

Thermochemical Conversion of Textile Waste to Useful Commodities and Fuel

Roozbeh Kalateh

Submitted for the degree of Doctor of Philosophy

Heriot-Watt University

School of Engineering and Physical Sciences

April 2021

The copyright in this thesis is owned by the author. Any quotation from the thesis or use of any of the information contained in it must acknowledge this thesis as the source of the quotation or information.

ABSTRACT

The quantity of textile waste has been increased significantly in the recent years and a considerable portion of this waste has been sent to landfills, causing environmental issues. This research has been carried out to address this issue and propose a method for textile waste conversion to useful commodities such as chemicals or biofuels with potential of application in a commercial scale.

Wool was selected as feedstock while gasification and pyrolysis were selected as the technologies with potential to facilitate the achievement of the objectives. Pyrolysis and gasification were carried out in bench-scale fixed bed reactor to check the feasibility of the pyrolysis for textile waste conversion. Furthermore, model compounds representing textile waste were pyrolysed with and without catalysts to evaluate if the properties of products could be modified.

5 different catalysts were used for pyrolysis of lignin, cellulose, and phenylalanine. The results indicated that Al-KIL2 and 20-ZSM5 had the potential to modify the properties of wool pyrolysis by-products and were used in wool pyrolysis in fixed bed. This decision was based on the increase in quantity of aromatics obtained in the oil products in based on the GC-MS analysis results.

High CO content of gas, char product properties and marketable products such as phenols in the oil obtained in pyrolysis and gasification using fixed bed reactor proved that these technologies were promising. Therefore, a novel scaled-up system (auger reactor) for textile waste pyrolysis was designed, built, and modified.

Comparing the findings of the gasification/pyrolysis of wool in the fixed bed and auger reactor, the conversion of feedstock to volatiles seemed to be more efficient in fixed bed while the properties of the char did not vary significantly. Regarding the oil products, while phenols and indoles were the prominent product in the fixed bed, ketones, nitriles and quinolines were the main products in the auger reactor.

Overall, the results indicated that up to 2 kg/h of textile waste feedstock on its own (without mixing with other material) can be pyrolysed/gasified in this system and by-products could be collected successfully. Furthermore, it was observed that residence time, heating rate and product collection method have been the main contributor for the difference between the small scale and scaled-up tests.

To my Parents,

For their continuous, selfless, and unconditional support

ACKNOWLEDGEMENT

I am grateful to my supervisor, Dr Aimaro Sanna, who provided me with guidance, knowledge and more importantly, his time during my PhD studies. I would also like to express my gratitude to The School of Engineering and Physical Sciences (EPS) of Heriot-Watt University, for providing the facilities for my PhD studies. Also, I would like to express my gratitude to Harris Tweed Authority for partially funding this research.

Special thanks to my brother Behzad Kalateh for always giving me the energy to move forward. Above all, I would like to express my utmost profound gratitude to my parents, Tayebeh Daryacheh and Ahmadreza Kalateh for their unconditional love and continuous encouragement, without whom I would have never had the opportunities that I have had.

DECLARATION STATEMENT

Research Thesis Submission

Name:	Roozbeh Kalateh		
School:	School of Engineering and Sciences		
Version: <i>(i.e. First, Resubmission, Final)</i>	Final Submission	Degree Sought:	PhD

Declaration


In accordance with the appropriate regulations I hereby submit my thesis and I declare that:

1. The thesis embodies the results of my own work and has been composed by myself
2. Where appropriate, I have made acknowledgement of the work of others
3. The thesis is the correct version for submission and is the same version as any electronic versions submitted*.
4. My thesis for the award referred to, deposited in the Heriot-Watt University Library, should be made available for loan or photocopying and be available via the Institutional Repository, subject to such conditions as the Librarian may require
5. I understand that as a student of the University I am required to abide by the Regulations of the University and to conform to its discipline.
6. I confirm that the thesis has been verified against plagiarism via an approved plagiarism detection application e.g. Turnitin.


ONLY for submissions including published works

7. Where the thesis contains published outputs under Regulation 6 (9.1.2) or Regulation 43 (9) these are accompanied by a critical review which accurately describes my contribution to the research and, for multi-author outputs, a signed declaration indicating the contribution of each author (complete)
8. Inclusion of published outputs under Regulation 6 (9.1.2) or Regulation 43 (9) shall not constitute plagiarism.

* *Please note that it is the responsibility of the candidate to ensure that the correct version of the thesis is submitted.*

Signature of Candidate:		Date:	09/04/2021
-------------------------	---	-------	------------

Submission

Submitted By <i>(name in capitals)</i> :	ROOZBEH KALATEH
Signature of Individual Submitting:	
Date Submitted:	09/04/2021

For Completion in the Student Service Centre (SSC)

Limited Access	Requested	Yes	No	Approved	Yes	No
E-thesis Submitted (mandatory for final theses)						
Received in the SSC by <i>(name in capitals)</i> :				Date:		

TABLE OF CONTENTS

1	Chapter 1 - Introduction	1
1.1	Aims & Objectives	3
1.2	Research Novelty	3
1.3	Thesis Arrangement	4
1.4	References	5
2	Chapter 2 - Literature Review	6
2.1	What is biomass	6
2.1.1	Biomass Characterisation & Classification	6
2.2	Textile Waste	8
2.3	Textile Waste Management Methods	9
2.3.1	Disposal	10
2.3.2	Recycling and Reusing	10
2.3.3	Anaerobic Digestion (Biochemical)	11
2.3.4	Fermentation (Biochemical)	11
2.3.5	Thermochemical Methods	12
2.3.6	Studies on Textile Waste Pyrolysis	24
2.3.7	Reactor Selection Conclusion	25
2.4	Auger Reactor (Pyrolyser) Applications Review	26
2.5	Wool Properties	30
2.5.1	Textile Dyes Review	34
2.6	Model Compounds	38
2.7	Catalysts	42
2.7.1	Catalysts Basics	43
2.7.2	Catalysts Selection	44
2.8	Model Compounds and Biomass Catalytic Pyrolysis	47
2.9	Summary & Conclusion	53
2.10	References	54
3	Chapter 3 – Methodology	72
3.1	Materials: Model Compound and Catalysts	72
3.1.1	Feedstock	72
3.1.2	Catalysts	73
3.2	Fixed Bed Pyrolysis	73
3.2.1	Non-Catalytic Pyrolysis/Gasification of Wool	74
3.2.2	Catalytic Pyrolysis of Model Compounds	77
3.2.3	Catalytic Pyrolysis of Wool	78

3.2.4	Large Scale Reactor Selection Procedure and Set-Up Arrangement	80
3.3	Products Analyses	80
3.3.1	Elemental Analyses (EA)	80
3.3.2	GC-MS	81
3.3.3	FTIR	81
3.3.4	TGA & MS	82
3.3.5	Surface Analysis	83
3.3.6	Catalyst Acidity	84
3.4	References	84
4	Chapter 4 - Auger Reactor Design	86
4.1	Initial Review	86
4.2	Design Requirements & Constrains	87
4.2.1	Feeding system	87
4.2.2	Cost and Sizing	87
4.2.3	Operations	88
4.3	Proposed Design.....	88
4.4	Design Decisions	90
4.4.1	Hopper Design Review	90
4.4.2	Furnace Review	94
4.4.3	Other Components of Design	95
4.5	Tests & Modifications	105
4.5.1	Option 1; Vertical auger feeder in the hopper	107
4.5.2	Option 2; Hopper with elongated outlet.....	107
4.6	Modified System Tests; Experimental Procedure	111
4.7	Chapter Conclusion & Recommendations	117
4.8	References	118
5	Chapter 5 - Model Compound Pyrolysis Results	121
5.1	Catalyst Characterisation	121
5.2	Model Compound Pyrolysis.....	123
5.3	Mass Balance & Product Distribution	123
5.4	Derivative Thermogravimetry (DTG) Data.....	126
5.4.1	Cellulose	126
5.4.2	Lignin	127
5.4.3	Phenylalanine.....	128
5.5	Gas Analysis	129
5.5.1	Cellulose Gas	130

5.5.2	Lignin Gas.....	130
5.5.3	Phenylalanine Gas	131
5.6	Oil Analyses	132
5.6.1	Cellulose Oil	132
5.6.2	Lignin Oil	138
5.6.3	Phenylalanine Oil.....	142
5.7	Discussion & Section Conclusion	147
5.7.1	KIL2.....	147
5.7.2	ZSM5	148
5.8	References	150
6	Chapter 6 - Small Scale Wool Pyrolysis & Gasification.....	152
6.1	Non-catalytic Wool Pyrolysis & Gasification.....	152
6.1.1	Product Distribution	152
6.1.2	Char Analysis	155
6.1.3	Gas Analysis	160
6.1.4	Oil Analysis	162
6.2	Catalytic Wool Pyrolysis	170
6.2.1	Product distribution.....	170
6.2.2	Char Analysis	171
6.2.3	Oil Analysis	172
6.3	Summary and Conclusion	177
6.3.1	Non-Catalytic Pyrolysis	177
6.3.2	Catalytic Pyrolysis	178
6.3.3	Next Chapter.....	179
6.4	References	179
7	Chapter 7 - Scale-up Wool Pyrolysis and Gasification Experiments Using A Customised Auger Reactor.....	181
7.1	Process Considerations	181
7.2	Mass Balance	182
7.3	Char analysis.....	183
7.3.1	Elemental Analysis of Char	183
7.3.2	FTIR of Char	185
7.4	Scrubbing Water & Gas.....	185
7.5	Bio-oil Analysis	189
7.5.1	Elemental Analysis of Oil	191
7.5.2	GC-MS of bio-oils	192

7.5.3	FTIR of Oil	198
7.6	Potential Application for Products and Separation Methods	198
7.7	Chapter Summary	200
7.8	References	201
8	Chapter 8 - Conclusion	203
8.1	Recommendations and Future Work	205
9	Appendices	207
9.1	Appendix A: Catalyst's Isotherms	207
9.1.1	Al-KIL2	207
9.1.2	Li-KIL2	207
9.1.3	20-ZSM5	208
9.1.4	30-ZSM5	208
9.1.5	60-ZSM5	209
9.2	Appendix B: DTG Vs. Temperature	210
9.2.1	Cellulose	210
9.2.2	Lignin	213
9.2.3	Phenylalanine	216

PUBLICATION AND CONFERENCE

Patent: Sanna, A., Kalateh, R., & Sun, D. (2019). Oil, method, and apparatus. (Patent No. WO 2019/043411 A1). World Intellectual Property Organization.

Conference Poster Presentation: Thermochemical conversion of textile waste to useful commodities; 25th European Biomass Conference and Exhibition, 2017, Stockholm, Sweden

CHAPTER 1 - INTRODUCTION

Due to technological advancements, efficient management system and globalisation, the cost of cloth's production has dropped considerably. This has led to a large increase in the volume of cloth purchased and consequently, textile waste has increased significantly in the last decades. These wastes are partially sent to landfill to decompose. Within European countries, Italy, and Germany each produce over 390,000 tonnes while France and UK each produce over 200,000 tonnes of textile waste annually [1.1]. Overall, textiles are the fastest growing sector in terms of household waste with over 2 million tonnes of textiles ending up in landfills every year globally [1.1, 1.2].

In total, of all the textile produced annually, 31 % ends up in landfills to decompose [1.3]. This decomposition has led to several environmental issues such as the production of greenhouse gases (methane) and groundwater contamination. Therefore, the Sustainable Clothing Action Plan (SCAP), launched in 2009, was aimed to increase the textile sector sustainability. SCAP 2020 commitment, as one of the paths, was placed to encourage retailers and government departments to sign up for voluntary waste, carbon, and water reduction targets for 2020 against a baseline on 2012. SCAP aimed to reduce the landfilled textile by 15% while the achieved target was 4% as of 2020 [1.4]. Therefore, actions needed to be taken to reduce the quantity of textile sent to landfills.

Other major sources of greenhouse gas emission are the use of fossil fuels and petroleum-based products. In addition to polluting the environment, fossil fuels are a finite source, and it is already believed that peak production of oil, natural gas and nuclear will be reached within a generation [1.5]. Their future consumption will not be sustainable given the strong energy dependency of the day-to-day life. Furthermore, the reduction of fossil fuels resources will result in consequential increase in prices. Therefore, renewable sources of energies are being developed to fulfil the requirement for sustainable energy.

Biomass and in particular bio-waste are considered the next step in generation of alternative products to replace conventional fossil fuels. The EU renewable energy directive [1.2] aims to achieve 14% renewable energy sources (RES) in transport fuels by 2030 [1.6]. Given that textile wastes and specifically natural fibres such as cotton and wool (making 29% of overall global fibre production) are considered as bio-waste, this research focused on proposing a solution for the problem of textile waste and use of fossil fuels through conversion of textile waste to fuel and useful commodities.

There are several methods to convert biomass to energy and useful commodities such as fermentation, anaerobic digestion, combustion etc. The thermochemical conversion of organic

wastes and more specifically thermo-catalytic cracking (catalytic pyrolysis/gasification) is another promising method. In pyrolysis, the textile waste could be depolymerised into useful commodities such as chemicals and fuels, under high temperatures and in presence of a carrier gas. Pyrolysis products are in three different phases: solid char, liquid oil, and gas. The gas phase can be utilised to make the process self-sufficient through use of CHP (Combined Heat and Power). The bio-oil can be further processed and upgraded to be used as fuels or as feedstock for the production of chemical commodities. Finally, the char can be used for several applications such as soil amendment, by which it will act as a carbon sequestration mean which can contribute to controlling the global warming effect.

Even though pyrolysis without the use of heterogeneous catalyst can lead to production of biofuels with some advantages over petroleum derived ones, there are important processing limitations that outweigh the advantages. Among the advantages, bio-oil can retain an acceptable percentage of the energy content of the original feedstock while withholding less nitrogen and sulphur compared to the petroleum product [1.7]. However, having an oxygen content of around 40 wt% makes this unstable for the conventional storage processes due to the existence of unsaturated compounds [1.8]. Additionally, several other issues such as high viscosity, low heating value, strong corrosiveness and more importantly, the complex composition of the oil represent unsolved challenges prior to integration into conventional facilities. Similar to petroleum refining, where catalysts can be used to influence the types of product obtained from the process of cracking, heterogeneous catalysis, either in-situ or ex-situ, can be utilised to overcome the issues mentioned earlier.

The literature indicated that there was a limited amount of research focused on developing and commercialising alternatives to sending textile waste to landfill for the disposal/recycling, including the pyrolysis of textile waste. Furthermore, most of the available systems which aimed at conversion of the textile wastes, either combined textile with other waste or changed the shape/structure of the feed (such as use of pellets). However, if textile waste conversion through pyrolysis/gasification was going to be commercialised, a specific reactor/system should have been designed which was capable of handling the textile waste in the same conditions as it is when being sent to landfills and at a large volume.

This research mainly focused on identifying the potential methods to convert textile waste to useful by-products followed by analysis/proposal of a method to scale such process up to a commercial one. In doing so, model compounds representing different textile wastes and textile waste itself were pyrolysed or gasified in a laboratory sized reactor to identify the potential of pyrolysis and gasification as a mean to convert textile waste to useful by-products. Furthermore, methods such

as change in operating conditions (such as temperature) and use of catalysts which had the potential to alter/improve the properties of by-products were tested. Additionally, feasibility of industrial-scale process was analysed through design and application of a novel arrangement.

1.1 Aims & Objectives

The aim of this research was to evaluate the potential of converting processed textile wastes by pyrolysis and gasification to chemical commodity and alternative fuel. The feasibility check of scaling up of this process to a commercial scale was also set as one of the aims of the research.

The objectives set for this research are listed below:

- I. Review of the potential methods for textile waste management
- II. Selection of reactor type considering the complex properties of textile waste; design and commissioning of the selected reactor arrangement for bench scale tests
- III. Textile waste pyrolysis/gasification and analysis of the products
- IV. Variation in test conditions (such as change of temperature and use of potential catalysts) to observe the possibility of modifying/improving the by-products quality
- V. Investigating the mechanism through which the pyrolysis took place on model compounds
- VI. Design and test of a scaled-up reactor and feeding system for textile waste processing
- VII. Analysis of the products for establishing their potential application

1.2 Research Novelty

This research focused on conversion of textile waste to fuels and chemical commodities. Most of the research carried out on biomass conversion and utilisation has been on lignocellulosic material and therefore significantly less focus has been put on textile waste conversion, which is mainly made of proteins and presents properties such as a very different density to lignocellulosic biomass. Furthermore, where textile biomass has been studied, it has been mixed with other wastes. Given that the use of textile waste for bioenergy could help in reducing the waste sent to landfill and mitigate drawbacks such as competition with food crops that exist with the use of lignocellulosic biomass, further research is required to facilitate such technology.

Only few papers have been published on possibilities of industrial sized thermo-chemical conversion plants for textile waste and utilisation of the process by-products. Most papers that consider processing textile waste in large scale are based on biochemical processes rather than thermochemical ones. However, the biochemical pathway had lacked success, due to the long residence time required and low conversions, making thermochemical methods a promising alternative.

In this Thesis, the effect of 5 catalysts in pyrolysis of three model compounds (lignin, cellulose, and phenylalanine) were tested in a lab-scale fixed bed reactor in addition to a thermo-gravimetric analysis to observe their potential to alter the properties of pyrolysis by-products. Afterwards, the fixed bed was used to pyrolyze/gasify wool waste (both catalytic and non-catalytic) and analyse the products through different tests. The system was scaled-up through designing, building, and testing a novel auger reactor arrangement. The products obtained from this scaled-up reactor were compared with the fixed bed reactor to evaluate the possibility of scale up.

1.3 Thesis Arrangement

- › Chapter 2 - Literature Survey: The nature of what biomass is and the advancements in biomass processing technologies are studied. Textile waste properties and potential methods for handling it are reviewed and catalyst which might improve the properties of the products of textile waste processing are studied. Also, the current stage of textile waste pyrolysis and application of auger reactors for biomass pyrolysis/gasification are reviewed
- › Chapter 3 – Methodology: The material's preparation, including the wool, model compounds and catalysts are listed. Next, the fixed bed (FB) system arrangements and the experimental procedures for catalytic and non-catalytic runs are discussed. Then, the methods utilised for analysing feedstock and products are detailed.
- › Chapter 4 – Auger Reactor Design: The detailed design of the scaled-up reactor, Auger Feeder (AF), is laid out and the overall operational procedures are listed. Afterwards, the issues observed, and actions taken for troubleshooting them are discussed
- › Chapter 5 – Model Compound Pyrolysis Results: The results for pyrolysis of model compounds with different catalysts in the fixed bed and TGA (Thermogravimetric analysis) are presented. These include the catalysts and pyrolysis by-products characterisation. Finally, based on the results, catalysts with promising results are selected to be taken forward for wool catalytic pyrolysis
- › Chapter 6 – Wool Pyrolysis and Gasification in Fixed Bed: The results of the wool pyrolysis (non-catalytic) at different temperatures, with different carrier gases, different condensation traps and different feedstock sizes are presented and compared. Afterwards, the results for wool pyrolysis/gasification and effects of the catalysts on by-products are discussed
- › Chapter 7 – Wool Pyrolysis in Auger Reactor: The results for pyrolysis of wool in the auger reactor at different temperatures are presented. Then, by-products obtained from pyrolysis/gasification in the fixed bed are compared with the ones obtained in the auger reactor.

- › Chapter 8 – Conclusion and Recommendations: A summary of the aims of the research are given. Then, the main findings of tests are given. Afterwards, the findings of the scale-up procedure are presented. Finally, recommendations on future work are listed.

1.4 References

- [1.1] LabFresh, “Fashion Waste Index,” LabFresh. [Online]. Available: <https://labfresh.eu/pages/fashion-waste-index?lang=en&locale=en>, [Accessed: 2020]
- [1.2] Waste Management World, “Textile reuse and recycling company expands in UK,” 2011. [Online]. Available: <https://waste-management-world.com/articles/2011/08/textile-reuse-and-recycling--company-expands-in-uk.html>.
- [1.3] WRAP , “Valuing our clothes,” 2012.
- [1.4] WRAP, “Sustainable Clothing Action Plan (SCAP),” [Online]. Available: <https://www.wrap.org.uk/sustainable-textiles/scap>. [Accessed 2020].
- [1.5] P.V.V. Prasad, J.M.G. Thomas, and S. Narayanan, “Global Warming Effects,” *Encyclopedia of Applied Plant Sciences*, p. 289–299, 2017.
- [1.6] European Commission, “Renewable energy directive,” August 2020. [Online]. Available: https://ec.europa.eu/energy/topics/renewable-energy/renewable-energy-directive/overview_en.
- [1.7] S. Weber, “The Afterlife of Clothes,” *Alternatives Journal*, vol. 41, pp. 26-29, 2015.
- [1.8] R. Consultancy, “Mapping the Development of UK Bio-refinery Complexes; A Report Prepared for the National Non-food Crop Centre,” 2007.

CHAPTER 2 - LITERATURE REVIEW

In this chapter, the general nature of biomass and types are discussed. Afterwards, the issues related to handling and disposing of textile waste are explained. Then, the potential technologies for textile disposal/conversion are listed and described, leading to a criteria-based selection. Finally, the employment of heterogeneous catalysis for improving the quality of the products obtained during processing of biomass using the selected methods are discussed.

2.1 What is biomass

Due to the versatility of biomass nature, there is no unified accepted description for what it specifically is. However, it could be simplified to compounds derived from organic matters. Based on what context it is being used, it can be described more specifically. For instance, in the bioeconomy (bio-technomy) term introduced by EU in 2012, biomass is “a biological resource from the land and sea, as well as waste, as inputs to food and feed, industrial and energy production [2.1]”

2.1.1 Biomass Characterisation & Classification

As an organic matter, the main elements of biomass are carbon, oxygen, and hydrogen in addition to less abundant elements such as nitrogen, sulphur, potassium, and calcium. The distribution of these elements is varied based on the type of feedstock used. For instance, in case of plant-based biomass, hydrogen normally makes up 6% of the biomass, while oxygen and carbon make up 40-44% and 42-47%, respectively [2.2]. These elements are mostly found in form of lipids, carbohydrates, and proteins. The variation in the ratio of these elements is one of the key factors in classifying biomass. Therefore, the following classification could be carried out [2.3]:

- › Carbohydrate-based: Made-up of carbon, hydrogen and oxygen. carbohydrate-rich carbohydrates can be categorised into:
 - Lignocellulosic: the main example of this type of biomass is wood and it mainly consists of cellulose, lignin, and hemicellulose
 - Starch: examples would be wheat, potato, corn etc. These are all high in polysaccharide reserves such as insulin
 - Sugar: monosaccharide such as glucose and sucrose such as sugar cane
- › Protein-based: Made of amino acid chains, proteins enable structural function of living matters. The main functional group of proteins are carboxylic acids and amines and therefore they have high nitrogen content. The biomass in this group can come both from plants (i.e., soybean) and animals (i.e., chicken, wool).

- › Lipid-based: Oil and fats are the main lipids found in the biomass which consist of fatty acids (tri-esters) and glycerol. Examples are some algae and rapeseed.

Other factors which matter in categorising biomass based on the chemical composition are water content (moisture), which can affect the heating value of the biomass and the conversion energy requirement. The range can be from 15 % for straws to 90% for algae [2.3]. The more the moisture content, the higher the processing and transportation costs are likely to be due to the additional complexities such as drying and storage.

Alternatively, biomass can be categorised based on the source of procurement. For instance, any biomass grown on agricultural land, which is any land permanently used for growing crops or pasture based on the Organization for Economic Co-operation and Development (OECD) [2.4], regardless of chemical composition, can be categorised as agricultural biomass. Similarly, any wood biomass obtained from forest can fall under the forest biomass. Additionally, any biomass, either plant or animal based, which is grown in water can be grouped as aquatic, such as microalgae.

Another source-based category can be wastes or by-products. This category can overlap with the above ones in the sense that agricultural or forestry wastes also fall in this category. All the wastes that are generated through production or consumption of organic compounds are considered biomass. Figure 2-1 illustrates a categorisation of biomass waste materials, potential major products and possible issue that could be arise from them.

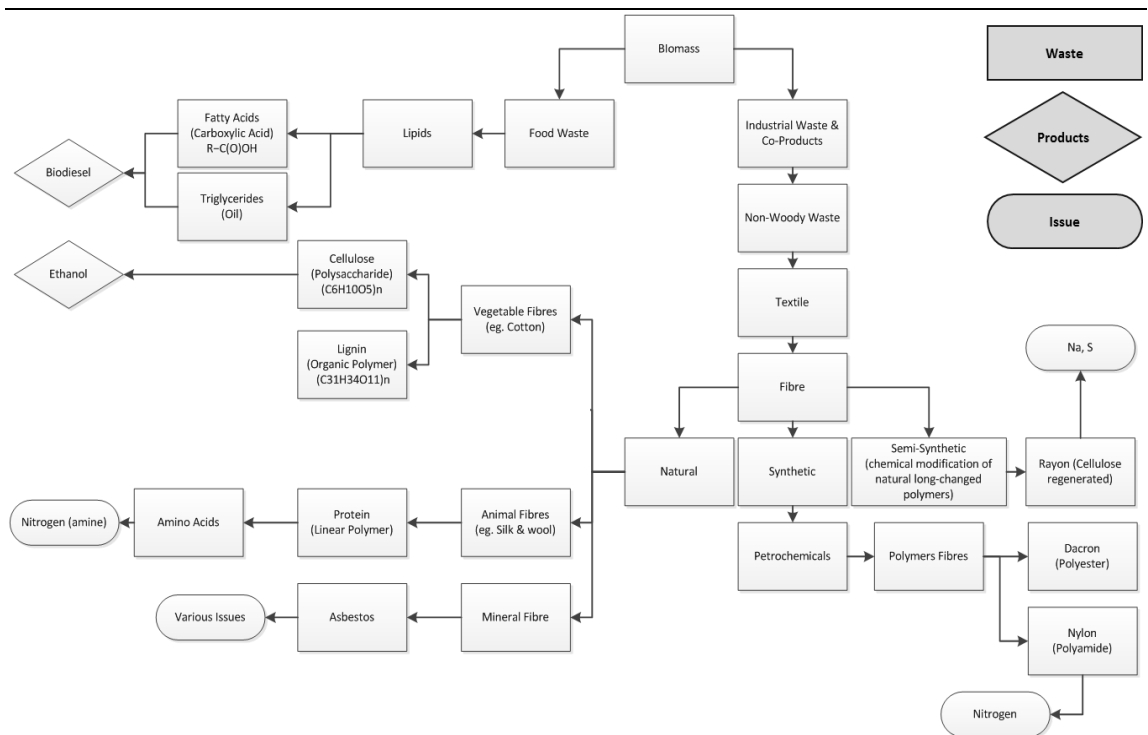


Figure 2-1: The categorisation of waste biomass

2.2 Textile Waste

Following transportation, food, and housing as the fourth contributor towards environmental issues contributors, fashion industry is one of the key sectors which requires further attention [2.5]. Despite all the recent innovations in all aspects of the industry such as production and care, which can potentially help in reduction of negative environmental effects [2.6], these might all be hindered or over-shadowed by the increase in the demand for purchasing more clothes by the consumers. For instance, just in the UK (based on HM Revenue & Customs), the consumption of clothes increased by almost 18% from 2012 to 2016, which including the amount of textile used can correspond to an increase of around 50,000 tonnes of textile per year. The fact that life span of garment utilisation has been reduced from 3.3 to 2.2 years in the current decade [2.7, 2.8], coupled with the increase in garment production will have a significant carbon footprint. The overall footprint in the UK has been above 26 million tonnes of CO₂ equivalent since 2016 with the highest contributors being the production and processing steps [2.8].

Sustainable Clothing Action Plan (SCAP) 2020, signed by more than 55% of UK retailers (based on production volume), required companies to reduce their negative environmental impact in several areas, namely [2.9]:

- › Carbon footprint reduction of 15%
- › Water footprint reduction of 15%
- › Waste to landfilled reduction of 15%
- › Reduction in waste arising over the whole product life cycle of 3.5 %

Each of the goals of the SCAP required in-depth research and technology innovation despite their interconnectivity. Since the initiation of the SCAP, several companies have taken steps to address each goal set in the plan. For instance, Marks & Spencer (M&S), Tesco and Sainsburys, all have set plans to commit to using sustainable cotton within the following decade, while ASOS has set plans to use different fibre mix through modifying their supply chain.

Another goal that needs to be addressed is the matter of waste to landfill reduction. For instance, over 200,000 tonnes of clothing are ended up in landfill in the UK annually [2.10]. As mentioned in Chapter 1, the objectives set by SCAP regarding the reduction in waste to landfill by 15% has not been reached as of 2020 (reduction of only 4%).

One of the materials which can have heavy negative environmental issues is wool, both due to high water consumption and extensive quantity of dyes used. Therefore, if more sustainable wool waste management technologies are developed, the environmental issues could be reduced through

reduction in soil contamination by dyes, water reduction if energy is extracted from the waste, and carbon footprint reduction.

As illustrated in Figure 2-1, the main building block of wool is protein. Protein itself is constituted of components such as alkyl phenols, aromatics (toluene), nitriles, heterocyclic amino acids and nitrogen containing aromatics. Similar to other biomass, wool can also be converted to biofuel which can overcome the issue of wool waste while having the simultaneous benefit of generating a renewable source of energy.

The high oxygen and protein content of the textile biomass is the main challenge that is limiting the advancement of textile biomass utilisation for bio-fuels purposes through pyrolysis. This is due to the fact that oxygenates contribute to the bio-oil thermal and storage instability [2.11, 2.12, 2.13]. Additionally, the high nitrogen content can reduce the value of the liquid products significantly due to the fact that it can cause serious environmental issues such as acid rain if used as fuel [2.14, 2.15]. Therefore, finding the suitable deoxygenation and nitrogen reducing methods have been set as one of the goals of this research. During this research, two different textile waste supplied by a clothing retailer in addition to 3 model compounds, namely cellulose, phenylalanine and lignin were utilised which have been discussed in more details in the following sections.

2.3 Textile Waste Management Methods

There are various paths that can be considered to manage textile waste beside disposal and reuse/recycle. The selection procedure can depend on multiple factors such as the economic factors, the feed composition, the quantity of the waste, the final desired products, and the residence time restrictions [2.16]. Some of these methods are listed below:

- › Disposal
- › Recycling and reusing
- › Biochemical methods
 - Fermentation
 - Anaerobic digestion
- › Thermal methods
 - Combustion
 - Torrefaction
 - Gasification
 - Pyrolysis

Each of the above methods have been explained and compared in the following sections.

2.3.1 Disposal

Disposal is currently the most commonly used method for handling the textile waste in the UK. For instance, up to 350,000 tonnes of textile are sent to landfill in the UK annually [2.17]. Even in major wool producing countries such as Australia or major wool consumers such as Italy, there was no significant record of managing pre-consumer or industrial waste by any means other than disposal [2.18]. However, this method does not represent a sustainable disposal method due to several economic and environmental issues. For example, the decomposition time could be long for some of the materials while some of the synthetic materials made from fossil fuels will not degrade at all. Also, even if they decompose, the release of methane during the process leads to an increase in greenhouse effects. Furthermore, the leaching of chemicals and dyes which are used during production can contaminate the soil and consequently the groundwater.

In order to dispose the clothing in the landfill, space is required. Therefore, extra costs are generated to make this land available. Also, this land requirement will increase annually due to the increase in global textile consumption. As an example, in USA, the 11 million tonnes of produced textile require 126 million cube yards to be stored [2.19].

As the environmental issues increase and space in landfills decreases, the probability of the introduction and enforcement of new regulations increases accordingly (and this has started). Therefore, more sustainable methods for handling textile wastes are desirable

2.3.2 Recycling and Reusing

Recycling and reusing are among the promising methods for handling textile waste. It has several advantages such as providing low-cost clothing for impoverished nations and reduction in carbon dioxide emissions. For example, collection of 1 kg of used textile can decrease the carbon dioxide production by 3.6 kg [2.20].

Textile recycling materials can be generally categorised into three groups of post-industrial, by-products of retail industry and post-consumer. The process of recycling itself can be divided into sorting, resorting, shredding, and pulling, carding, and spinning. Based on the requirements, the fibres then can be processed into different products.

Despite some positive aspects of these methods, several other issues suggested that these did not represent the desirable path for wool waste managements. Firstly, the re-use of the material might not be acceptable by some companies which target high-end and exclusive costumers due to the fact that it could lead to dilution of their brand. It may also result in the companies being dependant on recycling agencies and changing policies. Furthermore, the retail companies might lose their

financial opportunities such as generation of income from onsite power and other potential income source (e.g., chemical production). In addition, they might lose the chances of receiving government incentives through applying more sustainable technologies (e.g., Renewable Heat Incentives), through which, carbon sequestration could be achieved.

2.3.3 Anaerobic Digestion (Biochemical)

During anaerobic digestion, the biodegradable materials are broken down by micro-organisms in the absence of oxygen. Depending on the processing temperature, the anaerobic digestion can be divided into two groups of thermophilic and mesophilic. The mesophilic operates in a range of 35 to 40 °C, while thermophilic can go as high as 60 °C. The selection procedure would largely depend on the type of the feed. For instance, in case of the wool waste, if anaerobic digestion is selected to be utilised, a batch thermophilic system would be used [2.21].

This process converts hydrocarbons to methane and carbon dioxide. The process also produces a compost like solid and a liquid product, which can be utilised as fertiliser [2.22]. However, in case of textile, the application of this method was not justifiable. First of all, the capital cost of this method for an onsite digester could be relatively high compared to other potential methods [2.23]. Secondly, the experience in anaerobic digestion of textile is considerably limited while the operating cost of the process are potentially proportionally high in addition to the fact that the process might not be flexible enough to handle the expected variations in the textile feedstock. And finally, anaerobic digestion has a very long residence time (weeks), which might not be in sync with the continuous production system of most retailers.

For example, based on a case study on anaerobic digestion of wool produced by the Scottish biofuel program, it has been proven that this method was not promising for several reasons. For instance, the process was not able to break down the high keratin content of the wool without use of costly pre-treatment processes [2.24]. Therefore, it was concluded that it will not be commercially viable to apply anaerobic digestion to wool feedstock.

2.3.4 Fermentation (Biochemical)

During Fermentation process of biomass, the organic molecules are converted into products such as alcohols by microorganisms such as bacteria and yeast in the absence of oxygen [2.25]. However, similar to the other biochemical method, Fermentation anaerobic digestion is not promising for wool biomass processing due to the fact that the complex amino acid structure of this feedstock cannot be broken down to simpler units.

2.3.5 Thermochemical Methods

During thermochemical process, heat is used in order to convert biomass; As other types of biomass, textile waste can be converted to useful by-products. Depending on the processing temperature and whether oxygen is present, the thermochemical procedures can be categorised as shown in Table 2-1.

Table 2-1: Thermochemical methods

Methods	Temperature (°C)	Oxygen	Residence time (s)
Torrefaction	200-400	No	>300
Slow pyrolysis	400	No	>86400
Intermediate	500	No	10-30
Fast pyrolysis	500	No	1
Gasification	750-900	Yes	Variable
Combustion	>1500	Yes	-

2.3.5.1 Combustion

In this method, the biomass feed is directly burned either within a fixed or fluidised bed reactor in the presence of excess oxygen. Even though this method is the dominant mean of biomass utilisation, applying it to wool waste can have several drawbacks. For instance, due to the nitrogen and sulphur content of the feed, the resulting gas will contain NO_x and SO_x. Additionally, since heat is one of the main products of this process, this means that converting it to other energy sources such as electricity is required onsite if it is going to be utilised [2.26]. Additionally, and more importantly, having a limiting oxygen index of higher than 21% for wool coupled with an ignition temperature of above 580°C means that it will not burn readily [2.27].

2.3.5.2 Torrefaction

In this process, biomass is heated at relatively low temperatures and atmospheric pressure in order to upgrade it to a product with better fuel characteristics. Also, this coal-like material could be stored more easily due to the decrease in water absorption abilities and degradation possibilities [2.28]. Another name that is normally used for this process is roasting [2.29]. This method is generally used to dry and prepare the biomass feed for other thermochemical conversion methods such as gasification and pyrolysis. By doing so, the energy requirement for removing the water content of the biomass is reduced [2.30].

The gas released during the process is mainly water vapour and the volatiles decomposed from cellulose, hemicellulose, and lignin. These volatiles are hydrogen, carbon oxides, aromatics, light

hydrocarbons, and volatile organic oxygenates [2.31]. The remaining solid, normally referred to as bio-coal, includes ash, carbohydrates and char and can be changed into pellets in order to intensify the energy density and mass of it [2.32, 2.33].

Despite the various advantages and available markets for the products of this method, such as steel production and coal-fired power plants, this method was deemed unsuitable for the purpose of textile waste handling. As mentioned previously, this method is generally used as a precursor to pyrolysis/gasification to remove the moisture since the volatiles released through this method is around 25%, leaving 75% of the feedstock behind [2.34]. Therefore, utilising it, will not remove the issue of sending the waste to landfill.

2.3.5.3 *Pyrolysis*

Pyrolysis is the thermal decomposition of biomass at temperatures around 500 °C in absence of oxygen, resulting to three different products: biogas, biochar, and bio-oil. In pyrolysis, prior to depolymerisation in which the lower molecular weight substances get separated from the polymer, the polymer back bone is separated into two main high molecular weight chains, called random scission. These processes are normally followed by side group elimination during which, by removal of atoms and molecules from the backbone of the polymer chain, unstable unsaturated chains are left behind, which can lead to other reactions such as aromatisation [2.35]. These steps are not always followed in this order and can be varied depending on the feedstock.

Depending on the residence time of the reaction, pyrolysis can be sub-categorised into fast, intermediate, and slow [2.36, 2.37]. The compositions of the gas, solid and the liquid are dependent on several factors such as the reactor type, temperature of the process, heating rate, feedstock composition, particle size and reactor pressure. Table 2-2 illustrates the expected product distribution dependence on the type of pyrolysis applied. It should be noted that these data should only be used as an illustration of the effect of residence time rather than exact values since other factors such as feedstock composition play an important role in the product distribution.

Table 2-2: Product distribution dependence with pyrolysis model [2.38, 2.39]

Mode	Product Distribution (%)		
	<i>Gas</i>	<i>Liquid</i>	<i>Solid</i>
Fast	13	75	12
Intermediate	25	50	25
Slow	35	30	35

The liquid product is called bio-oil and 30% to 75% of the biomass can be converted to it depending on the path used [2.40]. The resulting bio-oil can include different by-products according to the type of the feed used.

Some of the products are detrimental to the further use of the bio-oils as fuel. For example, carboxylic acid and phenols can have corrosive effects, while aldehydes and ketones make the bio-oil unstable and reactive [2.40]. The resulting corrosiveness and instability cause issues during handling and storage of the bio-oil.

On the other hand, hydrocarbons such as aromatics can be valuable if appropriately separated. Furthermore, products such as phenol and its derivatives, if separated efficiently, could be valuable. For example, phenol has a wide range of application in industry; it is used as feedstock for production of explosives, plastics, or common drugs [2.40].

Since the produced liquid in this process has the potential to be used directly as a feed to other chemical process or as a fuel source, the fast pyrolysis, which has the highest yield of liquid, followed by intermediate pyrolysis were deemed promising. The produced liquid has several advantages over the solid feed such as [2.41]:

- › reduced transportation and storage cost
- › potential upgrading using existing crude-oil refinery technologies
- › reduced carbon footprint due to almost carbon neutrality of the process

However, if bio-oil is going to be considered as a viable substitute for fossil fuel derivatives, its properties such as oxygen to carbon ratio should be comparable to crude oil. Table 2-3 [2.40] shows the properties of bio-oil from lignocellulose biomass in comparison to that of crude oil.

Table 2-3: Bio-oil and crude oil comparison

Properties	Bio-oil (Lignocellulosic)	Crude oil
C (wt%)	55-65	83-86
O (wt%)	28-40	<1
H (wt%)	5-7	11-14
S (wt%)	<0.05	<4
N (wt%)	<0.4	<1
Ash (wt%)	<0.2	0.1
H/C	0.9-1.5	1.5-2.0
O/C	0.3-0.5	0

As illustrated in Table 2.3, some of the properties of the bio-oil such O/C ratio require to be modified in order to make the bio-oil quality comparable to crude derived liquids. For example, a

bio-oil with heating value of 18 MJ/kg can be converted to one with much higher heating value (44 MJ/kg) by using catalytic processes [2.31]. However, this process will reduce the bio-oil yield as a sacrifice to increase the heating value.

Based on the above considerations, it is envisaged that the solely production of bio-oil as disposal of wool waste does not represent a viable pathway, due to the extent of post-processing required to render the bio-oil compatible to crude-oil based fuels. Therefore, use of catalysts for modifying the properties of the products should be considered.

The solid product of pyrolysis and gasification is called biochar. In case of pyrolysis, it normally has more than 50% carbon. One of the most common and direct applications of biochar is its use as soil amendment [2.42]. Also, despite some disagreements, most studies agree that since the carbon in the biochar will be stable for hundred years [2.43], it can be effectively utilised as a mean of carbon capture and sequestration.

The market for biochar is expanding rapidly. This increase is mainly due to the interest from the agricultural market towards utilisation of biochar in order to improve water holding capacity of the soil and crop yield, natural carbon sequestration properties of biochar and increased government initiatives [2.44]. For instance, the American Power Act of 2010 has several provisions, which support the biochar initiatives. Moreover, several non-government or non-profit organizations are also promoting its production and usage, such as International Biochar Initiative (IBI), a member-based organization promoting good industry practices, stakeholder collaboration, and environmental and ethical standards to foster economically viable biochar systems globally; and United States Biochar Initiative (USBI), a non-profit organization promoting the sustainable production and use of biochar in the U.S [2.45].

If the pyrolysis processing parameters such as temperature are controlled and the biochar is in-situ activated (e.g., using steam), the activated carbon can be a valuable by-product to be obtained. The same product will result from low temperature gasification.

The main application of activated carbon is in the removal of contaminants from either water or gas. This phenomenon is facilitated due to attractive forces between the contaminant surface chemistry and the surface of the carbon. This adsorption can also be used in multiple other industrial processes, which require purification or separation such as medicine, food industry (decaffeination) and metals extraction [2.46]. Activated char also has been used for the development of new textile product [2.47].

Activated carbon is characterised by several physical and activity properties such as pore size distribution, surface area, product density, ash content, mesh size and abrasion resistance [2.46].

Therefore, the selected process condition will determine the activated carbon properties and the potential applications. For example, different activation methods such as the gas treatment (CO₂–physical activation) or chemical treatment (NaOH) can change the final product properties significantly [2.48].

The gas product of the pyrolysis mainly consists of carbon monoxide, carbon dioxide, hydrogen, and light hydrocarbons (e.g., CH₄, C₂H₆). The composition of the gas mainly depends on the feedstock and process conditions [2.49]. This combustible gas (excluding CO₂) could be used to run the pyrolysis process itself or be used within a CHP plant onsite if significant amount of it is produced (e.g., in gasification mode).

Most research and developments have focused on testing different reactor configurations with a variety of feedstock. In the last 20 years, numerous researches have been working on laboratory scale reactors based on technological concepts of fast pyrolysis, where high yields of bio-oil and operational efficiency are the main goals. The reactor, which is the “core” of the conversion process can be classified as below [2.38]:

- › Fixed bed reactor
- › Bubbling fluidized-bed reactor
- › Circulating fluidized-bed reactor
- › Rotating cone
- › Vacuum pyrolysis reactor
- › Rotary Kiln
- › Screw/auger reactor
- › Microwave pyrolysis and hydro pyrolysis reactor

It is important to note that the above reactor configurations can also be used for gasification purposes.

Fixed Bed

Fixed bed reactor has been used in several laboratory scale researches and investigations as the simplest arrangements for pyrolysis. This reactor type is particularly useful in terms of simulating thermal processes in laboratory scale, due to good accessibility and facilitating operation under similar conditions to scale up process with good accuracy.

However, there is limited commercial scaled application for biomass conversion purposes. The possible reasons for this could be the probable issues such as maintenance, clogging caused by produced tar, or increase in the resistance to the gas flow in the reactor [2.50].

Fluidised Bed

The operational mechanism of both the bubbling and circulating fluidised bed are well understood and several documents are available on their pilot and commercial application. As illustrated in Figure 2-2, the biomass feed is injected into the heated bubbling bed using a screw feeder. Additionally, sometimes a carrier material such as sand is used alongside the gas flow in order to improve the heat transfer and temperature control in the reactor. Also, due to the lack of the mechanical parts within the reactor, the scale up procedure is not as complex as other reactor arrangements.

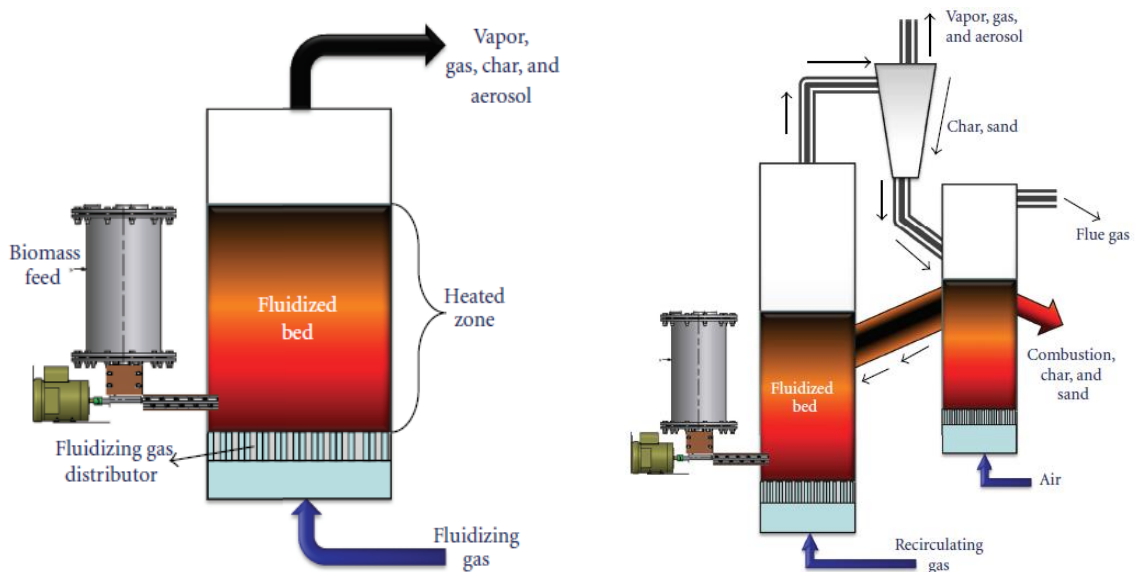


Figure 2-2: Fluidised bed reactor arrangement (bubbling- left, Circulating, right) [2.49]

However, one of the main issues regarding the utilisation of this method is its high capital and operation cost. In other words, significant investment is required for purchasing gas blowers required to maintain fluidised the beds. Also, the energy consumption for fluidising the material is significant [2.50]. Above all, fluidising processed wool feedstock can pose challenges regarding the mixing in the reactor, and this has prevented the selection of this method as the suitable path.

Circulating beds are a more complex version of the bubbling bed with the main aim to improve char quality through increasing the gas velocity and reflux. However, issues such as low heat transfer rate and even increased cost of gas injection [2.50], and the matters regarding the type of feed, render this method not applicable for the wool waste.

Rotating Cone

In the rotating cone arrangement, a technology developed at the University of Twente, the biomass feed and heated sand are sent to a high-speed rotating cone (Figure 2-3), where the high rotating speed of the cone in the absence of the oxygen, causes a quick and simultaneous mixing and heat

transfer process [2.51]. The process is self-sufficient in case of the energy since it uses the produced biochar as the fuel source. However, it should be noted that the process uses almost all the produced biochar as the fuel itself and therefore the main product of this process is the liquid bio-oil. Additionally, the maintenance of the process could be costly because the cone is operating with high rotating speed, which could lead to frequent equipment failure. Similar to the case of the fluidised bed, the downward and continuous flow of the processed wool with no external mechanical force is not practical. Therefore, this method should be discarded as a suitable method for wool pyrolysis.

Vacuum Pyrolysis:

Vacuum pyrolysis is another promising method for biomass conversion. In this technology, the organic feedstock polymeric structure is decomposed into primary fragments under reduced pressure when heated. The main difference between this technology and atmospheric pyrolysis, besides the lower pressure, is the continuous and immediate removal of the produced vapour by a vacuum pump which will prohibit the secondary reactions such as cracking and repolymerisations [2.52]. The removed gases are condensed as pyrolytic oils. The other products obtained from the process (water and charcoal) are predicted to have higher quality since their chemical characteristics are closer to the original feed [2.53]. Therefore, this arrangement (Figure 2-3), can be operated at reduced temperature and heat input due to the lower operating pressure in addition to the appropriate control over the vapour residence time [2.50].

However, there are several operational issues associated with the application of this method. As illustrated in the Figure 2-3, recovering the products requires a complex design for the outlets. Furthermore, there are several generalised issues such as, large equipment size, high capital cost and low heat and mass transfer rate which are embedded with the utilisation of this technology [2.54]. Therefore, this technology is considered unsuitable for this research project.

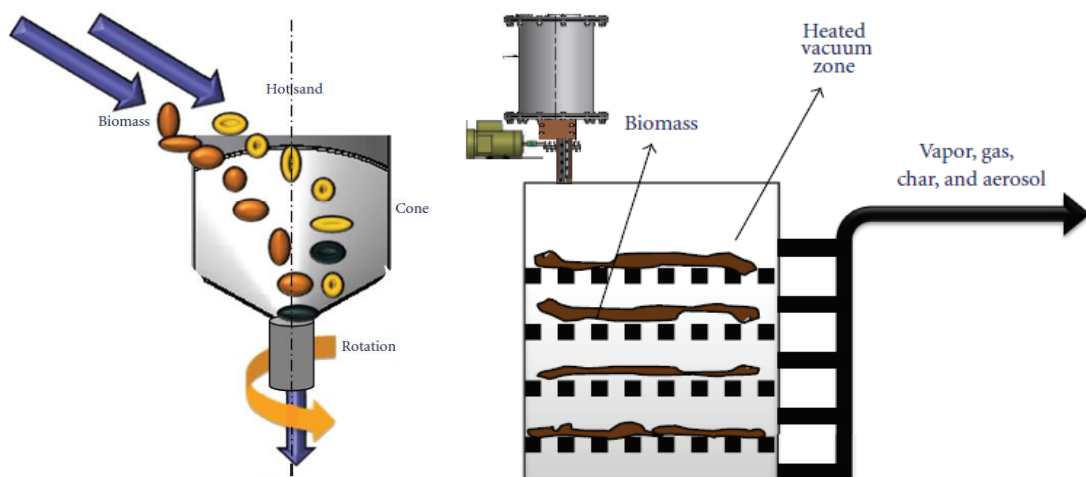


Figure 2-3: Schematic of circulating cone (left) and vacuum (right) Reactor [2.49]

Rotary Kiln

Another possible technology, Rotary kilns, has recently attracted major attention for the thermal processing of wastes, due to their advanced state of development and their relatively simplicity.

A rotary kiln is a pyro-processing device typically used to raise up materials to high temperature (calcination) in a continuous process. Materials produced using rotary kilns include cement, lime, refractories, and waste treatment.

The two basic types of rotary kilns – direct fired and indirect fired (calciners) – can be found supporting processes in mineral, agriculture, and other material processing industries. The design and operation of a rotary kiln are critical to its efficiency. If designed incorrectly or operated improperly, a rotary kiln will inadequately treat materials and drastically increase operating costs.

Rotary kiln gasifiers are a proven technology and are considered robust and dependable. These gasifier systems are comprised of a primary rotary kiln reactor, a secondary combustion chamber, flue gas treatment units and a control system. Rotary kiln gasifiers can be specifically designed to treat MSW, sludge, and hazardous solid waste.

Rotary kilns have the advantage of being able to operate over a wide temperature range depending on the design and refractory used and can handle a wide variety of waste types. For solid waste application, these gasifiers systems have a specially designed afterburner to assure maximum oxidation and minimal particulate emissions. They can be fitted with various options for emissions control, heat recovery to steam, hot water, and electricity [2.55]. However, they are limited as to waste capacity per unit compared to fluidized bed designs and might encounter flow issues with wool feedstock.

Auger

Another promising technology is the auger or screw reactor configuration (Figure 2-4). As described earlier, almost all the discussed pyrolysis technologies with the exception of the rotating cone reactor include a screw feeder as part of their design. In this technology, the use of the auger is extended. The biomass feed is transported through a heated zone (either direct or indirect heating) by the auger and the temperature of the feed is increased to the required pyrolysis temperature during this transportation. This desired temperature could be controlled by manipulating the feeding rate (auger rotating speed), mode of heating, biomass particle size, flight-pitch, and auger diameter [2.50]. This variety of controllable variables leads to the overall expected controllability of the residence time of the feed in the reaction in this technology.

This technology has some minor disadvantages such as mechanical wear and tear due to the existence of the moving parts, which could be overcome easily through careful and customised design. Additionally, other advantages of this technology such as simplicity, low energy requirement and lack of a requirement for excess amount of gas flow [2.50], outweigh the minor disadvantages.

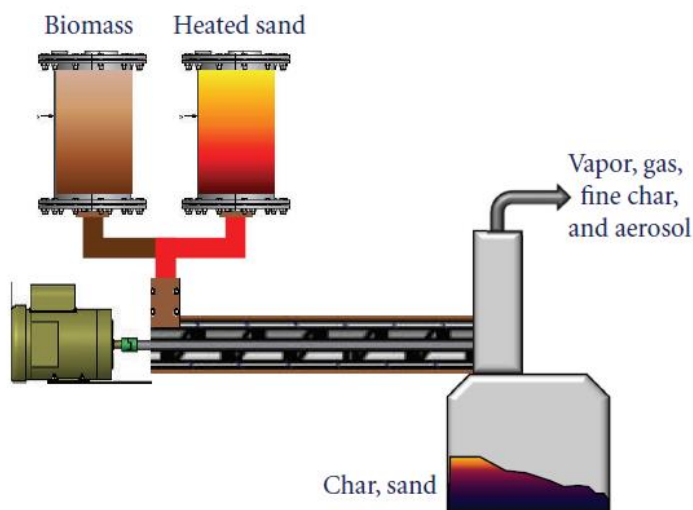


Figure 2-4: Schematic of screw feed (auger) reactor

Comparison of Technologies

Other methods such as microwave pyrolysis, hydro pyrolysis and ablative pyrolysis reactors were considered unsuitable for the current research in hand either due to their immaturity or repetitive unsuccessful scale ups based on multiple reports [2.38, 2.50].

Table 2-4 illustrates a comparison amongst the discussed pyrolysis technologies based on their expected bio-oil yield and versatility alongside some other aspects. However, it should be noted that several operational factors such as residence time and temperature can affect the bio-oil yields and the values in the table below are indicative only and in most cases, a maximum expected value.

Table 2-4: Pyrolysis technologies comparison [2.50]

Reactor (pyrolizer)	Bio-oil yield (%)	Operational complexity	Particle size	Biomass variability	Scale up	Inert gas flow
Fixed bed	75	Medium	Large	High	Hard	Low
Bubbling bed	75	Medium	Small	Low	Easy	High
Recirculating bed	75	High	Medium	Low	Hard	High
Rotating cone	70	Medium	Medium	High	Medium	Low

Auger	70	Low	Medium	High	Easy	Low
Vacuum	60	High	Large	Medium	Hard	Low

Because of the nature of processed wool waste, the feeding into the reactor should be forced by some method. The information in the literature suggested that the auger reactor is the most promising technology for the conversion of textile waste due to the ease of scale up procedure and low operating complexity.

2.3.5.4 Gasification

Waste-to-Energy technologies are emerging as promising routes for reducing the fossil fuel dependency of the world's energy supply. Heating biomass at temperature within the range of 700 to 1000 °C in the presence of limited amount of oxygen is called gasification. In contrast to pyrolysis, in which the main product is the condensable liquid phase, the main product is the volatile gas phase (syngas) in gasification. Syngas consists of hydrogen, carbon monoxide, carbon dioxide and methane in addition to tar and char [2.56, 2.57]. The produced syngas can be utilised in several processes. For instance, it can be combusted to generate heat and electricity in CHP units, further processed to diesel through Fischer Tropsch process or used as an intermediate to synthesise ammonia and fertilizers [2.58].

A typical gasifier (the equipment in which gasification occurs) generally consists of 5 zones as illustrated in Figure 2-5, they are listed below:

- > Drying zone
- > Distillation zone
- > Reduction zone
- > Hearth Zone
- > Ash zone

Figure 2-5 illustrates the two main types of gasifiers, concurrent and counter-current, and the division of the above stages within them. On the left, the counter current gasifier is illustrated. In this system, the air entering from the bottom facilitates the combustion while the reduction reactions occur in the upper zones of the reactor. The heat transfer carried out by forced convection and radiation from lower zones causes the pyrolysis to take place in the upper regions. While the ashes are left for collection at the bottom of the reactor, the tars and volatile leave the system with the gas stream.

The formation of this tar and ash can lead to operational issues. For example, the ash can cause corrosion and erosion. Similarly, the tar formation can reduce the process thermal efficiency

through reducing the heat transfer rate [2.59]. In addition, tar contaminants, particulate matters, and sulphur in the syngas [2.60] are becoming more and more important issues, as the environmental regulations for the emissions are getting stricter.

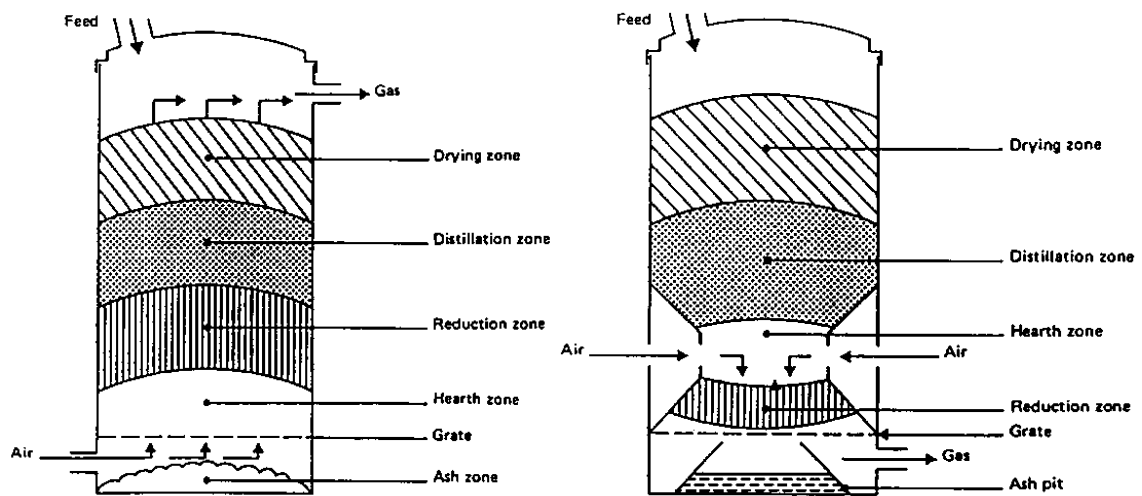


Figure 2-5: The two main gasifier types [2.58]

As illustrated in Table 2-5, regardless of the class, all the tars have molecular weight higher than benzene. The gasification temperature is an operating parameter that strongly influences the tar level in addition to the products distribution. High operating temperatures (at least 750 °C) are required to reach high carbon conversion of the feedstock and low tar content in the resulting product gas. However, at gasification temperatures exceeding 850 °C there is a rapid increase in the formation of 3- and 4-ring aromatics (class 4 and 5) together with other unwanted by-products [2.60, 2.61]. Therefore, temperature between 750 and 850 °C is desired in terms of reduction of tar production.

A different type of primary tar reduction measure is the use of bed additives or catalysts. There exist numerous studies that discuss the selection of the most appropriate additives/catalysts for tar abatement [2.62, 2.63]. The ideal catalyst material is cost-effective and combines a high efficiency with a high selectivity towards tars (as opposed to high quality syngas components) [2.60].

Despite having several advantages such as simplicity, high efficiency and adaptability to various feedstock, disadvantages such as tar carried over in the gas stream, gas channelling in the equipment (which could lead to explosions), feed preparation (drying and grinding), oxygen input, reactor cleaning and maintenance are the main limitations of the counter-current configuration [2.50]. For instance, if the feed is not homogeneous, the reactions will not take place evenly and therefore the quality of the product might be affected [2.60]. This means that normally, further treatment of the

products will be required in order to make them usable either directly as fuel or as feed to other processes.

Table 2-5: Tar classification [2.64]

Class	Description	Component
1	GC Undetectable: Heaviest tars at highest concentrations; even at very low concentration	Gravimetric tars
2	Heterocyclic Component: Generally high-water solubility due to polarity	Pyridine, phenol, cresol, quinoline
3	Aromatic Component: Light hydrocarbons, i.e., no issue regarding their condensation but water solubility could be an issue	Xylene, styrene, toluene
4	Light Polyaromatic Hydrocarbons (2-3 rings PAH's): Condense at high concentrations and intermediate temperatures	Naphthalene, methylnaphthalene, biphenyl, ethenylnaphthalene, acenaphthylene, acenaphthene, fluorene, phenanthrene, anthracene
5	Heavy Polyaromatic Hydrocarbons (4-5 rings PAH's): Condense at high temperature and low concentrations	Fluoranthene, pyrene, benzo-anthracene, chrysene, benzo-fluoranthene, benzo-pyrene, perylene, indeno-pyrene, dibenzo-anthracene, benzo-perylene

In order to overcome the above issues, the concurrent (right in Figure 2-5) system has been proposed. Additionally, due to the lower levels of organic condensate in this arrangement, it normally results more environmentally friendly compared to the counter current arrangement.

However, there are several issues that make the use of this arrangement unsuitable for the thermochemical conversion of textile waste. For instance, textiles feed can cause flow problems and therefore result in excessive pressure drop within the system. In other words, since the feedstock motion into the reactor is achieved mainly by “assisted” gravity flow, the textile waste will not flow smoothly using this gasification configuration. Moreover, since they do not have any internal heat exchanger, they are less efficient than the counter-current arrangement.

2.3.6 Studies on Textile Waste Pyrolysis

Recently, there have been an increasing interest in research on pyrolysis of textile waste despite the fact that the numbers of studies on textile waste pyrolysis on its own (rather than co-pyrolysis with another feedstock) are still limited compared to other biomass feedstock. Furthermore, records of these researches are limited in literature. Table 2-6 lists some of these studies and the reactor type utilised in addition to summarising the work which has been carried out.

Table 2-6: Examples of textile pyrolysis [2.65]

Feedstock	Reactor	Summary of work	Product Break-Down ¹ (%)	Ref.
Natural Textile (Mainly Cotton)	Fixed Bed	<ul style="list-style-type: none"> > The reactor used was 64 cm long with a diameter of 5 cm > Nitrogen was used as the carrier > Pyrolysis temperatures of 300 to 900 °C were used > Heating rate of 10 °C/min 	Char – 20 Oil – 40 Gas – 40 ²	[2.66]
Acrylic Textile Waste	Static Bed (Batch)	<ul style="list-style-type: none"> > The reactor was 25 cm long with a diameter of 3 cm > Pyrolysis temperature of 500 to 900 °C were used > Heating rate of 5 °C/min 	Char – 48 Oil – 42 Gas – 10 ³	[2.67]
Textile	Batch	<ul style="list-style-type: none"> > The textile was 30% polymer and 70% cotton > Reactor was 50 cm long with a diameter of 12.5 > Nitrogen was used as the carrier > Heating rate of 10 °C/min > Pyrolysis temperature of 400 to 600 °C were used 	Char – 23 Oil – 34 Gas – 43 ⁴	[2.68]
Combed Cotton	Fixed Bed	<ul style="list-style-type: none"> > Pyrolysis temperature of 450 to 600 °C were used > Heating rate of 5 °C/min 	Char – 16 Oil – 30 Gas – 54 ⁵	[2.69]

¹ The values are approximate and taken at highest pyrolysis temperature reported

² Data for pyrolysis at 800 °C

³ Data for pyrolysis at 900 °C

⁴ Data for pyrolysis at 600 °C

⁵ Data for pyrolysis at 600 °C

As stated in Table 2-6, with exception of pyrolysis of acrylic textile waste, a product distribution which consists of less than 25 % char and over 75% of volatiles in form of oil and gas could be expected from pyrolysis of textile waste at high temperatures. However, the properties of the type of textile waste utilised and conditions of pyrolysis such as temperature can affect this distribution significantly. Furthermore, the range of temperatures varied significantly (from 300 to 900 °C) in these studies.

In addition to the works reported in Table 2-6, some other more recent works have been done on textile pyrolysis. For instance, Balcik-Canbolat et.al. pyrolysed comingled waste textiles in a batch reactor at temperatures ranging from 500 to 700°C with heating rates of 25 to 50 C.min⁻¹ [2.68]. The study was done to analyse the evolved gas and char products and therefore the analysis of oil was omitted from this study. Maximum volatile content of 83% was reported with CO, CO₂, H₂ and CH₄ as main components in gas.

Chen Weng et.al. pyrolysed small samples (smaller than 1.2 mm) of three different textile feedstocks (cotton, wool, and polyester) in CO₂ environment using Thermogravimetric-Fourier transform infrared spectrometer at 300 to 500°C [2.69]. Experiments concluded that cotton was the most reactive compounds with pyrolysis starting at 300°C followed by polyester with wool being the least reactive compound with the least sensitivity to change in temperature.

Samy Yousef et.al. pyrolysed blue and black jeans (cellulose, polyester, and dyes) at 800 °C. Pyrolysis was carried out with 300 g of material and heating rate of 20 °C/min in a vertical fixed bed reactor and using nitrogen as injected gas. Char, oil, and gas made up 17.8%, 37.5 and 44.7% of the products, respectively. Heavy metals which were part of the waste (as part of the dyes) were extracted and used as catalysts which increased the yield of bio-oil by around 20% and reduced pyrolysis time by 15% [2.70].

2.3.7 Reactor Selection Conclusion

Base on the literature review on the current available thermo-chemical processes, it was decided to pyrolyze the textile waste by using fixed bed arrangement in the laboratory scale with the possibility of scale up with utilisation of an auger arrangement if the results of the laboratory scale was deemed promising.

Pyrolysis was selected due to the proven record of this method for other sources of biomass and the numerous available arrangements to implement it. Fixed bed was selected due to the simplicity and proven applicability of it to different kind of biomass feed [2.73, 2.74]. However, as explained previously, the scale up of this method was not practical and another method was required for scale up implementation.

Due to the nature of the wool, i.e., tanglement of the feed particles together and resistance to flow, auger pyrolizer was deemed a suitable method since it can drive the feed all the way through the process (from feeding to product collection). The design of the reactors and their arrangements are discussed in chapters 3 and 4 while some of application of auger (screw) reactors for biomass are reviewed in section 2.4

2.4 Auger Reactor (Pyrolyser) Applications Review

Recently, vast interest has been attracted towards use of auger reactors for pyrolysis. Most of the applications of this method have been by universities and research institutes [2.75]. Table 2-7 illustrates some of these studies and application. The feedstock range for auger Pyrolyser can be vast and it could include agricultural waste, sewage sludge, food waste, plastic waste, and other miscellaneous waste. However, as can be seen from Table 2-7, the application of this method for textile waste has been close to no existence and this presents an opportunity for further investigation on the matter.

Almost in all the processes presented in Table 2-7, the feed is introduced to the pyrolysis process via a hopper. Then, the feed is introduced into a heated medium either directly with the auger reactor (one auger) [2.76, 2.77, 2.78] or with an additional auger [2.75, 2.76, 2.79] for control over the feeding rate. The reactor (heated section) itself is generally divided into two types. One uses the auger feeder as the sole reaction zone [2.80, 2.81] while the other method passes the gas through an additional reactor [2.82, 2.83] (mostly fixed bed) for further reaction and conversion. The second reactor can also be a catalytic one [2.75]. The auger itself is installed horizontally in most of the arrangements while horizontal installation can also be observed in some of the reactors such as the pyrolysis process developed by the Research and Development Institute for Agri-Environment in Quebec [2.84]. Additionally, a single or twin auger can be installed in the reactor based on the feed characterisation [2.75].

Table 2-7: List of auger applications for biomass pyrolysis [2.75]

Company/University	Country /Year	Auger Type	Feedstock	Moisture Content (wt%)	Particle Size (mm)	Feeding Rate (Kg/h)	T (°C)	Reactor Length (cm)	Auger ID (cm)	Ref.
Maharakham University	Thailand /2013	Counter Rotating Twin Screw	Cassava, Rhizome	0	0.3-0.4	0.4	500-700	45	4.4	[2.79]
European Bioenergy Research Institute–Ebri	UK/ 2014	Twin Co-Axial Screw	pelletised wood and barley straw	3-11.9	-	15	450	180	20	[2.85]
Michigan State University	USA/ 2015	Single Auger	Food Waste (Spent Coffee Grounds)	3	0.1-2	1.5	429-571	-	-	[2.80]
University of Leeds	UK/ 2012	Single Auger	Waste Wood Pellet	7.8	-	0.24	500	54	6.2	[2.82]
Slovak University of Technology	Slovak Republic / 2016	Single Auger	Shredded Tire and Wood Pellets	0.5-3.3	2 By 5 To 5 By 5	0.1	650 - 850	30	2.5	[2.86]
Washington State University	USA/ 2010	Single Auger	Firewood	0	2	1.5	120-800	58.5	10	[2.75]
University of Caxias Do Sul	Brazil/ 2015	Single Auger	Wood Pellets (MDF)	7.3	<0.21	1.9	400-600	200	20	[2.76]
Iowa State University	USA/ 2014	Twin Auger	Wood Waste, Switchgrass	5.84	<0.75	0.25	425-625	55.9	2.5	[2.87]
Instituto De Carboquímica	Spain/ 2013	Single Auger	Waste Tire	0.8 - 6.21	2 To 20	15	500-600	87	7.5	[2.88] [2.75]
Karlsruhe Institute of Technology	Germany /2016	Twin Auger	Lignocellulosic	5.9 - 10	<0.5	20	500	59	4	[2.89]

Institute for Technical Chemistry (Itc)	Germany / 2018	Single Auger	Wood Chips and Sewage Sludge	8.8 - 10	2 To 8	4	350 - 500	200	15	[2.77]
Chosun University	South Korea/ 2011	Single Auger	Swedge Sludge (Dried)	5.6	5 To 10	-	385 - 500	>250	-	[2.90]
University of Tennessee	USA/ 2014	Twin Auger	Pine Wood	8	< 4	20	500 - 550	-	-	[2.91]
Mississippi State University	USA/ 2016	Single Auger	Pine Wood	8 - 10	2.5		450	101.6	7.6	[2.75]
Mississippi State University	USA/ 2013	Single Auger	Pine Wood	6 - 10	2 To 4	7	300-450	114	7.6	[2.92] [2.75]
Delian University of Technology	China/ 2017	Single Auger	Pine Sawdust and Sewage Dust	1.4 - 6.3	1 To 2	6	400 - 900	120	4	[2.75]
Beijing University of Chemical Technology	China/ 2017	Microwave Assisted Auger	Textile Dyeing Sludge	1.4	<1	2.5	450 - 750	40	4	[2.75]
University of Basque Country	Spain/ 2016	Single Auger	Woody Biomass Waste	10.8	0.5 To 2	3.9	900	-	-	[2.93] [2.75]
University of Seoul	South Korea/ 2016	Single Auger	Tyre Rubber	0.4	1 To 2	0.3	338	70	2.8	[2.75]
Research and Development Institute for The Agri-Environment	Canada/ 2016	Vertical Single Auger	Wood Pellets, Pig Manure	6.5 - 13	1 To 3.8	1.08	450-600	25.4	2.5	[2.75]
Laval University	Canada/ 2015	Single Auger	Wood Chips	8	<2	0.47	450			[2.75]

Memorial University of Newfoundland	Canada/ 2016	Single Auger	Wood Shaving and Sawdust	0.1 - 2.2	2	7.5	400 - 500				[2.75]
Guangzhou Institute of Energy Conversion	China/ 2014	Single Auger	Pine Wood	6 - 8	<1	20	400 - 600	300	15		[2.94] [2.75]
Institute Branch Sulzbach-Rosenberg	Germany / 2017	Single Auger	Digestate	15	-	1.6	450				[2.75]
University of Idaho	USA/ 2014	Single Auger	Potato Peel	4.3 - 5.5	<1	0.5	450	90	5		[2.75]
University of Leoben	Austria/ 2013	Twin Auger	Agricultural Residue	6.8 - 11	<8	10	900	230			[2.78]
Texas A&M University	USA/ 2015	Single Auger	Rice Straw	9.2	<2	6	500	150	10		[2.95]
Shanghai Jiao Tong University	China/ 2016	Single Auger	Rice Husk and Corn Stalks	16.7 - 17.6	<10	0.35	350 - 525	50	2.6		[2.75]
Vellore Institute of Technology	India/ 2017	Single Auger	Mesquite Sawdust	8.3 - 15.3	2	10	475 - 525	120	30		[2.75]
Auburn University	USA/ 2010	Single Auger	Pine Wood Chips	5.79	0.6 To 0.84	0.5	425 - 500	-	-		[2.75]

The heating method of the reaction zone is normally done through electrical furnace while the arrangement can be varied. For example, the pyrolyser utilised by Michigan State University uses three 6 separate electrical heaters (3 pairs of heaters) which can be adjusted to have three differentiated heating zones at different temperatures [2.80]. In contrast, the Washington State reactor is heated through a singular furnace [2.75]. Another method for application of heat to the reaction is use of heat carries. For instance, Iowa university uses different heat carriers such as sand and steel shot [2.96]. The carrier is heated prior to entering the auger and is fed into the auger separately.

The products are generally divided into two phases after the reaction: solid and gas. The solid product is collected in a container at the end of the auger while the gashouse product is passed through different types of condensation trains to facilitate the separation of the liquid product (condensable) from it. In most cases, the gas leaves the reactor at the end of the reactor and after the auger has left the heated zone. However, alternative arrangements can be set up. For example, in the STYX plant by Karlsruhe Institute of Technology, the gas is extracted at several point from within the heated zone and sent to the condensation train [2.75]. In the condensation train, one or several condensers are used with several coolants' mediums such as ice bath chilled water.

In addition to the application by researching bodies, several attempts have been being made to commercialise this process. For instance, a single auger system by ABRI-TECH in Canada is capable of processing 25 kg/h and it can be rapidly installed due to skid mountable design [2.97]. Another example would be the PYREC 500 plant (operating since 2009 in Switzerland) which utilises twin screw slow pyrolysing to process 1500 t/y of biomass [2.98]. A more comprehensive list of other applications of auger pyrolysers can be found in the scientific journal titles "Auger reactors for pyrolysis of biomass and wastes" [2.75].

2.5 Wool Properties

Wool is a natural fibre and unlike other natural fibres such as cotton which have homogenous structure, wool has a complex heterogenous structure consists mainly of a protein called keratin. Wool owes most of its properties such as flexibility towards being stretched and shape retaining to this protein structure. Natural wool, however, does have other components (impurities) besides the fibre itself. These impurities which might make up around 40% of raw wool, can range simply from dirt and vegetation debris to wool grease (mainly made of fatty acids and esters [2.99]). These are removed from the wool during the processing stage [2.100].

Table 2-8 compares the elemental composition of keratin (as generalised wool composition) to that of lignocellulosic biomass [2.101, 2.102]. Since the properties of each sample may be slightly different, this table should only be used as a generalised example.

Table 2-8: Wool elemental component

%	Carbon	Hydrogen	Oxygen	Nitrogen	Sulphur
Keratin	50	12	10	25	3
Lignocellulosic	44-53	5-7	40-51	0.1-2	N/A

The processed wool waste presents a C and H content similar to those of lignocellulosic materials, while the high percentage of N content is due to high protein content in the wool waste. From a biochar utilisation perspective, the presence of 12-15% N would make the material as an excellent soil amendment compared to lignocellulosic biochar while it would be detrimental as fuel due to NO_x emission. It is interesting to highlight that previous work indicated that N could be removed from syngas (presented as NH₃) by scrubbing and be re-used for example for growing microalgae or fertiliser production [2.103].

Table 2-9: Natural fibres properties [2.104]

Fibre property	Wood (Pine)	Cotton	Silk	Wool
Specific gravity	0.35- 0.64 [2.105]	1.52	1.34	1.31
Moisture regains (%)	7 [106]*	7.5	10	14-18
Heat of combustion (MJ/kg)	20-22 [2.107]	17	N/A	21

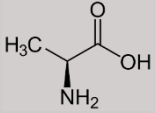
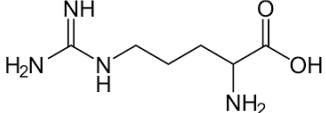
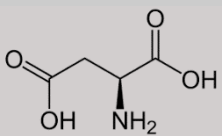
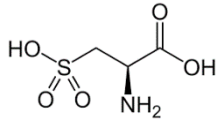
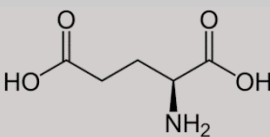
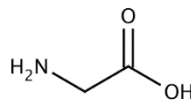
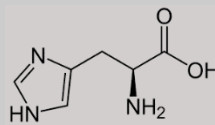
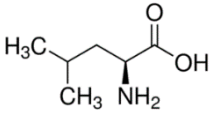
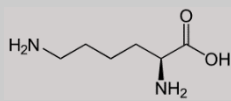
*This value corresponds to the wood moisture content rather than moisture regain

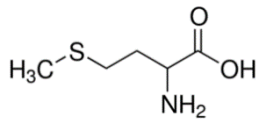
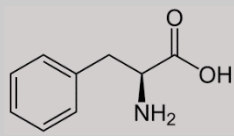
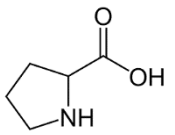
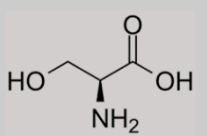
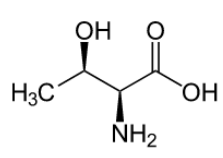
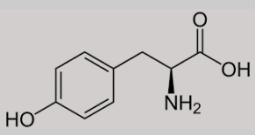
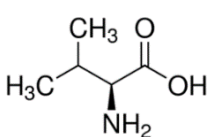
Table 2-9 summarises the properties of wood, wool, and other natural fibres. As it can be observed, the heat of combustion of wool is approximately the same as pine wood which has been the subject of several pyrolysis studies. Therefore, study of wool pyrolysis has high potential. However, the properties of wool are vastly different to that of wood. For instance, the specific gravity of wool is at least double of the wood while the compressibility of shredded/sliced wood and wool are different due to the nature of the materials.

Proteins are made up of amino acids which have amine and carboxyl functional groups in their structure. To ascertain which products are expected from wool thermal decomposition, its constituent amino acids should be considered. Table 2-10 reports the amino acids of two different unprocessed wool samples and the average composition [2.108, 2.16]. It should be noted that the wool amino acid composition can be varied significantly even along a single fibre and large deviations exists between different breeds or even different animals of the same breed [2.99]. Each

of these amino acids have a side chain and can be grouped into polar, non-polar, acidic, and basic based on these side groups. Generally, polar side chains have higher chemical reactivity compared to the non-polar ones [2.99].

Table 2-10 Amino acids of wool

	Sample 1 ($\mu\text{mol/g}$)	Sample 2 ($\mu\text{mol/g}$)	Average ($\mu\text{mol/g}$)	Chemical Structure
Alanine	460	469	465	
Arginine	550	600	575	
Aspartic acid	500	560	530	
Cysteic acid	1000	700	850	
Glutamic acid	980	1049	1015	
Glycine	700	757	729	
Histidine	66	82	74	
Leucine	630	676	653	
Lysine	220	269	245	

Methionine	39	44	42	
Phenylalanine	230	257	244	
Proline	590	522	556	
Serine	920	902	911	
Threonine	550	572	561	
Tyrosine	290	349	320	
Valine	460	486	473	

Hard keratins, i.e., hair and wool, have high concentrations of sulphur which is mainly due to the existence of Cystine. The main reason for lower solubility and higher stability of wool compared to other proteins is the formation of cross-links of disulphide bonds in cystine [2.109]. As illustrated in Figure 2-6, the disulphide cross-links are not the only bonds between peptides (short amino acid chains).

The hydrophobic bond occurs between hydrophobic groups in amino acids like phenylalanine and valine and is a non-covalent one [2.99]. The hydrogen bonds are formed between the carboxyl groups and amino or the CO and NH. The ability of the wool to be combined with acids and alkalis

is due to its amphoteric properties which in turn is the result of approximate equity between acidic carboxyl group and basic amino group in this fibre [2.99]

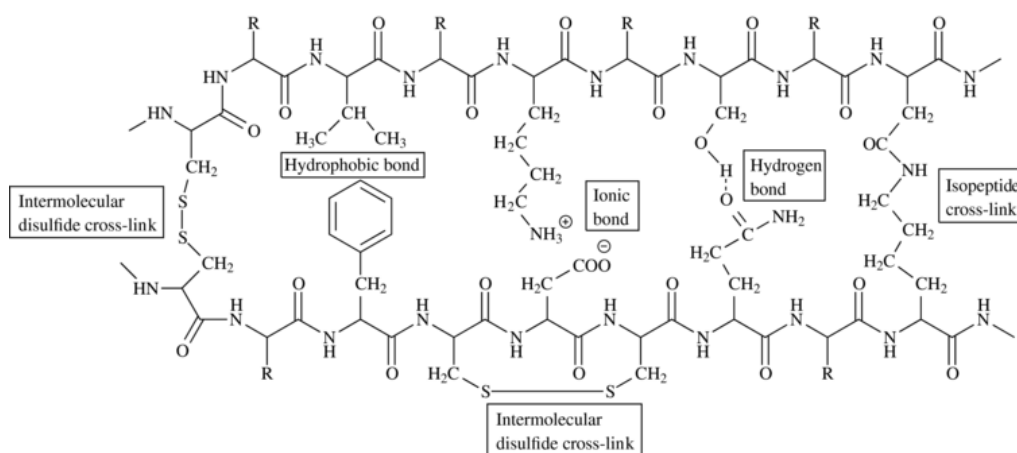


Figure 2-6: Chemical structure of wool [2.111]

Besides proteins, other materials are presented in the wool structure; mainly lipids and small quantities of polysaccharides [2.99]. On a mass basis, the lipids constitute 1% of the wool (Merino wool) [2.110]. Lipids can be divided into 3 main groups: polar, sterols and fatty acids. Palmitic, stearic, oleic and 18- methyleicosanoic acid are the main fatty acids while ceramides, cholesterol sulphate and glycosphingolipids are the main sterols [2.110].

2.5.1 Textile Dyes Review

The properties of raw wool were discussed in the previous section. However, the application of dyes on wools for use, for example in fashion industry, changes the properties of the wool. Therefore, the study of the textile dyes was deemed essential. The main types of textile dyes are reviewed in this section.

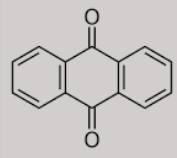
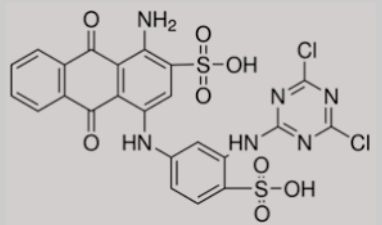
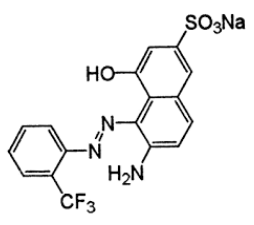
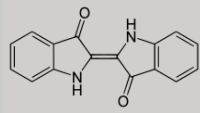
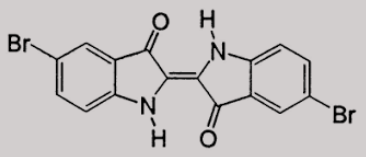
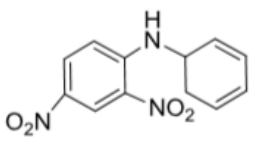
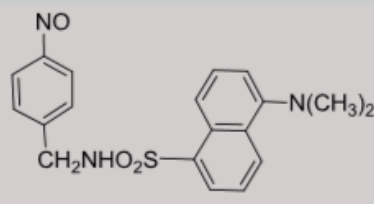
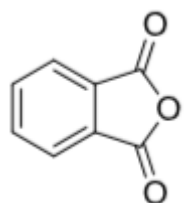
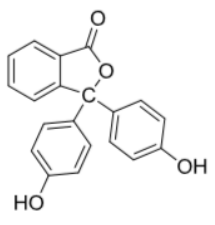
Dyes exhibit colours for the following four reasons and lack of one of these features can eliminate this property of dyes [2.112]

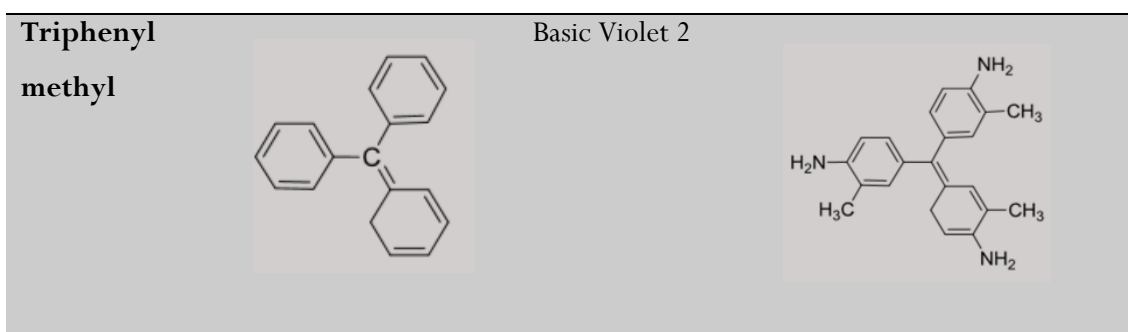
- › Absorption of light visible spectrum
- › Electron resonance
- › Alternating single and double bond structure
- › Existence of a minimum of one colour bearing group called chromophore

A list of know dyes is produced and updated regularly by the Colour Index International and each colorant is given Colour Index (CI). According to chemical type, dyes belong to 25 structural classes based on the CI [2.113]. Chromophores are responsible for these colours and 7 of them are

presented in Table 2-11. It should be noted that chromophores exist as results in a colour when they are part of conjugated group rather than on their own [2.112].

Table 2-11: Dye classification based on chromophores [2.114]

Class	Chromophore	Example Colour	Example Structure
Anthraquinone		Reactive Blue 4	
Azo	$-N=N-$	Acid Red 337	
Indigoid		C.I. Vat Blue 35	
Nitro	$-N=O$	Disperse Yellow 14	
Nitroso	$-N=O$	Fluorescent-labelled nitroso	
Phthalein		Phenolphthalein	



In addition to chromophores, most dyes contain another component which can affect the solubility of dye or shift the colour of the dye while not being responsible for the colour of dyes. These are called auxochromes and some examples of them are sulphonic acid, amino, carboxylic acid, and hydroxyl group [2.112].

Another categorisation method can be based on the chemical structure. Table 2-12 lists the class of dyes based on this categorisation [2.114, 2.115, 2.116]. Furthermore, the main application of the dyes in addition to a summarised description on the behaviour of the class is given.

Table 2-12: Dye classes and their description/application [2.114, 2.115, 2.116, 2.117, 2.118]

Class	Description/Notes	Application
Azoic	<ul style="list-style-type: none"> > Contains Azo group > Ingrain¹ > largest class of synthetic dyes 	<ul style="list-style-type: none"> > Cellulosic
Vat	<ul style="list-style-type: none"> > Name refers to the preparation method > water insoluble > readymade > Cannot be directly applied to textile 	<ul style="list-style-type: none"> > Cellulosic (cotton, linen) > Viscose
Reactive	<ul style="list-style-type: none"> > Dye chemically reacts with the textile > Form covalent bond with the substrate > Water soluble 	<ul style="list-style-type: none"> > Wool (other animal fibres) > Cellulosic (cotton) - rarely > Nylon
Sulphur	<ul style="list-style-type: none"> > Water insoluble > Can become soluble by use sodium sulphide > Dying is done under high temperature, and large quantities of salt > 	<ul style="list-style-type: none"> > Cellulosic (cotton, linen)
Disperse	<ul style="list-style-type: none"> > Dye available as paste or powder > Dye is dispersed into water for the colouring procedure (dissolved in fibre) > Water insoluble > Require additional steps such as heat, pressure, and dye carrier to be applied 	<ul style="list-style-type: none"> > Synthetics (Polyester, polyamides)
Direct	<ul style="list-style-type: none"> > Named due to capability to be directly applied (to cellulosic textile (no requirement for affixing agent) > Water soluble 	<ul style="list-style-type: none"> > Rayon > Cellulosic (cotton, linen)

	> Anionic	
Acidic	> Water soluble	> Wool (other protein fibres)
	> Anionic	
	> Na salt of sulphuric acid	> Polyamides
	> Direct affinity towards protein fibres	
Basic	> Water soluble	> Polyester
	> Normally used with a mordant ²	> Acrylic
	> Bright dyes	
	> Normally used as after treatment for already dyed textile	

1 Two chemical components react (either on the surface or within the fibre) to form the dye – dye is produced during the dyeing process inside the fibre [2.119]

2 Chemical agent which by forming insoluble compound with the dye, sets dye on the textile [2.117] [2.118]

As illustrated in Table 2-12, acidic and reactive dyes are the main classes applied to wool. Commercial wool dyeing is normally done through aqueous acid solutions via batch method with the ratio of wool to liquor being anything between 1:10 to 1:60 [2.99].

Reactive dyes normally have a molecular weight of 500 to 900 g/mol and contain a sulphonic acid group. Furthermore, they side chain of amino acids in wool (for example hydroxyl group, amino and thiol) can form covalent bonds with these dyes [2.99].

Another dye class used for wool is acidic dye. There are several reasons for which wool uptake acidic dyes. These are listed below [2.99]:

- > The electrostatic interactions of dye anions (negatively charged) and wool amino groups (passively charged); more dominant in case of lower molecular weight dyes – Important for attraction of dyes to the surface of the fibre
- > Van der Waal's forces; more dominant in case of higher molecular weight dyes
- > Interaction of wool fibre hydrophobic (as a result of non-polar side of amino acids) with hydrophobic parts of dye; more dominant with higher molecular weight dyes
- > Hydrogen bonds

Acid dyes themselves can be categorised into three groups based on their dyeing behaviour [2.120]:

- > Levelling; Low molecular weight (300-400 g/mol) [2.99]. Poor fastness to washing since dye molecules can migrate in and out of the wool fibre; normally used for pale and bright shades [2.121].
- > Milling; wool is treated with weak alkaline solution coupled with mechanical action. Higher molecular weight (600-900 g/mol) compared to levelling type [2.99]; also, less water soluble due to having fewer sulphonate groups. Bonding to the fibre is through ionic and intermolecular forces [2.122]. Generally, the aromatic ring has a hydrophobic side chain (e.g., dodecyl group) [2.99].

- › Super milling: similar to milling type, however due to the presence of long chain alkyl groups, they show more hydrophobic behaviour [2.122].

2.6 Model Compounds

In order to study the effect of thermo-chemical processes on wool in a more isolated manner, it was decided to study model compounds representing the properties of wool closely. Representing the proteins in wool, one of the amino acids with the broadest functional groups was selected. In other words, one which could represent not only the carboxylic acid group, but also aromatics. Looking at the most abundant amino acids in Table 2-10, cysteic acid contains sulphur, which is an undesirable element, and attempts should be made to remove it from the potential products. Coming down the table, most of the substance either just have one or double carboxylic acid groups and no other functional group. Two of the compounds which are except from this are phenylalanine and tyrosine, which have a benzene ring included in their structure. Either of these components could have therefore been a good choice for a model compound representing wool. Phenylalanine was selected as the optimum and final choice in order to keep the model compound as simple as possible. This way, analyses of the reaction would have been carried out more accurately while having all the required functional groups presented in analyses.

There has not been as extensive of a range of studies on phenylalanine pyrolysis compared to lignocellulosic model compounds. Most of the studies had been on pyrolysis of phenylalanine in tobacco due to the phenylalanine being a key element in tobacco. Studies have mostly been carried out in conditions ranging from 450 to 950°C [2.123, 2.124]. They agree on a mostly similar pathway for phenylalanine pyrolysis where difference in the order of the reactions and occurrence of the secondary and side reactions are determinant in the final product distribution.

The process could include decarboxylation whereby separation of the carboxyl group, nitrile amides are formed. Alternatively, cinnamic acid could be initially formed by the removal of the amine group (deamination). The intermediates produced from the above processes, are then further reacted and reformed (Figure 2-7). Paterson (1972) [2.123] isolated the products obtained from both paths and concluded that the decarboxylation paths is the dominant one with the deamination path having a limited degree of effect.

Following either of the steps, decarboxylation or deamination, production of the NH_3 and CO_2 are expected in the gas product. Also, depending on the temperature of the process, some CO , N_2 and H_2 are going to end up in the gas. For instance, carbon dioxide can shift to CO depending on the temperature of the system and availability of hydrogen. Similarly, ammonia can be converted to N_2 and H_2 if temperature gets close to 600°C [2.123]. Finally, formation of HCN in the gas is expected as the result of decarboxylation path.

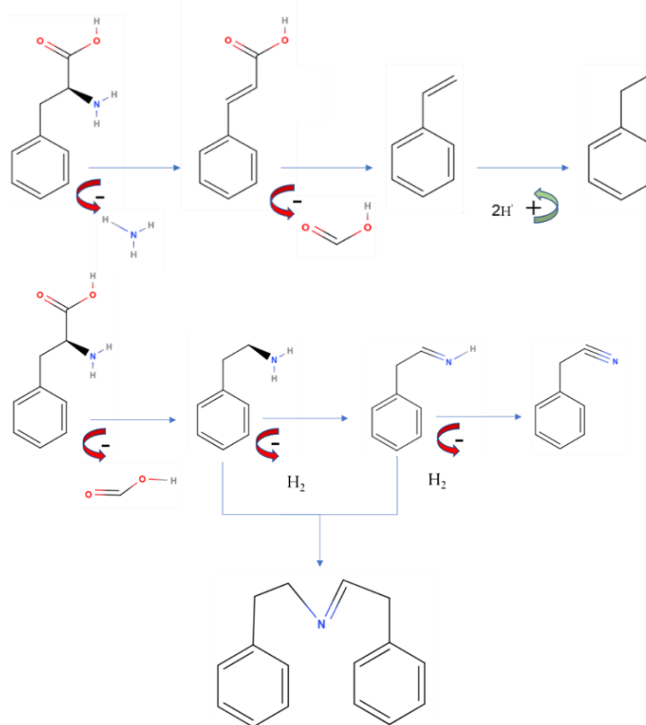


Figure 2-7: Phenylalanine decarboxylation (bottom) and deamination (top) path

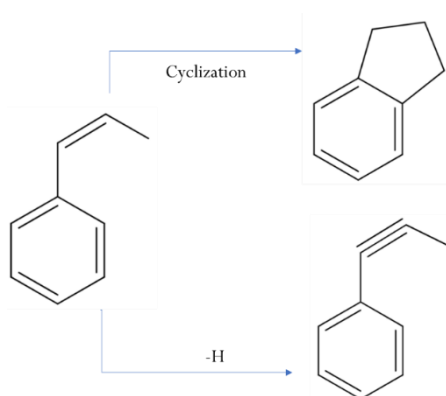


Figure 2-8: Competition of paths in phenylalanine decomposition example

There are two other mechanisms by which the pyrolysis products of phenylalanine are formed: homolyses and cyclization. During homolyses, molecules are dissociated into radicals, which then can later react to form other substances. This process is more likely to remove the carbon

compounds under high temperatures [2.124]. In fact, the decarboxylation and deamination process are both dependant on an initial homolyses of the feed. One of the processes through which these radicals can react is cyclization. The paths taken are most likely to compete when forming new compounds and the aim should be to facilitate conditions under which the desired product is favourable (Example in Figure 2-8). The effect of the catalysts in the product formation and distribution is discussed in the results chapter (Chapter 5).

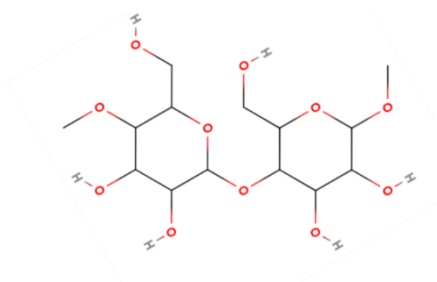


Figure 2-9: Cellulose Structure

In addition to protein, the processed wool waste normally also contains cotton due to the stitching or existence of mixed fibre for tailoring purposes. Therefore, a model compound representing cotton waste needed to be studied alongside phenylalanine. Cellulose which is formed in bundles of fibres attached together strongly and is composed of D-glucose polymers [2.125], was selected to do this representation since it forms around 90% of cotton fibre [2.126].

Cellulose, a polysaccharide, has its monomer constructed from two glucopyranose unites as illustrated in Figure 2-9. Based on the data in the literature, the main decomposition of cellulose starts from 300°C and if the temperature is increased to 370°C, a weight loss of 70% could be expected, which is mainly composed of condensable vapours [2.127, 2.128]. As the temperature goes higher than the 400°C thresholds, the higher the chance of aromatic formation becomes [2.129].

The first step reaction at low temperatures, below 300°C, mainly will lead to generation of intermediates called anhydro-cellulose which will react further to make other substances [2.130]. Additionally, as expected, water will be lost at low temperatures, which can affect the final products by facilitating benzene formation through making a good condition for generation of carbon-to-carbon unsaturated bonds [2.131].

As the temperature increases to around 400°C, the depolymerisation gets further promoted and compounds such as levoglucose and levoglucosenone, generally anhydro-saccharides, are formed. [2.132]. Similar to phenylalanine, these products will undergo secondary processes to generate

secondary products. Figure 2-10 illustrates the steps involved during pyrolysis of cellulose at different temperatures.

Finally, in order to compare the textile waste and its representing model compounds with lignocellulosic biomass which has been studied extensively, lignin was selected to be analysed under the same pyrolysis conditions. Lignin, a complex polymer, is made up of 3 phenylpropane cross chains, coniferyl alcohol, sinapyl alcohol, and coumaryl alcohol (Figure 2-11), for which the amount of each of them in the lignin is dependent on the source feed is obtained.

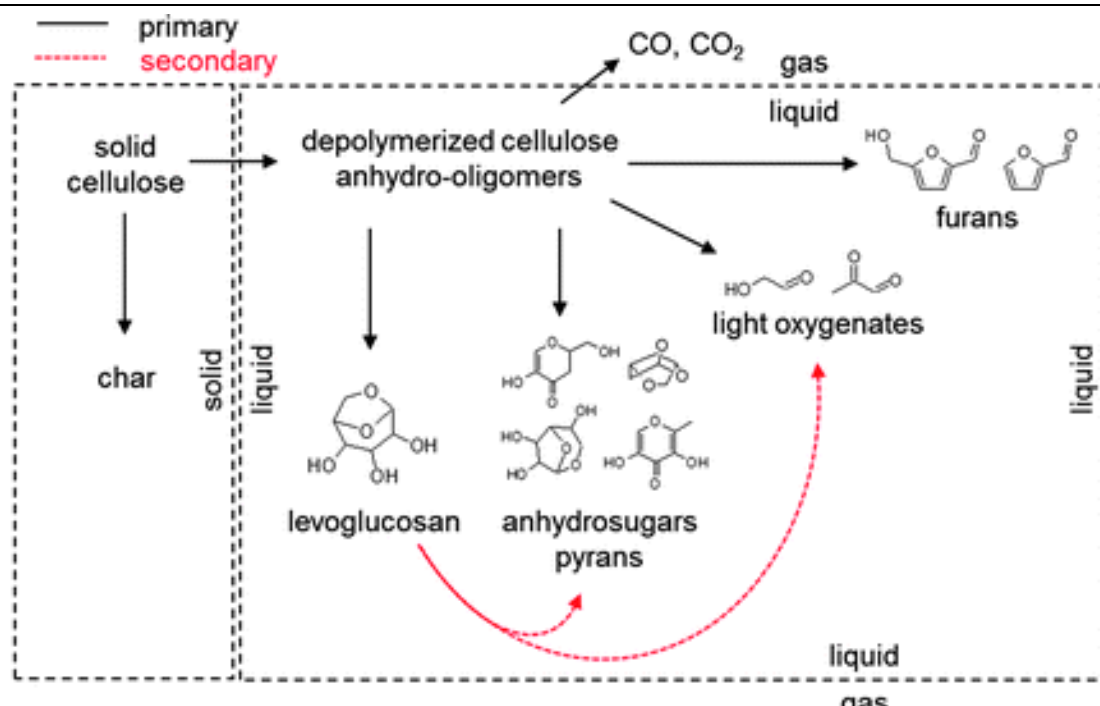


Figure 2-10: Cellulose decomposition path [2.71]

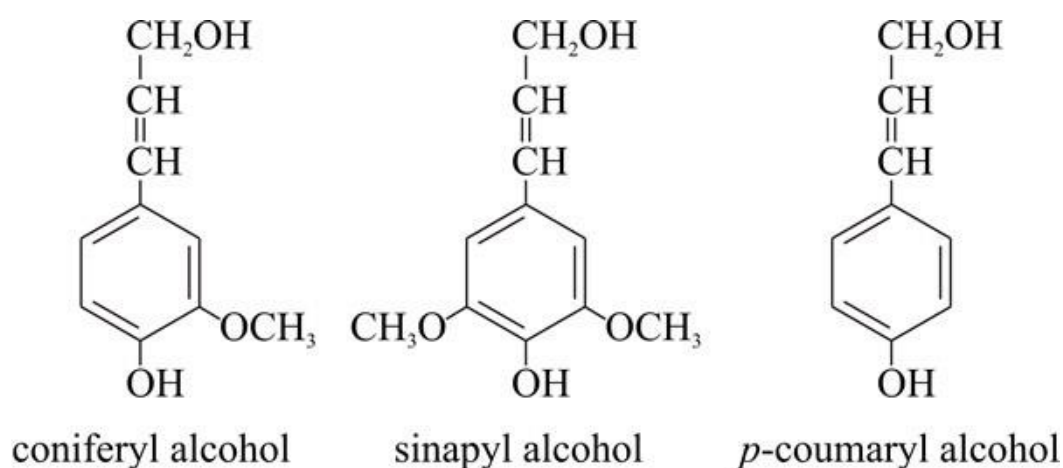


Figure 2-11: Major phenylpropanes in lignin structure [2.72]

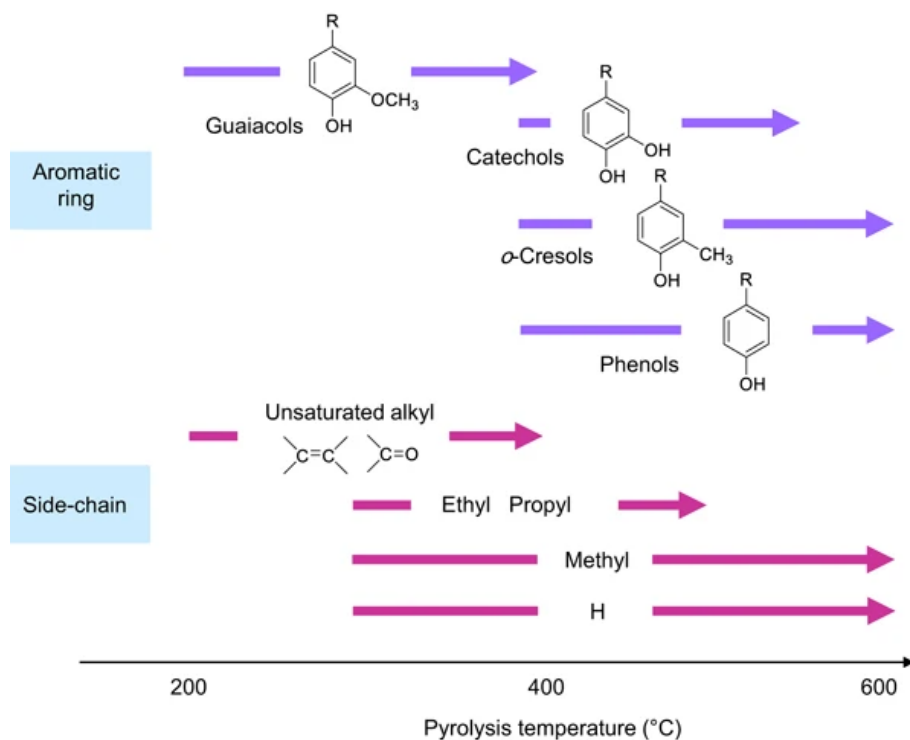


Figure 2-12: Lignin decomposing path [2.190]

Due to the complexity of the molecule, the initial decomposition temperature can have a wide range, typically between 200 to 450°C [2.133]. The initially decomposed compounds are expected to be mostly uncondensable low molecular weight compounds resulting from the breaking of the weak propyl chains between the monomers [2.134]. At lower temperature, around 180 °C, the hydroxyl group at the end of the chains are released and dehydration will occur. Since the benzene chains within the structure of the lignin are stable, therefore, more complex aromatic compounds resulting from linkage between these rings are expected. As mentioned, the pyrolysis path of lignin can be complex. For instance, Figure 2-12 illustrates the temperature dependency of product distribution during lignin pyrolysis for aromatic side chains.

2.7 Catalysts

Even though pyrolysis without the use of heterogeneous catalyst can lead to products with superiority over the ones obtained from petroleum, there are some important processing difficulties that outweigh the advantages. For instance, the bio-oil retains the energy content of the original feedstock to a degree while withholding less nitrogen and sulphur compared to the petroleum product [2.135]. But, having an oxygen content of around 40 wt% makes this unstable for the conventional storage processes due to the existence of unsaturated compounds [2.136]. Additionally, several other issues such as high viscosity, low heating value, strong corrosiveness and more importantly, the complex composition of the oil should be considered and solved prior to

integration into conventional facilities. Similar to petroleum refining where catalysts can be used to influence the types of product obtained from the process of cracking, catalysts, either in-situ or ex-situ, can be utilised to overcome the issues in bio-oil processing. Therefore, catalysts should have been screened for their capability of converting model compounds, which replicate textile properties, to char and non-condensable gases. The use of model compounds for screening with catalysts was preferred over the utilisation of solid biomass (wool) since using a solid biomass with a standard and unique composition was not realistically possible. For instance, the ash content of the biomass can play the role of catalyst itself while some constituent of the biomass can change the composition of final product [2.137].

2.7.1 Catalysts Basics

Catalysts are generally used during reactions to either reduce the activation energy or change the path of reaction mechanism, without the catalyst itself being consumed. When the activation energy is targeted, the temperature at which the reaction takes place can be lowered. Therefore, less energy is consumed. By using catalysts which target the reaction path, the products of the reaction can be modified.

Depending on the physical state of the catalysts and reactants, catalytic reaction can be divided into heterogeneous and homogeneous ones. In other words, if the catalyst and the reactants are presented in the same phase, a homogeneous reaction will take place. If they are presented in a different phase (e.g., solid catalyst and gas reactant), a heterogeneous reaction will happen. Normally, in the heterogeneous catalytic reactions, the reaction happens at the surface of the reactant. More specifically, the reactant molecules are adsorbed on the surface of the catalysts (the pores on the catalyst) prior to the reaction taking place. For this reason, the average size of pores and their area/volume, and therefore the overall available surface area for reaction is a key factor in the effectiveness of the catalysts and should be factored in when selecting an optimal catalyst for a reaction.

Another important categorisation of the catalysts could be based on base/acidity of the catalysts. Acid/base catalyses could be described in terms of Bronsted-Lowry and Lewis theory.

In the Bronsted-Lowry theory, an acid is described as any species which is capable of donating a proton, while a base is any species capable of receiving a proton. Meaning, the chemical structure of a Bronsted acid has a hydrogen that can be separated. In contrast, Bronsted base should contain at least one lone pair of electrons to accept a proton and consequently forming a new bond. In other words, a Bronsted acid is any species that can donate a proton (H^+ ion) while a Bronsted base is any

species which can accept a proton. Lewis Theory could be considered complimentary to Bronsted theory. In detail, a Lewis acid is an electron acceptor while a Lewis base is an electron donor.

Heterogeneous catalysts are generally made up of three parts: active phase, support (carrier) and the promotor. The active site of the catalyst which only makes up a limited weight percentage of the catalyst is where the principal chemical reaction takes place [2.138]. Several characteristics of the active site such as distribution on the support, particle size, electivity, purity, and type (metals, semiconductors, insulators) are determinant in the behaviour of the catalyst [2.139]. Catalyst supports could be made of clay, carbons or oxides which can withstand high temperatures such as silica and alumina.

The support's main function is to improve the accessibility of active phase to the reactants. Therefore, the support should have high surface area and proper pore size distribution. Also, maintaining this high surface area over time and resistance to poisoning is an important criterion when choosing the support. Therefore, the chosen material should be mechanically stable. Finally, promoters are added to the catalyst to improve its effect in a reaction. While normally not catalytic in their nature, they can interact with the active phase of the catalyst to modify the products of the reaction.

Since 1950s, heterogeneous acidic catalysts have been the main choice in petrochemical industry and therefore have been studied extensively. This success has been to their capability of cracking facilitated by their acidity [2.140]. These reasons have been complimented by other favourable properties of heterogeneous catalysts such as recyclability and easy removal. This proven record and the fact that one of the main goals of this study was the integration capability of the textile waste products in the current refinery systems, it was decided to use heterogeneous catalysts.

2.7.2 Catalysts Selection

When selecting the catalysts, factors such as surface area, acidity/basicity, pore size and pore size distribution are important. The surface area will determine the total area available for the collision and therefore the cracking, while the physical dimensions of the pore will determine the ease of access for materials to proceed through and the level of cracking that is undergone. Meanwhile, the pore size distribution is an important factor to determine the efficiency of transportation of reactants and products to and from the catalyst's active sites.

Zeolites have long been utilised for catalytic cracking processes and as sorbents [2.141]. They are a favourable catalyst material due to their shape selectivity and acidic properties [2.142]. The presence of 10-membered rings with a three-dimensional structure combined with medium pore sizes [2.143] of ZSM5 makes it one of the best performers when it comes to aromatics production [2.144, 2.145] (Figure 2-13).

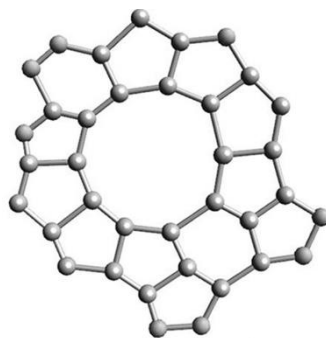


Figure 2-13: Structure of ZSM5 [1.179]

In IUPAC nomenclature, catalysts are categorised into 3 separate groups based on their pore size: Macro porous (>50 nm), Mesoporous (2-50 nm) and microporous (<2 nm). In glucose pyrolysis, it has been shown that small pore zeolites such as ZK-5 contribute towards producing CO and CO₂ as their main product and the aromatic generation capability of large pore size zeolites such as SSZ-55 is hindered by production of high yield of coke [2.145]. Additionally, the specific ring structure of ZSM5 can avoid the occurrence of unfavourable side reactions which leads to higher aromatic production [2.146]. Shirazi et al [2.147] found that altering the silicon to aluminium ratio (Si/Al) in zeolites affected the Brunauer-Emmett-Teller (BET) surface area and crystal size. It was found that as the ratio was increased from 10 to 50, the BET surface area increased from 355 to 392 m²/g and the crystal size also increased from 1 to 9 μm. Shirazi also investigated the effect of the molar ratio on the acidity of the zeolite by means of ammonia temperature programmed desorption (NH₃-TPD) for the evaluation of the ZSM-5 acidity. Bronsted acid sites are formed by aluminium atoms connected to silicon by a so-called “bridging hydroxyl” where the negative charge generated is compensated for by a proton. This site is believed to be the main catalytic centre [2.147]. Lewis’s acid sites are instead composed of aluminium with low coordination or Si⁺ ions formed from dehydroxylation in the thermal treatment at T > 500°C. These sites are also of importance in many catalytic processes (i.e., Friedel-Crafts reactions), acting as an electron pair acceptor and thereby giving rise to charge transfer processes. The acidity of a zeolite is therefore related to its aluminium content, and one expects a linear increase in the overall acidity with increasing aluminium content in the zeolite [2.148]. This measures the temperature required for an adsorbed molecule to desorb from the surface. Measuring across the same molar ratio from 10 to 50, this yielded a decrease in

acidity of the zeolite. They found evidence of aluminium in extra-framework positions as the ratio decreased. Rodriguez-González et al. also studied the properties of ZSM5 [2.148] by means of NH₃-TPD and nuclear magnetic resonance (Al-MAS-NMR) spectroscopy. They had consistent findings with Shirazi et al. that the NH₃-TPD profile had two desorption peaks, which indicated acid sites of different strength. This work indicated that the lower the Si/Al ratio, the more acidic the sample is. This shows that acidity is directly proportional to the aluminium content of the catalyst. They concluded that a Bronsted site would be the main catalytic zone for the particle, approximating that 72% of aluminium atoms were Bronsted acid sites.

For zeolite catalysts, it seems that both the surface area and acidity are dictated by the Si/Al ratio. The acidity of the sample increases linearly with the aluminium content [2.149] and according to the findings of Shirazi et al, the surface area increases linearly with increasing the Si/Al ratio [2.147]. Due to this variation in performance by manipulating the Si/Al ration, it was decided to test three ZSM5 catalysts with three Si/Al ratios; namely 20-ZSM5, 30-ZSM5 and 60-ZSM5 to find the optimal one for conversion of model compounds representing the textile waste and textile waste itself.

Despite the fact that catalysts such as ZSM5 have been intensely investigated for the catalytic pyrolysis of biomass [2.150], mesoporous silicates such as KIL-2 (Kemijski Institute Ljubljana) have received much less attention [2.151, 2.152]. Additionally, microporous zeolite can have limitations when it comes to converting large molecules due to the size of pores. Therefore, to test the effect of increasing the pore size of the catalysts on improving the diffusion of reactant molecules on the active site of the catalysts, it was decided to use mesoporous catalysts.

Produced in Ljubljana at 2010, KIL-2 is a relatively novel mesostructured wormhole silicate support with interparticle and textural porosity [2.153]. Due to the novelty of KIL2, number of researches and experiments were limited on it. Popova et.al. used KIL2 impregnated with different quantities of ZrO₂ and sulphates to vary the acidity (both strength and type) of the catalysts for catalytic esterification of glycerol with acetic acid [2.154]. Compared to pure zirconia, KIL2 supported zirconia proven to be more active and efficient for esterification reaction.

In another research, Popova et.al. compared Co/KIL2 with Co/SBA15 during oxidation of toluene. It was concluded that the interparticle mesa porosity of KIL2 made it an effective catalyst for removal toluene in gas phase. It was also concluded that compared to the SBA15, the lower cost, stability, and high catalytic activity of KIL2 made it a catalyst with higher potential to remove the volatile organic compounds [2.155].

Due to the high surface area of it and hydrophilic properties, KIL2 has also been used for sorbent. For instance, FeKIL2 with a surface area of 712 m²/g was used as part of two component composite for sorption-based solar energy storage [2.156].

The mentioned properties such as low cost, high surface area, efficiency in removal of volatile and the capability of being functionalised by metals, made KIL2 a promising support for catalysed biomass conversion. Therefore, two different KIL-2 based catalysts, one loaded with aluminium (Al-KIL2) and one loaded with lithium (Li-KIL2) were included in the testes to allow a comparison between acidity and alkalinity using the KIL-2 catalysts, with lithium being basic.

The final list of the catalyst which were used in the experiments are therefore as below:

- › Al-KIL2
- › Li-KIL2
- › 20-ZSM5
- › 30-ZSM5
- › 60-ZSM5

2.8 Model Compounds and Biomass Catalytic Pyrolysis

In section 2.4, some of the applications of auger reactors for pyrolysis of biomass were reviewed. In this section, the applications of catalytic pyrolysis on the selected model compounds in addition to catalytic pyrolysis of biomass are reviewed.

While work on catalytic pyrolysis of phenylalanine has been limited, studies on other amino acids could be found. Furthermore, numerous studies have been carried out on lignocellulosic model compounds (cellulose and lignin) catalytic pyrolysis. However, since the full account for all of these studies would have been exhaustive and out of the scope of this work, Table 2-13 only lists some examples of these studies alongside a short summary of what has been carried out in addition to the observation on the effects of the catalyst application.

Table 2-13: Examples of catalytic pyrolysis of model compounds

Model Compound	Catalyst	Summary of Work/ Effect of Catalyst	Year	Ref.
Cellulose	Zn/ZSM-5 FePO ₄	› The most dominant groups in the bio-oil were levoglucosenone › Bronsted and Lewis acid sites promoted the production of furans in the bio-oil	2015	[2.156]

Cellulose	HZSM-5	› Catalyst decreased the gas by-product while increasing the liquid and char	2010	[2.157]
Cellulose	Al-MCM-4, Ce-Al-MCM-41	› The mesoporous catalyst decreased the liquid and char while increasing the gas › Broke long chain carbons to low-carbon chains › More toluene and 2 methoxy-phenol production in catalytic runs	2012	[2.158]
Cellulose	Ce _{0.8} Zr _{0.2} -xAl _x O ₂	› Catalyst facilitates production of aromatics under 400-550°C › Furan is promoted at lower temperature of less than 350°C › Higher acidity catalyst promoted the generation of toluene and benzene	2020	[2.159]
Cellulose	CaO, MCM-41, ZSM-5, and SAPO-34	› ZSM5 was the most effective catalyst for formation of light olefins › With the combination of 85% ZSM-5 and 15% CaO, the highest yield of light olefins was obtained	2019	[2.160]
Cellulose*	ZSM-5	› ZSM-5 increased the yield of bio-oil › The nitrogen-containing components and acids were reduced significantly via use of the catalyst › Furan and ketone generation was promoted through use of catalyst	2018	[2.161]
Cellulose	HZSM-5	› The catalysts utilised were metal modified (Fe and Ga) › Ga improved aromatic production while Fe had the opposite effect › Both catalysts favoured production of monoaromatics over polyaromatics	2018	[2.162]
Cellulose	SAPO Type	› SAPO catalysts promoted production of furans while reducing sugar content	2018	[2.163]

		<ul style="list-style-type: none"> › The SAPO catalysts with milder acidity favoured furan generation. › Optimum temperature for furan generation with SAPO catalysts was deemed to be 500 to 600 °C 		
Cellulose	Al ₂ O ₃	<ul style="list-style-type: none"> › Effect of pyrolysis temperature and ratio of catalyst to cellulose on product distribution was evaluated under ammonia atmosphere › At 400 °C and cellulose to catalyst ratio of 0.5, carbon yield of nitrogen containing compounds was 9.7% 	2017	[2.164]
Cellulose	TiO ₂ , ZSM-5	<ul style="list-style-type: none"> › Main product of non-catalytic runs was levoglucosan › With use of the TiO₂ at 500 °C (in-situ), production of levoglucosan was reduced and new aromatics such as toluene, benzene and naphthalene were introduced › Under the same conditions as above, use of ZSM-5 oxygenated compounds such as benzofuran, acetone and furan were observed with low yield › For the ex-situ runs, catalysts were comparable regarding the production of aromatics 	2020	[2.165]
Hydrolysis Lignin	Zeolite X, Zeolite Y, ZSM-5	<ul style="list-style-type: none"> › Bronsted acid sites played an important role in breaking and deoxygenating of the pyrolysis vapour products to phenolics and monoaromatics › The best condition was at 450°C and with ZSM-5, yielding 57.4 wt% of oil 	2018	[2.166]
Milled wood lignin	HZSM-5	<ul style="list-style-type: none"> › Different Si/Al mole ratio ZSM-5 was used 	2015	[2.167]

		<ul style="list-style-type: none"> › Toluene, benzene, and p-xylene were the main aromatic products › Other catalytic pyrolysis was phenolics › The HZSM-5 acidity was inversely proportional to the ratio of Si/Al ratio while the formation of aromatics was directly proportional to acidity › Aromatics increased by increasing the pyrolysis temperature (up to 700 °C was tested) 		
Kraft Lignin	ZSM-5	<ul style="list-style-type: none"> › Microporous, nano porous and mesoporous ZSM-5 were studied › Pyrolysis carried out between 400 to 600 °C in a fixed bed › Conventional ZSM5 (microporous) showed more selectivity towards monoaromatics › Mesoporous and nano-porous ZSM-5 demonstrated high selectivity towards alkyl phenols › Highest production of coke, water, and non-condensable gases through use of nano-porous ZSM-5 	2018	[2.168]
Corn Straw Lignin	TiO ₂ (with loaded Fe, Cu, Mo)	<ul style="list-style-type: none"> › Catalysis carried out at 350-650°C in a fixed bed › With TiO₂, the selectivity for phenols reached 86% › Fe and Cu decreased the yield and selectivity for phenols while an increase in aromatic ketones was observed › The Mo addition increased the yield and selectivity of phenols 	2019	[2.169]
Kraft Lignin	HZSM-5, Y-Zeolite, Pd/C	<ul style="list-style-type: none"> › The pyrolysis over acidic catalysts favoured production of aromatic 	2015	[2.170]

		hydrocarbons, specially one to three ringed ones, coupled with deoxygenated phenolic structures		
		› Comparing catalytic and non-catalytic runs, only Y-zeolite caused a significant difference in product distribution		
Leucine, Proline	ZSM-5	› Catalytic pyrolysis was carried out in a micro-furnace at 650 °C	2016	[2.171]
		› The simple structure of leucine resulted in hydrocarbon due to easier detachment of ammonia		
		› Larger nitrogen containing heterocyclic compounds were found in proline due the cyclic nitrogen structure of the model compound (the char contained 28% of the original nitrogen in it compared to the 4.3% in the leucine char)		
		› Decarboxylation to CO ₂ seemed to be the favoured in the un-catalytic runs while decarbonylation to CO was the main pathway for catalytic runs		
		› Product distribution was highly dependent on the chemical structure of model compound		
Phenylalanine, leucine, proline, aspartic acid	HZSM-5	› Drop quartz reactor was used at 500 °C	2018	[2.172]
		› The increase in temperature favoured conversion of nitrogen to NH ₃		
		› Phenylalanine (containing aromatic group) and leucine (saturated side chain) promoted NH ₃ and aromatic generation		

- › In case of nitrogen ring amino acids (proline), the coking of catalyst caused by generation of nitrogen containing heterocyclic compounds reduced the cracking effectivity of the catalyst

*Cellulose was co-pyrolysed with microalgal polysaccharides

Numerous research studies have been carried out on the effect of catalyst pyrolysis on conversion of lignocellulosic biomass. However, limited data could be found on catalytic pyrolysis of wool biomass. Table 2-14 lists some examples of the application of the catalysts on biomass alongside the effect of variation in pyrolysis conditions on product distribution.

Table 2-14: Examples on biomass pyrolysis and effect of catalyst on product distribution [2.174, 2.175]

Biomass	Catalyst	Reactor Type	T (°C)	RT (s)	Oil (%)	Gas (%)	Solids (%)	Ref.
Cotton Stalk	HZSM-5	Fixed Bed	600	-	56	19	19	[2.176]
Sugarcane	La/HZSM-5	Fixed Bed	600	10	3.8	57	21.7	[2.177]
Soybean Straw & Soap stock	ZSM-5	Microwave Oven	550	-	49	28	29	[2.178]
Rice Husk	La/HZSM-5	Fixed Bed	600	10	4.0	53.5	20.4	[2.177]
Rape straw	HZSM-5	Fixed Bed	500	-	32	39	29	[2.179]
Sawdust	La/HZSM-5	Fixed Bed	600	10	4.8	40.8	31.3	[2.178]
Pine	H-Beta	Fluidised Bed	450	-	28.9	49.4	21.7	[2.179]
Pine Wood	ZSM-5	Auger Reactor	500	2	50.3	26.2	13.6	[2.180]
Corn Stover	ZSM-5	Microwave Oven	550	-	36.5	35.2	28.3	[2.181]
Beech Wood	Al-MCM-41	Fixed bed	500	4.5	48.4	7.5	37.4	[2.182]
Rice Husk	ZnO	Fixed Bed	550	-	47.0	21.4	31.6	[2.183]

Rice Husk	ZSM-5	Fixed Bed	490-540	0.0 1	38.3	19.5	42.3	[2.184]
Rice Husk	AL-MCM-41	Fixed Bed	490-540	0.0 1	40.0	18.8	43.2	[2.184]
Poplar Wood	HZSM-5	Fluidised Bed	425-450	3	32.8	46.8	20.3	[2.185]
Canadian Pinewood	α -Al ₂ O ₃	Fixed Bed	450	-	61.5	10.5	17.6	[2.186]
Pine Sawdust	ZnO	Fluidised Bed	400	-	57	20	12	[2.187]
Ferula orientalis L. Stalks	ZnO	Fixed bed	500	-	45.2	30.5	24.3	[2.188]
White Pine	Na ₂ CO ₃ / γ -Al ₂ O ₃	Fixed Bed	500	4	37	23	19	[2.189]

Note: RT stands for Residence Time

2.9 Summary & Conclusion

In this chapter, the issues regarding the increase in production of textile waste and its potential to be used as a renewable source of energy in addition to generation of other useful by-products were reviewed. Afterwards, methods through which these objectives could be achieved were listed and briefly explained. This was carried out through reviewing other researches and commercial applications of biomass pyrolysis. Consequently, pyrolysis through fixed bed reactor followed by scaling up with use of auger pyrolyser was suggested to be taken forward.

It was decided to use wool as the biomass feedstock for the pyrolysis. To understand the path through which pyrolysis takes place, three model compounds, namely cellulose, lignin and phenylalanine were selected. To potentially improve/alter the quality of the bio-oil obtain, the use of catalyst was suggested, and it was decided to use three ZSM-5 (20-ZSM5, 30-ZSM5 and 60-ZSM5) and two KIL2 (Al-KIL2 and Li-KIL2) catalysts.

2.10 References

- [2.1] European Commission, "Commission proposes strategies for sustainable bioeconomy in Europe," Brussels, 2012.
- [2.2] I. Lewandowski, "Bioeconomy, Shaping the Transition to a Sustainable, Biobased Economy," Stuttgart: Springer, 2018, p. 80.
- [2.3] J.Sanchez, M.D. Curt, N. Robert, J. Fernandez, "Biomass Resources," in *The Role of Bioenergy in the Emerging Bioeconomy*, Madrid, Elsevier, pp. 25-111, 2019
- [2.4] OECD, "OECD Agricultural Outlook," OECD Publications, Paris, 2002.
- [2.5] EEA, "Environmental Indicators Report," 2014.
- [2.6] K. Fletcher, Mathilda Tham, "Other Fashion Systems," in *Routledge Handbook of Sustainability and Fashion*, 2015.
- [2.7] Wrap, "Measuring the Active Life of Clothes," 2013.[Online]. Available: <https://www.wrap.org.uk/sustainable-textiles/scap/extending-clothing-life/report/measuring-active-life-of-clothing>
- [2.8] WRAP, "Valuing Our Clothes, the true cost of UK fashion retail," 2017.
- [2.9] WRAP, "Sustainable Clothing Action Plan (SCAP)," 2019. [Online]. Available: <http://www.wrap.org.uk/sustainable-textiles/scap>. [Accessed December 2019].
- [2.10] WRAP, "Textiles - Overview," WRAP, 2020 . [Online]. Available: [wrap.org.uk/content/textiles-overview](http://www.wrap.org.uk/content/textiles-overview). [Accessed June 2020].
- [2.11] G. Liu, M.M. Wright, Q. Zhao, R.C. Brown, K. Wang, "Catalytic pyrolysis of amino acids: Comparison of aliphatic amino acid and cyclic amino acid," *Energy conversion and management*, vol. 112, pp. 220-225, 2016.
- [2.12] W.H. Chen, B.J.Lin, M.Y. Huang, "Thermochemical conversion of microalgal biomass into biofuels: a review," *Bioresour technology*, vol. 184, pp. 314-27, 2014.
- [2.13] C. Dorado, C. Mullen, A. Boateng, "H-ZSM5 catalysed Co-pyrolysis of biomass and plastics," *ACS Sust Chem Eng*, vol. 2, pp. 301-11, 2014.

- [2.14] B. Maddi, S. Viamajala, S. Varanasi, “Comparative study of pyrolysis of algal biomass from natural lake blooms with lignocellulosic biomass,” *Bioresour Technol*, vol. 102, 2011.
- [2.15] Z. Du, M. Mohr, X. Ma, Y. Cheng, X. Lin, “Hydrothermal pretreatment of microalgae for production of pyrolytic bio-oil with a low nitrogen content,” *Bioresour Technol*, vol. 120, 2012.
- [2.16] J.H. Bradbury, G.V. Chapman and N.L.R. King, “Analysis of the Major Historical Components Produced by Ultrasonic Disintegration,” *The Chemical Composition of Wool*, pp. 353-64, 1965.
- [2.17] WRAP, “Valuing our clothes,” 2012. [Online]. Available: https://www.wrap.org.uk/sites/files/wrap/valuing-our-clothes-the-cost-of-uk-fashion_WRAP.pdf
- [2.18] K. Caulfield, “Sources of Textile Waste in Australia,” *Apical International Pty Ltd*, 2009.
- [2.19] P. Mckendry, “Energy production from biomass (part 2),” *Conversion technologies. Bioresource Technology*, pp. 47-54, 2002.
- [2.20] M. Wallander, “Why Textile Waste Should be Banned from Landfills,” Triple Pundit, 2 January 2012. [Online]. Available: <http://www.triplepundit.com/2012/01/textile-waste-be-banned-landfills/>. [Accessed 2016].
- [2.21] “Anaerobic Digestion,” Wrap, 2016. [Online]. Available: <http://www.wrap.org.uk/content/anaerobic-digestion-1>.
- [2.22] Biomass Energy Center, “Anaerobic Digestion,” 2011. [Online]. Available: http://www.biomassenergycentre.org.uk/portal/page?_pageid=75,17509&_dad=portal&_schema=portal. [Accessed 2016].
- [2.23] L. Arsova, “Anaerobic digestion of food waste: Current status, problems and alternative products,” Columbia University, 2010.
- [2.24] Scottish Biofuel Programme , “Wool: A Pyrolysis and Anaerobic Digestion Case Study,” Edinburgh.
- [2.25] Scottish Biofuel Programme , “Fermentation,” Edinburgh, 2016.

- [2.26] Biomass Energy Centre, "Combustion," 2011. [Online]. Available: http://www.biomassenergycentre.org.uk/portal/page?_pageid=75,17502&_dad=portal&_schema=PORTAL.
- [2.27] Textiles F.R. Limited, "Fibres and Flammability," 2018. [Online]. Available: <http://textilesfr.co.uk/technical/fibres-and-flammability/>.
- [2.28] BTG - Biomass Technology Group, "Torrefaction," 2016. [Online]. Available: <http://www.btgworld.com/en/rtd/technologies/torrefaction>.
- [2.29] A. Mourant, "Biomass: When could torrefaction be commercially viable?," *Renewable energy focus*, 10 May 2013. [Online]. Available: <http://www.renewableenergyfocus.com/view/32330/biomass-when-could-torrefaction-be-commercially-viable/>. [Accessed 2016].
- [2.30] A. Austin, "French torrefaction firm targets North America," *Biomass Magazine*, February 2012. [Online]. Available: Austin, Anna (April 20, 2010). "French torrefaction firm targets North America". *Biomass Power and Thermal*. Retrieved February 29, 2012 .
- [2.31] C. M. Saffron, "Thermochemical Processes for Biomass Conversion of Bioenergy," in *Michigan State University* , New York, 2013.
- [2.32] Dutch Torrefaction Association , "Torrefaction: The future of energy," 2012.
- [2.33] A. S. S. Xiu, "Bio-oil production and upgrading research: A review," *Renewable and Sustainable Energy Reviews*, pp. 4406-4414, 2012.
- [2.34] Ronsse, F., Dickinson, D., Nachenius, R. & Prins, W., "Biomass pyrolysis and biochar characterization," *Department Of Biosystems Engineering, Faculty of Bioscience Engineering, Ghent University (Belgium)*, Vienna, 2013.
- [2.35] CDS Analytical, "Degredation Mechanisms, Side Group Elimination," Oxford, USA, 2017.
- [2.36] C. R. French, "Catalytic pyrolysis of biomass for biofuels production," *Fuel Processing Technology*, pp. 25-32, 2010.
- [2.37] A. Bridgwater, "Review of fast pyrolysis of biomass and product upgrading," *Biomass and Bioenergy*, pp. 68-94, 2012.

- [2.38] Ronsse, Prof. F., "Report on biochar production techniques," *Department of Biosystems Engineering*, Ghent University, 2013.
- [2.39] T. Dickerson, J. Soria, "Catalytic Fast Pyrolysis: A Review," *Energies*, pp. 514-538, 21 January 2013.
- [2.40] R. Maximino, "Pyrolysis of Biomass Residues in a Screw Reactor," *Tecnico Lisboa*, Lisbon, 2013.
- [2.41] The University of Edinburgh, "What is Biochar," *UK Biochar Research Centre*, [Online]. Available: <http://www.biochar.ac.uk/>.
- [2.42] Lijian Leng, Huajun Huang, Hui Lic, Jun Lia, Wenguang Zhou, "Biochar stability assessment methods: A review," *Science of the total environment*, pp. 210-222, 2019.
- [2.43] Grand View Research, "Biochar market analysis by technology (pyrolysis, gasification), by application (agriculture) and segment forecast to 2022," *Grand View Research*, 2016.
- [2.44] International Biochar Initiative, "The state of the biochar industry report," 2015.
- [2.45] J. M. John Sherbondy, "What is Activated Carbon," *TIGG*, 2015. [Online]. Available: <http://www.tigg.com/what-is-activated-carbon.html>.
- [2.46] P. Kandhavadi, C. Vigneswawran, T. Ramachandran, B. Geethamanobari, "Development of polyester-based bamboo charcoal and lyocell-blended union fabrics for healthcare and hygienic textiles," *Journal of industrial textiles*, vol. 41, pp. 142-159, 2011.
- [2.47] Thomasnet, "Producing Activated Carbon," 2016. [Online]. Available: <http://www.thomasnet.com/articles/chemicals/producing-activated-carbon>.
- [2.48] S. Amin, "Review on biofuel oil and gas production processes from microalgae," *Energy Conversion and Management*, pp. 1834-1840, 2009.
- [2.49] M. Verma, S. Godbout, S.K. Brar, O. Solomatnikova, "Biofuels Production from Biomass by Thermochemical Conversion Technologies," *International Journal of Chemical Engineering*, 2012.
- [2.50] A. Toussaint, "BTG-BTL Pyrolysis Process," *btg-btl biomass-to-liquid*, 2016. [Online]. Available: <https://www.btg-btl.com/en/technology>.

- [2.51] R. Rabe, "A model for the vacuum pyrolysis of biomass," *The University of Stellenbosch*, Stellenbosch, 2005.
- [2.52] N. Cao, H. Darmstadt, C. Roy, "Thermogravimetric study on the steam activation of charcoal obtained by vacuum and atmospheric pyrolysis of softwood bark residue," *Carbon*, pp. 471-479, 2002.
- [2.53] A. Bridgwater, "Principal and practices of biomass fast pyrolysis for liquids," *Journal of analytical and applied pyrolysis*, pp. 3-22, 1999.
- [2.54] Enviropower, "Rotary Kiln Systems," 2014. [Online]. Available: www.eprenewable.com/rotary-kiln-systems-0-5mw-to-10-mw.
- [2.55] Biofuel.org, "What is syngas?," 2010. [Online]. Available: <http://biofuel.org.uk/what-is-syngas.html>. [Accessed 2016].
- [2.56] M.F. Demirbas, M. Balat, "Biomass pyrolysis for liquid fuels and chemicals : A review," *Scientific and Industrial Research*, pp. 514-538, 2007.
- [2.57] E. Suali, R. Sarbatly, "Conversion of microalgae to biofuel," *Renewable and Sustainable Energy Reviews*, pp. 4316-4342, 2012.
- [2.58] Food and agriculture organization of the united nations, "Wood gas as engine fuel," *FAO Forestry Department*, 1986.
- [2.59] A. Bosman, S. Wasan, L. Helsen, "Waste to clean syngas: Avoiding tar problems," in *2nd International Enhanced Landfill Mining Symposium*, 2013.
- [2.60] L. Devi, K.J. Ptasinski, G. Janssen, "A Review of the Primary Measures for Tar Elimination in Biomass Gasification Processes," *Biomass and Bioenergy*, pp. 125-140, 2003.
- [2.61] G. Young, "Municipal Solid Waste to Energy Conversion Processes - Economic, Technical and Renewable Comparisons," *John Wiley & Sons, Inc*, New Jersey, 2010.
- [2.62] D. Sutton, B. Kelleher and J. R. H. Ross, "Review of Literature on Catalysts for Biomass," *Fuel Processing Technology*, pp. 155-173, 2001.
- [2.63] Energy Research Centre of the Netherlands, "Classification System," *ECN*, June 2009. [Online]. Available: <http://www.thersites.nl/classification.aspx>. [Accessed 2016].

- [2.64] D. Czajczynska, L. Anguilano, H. Ghazal, R. Krzyczynska, A.J. Reynolds, N. Spencer, H. Jouhara, "Potential of pyrolysis processes in the waste management sector," *Thermal Science and Engineering Progress*, pp. 171-197, 2017.
- [2.65] R. Chowdhury, A. Sarkar, "Reaction Kinetics and Product Distribution of Slow Pyrolysis of Indian Textile Wastes," *International Journal of Chemical Reactor Engineering*, 2012.
- [2.66] M.A. Nahil, P.T. Williams, "Activated carbons from acrylic textile waste," *Journal of Analytical and Applied Pyrolysis*, pp. 51-59, 2010.
- [2.67] Y.B. Yang, A.N. Phan, C. Ryu, V. Sharifi, J. Swithenbank, "Mathematical modelling of slow pyrolysis of segregated solid wastes in a packed-bed pyrolyser," *Fuel*, pp. 169 - 180, 2007.
- [2.68] C.B. Canbolat, B. Ozbey, N. Dizge, "Pyrolysis of commingled waste textile fibers in a batch reactor: Analysis of the pyrolysis gases and solid product," *International Journal of Green Energy*, 2017.
- [2.69] C. Wen, Y. Wu, X. Chen, G. Jiang & D. Liu, "The pyrolysis and gasification performances of waste textile under carbon dioxide atmosphere," *Journal of Thermal Analysis and Calorimetry*, 2016.
- [2.70] S. Yousef, J. Eimontas, N. Striūgas, M. Tatariants, M. A. Abdelnabyd, S. Tuckutee, L. Kliucininkas, "A sustainable bioenergy conversion strategy for textile waste with self-catalysts using mini-pyrolysis plant," *Energy Conversion and Management*, 2019.
- [2.71] M.S. Mettler, A.D. Paulsen, D.G. Vlachos and P. J. Dauenhauer, "Pyrolytic conversion of cellulose to fuels: levoglucosan deoxygenation via elimination and cyclization within molten biomass", *Energy and Environmental Science*, 2012
- [2.72] A. Keshwani, B. Malhotra, H. Kharkwal, "Natural polymer based detergents for stain removal", *World Journal Of Pharmacy And Pharmaceutical Sciences*, 2015
- [2.73] M. S. Ö. Sibel Barışçı, "The Disposal of Combed Cotton Wastes by Pyrolysis," *International Journal of Green Energy*, 2014.
- [2.74] R. Miranda, C. Sosa_Blanco, D. Bustos-Martinez, C. Vasile, "Pyrolysis of textile wastes, I. Kinetics and yields," *Journal of Analytical and Applied Pyrolysis*, pp. 489 - 495, 2007.

- [2.75] F. Campuzano, R. C. Brown, J. D. Martínez, “Auger reactors for pyrolysis of biomass and wastes,” *Renewable and Sustainable Energy Reviews*, pp. 372-409, 2019.
- [2.76] S.D. Ferreira, C.R. Altafini, D. Perondi, M. Godinho, “Pyrolysis of Medium Density Fiberboard (MDF) wastes in a screw reactor,” *Energy Conversion and Management*, pp. 223-233, 2015.
- [2.77] M.T. Morgano, H. Leibold, F. Richter, D. Stapf, H. Seifert, “Screw pyrolysis technology for sewage sludge treatment,” *Waste Management*, pp. 487-495, 2018.
- [2.78] I. Agirre, T. Griessacher, G. Rösler, J. Antrekowitsch, “Production of charcoal as an alternative reducing agent from agricultural residues using a semi-continuous semi-pilot scale pyrolysis screw reactor,” *Fuel Processing Technology*, pp. 114-121, 2013.
- [2.79] S. Sirijanusorn, K. Sriprateep, A. Pattiya, “Pyrolysis of cassava rhizome in a counter-rotating twin screw reactor unit,” *Bioresource Technology*, pp. 343 - 348, 2013.
- [2.80] S. Kelkar, C.M. Saffron, L. Chai, J. Bovee, T.R. Stuecken, M. Garedew, et al., “Pyrolysis of spent coffee grounds using a screw-conveyor reactor,” *Fuel Processing Technology*, pp. 170-178, 2015.
- [2.81] T. Gopakumar, S. Adhikari, H. Revindran, R.B. Gupta, O. Fasina, M. Tu, “Physiochemical properties of bio-oil produced at various temperatures from pine wood using an auger reactor,” *Bioresource Technology*, pp. 8389-8395, 2010.
- [2.82] C.E. Efika, C.Wu, P.T. Williams, “Syngas production from pyrolysis–catalytic steam reforming of waste biomass in a continuous screw kiln reactor,” *Journal of Analytical and Applied Pyrolysis*, 2012.
- [2.83] V.K. Guda, H. Toghiani, “Altering bio-oil composition by catalytic treatment of pinewood pyrolysis vapors over zeolites using an auger - packed bed integrated reactor system,” *Biofuel Research Journal*, 2016.
- [2.84] P.Brassard, S.Godbout, V. Raghavan, J.H. Palacios, M. Grenier, D. Zegan, “The production of engineered biochar in a vertical auger pyrolysis reactor for carbon sequestration,” *Energies*, 2017.

- [2.85] Y. Yang, J.G. Brammer, A.S.N. Mahmood, A. Hornung, "Intermediate pyrolysis of biomass energy pellets for producing sustainable liquid, gaseous and solid fuels," *Bioresource Technology*, pp. 794 - 799, 2014.
- [2.86] J. Haydary, D. Susa, V. Gelinger, F. Čácho, "Pyrolysis of automobile shredder residue," *Journal of Environmental Chemical Engineering*, pp. 965-972, 2016.
- [2.87] D.L. Dalluge, T. Daugaard, P. Johnston, N. Kuzhiyil, M.M. Wright, R.C. Brown, "Continuous production of sugars from pyrolysis of acid-infused lignocellulosic biomass," *Green Chemistry*, 2014
- [2.88] J.D. Martínez, R. Murillo, T. García, A. Veses, "Demonstration of the waste tire pyrolysis process on pilot scale in a continuous auger reactor," *Journal of Hazardous Materials*, pp. 637 - 645, 2013.
- [2.89] E. Henrich, N. Dahmen, F. Weirich, R. Reimert, C. Kornmayer, "Fast pyrolysis of lignocellulosics in a twin screw mixer reactor," *Fuel Processing Technology*, pp. 151-161, 2016.
- [2.90] Y.N. Chun, S.C. Kim, K. Yoshikawa, "Pyrolysis gasification of dried sewage sludge in a combined screw and rotary kiln gasifier," *Applied Energy*, pp. 1105-1112, 2011.
- [2.91] P. Kim, S. Weaver, K. Noh, N. Labbé, "Characteristics of Bio-Oils Produced by an Intermediate Semipilot Scale Pyrolysis Auger Reactor Equipped with Multistage Condensers," *Energy & Fuels*, 2014.
- [2.92] Q. Li, P.H. Steele, F. Yu, B. Mitchell, E.B.M. Hassan, "Pyrolytic spray increases levoglucosan production during fast pyrolysis," *Journal of Analytical and Applied Pyrolysis*, pp. 33-40, 2013.
- [2.93] J. Solar, I. de Marco, B.M. Caballero, A. Lopez-Urionabarrenechea, N. Rodriguez, "Influence of temperature and residence time in the pyrolysis of woody biomass waste in a continuous screw reactor," *Biomass and Bioenergy*, pp. 416-423, 2016.
- [2.94] L. Bosong, L. Wei, Z. Qui, W. Tiejun W, Longlong M., "Pyrolysis and catalytic upgrading of pine wood in a combination of auger reactor and fixed bed," *Fuel*, pp. 61-67, 2014.

- [2.95] H. Nam, S.C. Capareda, N. Ashwath, J.E. Kongkasawan, “Experimental investigation of pyrolysis of rice straw using bench-scale auger, batch and fluidized bed reactors,” *Energy*, pp. 2384-2394, 2015.
- [2.96] J. Dalluge, T. Daugaard, P. Johnston, N. Kuzhiyil, M.M. Wright, R.C. Brown, “Continuous production of sugars from pyrolysis of acid-infused lignocellulosic biomass,” *Green Chemistry*, 2014.
- [2.97] A. Pattiya, “Fast pyrolysis,” in *Direct Thermochemical Liquefaction for Energy Applications*, Thailand, Elsevier, 2018, pp. 3-28.
- [2.98] M. Weaver, “Thermal Pre-treatment of Biomass for large Scale Application”, York: IEA Bioenergy, 2011.
- [2.99] J.A.Rippon, D.J.Evans, “Improving the properties of natural fibres by chemical treatments,” in *Handbook of Natural Fibres*, Woodland Publishing, 2012, pp. 63-140.
- [2.100] “The Chemical & Physical Structure of Merino Wool.,” 2006. [Online]. <https://csiropedia.csiro.au/wp-content/uploads/2015/01/6229343.pdf> [Accessed 2017]
- [2.101] D.S. Yengkhom, P. Mahanta, U. Bor, “Comprehensive characterization of lignocellulosic biomass through proximate, ultimate and compositional analysis for bioenergy production,” *Renewable Energy*, 2017.
- [2.102] M. Witczak, M. Walkowiak, W. Cichy, M. Komorowicz, “The application of elemental analysis for the determination of the elemental composition of lignocellulosic materials,” *Forestry and Wood Technology*, 2015.
- [2.103] T.Pröll, I. G. Siefert, A. Friedl, H. Hofbauer, “Removal of NH₃ from Biomass Gasification Producer Gas by Water Condensing in an Organic Solvent Scrubber,” *Industrial & Engineering Chemistry Research*, January 2005.
- [2.104] M. Hudson, “Fiber to Fabric,” *Ingeo Fibre Apparel Product Guidelines*, 2017.
- [2.105] Wagner, “Wood Species Types in Alphabetical Order,” 2019. [Online]. Available: <https://www.wagnermeters.com/specific-gravity/p/>.

- [2.106] X. Pham, B. Piriou, S. Salvador, J. Valette, "Oxidative pyrolysis of pine wood, wheat straw and miscanthus pellets in a fixed bed," *Fuel Processing Technology*, 2018.
- [2.107] R. Tomaz, J.W. Molina, M. Rípoli, "Energy potential of sugar cane biomass in Brazil," *Scientia Agricola*, 2000.
- [2.108] J. Lancashire, "Unit- chemistry of Garments: Animal Fibres," *Chemistry of Fibres, Textiles and Garments*, February 2015. [Online]. Available: http://wwwchem.uwimona.edu.jm/courses/CHEM2402/Textiles/Animal_Fibres.html. [Accessed 2016].
- [2.109] R. Asquith, "Crosslinking and self-crosslinking in keratin fibers," in *Chemistry of Natural Protein Fibers*, 1977, pp. 267-300.
- [2.110] D. Rivett, "Structural lipids of the wool fibre," *Wool Science Review*, pp. 1-25, 1991.
- [2.111] A.P. Pierlot, J.A. Rippon, J.R. Christoe, R.J. Denning, D.J. Evans, M.G. Huson, P.R. Lamb, K.R. Millington, "Wool: Structure, Properties, and Processing," in *Encyclopedia of Polymer Science and Technology*, Wiley, 2016.
- [2.112] International Agency for Research on Cancer, "Some Aromatic Amines, Organic Dyes, and Related Exposures," *IARC Monographs on the Evaluation of Carcinogenic Risks to Humans Volume*, France, 2010.
- [2.113] The Essential Chemical industry, "Colorants," 2013. [Online]. Available: <https://www.essentialchemicalindustry.org/materials-and-applications/colorants.html>.
- [2.114] S. Benkhaya, S.l. Harfi, A.E. Harfi, "Classifications, properties and applications of textile dyes: A review," *Applied Journal of Environmental Engineering Science*, pp. 311-320, 2017.
- [2.115] Textile School, "Types of Dyes – classification based on chemical structure," 2019. [Online]. Available: textileschool.com/383/types-of-dyes-classification-based-on-chemical-structure/.
- [2.116] Textile Fashion Studies, "Classification of Dyes," 2012. [Online]. Available: <http://textilefashionstudy.com/dyes-classification-of-dyes/>.

- [2.117] M.I. Kiron, "Dyeing Process, Different Types of Dyes, Classification of Dyes," *Textile Learner*, 2020. [Online]. Available: textilelearner.blogspot.com/2011/07/dyeing-process-different-types-of-dye_1720.html.
- [2.118] Textile Knowledge "Azoic Dyes," [Online]. Available: textileengg.blogspot.com/2015/11/azoic-dyes.html.
- [2.119] Britannica, "Azo dye chemical compound," [Online]. Available: britannica.com/science/azo-dye.
- [2.120] P. Richards, "Dye types and application methods," in *Colour Design, Theories and Applications*, Woodhead Publishing, 2012.
- [2.121] P. Richards, "Fabric Finishing: Dyeing And Colouring," in *Textiles and Fashion; Materials, Design and Technology*, Woodhead Publishing, 2014.
- [2.122] N. Sekar, "Acid Dyes," in *Handbook of Textile and Industrial Dyeing*, Woodhead Publishing, 2011.
- [2.123] J. Patterson, N.F. Haidar, E.P. Apadopoulos, W. Smith, "Pyrolysis of Phenylalanine, 3,6-Dibenzyl-2,5-piperazinedione, and Phenethylamine," *J. Org. Chem*, 1972.
- [2.124] S. Wang, B. Liu, Q. Su, "Pyrolysis–gas chromatography/mass spectrometry as a useful technique to evaluate the pyrolysis pathways of phenylalanine," *Journal of Analytical and Applied Pyrolysis*, 2004.
- [2.125] I. Pastorova, R.E. Botto, P.W. Ariszajaap, J. Boona, "Cellulose char structure: a combined analytical Py-GC-MS, FTIR, and NMR study," *Carbohydrate Research*, pp. 27-47, 1994.
- [2.126] Encyclopædia Britannica, "Cellulose, Plant Cell Structure," [Online]. Available: <https://www.britannica.com/science/cellulose>. [Accessed 2019].
- [2.127] H. Yang, R. Yan, H. Chen, et al, "Characteristics of hemicellulose, cellulose and lignin pyrolysis," *Fuel*, pp. 1781-8, 2007.
- [2.128] P.R. Patwardha, D.L. Dalluge, B.H. Shanks, et al, "Distinguishing primary and secondary reactions of cellulose pyrolysis," *Bioresource Technology*, 2011.

- [2.129] F.X. Collard, J. Blin, "A review on pyrolysis of biomass constituents: Mechanisms and composition of the products obtained from the conversion of cellulose, hemicelluloses and lignin," *Renewable and Sustainable Energy Reviews*, pp. 594-608, 2014.
- [2.130] J.L. Banyasz, S. Li, J. Lyons-Hart, "Gas evolution and the mechanism of cellulose pyrolysis," *Fuel*, 2001.
- [2.131] J. Scheirs, G. Camino, W. Tumiatti, "Overview of water evolution during the thermal degradation of cellulose," *European Polymer Journal*, 2001.
- [2.132] Q. Lu, X.C. Yang, C.Q. Dong, et al, "Influence of pyrolysis temperature and time on the cellulose fast pyrolysis products: analytical Py-GC/MS study," *Journal of Analytical and Applied Pyrolysis*, 2011.
- [2.133] D.K. Shen, S. Gu, K.H. Luo, et al, "The pyrolytic degradation of wood-derived lignin from pulping process," *Bioresource Technology*, 2010.
- [2.134] J. Cao, G. Xiao, X. Xu, et al, "Study on carbonization of lignin by TG-FTIR and high-temperature carbonization reactor," *Fuel Processing Technology*, 2012.
- [2.135] E. Heracleous, A. Lappas, D. Serrano, "Special thematic issue in Biomass Conversion and Biorefinery" *Biomass Convention*, Germany, 2017.
- [2.136] M. C. Samolada, A. Papafotica, and I. A. Vasalos, "Catalyst Evaluation for Catalytic Biomass Pyrolysis," *Energy & Fuels*, pp. 1161-1167, 2000.
- [2.137] M.R. Gray, W.H. Corcoran, G.R. Gavalas, "Pyrolysis of a Wood-Derived Material. Effects of Moisture and Ash Content," *Industrial & Engineering Chemistry Process Design and Development*, vol. 24, pp. 646-651, 1985.
- [2.138] S. Ch, "Heterogeneous Catalysis in Practice," *New York: McGraw-Hill*, 1980.
- [2.139] H. Hattori, "Heterogeneous Basic Catalysis," *Chem. Rev.*, 1995.
- [2.140] C. Falamaki, E. Mohammad and M. Sohrabi, "Studies on the Crystallization Kinetics of Zeolite ZSM-5 With 1,6-Hexanediol as a Structure-Directing Agent," *Zeolites*, vol. 19, no. 1, pp. 2-5, 1997.

- [2.141] B.Burger, K.Haas-Santo, M.Hunger, and J. Weitkamp, "Synthesis and Characterization of Aluminium-Rich Zeolite ZSM-5," *Chemical Engineering Technologies* , pp. 322-324, 2000.
- [2.142] S. Sang, F. Chang, Z. Liu, C. He, Y. He and L. Xu, "Difference of ZSM-5 zeolites synthesized with various templates," *Catalysis Today*, Vols. 93-95, pp. 729-734, 2004.
- [2.143] T.Q. Hoang, X. Zhu, T. Danuthai, L.L. Lobban, D.E. Resasco, "Conversion of Glycerol to Alkyl-aromatics over Zeolites," *Energy & Fuels*, 6 05 2010.
- [2.144] D. J. Mihalcik, "Screening acidic zeolites for catalytic fast pyrolysis of biomass and its components," *Journal of analytical and applied pyrolysis*, pp. 224-232, 09 2011.
- [2.145] J. Jae, G.A. Tompsett, A.J. Foster, K.D. Hammond, S.M. Auerbach, R.F. Lobo, G.W. Huber, "Investigation into the shape selectivity of zeolite catalysts for biomass conversion," *Journal of Catalysis* , pp. 257-268, 2011.
- [2.146] L. Shirazi, E. Jamshidi and M. R. Ghasemi, "The effect of Si/Al ratio of ZSM-5 zeolite on its morphology, acidity and crystal size," *Cryst. Res. Technol*, vol. 43, no. 12, pp. 1300-1306, 2008.
- [2.147] L. Rodriguez-Gonzalez, F. Hermes, M. Bertmer, E. Rodriguez-Castellon, A. Jimenez-Lopez and U. Simon, "The acid properties of H-ZSM-5 as studied by NH₃-TPD and Al-MAS-NMR spectroscopy," *Applied Catalysis A: General*, vol. 328, no. 2, pp. 174-182, 2007.
- [2.148] M. Crocker, R. H. M. Herold, M. H. W. Sonnemans, C. A. Emels, A. E. Wilson and J. N. van der Moolen, "Studies on the acidity of Mordenite and ZSM-5. 1. Determination of Brønstead Acid Site Concentrations in Mordenite and ZSM-5 by Conductometric Titration," *J. Phys. Chem.*, no. 97, pp. 432-439, 1993.
- [2.149] Z. Ma, L. Wei, W. Zhou, L. Jia, B. Hou, D. Li and Y. Zhao, "Overview of catalyst application application in petroleum refinery for biomass catalytic pyrolysis and bio-oil upgrading," *RSC Advances*, vol. 5, 2015.
- [2.150] D. Maucec, M. Mazaj, A. Ristic, V. Kaucic and N. N. Tusar, "Zinc Oxide Nanoparticles Immobilized On Ordered (Sba-15) And Disordered (Kil-2) Meoporous Silicate Supports," *Proceedings of the 4th Slovenian-Croatian Symposium on Zeolites*, 2011.

- [2.151] N. Linares, A. M. Silvestre-Alvero, E. Serrano, J. Silvestre-Albero and J. Garcia-Martinez, "Mesoporous materials for clean energy technologies," *Chem Soc Rev*, vol. 43, pp. 7681-7717, 2014.
- [2.152] N. Tusar, A. Ristic, G. Mali, M. Mazaj, I. Arcon, D. Arcon, V. Kaucic, and N. Z. Logar, "MnO_x Nanoparticles Supported on a New Mesoporous Silicate with Textural Porosity," *Chemistry; A European Journal*, pp. 5783-5793, 2010.
- [2.153] M. Popova, Á. Szegedi, A. Ristić and N. N. Tušar, "Glycerol acetylation on mesoporous KIL-2 supported sulphated zirconia catalysts," *Catalysis Science and Technology*, 2014.
- [2.154] M. Popova, A. Ristic, V. Mavrodinova, D. Maucec, L. Mindizova, N. N. Tusar, "Design of Cobalt Functionalized Silica with Interparticle Mesoporosity as a Promising Catalyst for VOCs Decomposition," *Springer Science+Business*, 2014.
- [2.155] A. Ristić, D. Maučec, S.K. Henninger, V. Kaučič, "New two-component water sorbent CaCl₂-FeKIL2 for solar thermal energy storage," *Microporous and Mesoporous Materials*, 2012.
- [2.156] H. Xia, X. Yan, S. Xu, L. Yang, Y. Ge, J. Wang, and S. Zuo, "Effect of Zn/ZSM-5 and FePO₄ Catalysts on Cellulose Pyrolysis," *Journal of Chemistry*, 2015.
- [2.157] F. W. Atadana, "Catalytic Pyrolysis of Cellulose, Hemicellulose and Lignin Model Compounds," *Virginia Tech*, 2010.
- [2.158] F. Yu, D. Ji, Y. Nie, Y. Luo, C. Huang, J. Ji, "Study on the Pyrolysis of Cellulose for Bio-Oil With Mesoporous Molecular Sieve Catalysts," *Applied Biochemistry and Biotechnology*, 2012.
- [2.159] W. Li, Y. Zhu, S. Li, Y. Lu, J. Wang, K. Zhu, J. Chen, Y. Zheng, "Catalytic fast pyrolysis of cellulose over Ce_{0.8}Zr_{0.2-x}Al_xO₂ catalysts to produce aromatic hydrocarbons: Analytical Py-GC × GC/MS," *Fuel Processing Technology*, 2020.
- [2.160] M. Yang, J. Shao, H. Yang, K. Zeng, Z. Wu, Y. Chen, X. Bai, "Enhancing the production of light olefins and aromatics from catalytic fast pyrolysis of cellulose in a dual-catalyst fixed bed reactor," *Bioresource Technology*, pp. 77-85, 2019.

- [2.161] B. Cao, Z. Xia, S. Wang, A. Abomohra, N. Cai, Y. Hu, C. Yuan “A study on catalytic co-pyrolysis of cellulose with seaweeds polysaccharides over ZSM-5: Towards high-quality biofuel production,” *Journal of Analytical and Applied Pyrolysis*, pp. 526-535, 2018.
- [2.162] G. Dai, S. Wang, Q. Zou, S. Huang, “Improvement of aromatics production from catalytic pyrolysis of cellulose over metal-modified hierarchical HZSM-5,” *Fuel Processing Technology*, pp. 319-323, 2018.
- [2.163] X. Chen, Y. Chen, Z. Chen, D. Zhu, H. Yang, P. Liu, T. Li, “Catalytic fast pyrolysis of cellulose to produce furan compounds with SAPO type catalysts,” *Pyrolysis, Journal of Analytical and Applied*, pp. 53-60, 2018.
- [2.164] Q. Yao, L. Xu, C. Guo, Z. Yuan, Y. Z. Y. Fu, “Selective production of pyrroles via catalytic fast pyrolysis of cellulose under ammonia atmosphere at low temperature,” *Journal of Analytical and Applied Pyrolysis*, pp. 409-414, 2017.
- [2.165] H. Ida, H. Ohtani, S. Karagöz, “Online fast pyrolysis of cellulose over titanium dioxide using tandem micro-reactor-GC-MS,” *Sustainable Chemistry and Pharmacy*, 2020.
- [2.166] H. Paysepar, K. Tirumala V. Rao, Z. Yuan, L. Nazari, H. Shui, “Zeolite catalysts screening for production of phenolic bio-oils with high contents of monomeric aromatics/phenolics from hydrolysis lignin via catalytic fast pyrolysis,” *Fuel Processing Technology*, pp. 362-370, 2018.
- [2.167] J. Kim, J. H. Lee, J. P. J. K. Kim, D. An, I. K. Song, J. W. Choi, “Catalytic pyrolysis of lignin over HZSM-5 catalysts: Effect of various parameters on the production of aromatic hydrocarbon,” *Journal of Analytical and Applied Pyrolysis*, pp. 273-280, 2015.
- [2.168] P.A. Lazaridis, A.P. Fotopoulos, S.A. Karakoulia, K.S. Triantafyllidis, “Catalytic Fast Pyrolysis of Kraft Lignin With Conventional, Mesoporous and Nanosized ZSM-5 Zeolite for the Production of Alkyl-Phenols and Aromatics,” *Chemistry*, 2018.
- [2.169] Z. Dong, H. Yang, P. Chen, Z. Liu, Y. Chen, L. Wang, X. Wang, and H. Chen, “Lignin Characterization and Catalytic Pyrolysis for Phenol-Rich Oil with TiO₂-Based Catalysts,” *Energy & Fuel*, 2019.
- [2.170] T. Ohra-aho, J. Linnekoski, “Catalytic pyrolysis of lignin by using analytical pyrolysis-GC-MS,” *Biorefining chemistry*, 2015.

- [2.171] G. Liu, M. M. Wright, Q. Zhao, R.C. Brown, K. Wang, Y. Xue, "Catalytic pyrolysis of amino acids: Comparison of aliphatic amino acid and cyclic amino acid," *Energy Conversion and Management*, pp. 220-225, 2016.
- [2.172] F. Wei, J. Cao, X. Zhao, J. Ren, B. Gu, X. Weisludge: A study of sewage sludge and model amino acids," *Fuel*, pp. 148-154, 2018.
- [2.173] S. Başakçılardan and Ş. Hacibektaşoğlu, "Catalytic Pyrolysis of Biomass," *Pyrolysis Energy Systems Engineering Department, Faculty of Engineering, Yalova University, Yalova, Turkey*, 2017. ,
- [2.174] R. Liu, Md. M. Rahman, M. Sarker, M. Chai, C. Li, J. Cai, "A review on the catalytic pyrolysis of biomass for the bio-oil production with ZSM-5: Focus on structure," *Fuel Processing Technology*, 2020.
- [2.175] X. Chen, Y. Chen, H. Yang, X. Wang, Q. Che, W. Chen, H. Chen, "Catalytic fast pyrolysis of biomass: Selective deoxygenation to balance the quality and yield of bio-oil," *Bioresource Technology*, pp. 153-158, 2019.
- [2.176] W. Huang, F. Gong, M. Fan, Q. Zhai, C. Hong, Q. Li, "Production of light olefins by catalytic conversion of lignocellulosic biomass with HZSM-5 zeolite impregnated with 6 wt.% lanthanum," *Bioresource Technology*, pp. 248-255, 2012.
- [2.177] L. Jiang, Y. Wang, L. Dai, Z. Yu, Q. Yang, S. Yang, D. Jiang, "Co-pyrolysis of biomass and soapstock in a downdraft reactor using a novel ZSM-5/SiC composite catalyst," *Bioresource Technology*, pp. 202-208, 2019.
- [2.178] X. Li, X. Zhang, S. Shao, L. Dong, J. Zhang, C. Hu, Y. Cai, "Catalytic upgrading of pyrolysis vapor from rape straw in a vacuum pyrolysis system over La/HZSM-5 with hierarchical structure," *Bioresource Technology*, pp. 191-197, 2018.
- [2.179] A. Aho, N. Kumar, K. Eranen, T. Salmi, M. Hupa, D. Y. Murzin, "Catalytic Pyrolysis of Biomass in a Fluidized Bed Reactor: Influence of the Acidity of H-Beta Zeolite," *Process Safety and Environmental Protection*, 2007.
- [2.180] G. Yildiz, M. Pronk, M. Djokic, K.M. Geem, F. Ronsse, R.V. Duren, W. Prins, "Validation of a new set-up for continuous catalytic fast pyrolysis of biomass coupled

- with vapour phase upgrading,” *Journal of Analytical and Applied Pyrolysis*, pp. 343-351, 2013.
- [2.181] N. Zhou, S. Liu, Y. Zhang, L. Fan, Y. Cheng, Y. Wang, Y. Liu, P. Chen, R. Ruan, “Silicon carbide foam supported ZSM-5 composite catalyst for microwave-assisted pyrolysis of biomass,” *Bioresource Technology*, pp. 257-264, 2018.
- [2.182] E.F. Iliopoulou, E.V. Antonakou, S.A. Karakoulia, I.A. Vasalos, A.A. Lappas, K.S. Triantafyllidis, “Catalytic conversion of biomass pyrolysis products by mesoporous materials: Effect of steam stability and acidity of Al-MCM-41 catalysts,” *Chemical Engineering Journal*, pp. 51-57, 2007.
- [2.183] L. Zhou, H. Yang, H. Wu, M. Wang, D. Cheng, “Catalytic pyrolysis of rice husk by mixing with zinc oxide: characterization of bio-oil and its rheological behavior,” *Fuel Processing Technology*, pp. 385-391, 2013.
- [2.184] J. O. Muhammad, S. AbuBakar, “Catalytic pyrolysis of rice husk for bio-oil production,” *Journal of Analytical and Applied Pyrolysis*, pp. 362-368, 2013.
- [2.185] O. D. Mante, A. Foster, “Catalytic conversion of biomass to bio-syn crude oil,” *Biomass Conversion and Biorefinery*, 2011.
- [2.186] M. Zabeti, T.S. Nguyen, H.J. Heeres, K. Seshan, “In situ catalytic pyrolysis of lignocellulose using alkali-modified amorphous silica alumina,” *Bioresource Technology*, pp. 374-381, 2012.
- [2.187] M.I. Nokkosmaki, E.T. Kuoppala, E.A. Leppamaki, A.O.I. Krause, “Catalytic conversion of biomass pyrolysis vapours with zinc oxide,” *Journal of Analytical and Applied Pyrolysis*, p. 1190131, 2000.
- [2.188] T. Aysu, M.M. Küçük, “Biomass pyrolysis in a fixed bed reactor: Effects of pyrolysis parameters on product yields and characterization of products,” *Energy*, pp. 1002-1025, 2014.
- [2.189] T.S. Nguyen, M. Zabeti, L. Lefferts, G. Brem, K. Seshan, “Conversion of lignocellulosic biomass to green fuel oil over sodium based catalysts,” *Bioresource Technology*, pp. 353-360, 2013.

[2.190] H, Kawamoto, "Lignin pyrolysis reactions", *Journal of Wood Science*, pp.117-132, 2017

CHAPTER 3 – METHODOLOGY

In this chapter, the feedstocks and catalysts used in the experiments are listed. Afterwards, methods to prepare these feedstocks for pyrolysis experiments are explained. Then, the fixed bed experimental procedure alongside the tests carried out on pyrolysis products are explained. Finally, decisions made on scaling up method are presented.

3.1 Materials: Model Compound and Catalysts

The characteristics of the feedstock, namely phenylalanine, cellulose, lignin, and waste wool, are discussed in this section alongside the synthesis procedure of the catalysts and their properties.

3.1.1 Feedstock

All the model compounds used were obtained from Sigma Aldrich and arrived in powder or crystalline form. The 98% pure phenylalanine crystals had a white to off white colour and had a carbon and nitrogen content range of 64.1% to 66.7 % and 8.2% to 8.8 %, respectively. It had a molecular weight of 165.19 g/mol with a melting point of around 270°C [3.1]. The white to off white in colour high purity microcrystalline cellulose powder had an average particle size of 51 µm and a bulk density of .6 g/mL at room temperature [3.2]. Finally, the light brown to dark kraft lignin had a density of 1.3 g/mL at room temperature with 5% moisture content [3.3].

The processed waste wool was supplied by Harris Tweed Authority and was received in two forms. As illustrated in Figure 3-1, one wool sample was made up of pieces with sizes ranging from 1 by 1 to 10 by 20 cm (left) and the other was made up of wool strings (loose waste). Furthermore, the wool supplied varied in colours regardless of size. This difference in colour could have potentially made some variation in the products due the differences in dye's structures. Dyes used in wool were reactive and acidic dyes. The preparation method of the wools for pyrolysis (cutting) was different based on the wool original size and has been discussed in the pyrolysis/gasification section. Table 3-1 illustrates the elemental analysis of the tweed waste and the heating value of it.

Table 3-1: Elemental Analysis and Heating Value of Tweed Waste

Elemental Analysis	C%	H%	N%	O%	H/C	O/C	Heating Value (MJ/kg)
Raw Tweed Waste	49.5	7.2	15.7	27.5	0.15	0.56	29



Figure 3-1: Wool samples used for pyrolysis; large samples (left), loose samples (right)

3.1.2 Catalysts

In this section, the synthesis procedure for ZSM5 and KIL2 catalyst are explained.

3.1.2.1 ZSM-5

Using LaTourette [3.4] and Widayat & Annisa [3.5] methods, a solution was prepared containing 56 grams of 98% pure sulfuric, 26.7 grams aluminium sulphate and 15 grams distilled water as the source of alumina. Then, to prepare the source of silica, 56 grams sodium hydroxide (40%) were mixed with identical amount of sodium silicate. After mixing and homogenising solution, A and B, crystallisation was carried out by leaving the solution for 7 hours in an autoclave reactor set at 200°C. Next, the produced ZSM-5s were let to dried after being washed with distilled water. Finally, the catalysts underwent calcination at 500°C for 7 hours.

3.1.2.2 KIL2

KIL2 were synthesised based on the methods found in literature [3.6] [3.7]. Initially, tetraethyl orthosilicate (TEOS, silica source) and template which consisted of triethanol amine (TEA), tetraethylammonium hydroxide (TEAOH) were added to each other and mixed with molar compositions of 1.0 TEOS:0.5 TEA:0.1TEAOH:11 H₂O, obtaining a homogenous gel. Then, the gel was dried in an oven for 24 hours at 50 °C after resting at room temperature overnight. Then, the gel was put in as stainless-steel autoclave set at 150 °C in ethanol for 48 hours. Finally, the template was removed by a 10 hours calcination procedure at 500°C in air flow with a ramp rate of 1 °C/min.

3.2 Fixed Bed Pyrolysis

Pyrolysis arrangements utilised for wool and model compounds, both catalytic and non-catalytic are presented in this section.

3.2.1 Non-Catalytic Pyrolysis/Gasification of Wool

Pyrolysis set-up used is presented in Figure 3-2 and Figure 3-3. It consisted of a fixed bed reactor, a gas distribution section, a tube furnace, and a condensation train. The fix-bed reactor was composed of a stainless steel (SS316) tubing with internal diameter of 2.5 cm and length of 39 cm. Tubing was placed into a Carbolite tube furnace with a heated length of 13 cm and a maximum operating temperature of 1000°C.

The arrangement was equipped with a movable probe to facilitate the feed introduction only when the desired temperature within the reactor was reached. The outside temperature of the furnace was illustrated on the body of the equipment. Additionally, a thermocouple was installed within the reactor to measure the temperature inside the reactor. Following this path, the temperature difference between inside and outside of the reactor in addition to the effect of the feed introduction on the temperature fluctuation could be observed.

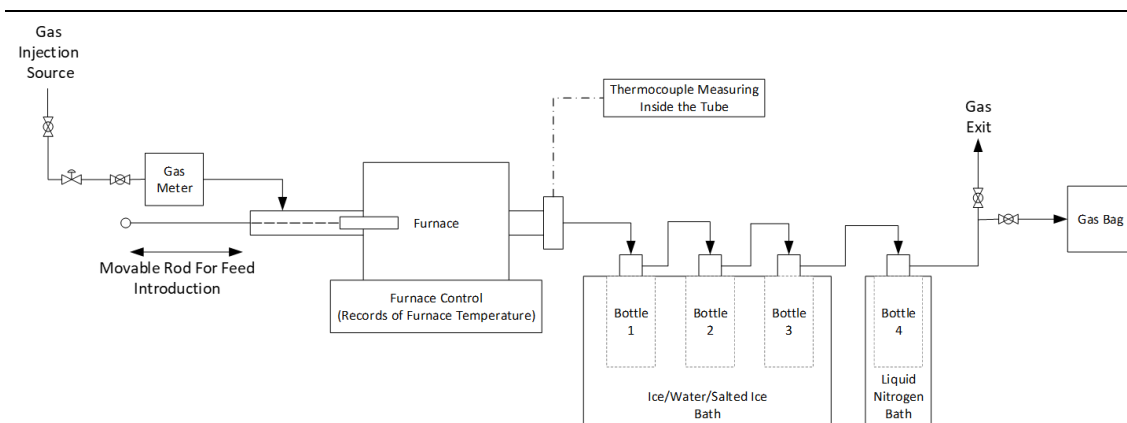


Figure 3-2: Schematic of fixed bed reactor set up

The gas was distributed and controlled via manometers and valves. The gas was injected in the reactor from one end and exited with the produced gas during the reaction from the other side. The exit was attached to a gas bag to collect the gas for further analysis if needed.

Four 500 mL glass condensers (Dreschel flasks bottles) were used as the condensation train. By doing so, the surface area and residence time for condensation was increased. Furthermore, by immersing different bottles in different cooling agents such as water, salt water or liquid nitrogen, products could be differentiated based on their boiling point. Due to the high temperature of the reactor outlet and the nature of the products, Viton tubing (6709) was used to connect the reactor to the condensation train.

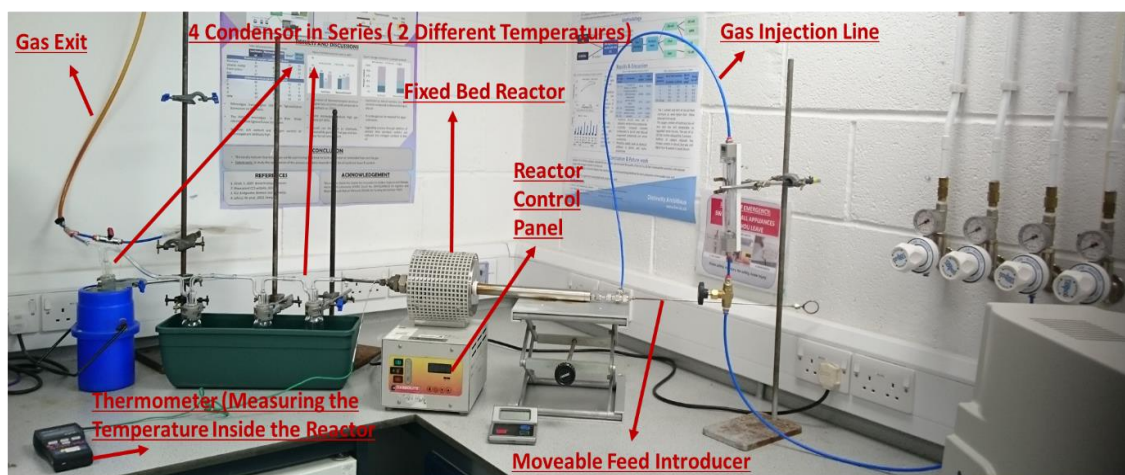


Figure 3-3: Picture of the laboratory pyrolysis arrangement

The feed to the reactor was loaded on to an alumina crucible boat with dimensions of 7 by 2 by 2 cm. The empty boat and the condensers were all weighed before the experiments. Additionally, feedstocks were also weighed prior to experiments using high precision scale (readable to 0.0001 g) with draft shield. This weighing procedure was repeated after the experiments to obtain the yield of products and product distribution. The percentage of gas was obtained by subtracting the sum of quantities of oil and char from feed weight.

The experimental procedure steps followed for the wool pyrolysis and gasification experiments were as following:

1. One gram of feed was loaded on to the boat
2. System was purged with nitrogen (pyrolysis) or CO₂ (gasification) gas for 20 minutes at 50 ml/min (reactor residence time of 28 seconds)
3. The reactor was heated up electrically to the desired temperature (350 to 900°C)
4. Feed was introduced via the movable sample holder into the heated section of the reactor when the desired temperature was reached. There was a temperature difference of 100 ± 12 °C between the tube (reactor) temperature and furnace temperature. The value recorded by the thermocouple placed inside the heated tube was used for introduction of feed.
5. Upon introduction of feed, temperature within the reactor dropped by 50 to 105 °C. It took another maximum of 2 minutes for the temperature records to come back to the pre-feed introduction value. This translated to heating rates of at least 25°C/min.
6. Overall, sample was held into the reactor at the elevated temperature for 15 minutes.
7. The condensable gas was collected in the condensers, 3 of which placed in ice (0°C) and 1 in liquid nitrogen (-196°C)

8. The incondensable gases were collected in a gas bag (1 L Tedlar bags) or released to atmosphere after enough gas was collected
9. The reactor was turned off and allowed to cool down for 2 hours
10. The solid char product was collected in small sealable plastic bags after weighing the boat
11. The liquid oil was collected after weighing the bottles. The procedure starts with diluting the oil with acetone (as a solvent) followed by collection in 10 ml vials and then drying the acetone out to obtain the pure oil products.

Different scenarios were created to evaluate the effect of several variables. The variables were as following:

- › The effect of temperature on final products (from 350°C to 900 °C)
- › Effect of feed size and type on product composition
- › The role of the carrier gas variation (N₂ and CO₂)

In more detail, 5 different temperature, 350, 500, 700, 800 and 900 °C, were selected to cover a large spectrum of temperatures. The large wool pieces which were described previously were cut in 1 by 4 cm to fit in the feed boat and the loose strings of wool needed to be de-tangling prior to loading to the bed. An example of the loaded boat with the large pieces of wool is shown in Figure 3-4.

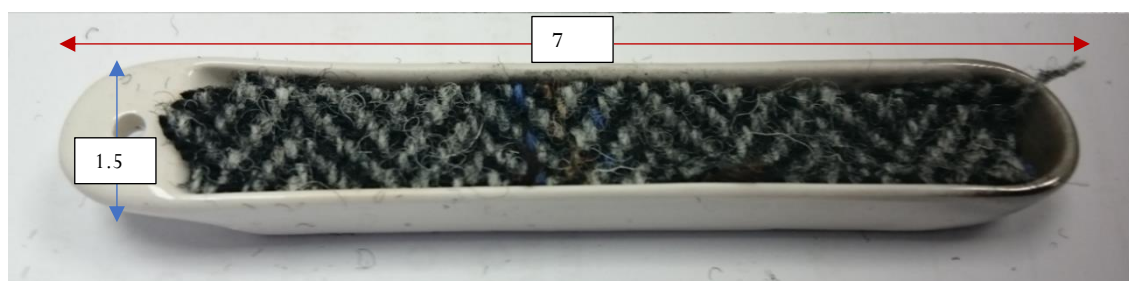


Figure 3-4: Loaded boat with large wool sample prior to pyrolysis

To cover all the of variables, 7 different scenarios were introduced as presented in Table 3-2.

Table 3-2: List of experiment scenarios carried out on wool in fixed bed.

Test No.	Temperature (°C)	Wool Size	Injected Gas
1	350	1 by 4 cm	N ₂
2	500	1 by 4 cm	N ₂
3	800	1 by 4 cm	N ₂
3	700	1 by 4 cm	CO ₂

4	800	1 by 4 cm	CO ₂
5	900	1 by 4 cm	CO ₂
6	800	Loose (Strings)	CO ₂
7	800	Loose (Strings)	N ₂

3.2.2 Catalytic Pyrolysis of Model Compounds

The same arrangement was used for the model compounds and catalytic experiments. However, since model compounds were pyrolysed to compare catalysts, variation of pyrolysis conditions was deemed unnecessary. Therefore, temperature was kept constant at 500°C for catalytic runs. Table 3-3 presents the tests carried out on model compounds.

Table 3-3: list of tests carried out on model compounds

Test No.	Model Compound	Catalyst
1	Cellulose	No Catalyst (Base Case)
2	Cellulose	Al-KIL2
3	Cellulose	Li-KIL2
4	Cellulose	20-ZSM5
5	Cellulose	30-ZSM5
6	Cellulose	60-ZSM5
7	Lignin	No Catalyst (Base Case)
8	Lignin	Al-KIL2
9	Lignin	Li-KIL2
10	Lignin	20-ZSM5
11	Lignin	30-ZSM5
12	Lignin	60-ZSM5
13	Phenylalanine	No Catalyst (Base Case)
14	Phenylalanine	Al-KIL2
15	Phenylalanine	Li-KIL2
16	Phenylalanine	20-ZSM5
17	Phenylalanine	30-ZSM5
18	Phenylalanine	60-ZSM5

In the catalytic tests, the sample and catalyst were weighted individually. The catalyst to sample mass ratio was set at 1:1 and 0.35 g of each were measured. Model compound and catalysts were then mixed using a pestle and mortar until a uniform and homogeneous powder was obtain. The

resulting mixture was added to the sample boat and the total mass of the boat measured. Then, the reactor and boat were set up as explained above, i.e., the boat was installed in the system while being kept out of the reactor until the desired temperature was reached inside the reactor. The rest of procedure was same as for the wool runs. For the non-catalytic runs, i.e., pyrolysis of model compounds on their own, 0.35 grams of feed was used while the rest of the procedure was kept the same.

3.2.3 Catalytic Pyrolysis of Wool

Due to the nature of wool samples, in-situ catalysis deemed not practical for scale up. In other words, similar to model compounds, if wool was going to undergo in-situ catalytic pyrolysis, wool feed should have been shredded/grinded to powder form to have a homogenous texture with catalysts to have a uniform contacting surface area. Furthermore, regeneration of catalysts would become an issue in in-situ catalytic pyrolysis of wool during scale up. Doing this in a large scale which was the optimal goal of the tests, was not practical. Therefore, the fixed bed arrangement was modified to ex-situ one (Figure 3-5).

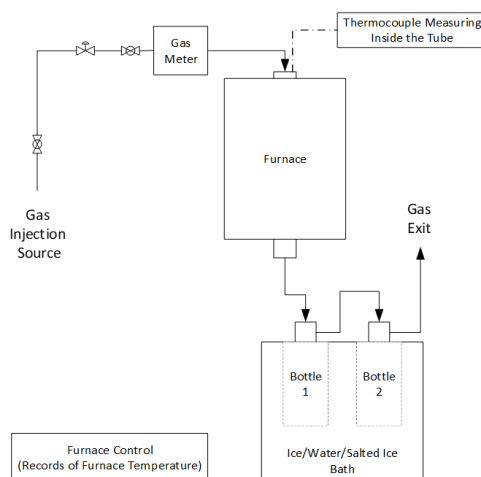


Figure 3-5: Schematic of the ex-situ fixed bed catalytic reactor.

The effect of temperature, feed size, injected gas and condensation system was evaluated in the non-catalytic runs. Therefore, the number of variables were reduced to increase the focus on the effect of catalyst on wool pyrolysis by-products. To do so, it was decided to remove the liquid nitrogen condensation trap, only use nitrogen, and use one size of wool (whole pieces of wool rather than strings ones).

Similar to in-situ arrangement, the configuration consisted of a furnace, a tube reactor, and a condensation train. Tube was 24 cm long with a diameter of 1.7 cm. Opposed to the in-situ arrangement where the length of the tube was more than 3 times of the furnace, in this arrangement

the tube and furnace length were almost identical (furnace length of 22 cm). However, to ensure that reaction occurred at the heated zone, a hollow tubing with length of 8 cm and diameter of 0.8 cm was used to support and keep the feedstock in the middle of the heated zone (Figure 3-6).

As illustrated in Figure 3-6, carrier gas (nitrogen) came in contact with wool first as it flew through the system. Evolved gas then came in contact with catalysts before exiting the reactor at the bottom. Mineral wool and metal mesh were used to avoid contact and mixing of the produced biochar and catalyst. Compared to in-situ case, the flowrate of injected nitrogen was increased (doubled to 100 mL/min). Since the reactor column was packed with wool feedstock in addition to mineral wool, this increase was necessary to overcome the back pressure caused by this packing. This in addition to the smaller size of the reactor, changed the residence time to 22 seconds.

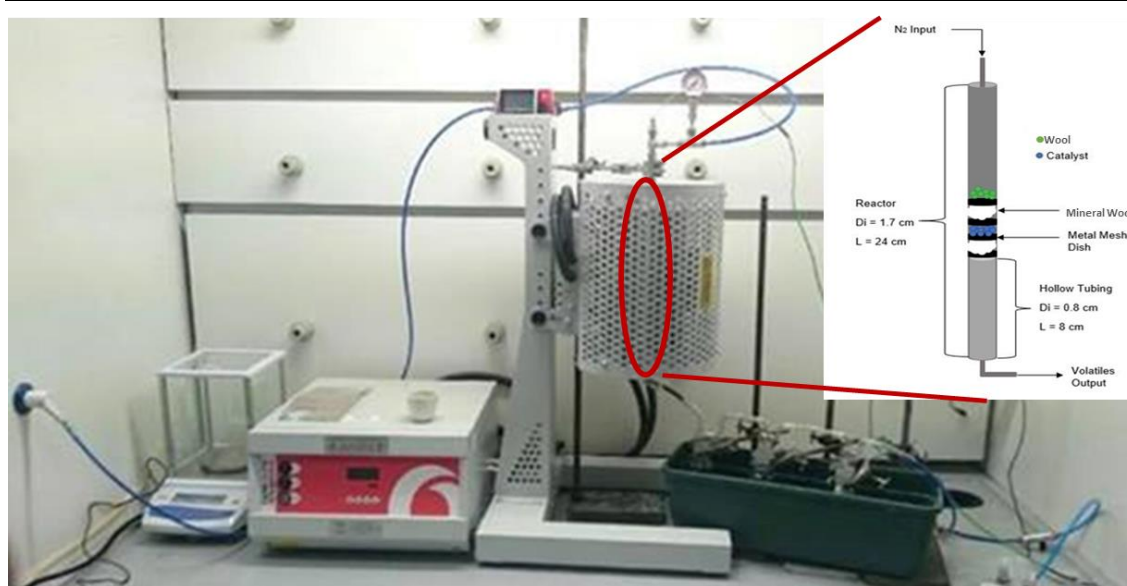


Figure 3-6: Ex-situ fixed bed configuration and order of material in the reactor tube

0.5 gram of wool and catalyst (overall feed weight of 1 gram) were added to the tube. Afterwards, the whole reactor (tube) was weighed using the same scale as in-situ case. After installing the tube in the furnace, the system was purged with nitrogen for 20 minutes. Then the furnace was turned on. Pyrolysis temperature was set at 500°C with a heating rate of 100°C/min. Reactor was kept at this temperature for 20 minutes to facilitate enough time for volatile generation. Reactor cool down period and product collection method were kept identical to the in-situ cases.

Al-KIL2 and 20-ZSM5 were used during wool catalytic pyrolysis. Since the heating rate and residence time was changed, in addition to wool catalytic pyrolysis with Al-KIL2 and 20-ZSM5, wool was pyrolysed on its own at 500°C using the new arrangement as a base case for comparison

with catalytic runs. For this tests, 0.5 g of wool was pyrolysed on its own with all the other elements staying the same.

3.2.4 Large Scale Reactor Selection Procedure and Set-Up Arrangement

It was decided to replicate wool pyrolysis tests using larger quantities of wool to analyse the practicality of industrial scale up for waste wool management. Initially, attempts were made to acquire and use currently established equipment to facilitate easy integration of the system in industrial scale. However, after reviewing the commercially available pyrolyser/gasifiers, it was concluded that due to the nature of the wool feedstock, a dedicated design was needed. Therefore, a wool feeder and reactor arrangement were designed. The design procedure/decisions made alongside the methodology used for wool pyrolysis in larger scale are presented in Chapter 4.

3.3 Products Analyses

In this section, the methodologies used to analyse feedstocks and catalysts in addition to pyrolysis by-products are explained.

3.3.1 Elemental Analyses (EA)

Elemental analyses were carried out using an Exeter CE-440 Elemental analyser in order to define the percentage of carbon, hydrogen, and nitrogen in the oil and char samples. To do so, samples were initially weighted in a small tin capsule to an accuracy of one millionth of a gram. This capsule was then inserted in the furnace (950°C) (Figure 3-7) where it was combusted in abundance of oxygen to form tin oxides which could reach temperatures above 1800°C. After vaporisation at this temperature, sample underwent complete combustion, forming H₂O, CO₂, N_xO_y and N₂ in addition to other by-products. Through use of scrubbing chemicals, undesirable by products such as sulphur, halogen and phosphorous were removed from inside the combustion tube.

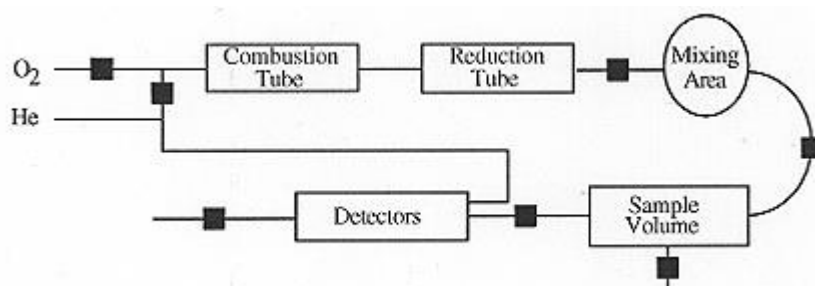


Figure 3-7: Schematic of Exeter CE-440 Elemental Analyser [3.8]

Afterwards, oxides of nitrogen were converted to N₂ and excess oxygen were removed by passing the gas through the reduction tube. Mixing area (downstream of the reduction tube) was used to homogenise these gases. The quantities of each gas (He, H₂O, CO₂ and N₂) were recorded in the

detector by series of thermal conductors. Eventually, the percentage of C, N and H was calculated from these readings and the weight of the sample. The amount of oxygen present in the gas is then calculated by difference ($O = 100 - (C + H + N)$). These values were then adjusted by factoring in the ash and water vapour quantities. Elemental analysis was carried out on the char and oil samples obtained from pyrolysis in addition to wool.

3.3.2 GC-MS

The GC-MS (Gas Chromatography-Mass Spectrometry) analysis is an essential tool for the identification of the variety of chemicals present in the liquid products (bio-oil) and the evaluation and optimisation of the process conditions in terms of producing high valuable compounds. The GC-MS tests were carried out using a GC 8000 series equipped with VG Trio 1000.

The column (length: 30m, inner diameter: 0.250; film: 0.25 μm) had temperature limits between 40 $^{\circ}\text{C}$ to 300 $^{\circ}\text{C}$. The oven was programmed to hold at 40 $^{\circ}\text{C}$ for 10 min, ramp at 5 $^{\circ}\text{C}/\text{min}$ to 200 $^{\circ}\text{C}$ and hold for 15 min, ramp at 10 $^{\circ}\text{C}/\text{min}$ to 240 $^{\circ}\text{C}$ and hold for 15 min, ramp at 10 $^{\circ}\text{C}/\text{min}$ to 260 $^{\circ}\text{C}$ and hold for 10 min. He was used as carrier gas with constant flow rate of 1.7ml/min and injector split ratio at 1:20 ratio. The end of the column was directly introduced into the ion source detector of VG Trio 1000 series. Typical mass spectrometer operating conditions were as follows: transfer line 270 $^{\circ}\text{C}$, ion source 250 $^{\circ}\text{C}$, electron energy of 70 eV. The chromatographic peaks were identified according to the NIST library to identify bio-oil components.

GC-MS tests were carried out on oil samples obtained from pyrolysis of model compounds, non-catalytic small-scale wool, catalytic pyrolysis of wool and large-scale wool.

3.3.3 FTIR

FT-IR (Fourier Transform Infrared Spectroscopy) was used to identify the functional groups present in the biochar and bio-oil samples. A PerkinElmer Frontier was for the analyses (Figure 3.8). During analysis, infrared radiation was applied to samples. The structure and molecular composition of the sample was then determined through analysing the wavelengths at which infrared light's energy was absorbed by the samples. Spectra data base were utilised to search the spectrum and assign the peaks observed on it to a function group.

To analyse char samples, sample were grinded using a pestle and mortar to form a uniform powder. Then, a base spectrum was obtained through running the FTIR machine with no sample in it. To analyse the oi samples, due to the high viscosity of them, they were diluted with acetone before analyses. Therefore, after running the machine with no samples loaded to it, acetone was analysed in itself. Therefore, acetone spectra could be subtracted from oil samples spectra.



Figure 3-8: PerkinElmer Frontier FTIR analyser used during analysis

3.3.4 TGA & MS

Thermogravimetric analysis was used to observe feedstock behaviour and change in behaviour by application of heat. Weight loss which could be due to decomposition, evaporation, desorption, and reduction could be detected by TGA. The TGA analysis were carried out using a TA Q500 (Figure 3-9)

As illustrated in Figure 3-9, three main parts of the analyser were the balance, furnace, and thermocouple. Furnace, coupled with the thermocouple, applied the heat in a controlled manner and with the assigned heating rate. The balance which was located in the casing and in an inert atmosphere, measured the change in the sample mass.

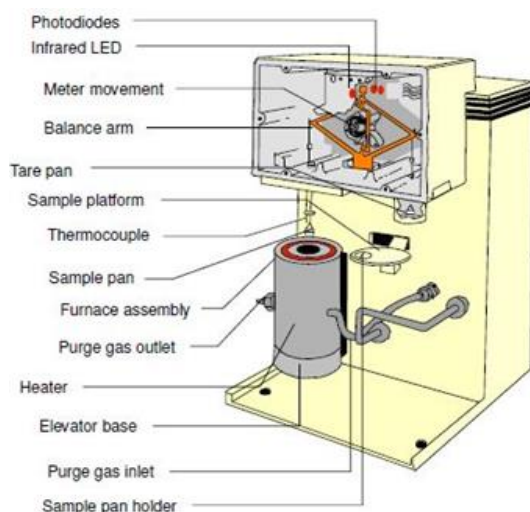


Figure 3-9: TGA Equipment schematic

Model compounds (with and without catalysts) and wool samples were analysed with the described configuration. Temperature program started with keeping the sample at 27 °C for 30 minutes and then increasing the temperature by 100 °C/min till it reached 500°C. It was then kept isothermal

for a further 15 minutes before cooling down to ambient temperature again. The samples for the TGA were kept between 15-20 mg and in the catalytic runs, the ratio of feedstock to catalysts was kept as 1:1. Furthermore, in catalytic runs, sample and catalysts were thoroughly mixed together. The gas flow was set to 20 mL/min of nitrogen. This analysis was carried out on catalyst on their own, model compound and wool.

Pyrolysis in TGA and decomposition of feed resulted in gas to be evolved. This gas was then fed into MS (Mass Spectrometry) analyser for the identification of the type and relative quantity of the gases. In this technique, gaseous ions were formed from samples via electron ionisation. Afterwards and before ion detection, mass to charge ratio of these ions were detected through use of magnetic fields. During ion detection, the relative abundance of each of ionic species were recorded. Then, to allow plotting the ion abundance vs mass to charge ratio, the ions were converted to electrical signals. MKS Cirrus MS was used for the test (Figure 3-10).



Figure 3-10: MKS Cirrus MS analyser used for gas analysis

3.3.5 Surface Analysis

BET (Brunauer–Emmett–Teller) analysis was carried out to figure out the available surface area of solid materials (char and catalysts) based on the assumption that the absorption occurs on multiple layers rather than just on a monolayer. Furthermore, analyses were carried out to identify the Langmuir surface area, pore volume pore width of catalysts and char. These surface analyses were carried out using a Micromeritics Gemini VII instrument (Figure 3-11).

Char and catalyst samples (quantities of 0.009 to 0.015 g) were degassed at 150 °C for a minimum of 4 hours before the run with the N₂ adsorption method at -195 °C. The surface area and pore size distribution of the samples were calculated by using the standard Brunauer–Emmett–Teller (BET) equation and the Barrett–Joyner–Halenda (BJH) method, respectively. All the surface area experiments were done at an environment with temperature of 77 K, hence liquid nitrogen was

used. Nitrogen adsorption was measured along an isotherm between partial pressures of 0.05 – 0.35 as this range was where the isotherm was maintained. This analysis was carried out on catalysts and char samples.



Figure 3-11: Micrometric Gemini VII and degassing heater configuration

3.3.6 Catalyst Acidity

To determine the surface acid strength of catalysts, temperature programmed desorption (TPD) was utilised. ChemBET TPR/TPD from Quantachrome instruments which were fitted with thermal conductivity detectors were used to perform CO₂ and NH₃ TPD. For 2 hours, 50 mg of samples were degassed in quartz U-tube using He at 200°C. The samples were then cooled down at room temperature using He. Afterwards, using 25 mL/min of 10% NH₃/He at 50°C, sample underwent NH₃ adsorption up to saturation. Then, to remove any ammonia from the surface, for 2 hours and at 50°C, sample was exposed to He at a flowrate of 25 ml/min.

Desorption was carried out with use of He at heating rate of 10 °C/min. Temperature with range of 50°C to 900°C was utilised to do so. Same procedures stated for NH₃ were carried out with CO₂. Acidities of synthesised catalysts were calculated from the NH₃ and CO₂ TPD curves peaks

3.4 References

[3.1] Sigma Aldrich, “L-Phenylalanine,” [Online]. Available:

<https://www.sigmaaldrich.com/catalog/product/sial/p2126?lang=en®ion=US>.

[3.2] Sigma Aldrich, “Cellulose,” Sigma Aldrich, [Online]. Available:

<https://www.sigmaaldrich.com/catalog/product/aldrich/435236?lang=en®ion=US>.

- [3.3] Sigma Aldrich, "Lignin," [Online]. Available:
<https://www.sigmaaldrich.com/catalog/product/aldrich/370959?lang=en®ion=US>.
- [3.4] B. Latourette, L. Raincy and C. Magnier, "Preparation of Zeolite of Type ZSM5". USA Patent 4,891,199 , 1990.
- [3.5] W. Widayat, A. N. Annisa, "Synthesis and Characterization of ZSM-5 Catalyst at Different Temperatures," *IOP Conference Series: Materials Science and Engineering*, 2017.
- [3.6] H. Song, J. You, B. Li, C. Chen, J. Huang, J. Zhang, "Synthesis, characterization and adsorptive denitrogenation performance of bimodal mesoporous Ti-HMS/KIL-2 composite: A comparative study on synthetic methodology," *Chemical Engineering Journal*, pp. 406-417, 2017.
- [3.7] M. Popova, A. Szegedi, H. Lazarova, A. Ristić, Y. Kalvachev, G. Atanasova, N. Wilde, N. N. Tušar, R. Gläser "Synthesis of biomass derived levulinate esters on novel sulfated Zr/KIL-2 composite catalysts," *Microporous and Mesoporous Materials*, pp. 50-58, 2016.
- [3.8] Heriot-Watt University, "Basic Theory and Operation," [Online]. Available:
<http://internal.eps.hw.ac.uk/services/analytical/chn-theory.htm>.

CHAPTER 4 - AUGER REACTOR DESIGN

In this chapter, decisions made in order to carry out the scale up of fixed bed are presented. Furthermore, the final arrangement of the scaled-up reactor and the modifications carried out to optimise the procedure are also discussed. Additionally, the test conditions and number of tests are listed.

4.1 Initial Review

Based on the initial literature review, the two most promising reactors for scaled-up pyrolysis/gasification were the auger and rotary kiln configurations. However, to reduce costs and risks associated with building a new system, available commercial reactors were considered first. For instance, the system illustrated in Figure 4-1, which is an example of a commercial concurrent downdraft small scale gasifier was considered as an appropriate choice for the purpose of this research due to the advanced stage (commercial stage) of the technique.

However, issues of this method impeded its further investigation. Firstly, as previously predicted, the vendors indicated that textile wastes presented poor flowing properties in this reactors configuration and would have resulted in frequent clogging of the feeding system due to the nature of the materials. Most of the vendors contacted (All power labs; MRC Green; Leaf Gasifiers; Trillion Gasifiers; Vulcan gasifiers; Superior gasification) stated that their reactors were not designed to work with waste and textiles. Only MRC Green package has been used for processing textile waste but mixed with wood chips (30% textiles: 70% wood chips). The vendor mentioned that using 100% textile waste will make operational issues within their system.

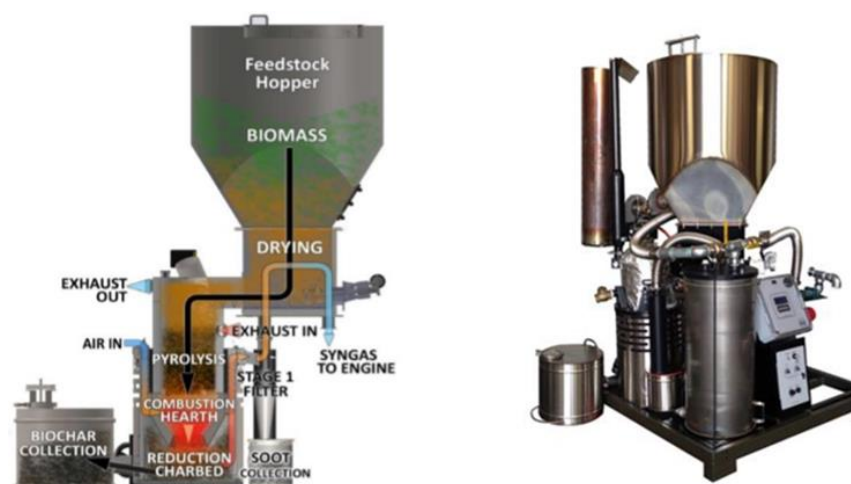


Figure 4-1: Some of the arrangements considered

Based on the above findings after contacting the vendors and the data presented in Chapter 2 regarding the advantages of auger reactors for wool pyrolysis, it was decided to design a reactor and feeding arrangement. In this chapter, once the requirements and constrains that are based on the feedstock are discussed, the basics of auger systems are listed prior to the presentation of the proposed system. Finally, the reactor testing and its consequent modifications are discussed.

4.2 Design Requirements & Constrains

The first step in designing procedure of the reactor was to clarify the objective of the reactor and consequently consider the constrains and limitations associated with the feedstock, the nature of the selected thermochemical methods and the available resources. Following are these constrains and why they were considered.

4.2.1 Feeding system

Due to the nature of the feedstock supplied by Harris Tweed, the designed system should have been capable of handling wool batches, which had different shape and density (Figure 3.1). Furthermore, the design should have had the capability of processing other forms of feedstock such as pebbled wool to evaluate other potential way to feed the wool to the reactor.

Since the uniformity and the general properties of the pyrolysis and gasification process are highly dependent on the residence time of the feed in the system, the rate of feed introduction in the combustion zone should have been controllable. Furthermore, the feedstocks should have been constantly mixed in order to avoid agglomeration of the wool pieces and consequently causing abnormality in the consistency of the feed introduced in the combustion zone.

4.2.2 Cost and Sizing

The reactor should have been capable of handling a volume of material which was large enough to be representative of a medium sized processing plant while keeping capital and operational costs to a minimum for a future deployment in small/medium enterprises. Also, the reactor should have been designed to be operable with minimum number of personnel to keep the costs down for new small size establishments. In case of the feeding rate, maximisation while keeping the costs to minimum both regarding the capital and operational cost was set as the goal.

Similarly, to reduce the budget required to operate the system, it should have been as reliable as possible to keep the cost of repair and delay in the process minimal. Therefore, all the connections should have been designed to be assembled by minimum number of personnel (ideally one) easily.

Additionally, the reactor should have been cleanable with a simple, quick, and sustainable procedure to keep the down time to a minimum

4.2.3 Operations

The efficiency and operability of the system is vastly affected by the system temperature and the pressure seal of the equipment. Therefore, a mean for leak-proofing of the system in addition to maintaining the high temperature of the heating zone should have been included. Also, a safe distance between the feeding zone and heating zone should have been thought of in order to keep the operation safe and assure the separation of the feedstock and products. This should have been coupled with appropriate thermal isolation of the tubing to avoid premature and unwanted condensation of vapours in the system.

The location of gas injection should have been designed in a manner to avoid back-flow of injected gas or produced gas. This should have been done simultaneously with the gas proofing of the system mentioned previously to assure continuous operation of the system was not interrupted.

Finally, a method to cleanse the incondensable gasses generated in the system should have been incorporated to test the practicality of the process regarding the emission standards.

4.3 Proposed Design

The design of the system should have addressed all the constrains and requirements discussed above. Therefore, a start to finish approach coupled with continuous communication with potential manufacturers was taken to draw an overall design of the system which was practical. The first stage of design was focused on the feeding system. Generally, augers are installed downstream of a storage unit for transportation of feedstock into the processing facilities. Although auger-type reactors have been successfully designed for wood feedstock (Table 2.7), practice in processing wool in an auger system with possibility of scale up to plant size was close to none and consequently, a method for storage should have been considered. This storage unit should have had the following constrains:

- › Gas-sealed
- › Maximised Capacity
- › Capable of handling wool feedstock without blockage

Complying with these requirements, a hopper was selected as the suitable storage method. A hopper coupling with an auger feeder is industry norm for delivering solid material into the system [4.1]. A hopper has the flexibility to store variety of feed load and integration of other techniques

into it to further assist the flow of the unconventional wool feed could be carried out. Furthermore, it is a low-cost equipment with no moving parts, keeping the CAPEX and OPEX to a minimum. However, modifications to the standard use of this arrangement, i.e., hopper coupled with auger feeder, was needed to satisfy the gas-sealed requirement. In other words, opposed to industry standard where continuous feeding from hopper onto the auger is carried out, a batch process in which the hopper was loaded, sealed, and connected to the auger was selected for the wool-dedicated set-up. However, the loading method of the hopper should have been designed to facilitate easy reloading of new batch for increasing the average flowrate of the system.

The next requirement needed to be addressed was the control of the feeding rate to manage the uniformity of the products and the overall process. This could have been managed by installation of controllable motor for the operation of the auger. However, a safe distance between the feed and heating zone should have been accounted for. Additionally, due to the lack of experience in textile waste pyrolysis via an auger feeder, an extra degree of separation between the heated zone and the feeding section would have made it possible to test these two sections/operations independently. Therefore, it was decided to install two auger feeders instead of one; the first one for pulling the feed down from the hopper outlet and transporting it to the second auger which transfers the feed through the heated zone. The additional hopper would have improved the mixing of feedstock [4.1] while reducing the possibility of wool pieces getting attached together (forming wool balls) prior to entering the heated zone. Both augers should have been controlled by a speed variable motor to control the feeding rate. Additionally, gas injection points were required for the process.

The next step was selection of the furnace. For this, it was decided to have a furnace that could reach temperatures over 1000 °C with minimum heated zone of 30 cm to allow enough residence time for the wool in the reactor. It was decided to research the market and find a furnace which could maximise the size of the heated zone within a small commercial scale. The sizing of other components of the system therefore were dependant on the dimensions of the furnace.

Finally, methods for collection of the products should have been considered. These consisted of gas, liquid, and solid products. The char should have been collected close to the exit of the heating zone to avoid the condensation of the produced bio-oil into it. To collect the liquids, first a condensation system should have been installed followed by a liquid container. Also, after collection of condensable gases, a gas scrubbing method was required to minimise the emission of toxic gasses such as NO_x into the environment. The overall schematic of the proposed system is illustrated in the Figure 4-2. As illustrated, it was decided to install the overall system on a movable bench for

ease of operation and transportation of the system. Next, the designing procedure of each section of this system is described followed by the detailed description of operational procedure.

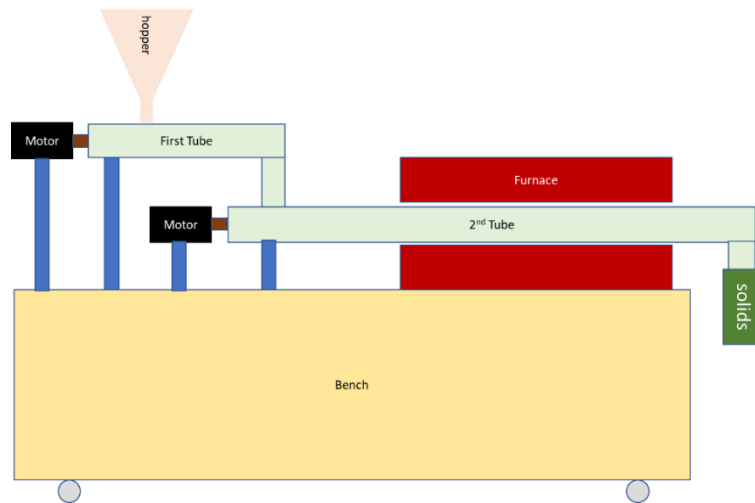


Figure 4-2: The overall schematic of the initial proposed system

4.4 Design Decisions

In this section, design decisions made to design and build the proposed design are discussed. The sub-sections in this chapter are inter-connected due to the design method taken.

4.4.1 Hopper Design Review

Hopper was the first equipment to be designed. Figure 4-3 illustrates the components of a typical hopper. The required hopper for the current design did not need the feeding conveyor since the process was a batch one. Similarly, since the primary role of the cylindrical part of the hopper was storage of the built-up material prior to falling into the hopper section, it was not needed in a batch process. Also, since the operation of the first tube and auger arrangement discussed previously was dependent on the design of the hopper outlet, also known as the feeder component in hopper, their design should have been carried out simultaneously.

The first step of design was to comply with the process storage requirements which itself required the consideration of several aspects such as discharge rate, safety, feed uniformity, etc. Therefore, the following objectives was set:

1. Storage capacity should have been maximised within the constrains
2. Hopper to be operated indoor
3. The feed should have only been kept in the reactor for less than a day (to avoid moisture build up in the feed)

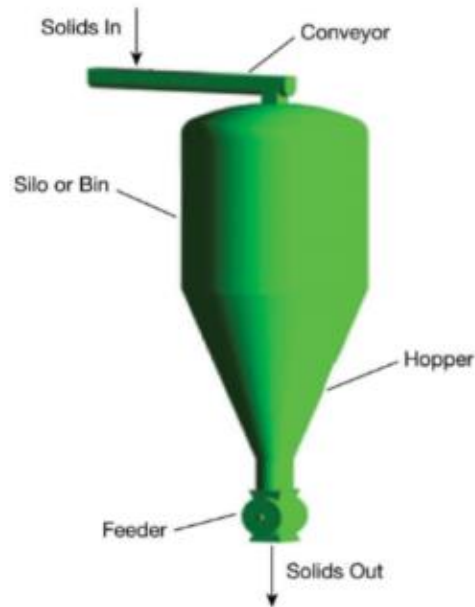


Figure 4-3: The typical components of a hopper feeding system [4.2]

-
4. The feed would have been at room temperature and pressure
 5. The feed was not going to be corrosive and therefore special fabrication was not needed
 6. The feed was not toxic and dangerous at room temperature
 7. The material shape and properties (density and structure) made it prone to segregation and agglomeration

With hoppers, a variety of issues associated with the flow of the material were expected. Some of them were [4.1, 4.2]:

- Flooding: a situation in which the fluid flow through the outlet of the hopper cannot be controlled
- Arching (bridging): as written in the title, in this situation, an arch is formed on the outlet of the hopper which blocks the flow of the material (Figure 4-4). If collapsed suddenly, it can lead to system failure or distribution to the flow rate of the feed.
- Ratholing: another flow blocking condition in which the flow of material from the hopper is localised, which leads to the formation of a stable channel. Issues such as reduced capacity of the hopper (as much as 90 % reduction in capacity) [4.2] or caking due to the stagnation of feed for long period of time
- Segregation: this could cause uniformity in the feed and consequently the product distribution. It can happen due to the difference in the density, size, or shape of the feed. It can lead to the build-up of material in the system and consequently lead to system failure

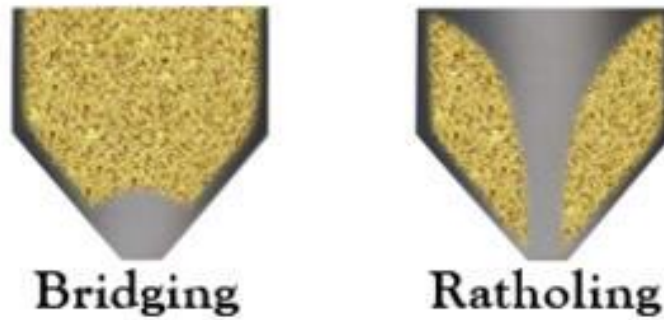


Figure 4-4: Some of the operational issues in flow out of hoppers [17]

Therefore, the next step was to predict which one of the above scenarios were most likely to happen and consider techniques to prevent them. This required a thorough understanding of the feedstock properties such as particle size, shape, density, moisture content. Understanding the above assisted in determining which type of flow pattern was more suitable for such as feed and therefore least likely to lead to the above operational issues.

There are generally two types of flow in hoppers: funnel and mass. In funnel flow (Figure 4-5), the system works on a first in/last out basis. In other words, the flow occurs in the centre of the hopper while the rest of the bulk material is stationary at the wall of the hopper. This system works best when the material consists of coarse material which do not form cakes if stayed stagnant for a long period of time or are free flowing [4.3]. In the case of the wool feedstock, However, the material was prone to agglomeration and was not free flowing. Therefore, this method was not considered the most economic method to be applied, due to the high potential of operational issues.

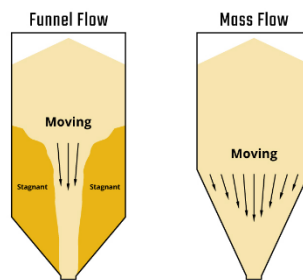


Figure 4-5: Two main flow types in Hopper [16]

To prevent these potential issues, mass flow, the other flow pattern option, could have been aimed for to store and feed wool. In a hopper with mass-flow design, the first in-first out design allows uniform feed flow. This is achieved because the feed flow is primary due to the angle of the hopper allowing feed to flow on the wall of it. Having the correct wall angle and right roughness of the

wall, therefore, are a key factor in achieving the desired design. Furthermore, the prevention of arching is highly dependent on the outlet size.

The next step was to decide the overall shape of the hopper. Generally, as illustrated in Figure 4-6, hoppers typically have 4 different construction arrangement. Regarding the opening however, there are two choices: square/rectangular or circular. A square opening has advantages such as lower manufacturing cost and larger volume per unit of height while suffering from issues such as stagnation of materials at the wall corners which could be a key issue regarding the wool feedstock [4.2].

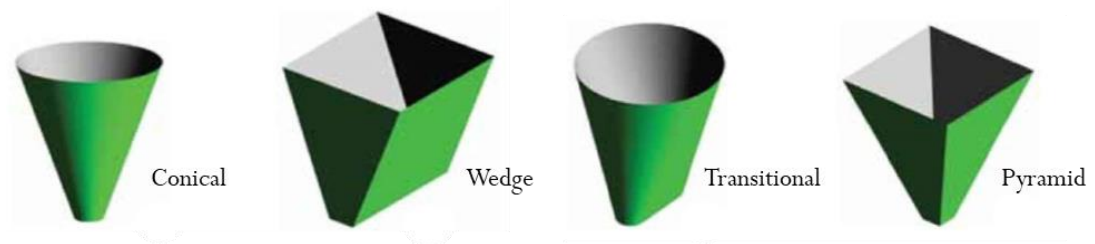


Figure 4-6: Typical hopper opening types

Another aspect previously mentioned was the fact that the designed system should have been in such scale that it could be installed in an indoor laboratory or small industry scale. Therefore, keeping the size and dimensions of the equipment as small as possible was one of the objectives. Satisfying this requirement, wedge and transitional hoppers typically need less headroom since mass flow can be reached in them with up to 12 degrees less steep [4.2]. Another important section was the outlet shape. Slotted hoppers can generally have higher flowrates due to the higher area of the outlet. These reasons led to choosing the transition hopper as the optimal one followed by the wedge shape. Both designs were expected to perform well with wool feedstock while avoiding stagnation of feed was prioritised to a less capital extensive choice. This decision meant that the opening needed to be rectangular rather than circular.

Eventually, the sizing procedure of the hopper was initiated. Various research has been done on how to size a hopper for achieving mass flow and most of these researches are derivatives or modifications of Andrew Jenike method was developed in 1950s [4.4]. However, there were some issues associated with this method application for wool flow. First, this method effectiveness is largely dependent on the nature of feed. This on itself was problematic because literature data on designing hopper parameters for wool were not available and most of the literature were focused on flow of particles, powders, and dense small material. Also, the properties of the supplied wool by Harris Tweed were variable and therefore the designed system needed to be flexible regarding the feedstock properties. Therefore, it was decided to design the hopper based on the overall system

requirements while building prototypes with the data which were resembled wool properties more closely.

4.4.2 Furnace Review

The first step of design, however, was to select a suitable furnace. To do so, several furnace vendors who could manufacture the design presented in Figure 4-2 were contacted. These companies were Carbolite (UK) (Figure 4-7), Nabertherm (Germany), Zhengzhou Technology (China), Shanghai Alarge (China) and Nanyang Xinyu (China).



Figure 4-7: Carbolite Furnace

Among them, Zhengzhou was selected as the manufacturer due to the advantageous quality/cost and their record of satisfied customers in the Europe. The furnace had a 60 mm internal diameter with a heated zone of 60 cm. Table 4-1 illustrates the properties of the furnace. The size of the rest of the reactor components were then based on the furnace.

Table 4-1: Design conditions of furnace

Max Temp.	1200°C for short time
Continuous Working Temp	$\leq 1100^{\circ}\text{C}$ (800-900 degree)
Temperature Zone	Single
Heating Rate	Suggestion $0\sim 10^{\circ}\text{C}/\text{min}$, max. $20^{\circ}\text{C}/\text{min}$
Temperature Control Accuracy	$\pm 1^{\circ}\text{C}$
Heating Element	Fe-Cr-Al Alloy doped by Mo
Furnace tilt angle	$0\sim 45^{\circ}\text{C}$
Max. Power	5kw
Heating zone	60cm
Working Voltage	AC 230V single phase, 50 Hz
Temperature Control	PID automatic control via SCR power control
Heating curves	30 steps programmable
Chamber material	Alumina Fibre

Next step was to decide on the material of construction. Since the furnace reached high temperatures, the material should have held its integrity at high temperature. In function of a potential scale-up of the reactor, stainless steel 310 (SS310) was selected as functional and cost-effective material. The alloy can withstand continuous temperatures of up to 1150 °C [5] and high resistance to corrosion and oxidation due to consisting of 20% nickel and 25% chromium [4.6]. Additionally, this combination makes this alloy suitable for situation where sulphur exists which is highly probable in wool pyrolysis. Table 4-2 illustrates the components of SS310. Also, due to the low thermal conductivity of SS310, the feeding section and heated part can be closer compared to use of other metals without risking the extension of reaction zone.

Table 4-2: Chemical composition of stainless steel 310

Carbon	0.25
Chromium	24.0-26.0
Nickel	19.0-22.0
Manganese	2.00
Silicon	1.50
Phosphorus	0.045
Sulphur	0.030

4.4.3 Other Components of Design

After finalising the furnace design, the overall size of the system was decided. Auger feeders in industry can have a large range of size, starting from shorter than 1 m to longer than 30 m [4.7]. As mentioned previously, the furnace had 60 cm of heated zone. In addition to that, there was a need for isolation around the furnace inlet and outlet to minimise unintended heat transfer. Generally, ceramics are used for this purpose. Initially, it was decided to size this section and supply the manufacture with the overall sizing of the second tube. However, the manufacture requested flexibility in this aspect of the job and offered to build and test the furnace so it would have sufficient thermal isolation. Therefore, they requested to be supplied with the size of the tube pieces which were out of the furnace and they would then design the overall system.

The design of the second tube started with an end to start approach. The distance between outlet of the furnace and the condensation system, i.e., the gas outlet, should have been minimised. Therefore, only enough length, just for the solid outlet and allowance for the solid container to pass the bench surface was allocated. Considering that the char particles were going to be small, the size of the outlet did not need to be too large or complicated. Therefore, a square opening with a side size of just smaller than the tube diameter, i.e., 45 mm was selected. In order to size the rest of the second tube, and consequently the inlet size of it, the auger was designed. This was necessary

because the efficiency and therefore the design of the auger was the key factor in the sizing of the inlet.

In order to design an auger, several design factors should have been considered. Figure 4-8 illustrates the main parts of a typical auger and the nomenclature. The drive shaft was attached to a rotary motor while the end shaft was fitted into the end bearing for support. The feed was then caught by the blade and drove through the tube. The whole system was supported by mounts (saddles) for avoidance of shaking and movements during operation. The size of the pitch, flight and core were determinants in the efficiency of the feed withdrawal. Therefore, each of these parameters was modified to create several auger arrangements.

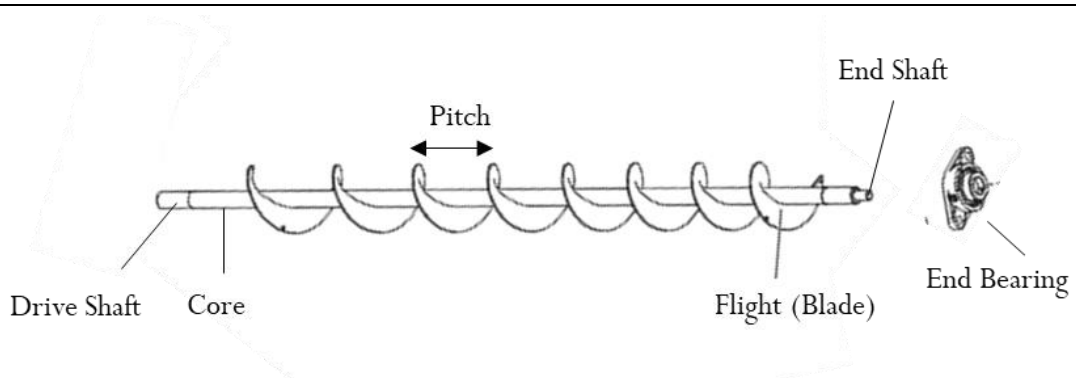


Figure 4-8: Auger main parts and nomenclature

Before continuing, the suitability of the other types of auger feeder, shaftless ones (without core), was considered. Typically, shaftless augers are the first choice for handling sewage sludge and in general sticky, high moisture, and sluggish feed [4.8] where the material could stick to the attachment point of the flight to the core [4.9]. Wool feedstock had some similarities to the material handled with shaftless augers. However, some of the drawbacks of it prevented further consideration of this system. Firstly, unlike shafted augers, shaftless ones touch the wall of tube due to the lack of central core. This is one of the reasons behind successful use of shaftless augers with high moisture feed [4.10] [4.11]. The wool feed does not resemble these properties. Furthermore, the nature of the wool feed makes it prone to built-up and backflow in the empty core of the shaftless augers. Finally, the type of material handled by the 2nd auger in the proposed system changed in the furnace with the pyrolysis reactions (conversion to char). Therefore, the shaftless augers were deemed unsuitable to handle the biochar formed, which had a fine powder and light particle shape.

The optimal design would have been one which distributed the empty space available in the auger pitch evenly underneath the hopper outlet. If this was not achieved and the auger was not designed efficiently, issues such as excessive power usage, high maintenance cost, variation in the

composition of feed, and quality issues due to non-uniform residence time and feed agglomeration [4.7] [4.12] could have occurred. J.W. Fernandez categorised these variations in industry into 6 main ones [4.13] (Figure 4-9):

1. Constant core, constant flight diameter, constant pitch
2. Constant core, tapered flight diameter, constant pitch
3. Constant core, constant flight diameter, variable pitch
4. Tapered core, constant flight diameter, variable pitch
5. Tapered core, expanding flight diameter, constant pitch
6. Tapered core, parabolically expanding flight diameter, variable pitch

The first decision made was for the type of pitch to be used. There are generally 3 different arrangements: full pitch, half pitch and 2/3 pitch. The full pitch is the standard type in which the pitch size is equal the flight diameter. This type is the most efficient in case of the volume of feed to be handled unless the system is inclined [4.14]. Since the nature of feed was not similar to the material typically handled in auger feeders, inclination would have not helped the flow since it was likely to form large agglomeration of feed and consequently would have led to blockage of system. Therefore, standard pitch was selected.

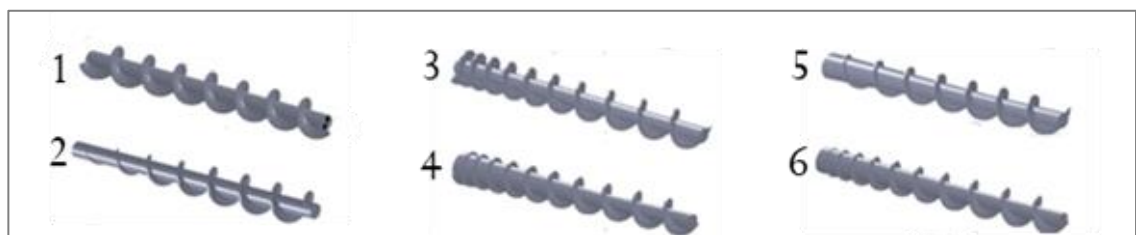


Figure 4-9: Types of auger [4.18]

Regarding the flight diameter, tapered ones could be beneficial in scenarios in which the feed material can move freely on top of each other in the tube, such as fine granules. However, using constant flight was deemed more suitable for wool due to the cohesiveness nature of it and constant requirement of the material to be assisted forward. The size of the flight therefore was selected as 48 mm to account for expansion of stainless steel under operational condition. Consequently, the pitch size was also selected to be 48 mm. The closeness of the flight size to the tube internal diameter was to avoid feed passage over the flight and stagnation along the tube. Also, increasing the gap would have decreased the capacity of the system due to reduction in effectiveness of the blades. Moreover, in this heated system, the blades themselves should have carried out the task of avoiding backflow. This was in contrast with non-heated systems with more standard feeding

material such as granules where the materials get compacted after drawdown by the blade, resulting in avoidance of gas backflow [4.15].

Finally, the core arrangement of the auger had to be set. The standard core size is between 30 to 35% of the flight diameter. W. Fernandez concluded that generally, hoppers with expanding pitch and tapered core perform noticeably better than a standard arrangement (i.e., arrangement No. 1) in improving the draw down from a hopper or other types of feeder (Figure 4-10). However, a larger shaft and more flights means that the auger will be heavier and therefore the operating, maintenance and capital cost are higher. Therefore, due to the uniqueness of the feed and to incorporate the advantages of both designs, it was decided to have a customised auger design.

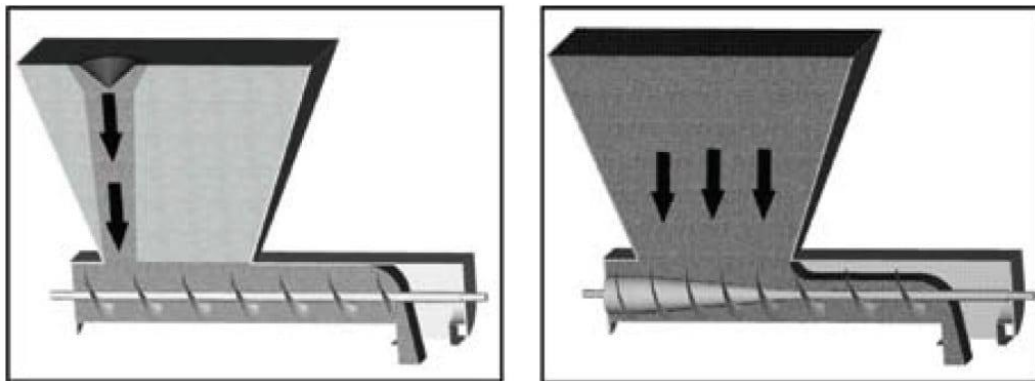


Figure 4-10: Tapered core performs better in facilitating mass flow (uniform flow) [4.14]

In this design, the first and second pitches were reduced by 25 and 20 % respectively and the rest of flights had standard pitch. Regarding the core, due to the size of feed material, it was decided to minimise the core size to maximise the probability of the wool pieces to be grabbed by the blades. However, to utilise the benefits of a tapered core arrangement, the core was enlarged by over 80 % along the first two pitches. This arrangement over the first two flights could have had the benefits of an arrangement in which the whole auger had tapered core and variable pitch arrangement without the cost sacrifices if the inlet dimensions of the tube were sized accordingly. Therefore, the inlet of the tube was designed to have a length of 8 cm.

Next step was to size the first tube. In order to avoid overflow of feed and make the controllability of the system more precise, the volume of the feed entering the first tube should have been kept smaller than the second one. This was achieved through reduction in the tube diameter by 30% to 35 mm. Consequently, the auger diameter was also reduced proportionally. Also, to maximise the feeding flow of tube 1 into tube 2, the width of both inlet of the 2nd tube and outlet of the 1st tube was set to 33 mm which was as close as possible to the internal diameter of the 1st tube.

Next, the outlet size of the hopper (1st tube inlet) was designed, due to the importance of the flow assurance from the hopper into the feeder. Following the previous decision on having a transitional hopper with a slotted rectangular opening, the width and length of the opening was assigned. For sizing noncircular orifices to avoid arching and other flow issues, established correlations derived by Beverloo [4.20] or Rose and Tanaka [4.21] could have been used. However, as mentioned earlier, the nature of the wool made these correlations near to non-relevant and therefore, it was decided to set the inlet size equal to that of the second tube while using the same auger arrangement for the same reasons. However, to assure that the selected sizes of inlets and outlets were reasonable, prototyping method was used.

It was decided to test openings made-out of cardboards with widths ranging from 2 to 5 cm with increasing size steps of 0.5 cm (since the size of wool pieces was 1 by 1 cm). Also, the length of the inlet was varied between 4 cm to 10 cm with 1 cm increase steps. Also, in order to replicate the auger design arrangement, a standard stand-alone auger that was available at the University workshop was utilised.

The tests were done with 2 different auger arrangement. A set of runs with the auger as it was and the rest with auger being modified to represent a model as close to the selected design shape as possible. To do so, the two first pitches of the auger were filled with putty to shape a taper and then covered with transparent tape to stimulate the frictional properties of polished stainless steel. Between 20 to 50 grams of wool were added to each slot size and the auger was rotated manually underneath it while being stabilised on a flat surface. The amount of wool was chosen on the basis to fill the slot without being in touch with the slot walls.

In case of the widths, any increase over 3.5 did not result in noticeable improvement in the flow. However, values below 2.5 resulted in random bridging in the slot. In case of the width, any increase over 7 cm did not improve the flow while values below 5.5 resulted in delayed accumulation of wool and eventual blockage of the system. The effect of auger design was the most noticeable one. While the standard auger performed better in drawing in the first feed, it left part of feed stagnant at the outer part of the slot. More precisely, the standard arrangement had higher flowrate and quick to grab the first wool pieces while the designed arrangement proved to provide more uniform and flawless flow.

The exact size of the first tube was not critical as long as it allowed the feed to be controlled between entering it and exiting it. Therefore, only an additional 80 mm, which was equal to the size of the inlet and outlet would have sufficed. However, after discussion with the manufacturer, it was

decided to elongate the first tube so the motor for operation of the second tube could be fitted underneath it.

Finally, the power of the motors was set. The system needed to be as flexible as possible due to the unknown behaviour of the system. However, to have exact values, the weights of the augers were needed to be known. After discussion with the manufacturer, it was agreed the motor selection to be carried out by them with the requirement being that it should have had operational range of 2 to 40 rpm. Table 4-3 and Figure 4-11 illustrate the sizes of the tubes and augers.

Table 4-3: Sizing of the augers and tubes

Number of Augers	2
Material of Augers (both)	Stainless Steel 310
Material of all the Tubing	Stainless Steel 310
No. Of Motors	2
Motors Rate (RPM)	2-50
Type of Augers	Helical or Sectional
Tubing 1, Length (mm)	380
Tube 1 Internal Diameter (mm)	35
Tube 1, Inlet Length (mm)	80
Tube 1, Inlet Width (mm)	30
Auger 1, Shaft Length (mm)	380
Auger 1, Flight Outside Diameter (mm)	33
Tubing 1, Outlet Length (mm)	80
Tubing 1, Outlet Width (mm)	33
Tubing 2, Length (mm)	1100
Tube 2, Internal Diameter (mm)	50
Tube 2, Inlet Length (mm)	80
Tube 2, Inlet Width (mm)	33
Auger 2, Shaft Length (mm)	1100
Auger 2, Flight Outside Diameter (mm)	48
Tubing 2, Outlet Length (mm)	45
Tubing 2, Outlet Width (mm)	45
Tubing 2, No. of Gas Orifices	2

Finally, the hopper was sized. Similar to tube and auger design, due to the non-typical type of feed, prototyping was utilised. Since the outlet was already set, the next design aspect was the side and end angle (Figure 4-12). To do so, 4 cardboards were cut and attached independently to the slot chosen as the hopper outlet. Initially, the end wall angles were fixed at 90 degrees while decreasing the side wall angle from 45 degrees. While doing so, 100 grams of feed was added to each arrangement with a 1 kg weigh putting on top of the feed to facilitate the flow of material. Initially, angles were decreased by 5 degrees steps to observe the effects. It was found that angles sharper than 15 degrees resulted in sudden flow of all feed to the outlet and agglomeration of feed resulting to blockage while angles over 20 degrees led to stagnation of feed on the walls. Therefore, angles

were decreased by 1 degree between 20 to 15. However, not any significant change was recognised between 19 to 15. This could have been due to the inaccuracies in the angle modifications since they were carried out by hand. Therefore, it was decided to choose 17 degrees as the side angle as an average of the two extremes.

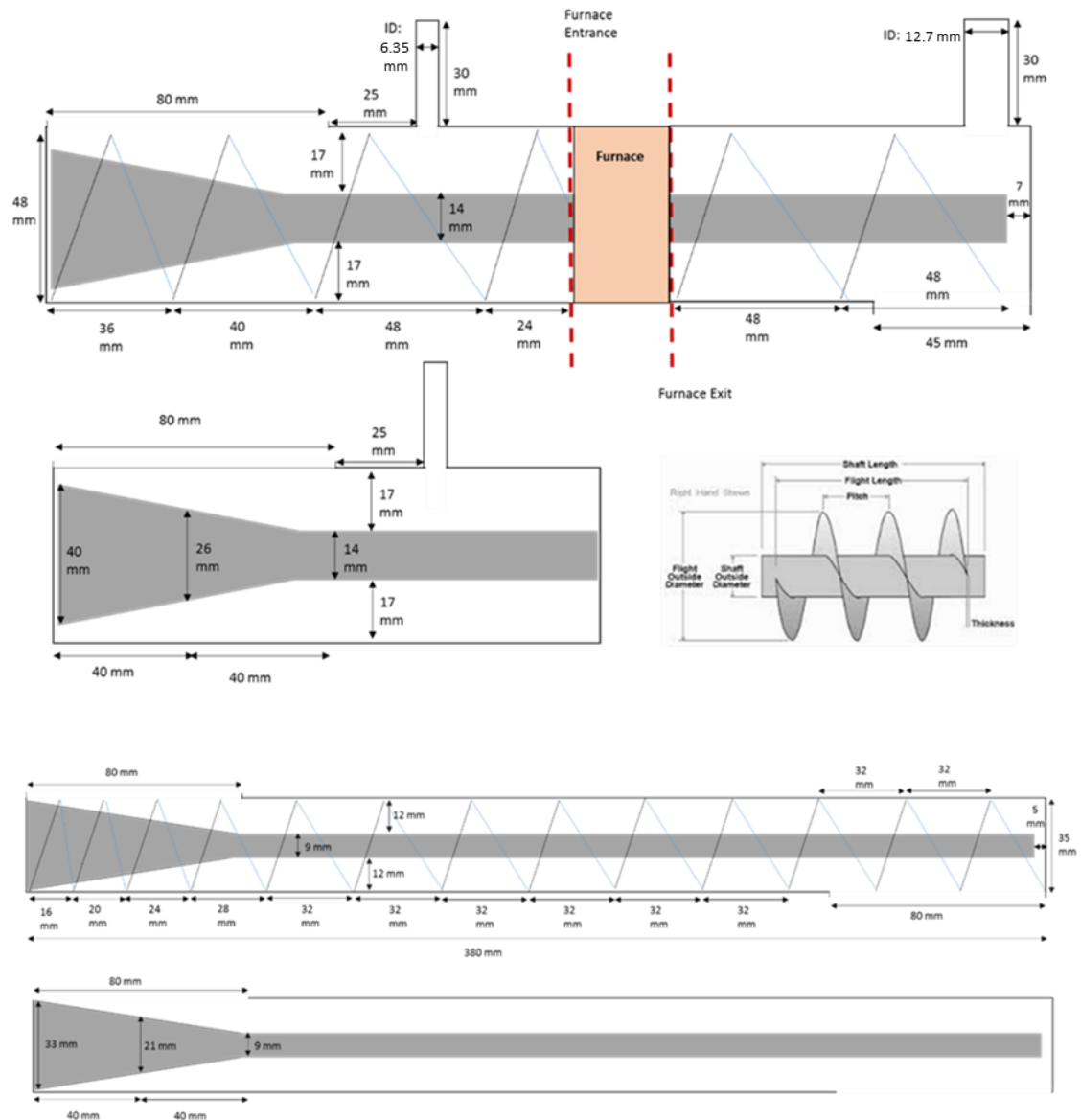


Figure 4-11: The sizing of 2nd tube (Top) and 1st tube (Bottom)

The same procedure for the side angles were followed by the end angles while keeping the side at 17 degrees. At this stage, decreasing the angle from 90 degrees was done to simulate a transitional hopper arrangement rather than a wedge shape. It was observed that an angle increases of over 20 would lead to stagnation while an angle of over 10 would improve flow control while resulting in smaller headroom. Therefore, 15 degrees was selected as the optimal angle. Regarding the height and consequently volume of the hopper which could have been detrimental in the flowrate out of the hopper, several approaches were considered. Initially, it was decided to assign a volume for the

hopper and then assign a height. This assumption would have worked if the volumetric flowrate of the wool was predictable. However, due to the variable compactness of the wool and uncertainties about the flow pattern of the wool, this method was redacted. Instead, it was decided to design the hopper as large as possible given the mechanical and space constrains. Therefore, after discussions with the manufacture, the overall height of the system was considered and largest height possible was 60 cm. This allowed for the system to be assembled by one person while not compromising its functionality.

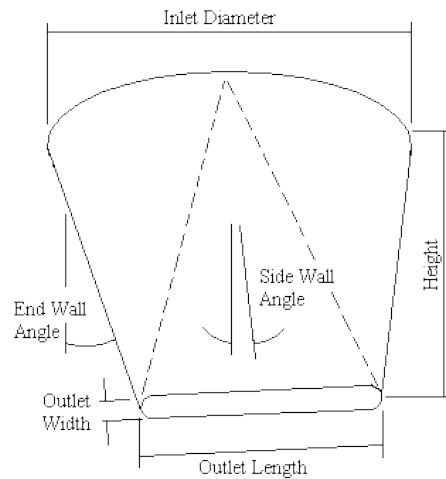


Figure 4-12: Nomenclature of a transitional hopper [4.19]

Since the start of the design, it was realised that the flow out of the hopper might need further assistance. This expectation was further proved during the prototyping, when the flow out of the hopper seemed slow and infrequent. That was why a weight was used to simulate the flow. In the actual design, it was decided to install a vibrator on the wall of the hopper. This was done due to the light weight of the feed. This hypothesis was tested by gently shaking the prototype. However, this was installed for applying programmed pulses to the hopper rather than continuous operation because it was predicted that this could cause the system and specially the joints (connections) to lose mechanical integrity in the long term.

Finally, the gas injection and extraction points were selected. Two possible locations were considered: the top of hopper and on the second tube, just before the furnace entrance. The top of the hopper would have been a good option since it would have covered the complete path of the reactor and therefore avoid any gas backflow. However, some operational issues such as pressure drop due to the requirement for the gas to pass the feed in stored in hopper were more probable. Additionally, extra volume to be purged by the gas would have increased the gas usage. Therefore, the entrance to the furnace was selected initially so the injection point would be as close as possible to the pyrolysis gas generation point. However, a secondary gas injection point was installed on top

of the hopper in case of gas back-flow issues during the tests. The size of the gas outlets and inlets were set as 0.5 inch (ID). After sizing all the design components, the schematic illustrated in Figure 4-13 was sent to the manufacturer while Figure 4-14 shows the final built auger reactor set-up at manufacturer facility.

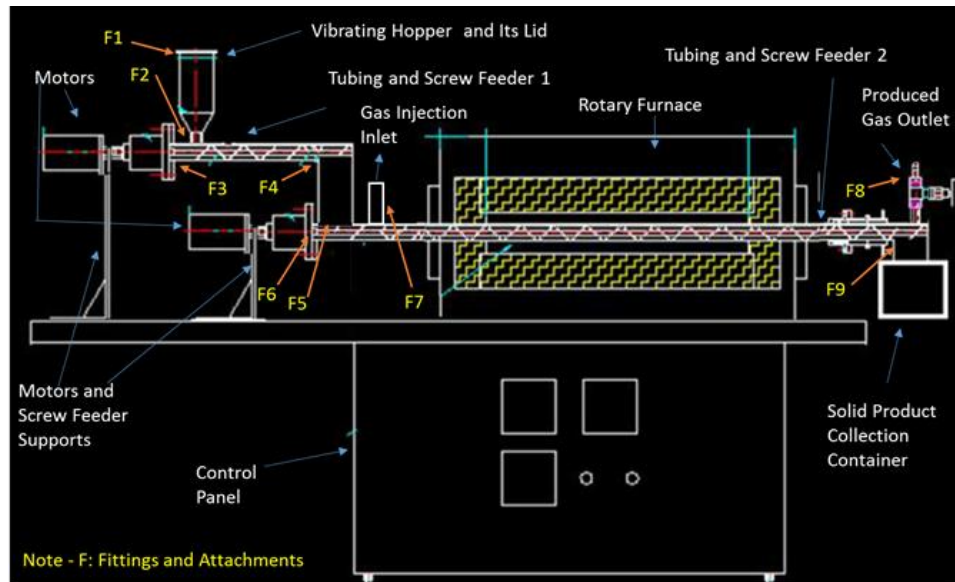


Figure 4-13: The final schematic of the reactor arrangement

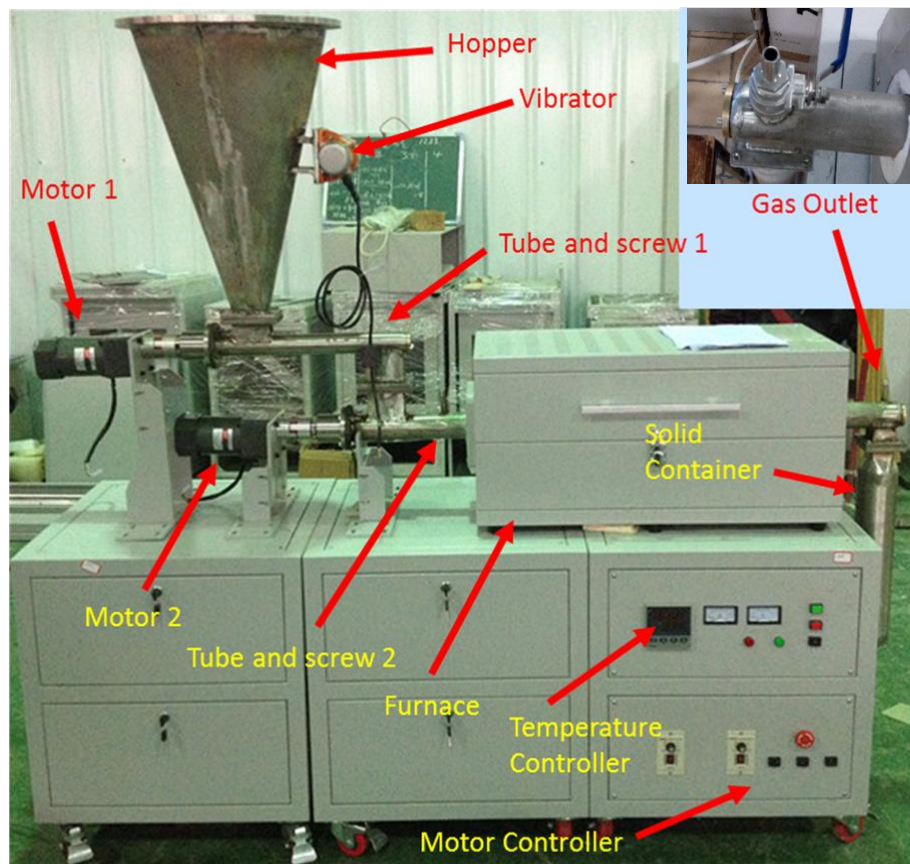


Figure 4-14: Pre-shipping arrangement of the reactor

To condense the condensable fraction of the gas produced, several condensation arrangements with different condensers such as Aldrich® super condenser, Aldrich® Liebig condenser, Quickfit® Liebig condenser and Quickfit® jacketed coil condenser with different contact surface areas were considered (Figure 4-15). After considering their efficiency in oil condensation, two Quickfit jacketed coil condensers in series were selected and a 250 mL Schlenk tube was installed at the bottom of each of them to collect the oil. This system gave an overall contact area of 800 cm² between the oil and the cold water, which was used as the cooling agent. In this arrangement, water was continuously run through the coils while the oil passed around it. This arrangement was selected to avoid blockage of gas flow caused by the condensation of the oil in the coil. If this system was successful, the water could be recycled back into system through installation of heat exchangers and pumps. Alternatively, in the future, the two 250 mL Schlenk tubes, which were being used for storage of the oil could get immersed in the water, ice, or liquid nitrogen for enhanced condensation capacity. This way, as well as increasing the contact area, the oil production might potentially increase.

Connection between the gas outlet and the condensers was carried out via a stainless-steel tube and rubber stopper with one hole in the middle. Stainless steel was used due to the high temperature of the gas coming out of the system and rubber stopper because of its expandability and being a good sealant. Furthermore, the tube was isolated with mineral wool covered with aluminium foil to minimise condensation in the tube leading to the condensers, facilitated by sudden temperature drop.

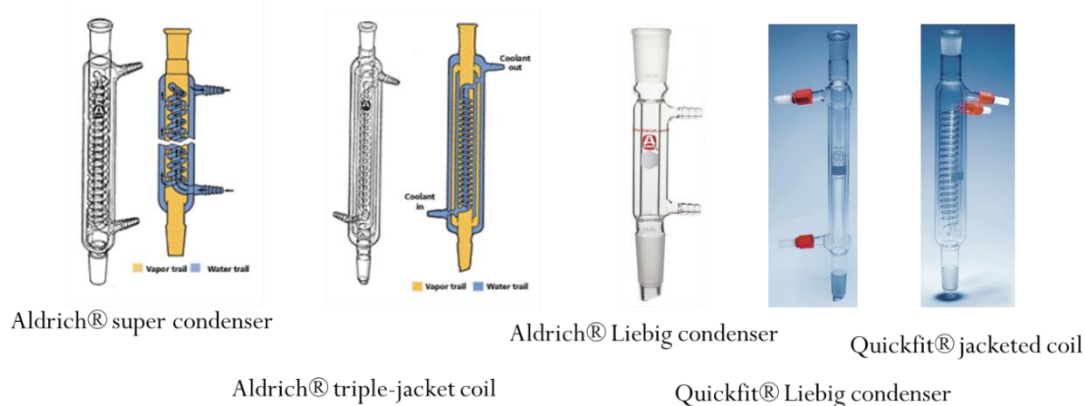


Figure 4-15: Considered Condensers (all acquired from Sigma Aldrich)

The condensers were connected to each other and to the water supply with laboratory flexible plastic tubes. Before emitting the gas into the atmosphere, it was scrubbed with water to remove not condensed acid pollutants and minimise the amount of the unwanted harmful components. The whole condensation and water scrubbing systems are illustrated in Figure 4-16.

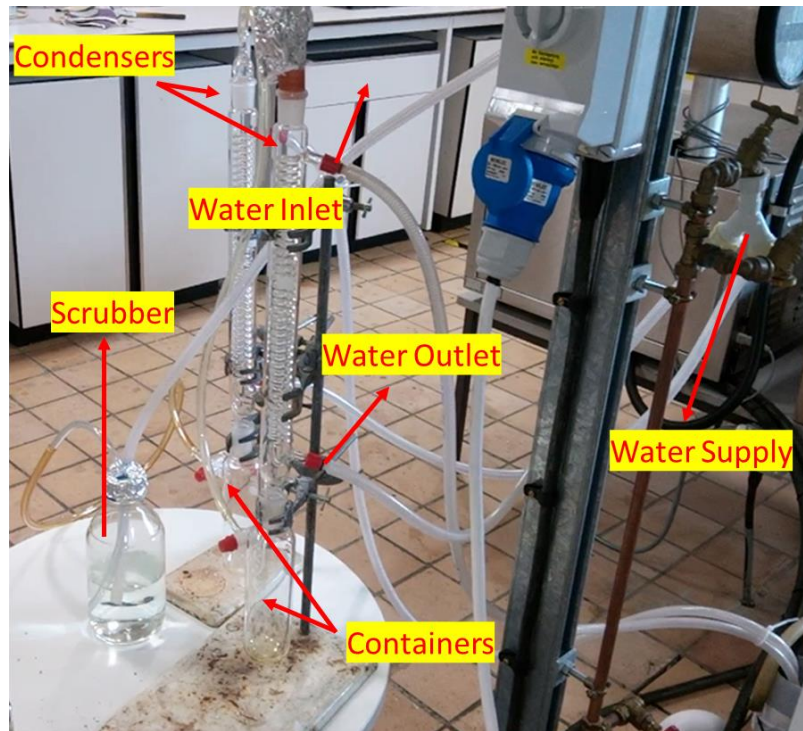


Figure 4-16: Condensation and water scrubbing system

Finally, the gas injection mechanism was set up. To do so, nitrogen and carbon dioxide gas cylinders with regulators were used. The cylinders were then attached to a digital flowmeter, outlet of which was connected to the injection point.

4.5 Tests & Modifications

After setting up the system and before starting the wool pyrolysis tests, the efficiency and feasibility of the feeding system was verified. The feeding system had 3 main parts

- > Hopper
- > Feeder
- > Auger reactor

Therefore, the following parameters were tested:

- > Flow of material in the hopper (consideration of issues)
- > Flow of material from hopper to the feeder
- > Flow in the feeder
- > Flow of the material from feeder to the auger reactor
- > Flow in the auger reactor

Prior to starting the tests, the feed size was assigned. Opposed to the fixed bed tests, where the feed was prepared on the site and manually for each test, to replicate a large-scale process, the feed

was also prepared for such a situation. Therefore, shredding the material in the industrial size scale was considered. To shred the material for this stage, several textile waste shredding companies such as “UNTHA UK”, “Valley Recycling”, “Clyde Recycling” and “Assured Security Shredding”, which had records of textile shredding were contacted and the requirements were discussed with them. Most of these companies were specialised in shredding for recycling, where the size of the shredded material was not important. Only Assured Security Shredding was able to shred the material in two cycles of shredding to make material as small as possible since their shredder could give 2 cm wide strings of textile in one pass. The material received from the shredding company was not uniform regarding the sizes of the pieces as expected. Therefore, it was decided to test with two different feed size conditions; one as it was received from the shredder and one with pieces which were further reduced in size to a uniform size of 1 by 1 cm.

The first test was carried out on the effectivity of the hopper and the vibrator attached. To isolate the hopper, it was suspended in air between two tables and loaded with 1 kg of feed. As expected, the initial issue observed was lack of flow out of the hopper. Except few pieces of wool, the rest agglomerated on the outlet top, forming lumps of wool. This was caused by tangling of wool strings together. The vibrator was incorporated in the system to overcome these foreseen issues. However, the hopper was too heavy to be vibrated efficiently, so that the vibrator became redundant, opposed to the cardboard prototype where the vibration was sufficient force to overcome wool entangling. Another issue was with the fabrication of the internal walls of hopper, which did not present a smooth internal surface, but the inside welding was visible and sharp edges restricted flow furthermore. Finally, the hopper was attached to the system to spot the potential issues with hopper as part of the whole system. This was also necessary to check the performance of the feeder and auger reactor.

The next identified issue was the size of the outlet size of the hopper and consequently the distance between it and the feeder inlet. The auger feeder itself, once it caught the wool in its flights, performed well and there was no issue in wool flow along the tube length. However, wool agglomeration occurred at the end bearing of the feeder tube. The reason was that the design of the bearing allowed some of the wool to get into it and get stuck. Regarding the second tube, the material flowed without any observed issues. All of these tests were carried out with the motor ratings set at two speeds of 5 and 40 to test the two extremes.

These issues justified a need to modify the system, either in material of construction or overall shape. In this new design, the following issues were addressed:

1. Weight of hopper

2. Fabrication of wall
3. Size of the hopper and consequently feeder auger opening
4. Bearing of the feeder

Changes 1 to 3 were carried out simultaneously due to the interdependency of the parts. Therefore, two different scenarios were considered and tested:

4.5.1 Option 1; Vertical auger feeder in the hopper

In this design, as shown in Figure 4-17, a vertical auger was used to mix the material and avoid packing of the wool pieces to one another. Initially, it was decided to design an auger feeder and attach it to a motor installed on the lid of the hopper. However, to minimise the cost and lead time, it was decided to test this system manually with the auger 1, which was already part of them system. To do so, the hopper was set mid-air with an operator rotating the auger at a low rotational speed at different angles.

During these tests, it was observed that except a minor increase in feeding efficiency, no significant or promising improvement was shown. For instance, the auger was only efficient on the area around the auger and the feeding process was stopped after increasing the flow of material by less than double the flow in the un-assisted method. In other words, the problem would have remained in this method despite minor improvements. Consequently, it was decided that option 2 should have been considered.



Figure 4-17: The schematic and testing condition of the proposed modification (Option 1)

4.5.2 Option 2; Hopper with elongated outlet

Since this was a completely new design for the hopper, it was decided to try and overcome all the issues simultaneously. Firstly, the length of the outlet was increased to intake larger volumes of the feed without any assist besides gravity. Similarly, the width of the opening was increased to let the

auger feeder pull in the material in contact with it despite the agglomeration. Next, to avoid blocking and ensure continuous flow of material, a rotary paddle with the minimum distance from the auger was designed. The paddle had three blades with 3 different angles. The reason for including 3 different blades was to avoid pressure on the blade by moving large loads of material and to have a flow pattern as uniform as possible in the length of the hopper outlet.

Similar to the original design, the prototyping method was used to size the new hopper. This time, some of the sizes were pre-assigned so the sections to be redesigned were:

- › Material of construction
- › Hopper shape
- › Hopper angles
- › Hopper opening

Firstly, it was decided to change the material of construction of the hopper to aluminium to reduce the weight of the hopper. As mentioned previously (section 4.3), despite having higher production cost, the transitional hopper was chosen over wedge hopper because of better flow while the flow was being assisted solely by gravity. However, for the redesign, since the flow was being assisted by the paddle, wedge hopper was selected to keep the costs lower. Furthermore, during the tests with transitional hopper, it was observed that because of the nature of the wool feed, the probability of the wool getting stuck in the edges of the hopper was minimal.

For setting the angle and dimensions of opening and paddle, a prototyping method using cardboard was chosen. Several scenarios including the size, shape, and location of the paddle in addition to the angle of the slope of the hopper were tested. Before making the prototype however, the size of the hopper opening was set. This time, to maximise the contact area between wool and blades of the feeder, it was decided to elongate the hopper opening as much as practically possible. Therefore, the opening size was tripled from 8 to 24 cm.

Initially, deciding to have three blades with same dimensions, a 24 cm long with three 8 cm blades was built out of cardboard. Since the paddle should have been installed on the wall of the hopper, 1 cm was added to the opening of the hopper. Figure 4-18 demonstrates the prototype made to test the best angle for the flow.

As shown above, the edges of the cardboard prototype were lined with aluminium foil to replicate the smoothness of the aluminium hopper wall. The angles of both sides were modified while the hopper was loaded with 200 g of wool. Simultaneously, the auger feeder was rotated manually to simulate the operational conditions. Finally, the dimensions of the new hopper were set which is illustrated in Figure 4-19.



Figure 4-18: The prototype made for setting the angle of the hopper (right hand side with no auger and deed, left with auger and wool in the hopper)

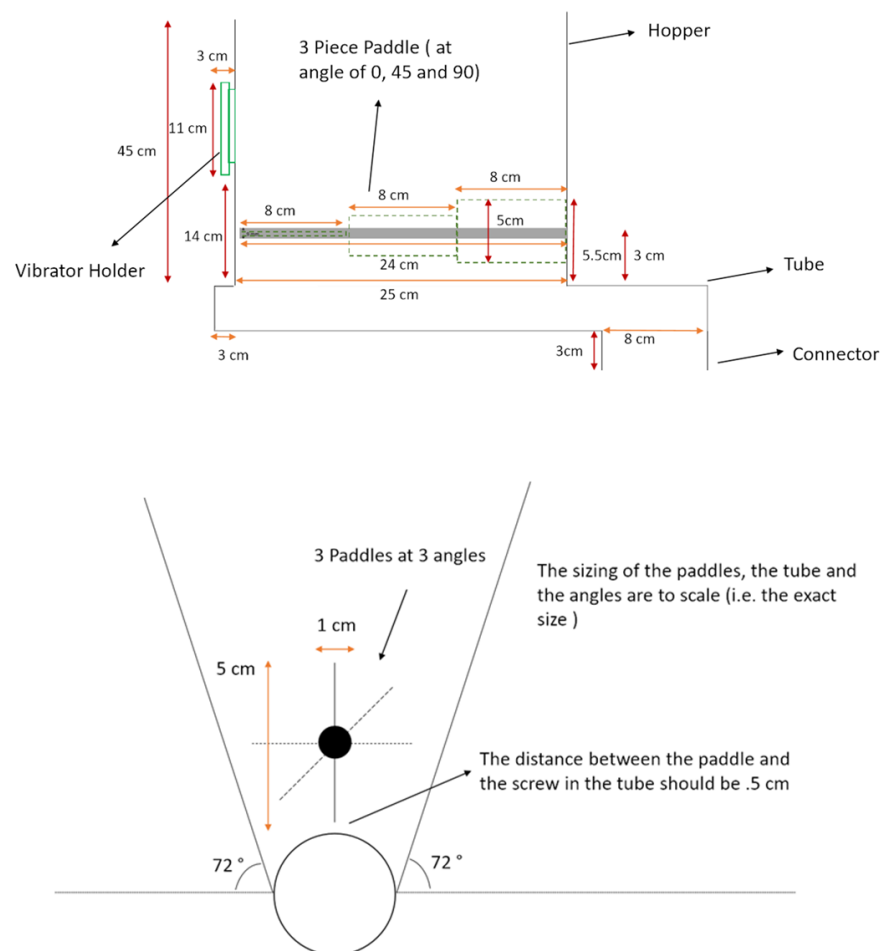


Figure 4-19: The dimensions of the new hopper arrangement

In the new design, the width of the hopper opening was set to the diameter of the feeder tube. This meant that the first tube needed to have cross sectional cut. Since cutting the stainless-steel tube was more costly than making a new tube from aluminium, a new tube was built. This did not have any negative effects regarding metal integrity because the system was heated up to 1000 C for 2 hours to observe the temperature increase of the feeder part which did not exceed 70 C. The hopper and the tube were screwed together to ease the removal of hopper from tube for cleaning purposes or in case the system gets clogged with material.

The paddle was designed to be installed on a stand over the motor for reactor auger. However, it was decided to operate it manually at the beginning to check its feasibility prior to allocating funds for the construction of the stand and purchase of the motor. Also, the height of the hopper was reduced for ease of access. Finally, the end bearing that initially was designed by the manufacture, was redesigned to have a solid construction without the gaps which increased the risk of material built-up (Figure 4-20). Also, the lid of the hopper was designed to be transparent with an extra gas injection point (Figure 4-21) to facilitate continuous observation of the state of the feeding process. The new hopper arrangement was draw using CAD and commissioned to a manufacture at Galashiels (Scotland). Figure 4-22 shows the CAD drawings alongside the final product.



Figure 4-20 Old bearing (left) Vs. the re-designed bearing (right)

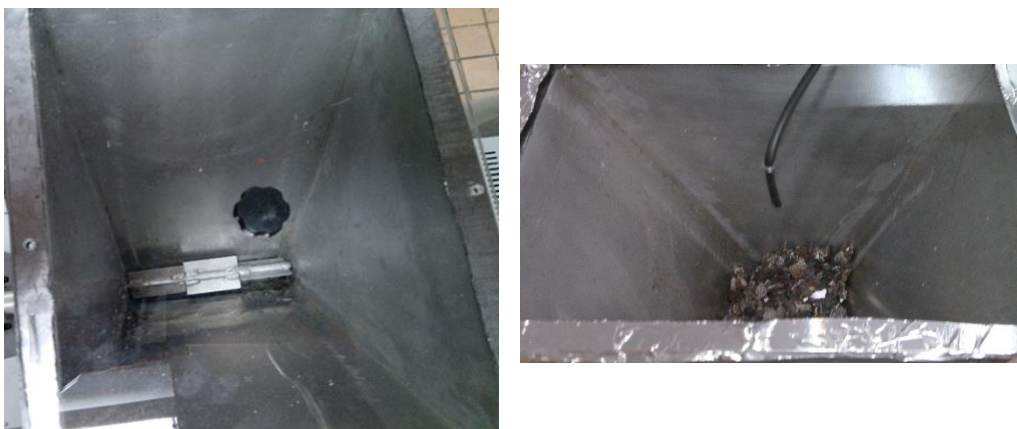
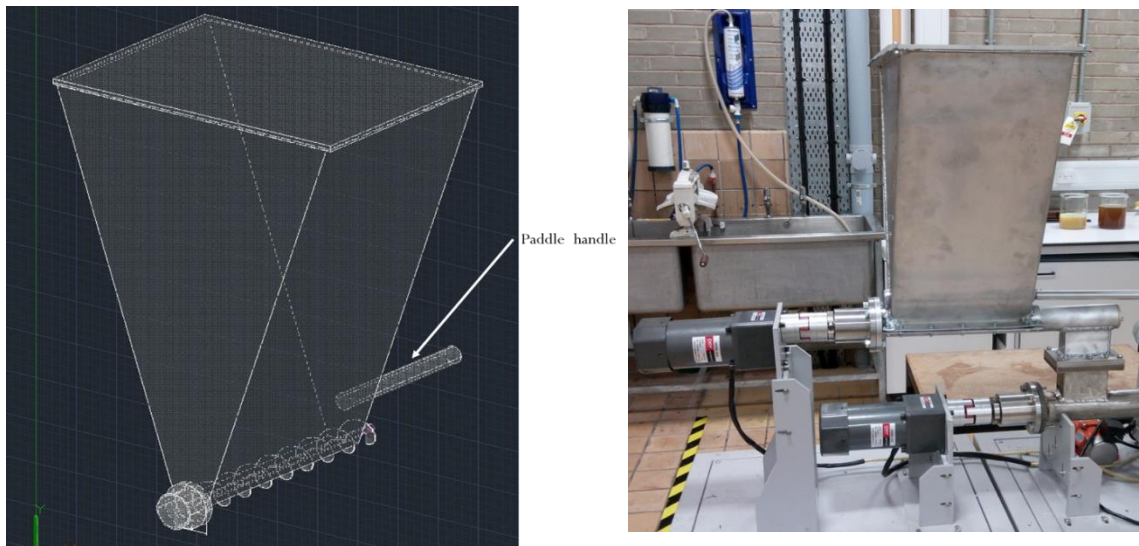


Figure 4-21: New transparent lid and 3 bladed paddle



4-22: CAD drawing and final arrangement of the new hopper

4.6 Modified System Tests; Experimental Procedure

In order to test the modified sections and the overall performance of the system, this time the system was tested at operational temperatures similar to the ones tested in the small-scale fixed bed. This was done to compare the results of the fixed bed with the scaled-up arrangement and consequently figure out the effectivity of the scale up. The results regarding the effect of scale-up in product quality and distribution are discussed in chapter 7.

To fully evaluate the best and possible operational conditions, the following criteria were considered:

- > Feed size
- > Speed of motors (both)
- > Hopper paddle speed
- > Temperature

Initially, the feed was used in the system in the same size received from the shredder. This meant that the size of wool pieces varied from 1 cm² to approximately 14 cm². Additionally, in this scenario, some of the paper attached to the wool material was also fed to the system. Predictably, some of the long strings of wool caused flow issues in the system when they got wrapped around the first auger. This led to agglomeration of the rest of the feed material around it and consequential blockage of system. Afterwards, wool was cut into 1, 2, 3 and 4 cm² pieces and each sample size was tested in the system. It was concluded that 2 cm² was the most fluent sample. For instance, the 1 cm² went through system with no issue but because of its small size, the augers were not always able to catch the pieces on the first rotation when they became in contact with a specific piece of

wool. Therefore, it took longer for a batch to go through the system. Larger samples also blocked the system on occasions, so it was decided to avoid them.

To achieve uniform flow rate, the optimal speed of motors and paddle rotation was selected through trial and error. These 3 (two motor speeds and 1 paddle speed) should have been adjusted in accordance with each other. If the rotational speed of the first auger was set too high, the system got blocked at the end of tubing one regardless of the other rotating parts. Similarly, if the paddle rotated at a high frequency, either excess material was fed into the system which led to blockage or it did not allow the wool to be grabbed by the tube in an efficient rate. In case of second tube, if the speed was too high, the char product was not pyrolyzed completely and on the other hand, if it was set at lower than optimal speed, feed got accumulated in the tubing connections and eventually system failed. Eventually, a ratio of 1:5 was selected for the revolution of first and second tube with the max speed of first and second tube being 10 and 40 rpm, respectively. The paddle rotation was set as 1rpm.

Finally, the amount of gas injected was set at 200 mL/min. The increase compared to fixed bed (discussed in chapter 3) was due to the increase in size of the reactor and therefore to reduce the residence time of the gas in large scale reactor. Higher volumetric velocities of gas were also considered but they resulted in turbulence in wool particles and carry over to the solid container. Velocities of lower than 145 mL/min resulted in back flow of gas. The selected flowrate resulted in residence time of 205 seconds. Table 4-4 lists the tests carried out in the auger reactor and summarises the decisions made for operating conditions such as motor speeds. Tests 4 and 5 were used for comparison of auger reactor with fixed bed in Chapter 7.

Table 4-4: List of tests carried out in auger reactor

Test No.	Motor 1 Speed (RPM)	Motor 2 Speed (RPM)	Feed Size (cm)	Paddle Speed	Injected Gas	Gas Flowrate (mL/min)	Temperature (°C)
1	10	40	2 by 1	1	CO ₂	200	350
2	10	40	2 by 1	1	CO ₂	200	500
3	10	40	2 by 1	1	CO ₂	200	800
4	10	40	2 by 1	1	CO ₂	200	900
5	10	40	2 by 1	1	N ₂	200	800

Before running all the tests discussed above, the system was checked for gas leaks. To do so, all the connections were bolted down, and the gas outlet was closed to let pressure built up in the system. Afterwards, nitrogen gas was passed through to check for leaks. A high temperature resistant gasket built from graphite with stainless steel (withstanding up to 500°C) was selected for connection to minimise the probability of any leak. Below, are the issues occurred during the gas leak tests in addition to the solutions applied for overcoming them. Furthermore, other issues and their respective solutions are also listed.

- › The surface of the reactor at multiple points such as connection part between tubes was not smooth and therefore feed got stuck and eventually accumulated in junctions
 - ✓ Since smoothing out inside of the tubes was not possible at a low cost, aluminium tapes which are smooth and can withstand operating temperatures of the system were attached on the walls of tubes and connection points from inside (Figure 4.23). This overcame the issues, but the tapes needed to be changed after every 2 runs, to keep the surface smooth and the wool pieces flowing



Figure 4-23 The added aluminium for smoothness of surface

- › Gas pressure drop occurred in the system after feeding. Due to the proximity of the auger to the tube walls, which was done to facilitate wool flow and eventually char flow in the system, the gas did not have enough space to flow through in the system. This caused gas back-flow and unwanted condensation in the system (Figure 4-24).
 - ✓ To solve this, the second auger blades were filed slightly only on one side to make space for the produced gas to flow

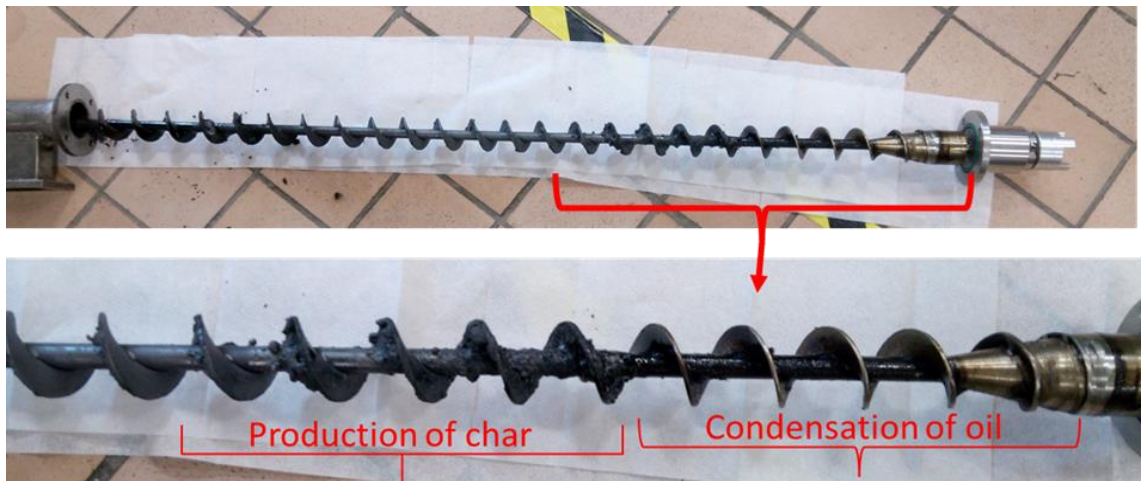


Figure 4-24: The effect of back flow and location of the feed on the auger on the product differentiation

- › Gas leak in the system was causing gas backflow and consequently oil condensation in the system leading to feed getting stuck to the surface and causing blockage.
 - ✓ To solve this, leak locations were identified. The lid of the hopper was a major leak source. First, the number of screws on the lid was increased from 6 to 10 and the closing bolts were changed to screw and nut for tighter fit. Then, an extra rubber gasket was added to the lid. These gaskets were glued to each side for ease of opening and closing and better gas proofing. Despite significant improvement, there still was some leak from the lid due to the thin aluminium material used which changed shape by screws tightening pressure. Finally, adding G-claps to each side of the hopper lid (4 claps) where leaks were happening, solved the issue.
- › The attachment of the new hopper to the feeder tube had circular connection with a cross sectional cut and attached together with bolts. There was a gasket in-between them for gas-proofing but there was large degree of leaks from this point (Figure 4.25).



Figure 4-25: The attachment point of the new hopper to the tubing 1 where leaks occurred; fire cement was used with additional aluminium tape on top of it

- ✓ Several options were considered such as welding the parts together, use of other thicker gaskets or using silicon sealant. However, each of them presented either financial or operational issues. Finally, fire cement was selected as the best option. Fire cement was the least costly option, quick and could withstand temperatures of up to 1200 °C. Additionally, it could be removed if needed for cleaning purposes opposed to the welding option.
- › Attachment points of tube 1 to 2 were un-even, causing gas leaks when there was high pressure in the system. Using the thin high temperature gasket at hand was not enough due to the large gap. Also, since temperatures as high as 500 °C could be expected at this point, thick rubber gaskets that could withstand this temperature were not available.
 - ✓ One option could have been to straighten the attachment point. However, this would have been costly due to the hard material (stainless steel) and time consuming. Finally, two high temperature gaskets with one rubber gasket in between was used to solve the issue (Figure 4-26). In this manner, the rubber gaskets were not in contact with hot metal surface

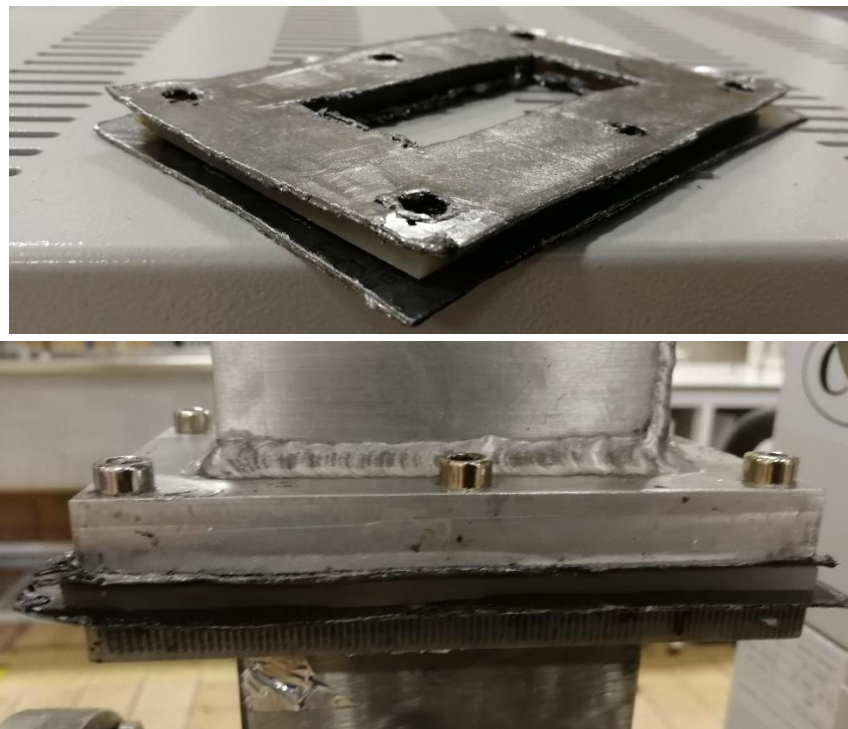


Figure 4-26: Gasket arrangement to avoid gas leak

- › Condensation occurred in the solid container. The solid container was at room temperature with no mean of heating. This would have led to condensation of the gas in the tubing and container due to the rapid heat loss. Consequently, operational issues such as blockage and contamination of products would have happened.

- ✓ To prevent this, the tube and solid container were wrapped with heating tape (Figure 4-27) in addition to glass wool and aluminium foil. This way, the heating tape will keep the gas above the boiling point and glass wool is used to insulate the heat generated by it.
-



Figure 4-27: Heating tape around the solid container and end of tubing

- › Oil condensation in the connection part between pyrolizer and condensers
 - ✓ Since the metal tubing connecting the reactor to the condensers was not heated, condensation happened in the tube which restricted the flow. Therefore, opposed to the initial isolation, which was one layer of mineral wool, 4 layer of mineral wool, aluminium foil, tube isolating sleeve (withstanding temperatures of up to 100 °C) and aluminium tape was used which largely improved the isolation (Figure 4-28).
-



Figure 4-28: Sleeve, the inner second thermal isolation layer on top of mineral wool (right), third layer of isolation, aluminium tape (left)

- › Oil got condensed in the tubes attaching the two condensers together and partially blocked the tubes leading to pressure drop in the system

- ✓ In the original set-up, condensers were attached to each other by long tubing which increased the possibility of oil condensation in them. In the new set-up, one of the oil collection bottles was removed and the two condensers were attached directly to each other to eliminate this issue (Figure 4-29)

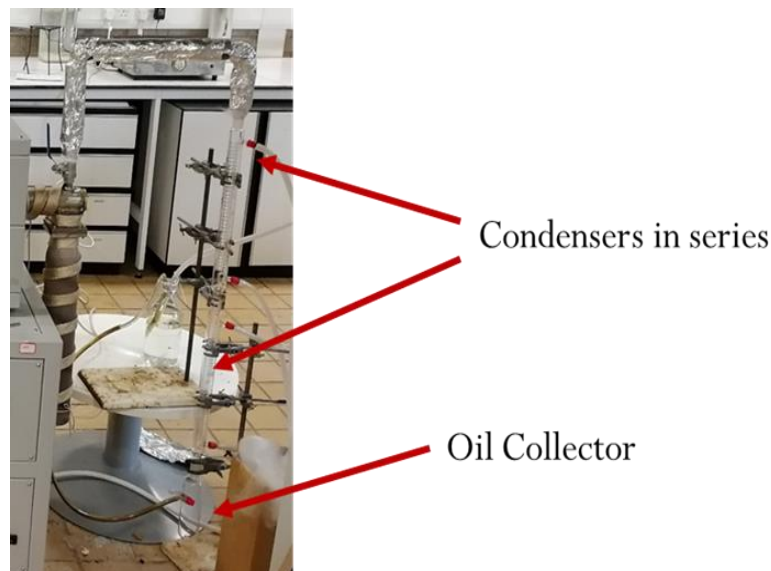


Figure 4-29: The new condensation arrangement; removal of tubing and direct attachment of the condensers

4.7 Chapter Conclusion & Recommendations

Overall, despite several challenges, the scale up procedure was promising. By-products (char, oil, and gas) were produced as expected and flow of wool through the system was controlled. Modifications that were carried out were successful in eliminating the gas leaks and minimising obstruction of flow by wool. Also, condensation of oil in the solid container and tubing upstream of the condensation traps and in the reactor itself, were reduced significantly through use of heating tapes and isolation.

To improve the flow of gas, one improvement that is recommended could be to add small (less than 0.5 cm) holes on the blades of the auger. Furthermore, addition of gas extraction points alongside the reactor and in the heated zone could improve the gas flow and reduce gas condensation in the system even more. Using a cooling system with lower temperature to reduce the temperature of the condensation medium would improve the condensation efficiency. Furthermore, recycling the cooling medium in a loop would reduce the operational costs of the process. Alternatively, if the proposed reactor is used within the textile manufacturing facility where hot water is likely to be required (for instance for dyeing purposes at around 70 °C), a heat exchanger or waste heat recovery unit could be used on the cooling system to increase the energy efficiency of the system. The

produced gas could also be integrated into a CHP (Combined Heat and Power) arrangement to reduce the energy requirement of the system.

The current hopper could hold over 1 kg of wool per batch and considering the rotational velocity of 10 RPM in the first auger, if the size of hopper is increased in future, potentially over 10 kg/h of wool can be pyrolysed in this system. However, there were some bottlenecks to achieve this flowrate. For instance, some large parts of wool could have still blocked the inlet of the second tube. This occurrence interrupted continuous and uniform flow of wool on occasions. Since it was observed that elongation of the outlet of the hopper (inlet of first tube) improved the flow of wool from the hopper to the first tube significantly, it is envisaged that elongating the connection between two tubes can overcome this issue and facilitate the system to achieve its maximum flowrate. With the current arrangement, flowrates of up to 2 kg/h (30 minutes for the 1 kg to be pyrolysed) was achieved. However, due to the issues such as blockage of system, an average flowrate of 0.5 kg/h could be recorded as the more achievable flowrate.

4.8 References

- [4.1] F. Campuzanoa, R.C. Brown, J.. Martínez, "Auger reactors for pyrolysis of biomass and wastes," *Renewable and Sustainable Energy Reviews*, p. 2019.
- [4.2] E. Maynard, "Ten Steps For Effective Bin Design," *American institute of Chemical Engineers*, pp. 25-32, 2013.
- [4.3] A. Jenike, "Storage and Flow of Solid," *University of Utah Engineering Station*, Utah, 1976.
- [4.4] R. B. R. F. MSA Bradley, "Methods for Design of Hoppers. Silos, Bins and Bunkers for Reliable Gravity Flow, for Pharmaceutical, Food, Mineral and Other Applications," *University of Greenwich*, Chatham , 2011.
- [4.5] Sandmeyer Steel Company, [Online]. Available: <https://www.sandmeyersteel.com/310-310S.html>.
- [4.6] Azo Materials, "Stainless Steel - Properties and Applications of Grades 310/310s Stainless Steel," [Online]. Available: www.azom.com/article.aspx?ArticleID=4392.
- [4.7] H. Zareiforoush, M. Komarizadeh, M. Alizadeh, M. Masoomi, "Screw Conveyors Power and Throughput Analyses Dring Horizontal Handling of Paddy Grains," *Journal of Agricultural Science*, 2010.

- [4.8] K. Abdulbaki, J. Jarjour, S.J. Kim, S. Nagib, "Pyrolysis Feeder," *McGill University*, 2016.
- [4.9] B. Mecke, "Shaftless Screw Conveyors: A Perfect Solution for Handling Bulk Solids," KWS, 2012. [Online]. Available: <https://www.kwsmfg.com/resources/articles/shaftless-screw-conveyor-article/>.
- [4.10] Shaftless Screw Conveyor, [Online]. Available: <https://www.imix.net.in/shaftless-screw-conveyor/>.
- [4.11] KWS, "Shaftless Screw Conveyor Engineering Guide," [Online]. Available: <https://www.kwsmfg.com/engineering-guides/shaftless-screw-conveyor/>.
- [4.12] P. Owen, "Screw Conveyor Performance: Comparison of Discrete Element Modelling with Laboratory Experiments," *Computational Fluid Dynamics in the Minerals and Process Industries*, 2009.
- [4.13] J.W. Fernandez, P.W. Clear, W. McBride, "Effect of Screw Design on Hopper Draw Down by a Horizontal Screw Feeder," *Seventh International Conference on CFD in the Minerals and Process Industries*, 2009.
- [4.14] G. Mehos, D. Morgan, Jenike & Johanson, "Hopper Design Principles," *Chemical Engineering Essentials for for the CPI Professionals*, 2016. [Online]. Available: <https://www.chemengonline.com/hopper-design-principles/?printmode=1>.
- [4.15] K.R. Cummer, R.C Brown, "Ancillary Equipment for Biomass Gasification," *Biomass and Bioenergy*, 2002.
- [4.16] E. Sinnott & C. Stephen, "Coffee Storage: Options for Mid- to Large-Sized Roasteries," *Modern Process Equipment*, Chicago, 2018.
- [4.17] Velodyne, "What is product bridging and rat-holing? And how can it be prevented?," 2016. [Online]. Available: velodynesystems.com/blog/2016/06/09/what-is-product-bridging-and-rat-holing-and-how-can-it-be-prevented/.
- [4.18] J.W. Fernandez, P.W. Clear, W. McBride, "Effect Of Screw Design On Hopper Draw Down By A Horizontal Screw Feeder," *Seventh International Conference on CFD in the Minerals and Process Industries* , 2009.

- [4.19] Ajax, "Hopper Volume," [Online]. Available:
<http://www.ajax.co.uk/TransitionHopper.htm>.
- [4.20] W. A. Beverloo, H.A. Leniger, J. van de Velde, "The flow of granular solids through orifices," *Chemical Engineering Science*, 260–269. 1961
- [4.21] H.E. Rose, T. Tanaka, "Rate of discharge of granular materials from bins and Hoppers," *The Engineer*, 465-469, 1959

CHAPTER 5 - MODEL COMPOUND PYROLYSIS RESULTS

In this chapter, after characterising ZSM-5 and KIL-2 catalysts in section 5.1, a summary of the methodology carried out for comparison of model compound pyrolysis with different catalysts is given in section 5.2 followed by the presentation of the results in sections 5.3 to 5.6. The results for each type of analysis for each model compounds are discussed and summarised in section 5.7.

5.1 Catalyst Characterisation

Results for the analysis carried out to characterise the catalysts are presented in Table 5-1. The water weight loss corresponds to the amount of water released when the catalysts were heated up to 500°C during TGA analysis. This characterisation will be useful during the mass balance calculation to determine the product distribution of pyrolysis.

The surface analyses were carried out on the catalysts to establish the available areas for the reactions to take place. BET surface area, Langmuir surface area, and median pore width were obtained for each catalyst.

Table 5-1: The properties of the catalysts

Properties	Unit	Li-KIL2	Al-KIL2	20-ZSM5	30-ZSM5	60-ZSM5
Weight Loss	%	16.53	18.15	19.00	18.00	18.43
BET (Surface Area)	m ² /g	23.80	896.09	361.99	361.79	376.18
Langmuir	m ² /g	58.76	1564.04	546.67	564.42	589.22
Max Pore Volume	cm ³ /g	0.01	0.37	0.16	0.17	0.17
Median Pore Width	nm	1.52	0.95	0.95	0.95	0.95

As tabulated in Table 5-1, the ZSM5 catalysts showed an increase of the surface available from 361.99 m²/g (20-ZSM5) to 376.18 m²/g (60-ZSM5). Although, the BET of the 30-ZSM5 was almost identical to that of 20-ZSM5, the experimental error in the readings for 20-ZSM5 and 30-ZSM5 were ± 3.35 m²/g and ± 4.65 m²/g, respectively; meaning the trend could still be observed. The Langmuir surface areas followed the trend more clearly for increasing the Si/Al molar ratio. The BET trend was found to be consistent to that observed by Shirazi et al [5.1]. The decrease of surface could be related to the incorporation of Al in the framework of ZSM5.

The BET surface area of Al-KIL2 was by far the largest at 896 m²/g (isotherms can be found in Appendix A). As mentioned in chapter 2, KIL2 is a novel disordered mesoporous silica support

with limited experience of being incorporated with metals. However, due to the similarity in physical structure to SBA-15 (ordered mesoporous silica), for which there has been extensive research, behaviour of KIL2 support when incorporated with metals could be correlated. In case of BET surface area, the relationship with Si/Al ratio was similar to the one in ZSM5 case after a certain threshold ratio [5.2]. In other words, if the ratio of Si/Al ratio is higher than a certain value, the BET surface area increases compared to the original support. However, it should be noted that other criteria such as the synthesis temperature could affect the BET surface area [5.3]. In this case, since the BET surface area of the KIL2 support was 545 m²/g, it could be assumed that Si/Al ratio was over the threshold value. This increase in surface area could be explained by several factors. For instance, the addition of aluminium could improve the structure regularity and ordering of the material and therefore increase the internal surface area of the disordered support, despite the fact that external surface might be reduced due to the blockage of the some of the pores on the surface by aluminium [5.3].

Li-KIL2 had by far the smallest BET surface area. It was highly probable that the disordered pores of the KIL-2 support were filled with the lithium. This was because silica supports generally have pores which are larger than lithium [5.4].

The median pore width of all the catalysts were similar with the exception of Li-KIL2. This property can assist this catalyst to perform better in processes where the size of the feedstock molecules is larger, and the reaction takes place on the surface of the catalyst. In this research this might have been the case with lignin catalytic pyrolysis. On the contrary, the pore volume of Li-KIL2 was the smallest one compared to the other catalysts with Al-KIL2 having by far the largest pore volume.

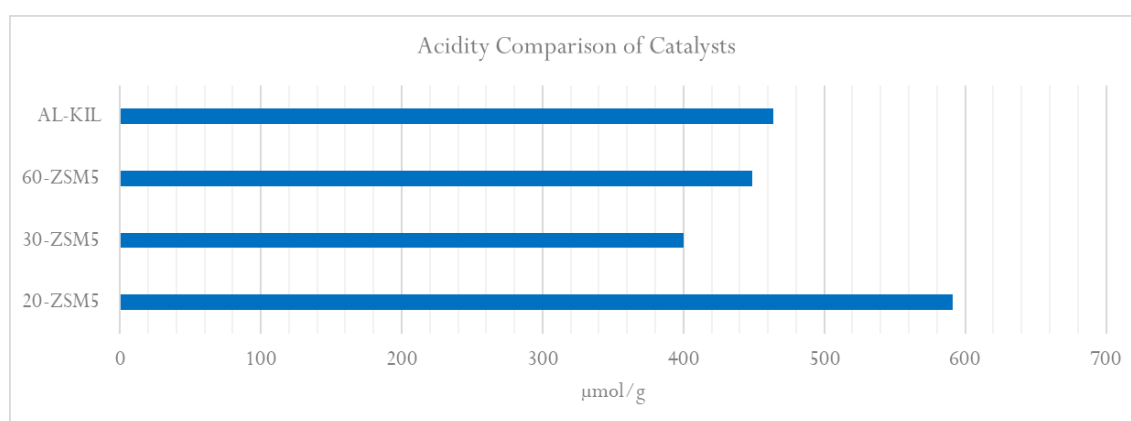


Figure 5-1: Comparison of acidity sites for ZSM5 catalysts

Figure 5-1 demonstrates the acidity comparison of ZSM-5 catalysts. The results indicated that the molar ratio of Si/Al of the ZSM-5 had a significant effect on their total acidity, with the 20-ZSM5 having the largest number of acid sites (>590 μmol/g) compared to the other two samples. The

Al-KIL2 acidity was expected to be higher than the ZSM5 due to the existence of aluminium while the reverse of this was expected from Li-KIL2. However, while acidity of Al-KIL2 was higher than two of ZSM-5 samples, it was lower than the acidity of 20-ZSM5. The acidity values were used for qualitative comparisons of catalyst's behaviour rather than quantitative comparison.

5.2 Model Compound Pyrolysis

All the model compounds and catalysts combinations were pyrolysed in both the TGA and fixed bed reactor. This was carried out to observe the effect of increasing the feed size. However, it should be noted that other factors such as heating rate were different between these two methods. TGA also facilitated the observation of temperatures at which decomposition of material started and temperature/time at which the maximum decomposition rate took place. Furthermore, TG-MS results were used to observe the composition of the gas produced. GC-MS analysis was carried out on the oil produced in the fixed bed reactor to observe the components found in the oil and compare the effectivity of the catalysts. All of these analyses should be considered simultaneously to clarify the behaviour of catalysts on each model compound. This has been carried out in Section 5.7.

Both the TGA and fixed bed tests were carried out at 500°C and with use of nitrogen as the carrier gas. The ratio of feed to catalyst was kept at 1:1 for both the TGA and fixed bed runs while the heating rate for the fixed bed and TGA were at least 25 °C/min and 100 °C/min, respectively.

5.3 Mass Balance & Product Distribution

Figure 5-2 to Figure 5-3 compare the quantity of chars and volatiles produced in the TGA and fixed bed. In case of cellulose, the use of catalysts increased the char production compared to the non-catalytic runs. In more details, the amount of char produced in the fixed bed during non-catalytic pyrolysis of cellulose was less than 9% at 500°C which matched the values reported in literature [5.5]. It should be noted that the main purpose for application of catalysts was to reduce the oxygenated by-products and the distribution of products on its own could not be indicative of the effectivity of the catalyst. However, one reason behind the increase in the char content in the catalytic tests could be the condensation of the large oligomers on the surface of the char or coke formation on the surface.

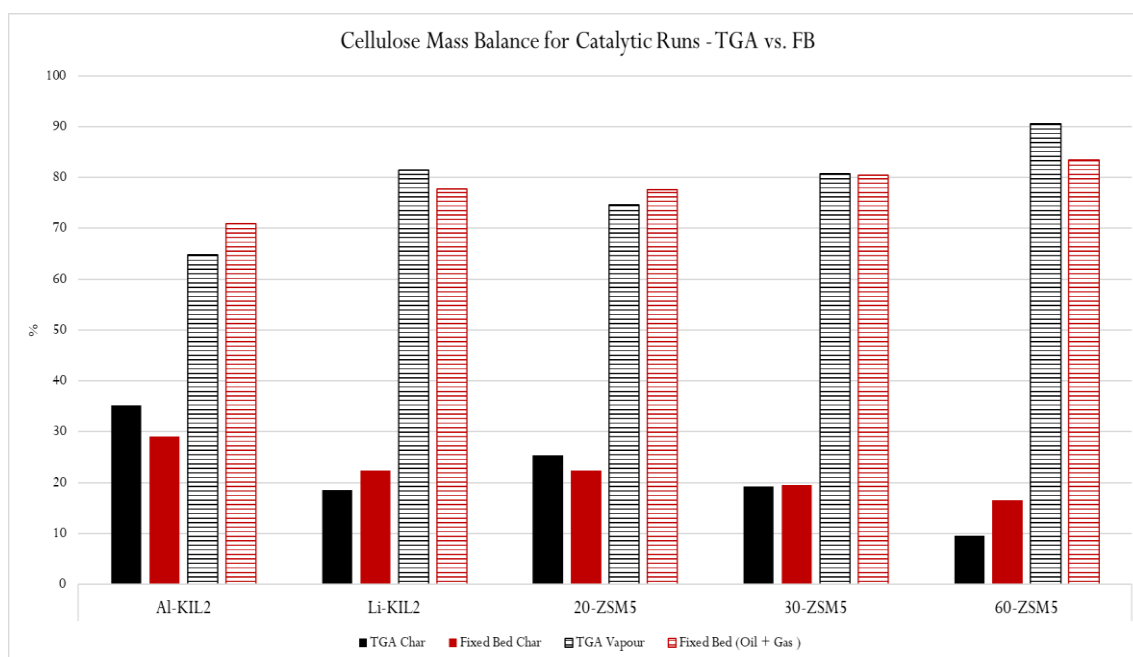


Figure 5-2: Cellulose mass balance comparison of TGA and fixed bed (FB)

The maximum difference between the TGA (Appendix B) and fixed bed could be observed in 60-ZSM5 case, which was less than 8%. However, since the trend observed was the same for all the cases regardless of the scale of the process, this difference was acceptable. For instance, the least amount of char was obtained through use of 60-ZSM5 while Al-KIL2 maximises the char production for both the TGA and fixed bed. One reason behind the difference in char fraction between fixed bed and TGA could be the difference in the heating conditions. In the fixed bed, the temperature was at 500 °C when the feed was introduced while in the TGA the temperature was increased at a heating rate of 100°C/min. For instance, in pyrolysis of pine wood, it was observed that while keeping all the conditions the same except the time constrains, the biochar yield was decreased from 24% to 12% at 500°C [5.6].

Another reason for the difference in char production in fixed bed compared to TGA could be the increased residence time in the fixed bed. The reactor had to be left to cool down prior to disassembling the reactor and collecting the product in the fixed bed while the feed exited the reactor more quickly after the conclusion of the heating process. This means that the feedstock spent more time in the heated environment of the reactor in the fixed bed. This could facilitate further conversion of feedstock to volatiles and further secondary reactions. Therefore, in most cases, the results of TGA were prioritised over fixed bed results for identifying the conversion percentage of the samples to char and volatiles (oil + gas).

Initially, the TGA results for ZSM-5 catalysts indicate that acidity did not play a significant role in conversion of the feed to vapours in cellulose case. This observation was made by comparing 30-

ZSM5 and 60-ZSM5 which had similar acidity, but production of char was almost halved when 60-ZSM5 was used compared to 30-ZSM5. However, this reduction in char production could be due to the higher BET surface area of 60-ZSM5, facilitating higher surface contact for reaction. Another observation could be that higher acidity can promote higher char production. This observation was based on the high char production in the two most acidic catalysts, namely Al-KIL2 and 20-ZSM5. This phenomenon is due to condensation of higher molecular weight components (coke) produced during secondary reactions which are facilitated by higher acidity, coupled with higher surface area in case of Al-KIL2. Overall, ZSM5 catalysts performed better in conversion of cellulose to volatiles compared to KIL2 catalysts regardless of the scale of the pyrolysis (TGA or fixed bed).

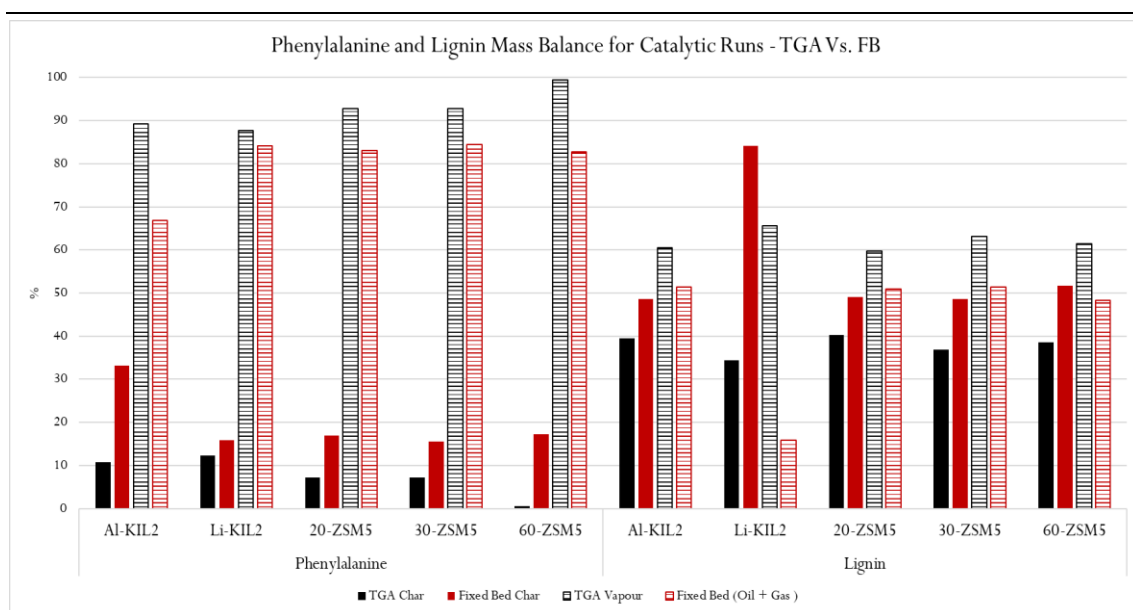


Figure 5-3: Lignin and phenylalanine mass balance comparison of TGA and fixed bed

Based on literature, a char percentage of over 40% was to be expected from un-catalytic pyrolysis of lignin [5.8]. The results obtained for char percentage in TGA (48%), and fixed bed (51%) matched with this expectation. As predicted, the char production was larger for lignin pyrolysis compared to cellulose [5.20] due to its more complex structure of cross-linked polymers. Comparing the TGA results, acidity of the catalysts seemed to be the dominant driver for conversion of the lignin to char. In other words, the higher the acidity of the catalyst, the higher the amount of char produced.

Phenylalanine had considerably less char compared to lignin and cellulose. Available surface area of the catalysts did not have significant effect on the char production. This observation was based on comparison of 30 and 60-ZSM5 which have almost identical BET surface area while having vastly different quantity of char. This could have been due to the smaller size of phenylalanine compared to cellulose and lignin. TGA data did not indicate existence of any trends with acidity either.

However, fixed bed data indicated that increase in acidity increased char production. In case of Al-KIL2, high acidity and high surface area could have resulted in secondary reactions leading to precipitation of products on surface of char. Other characteristic indicators of oil, char and gas were required to clarify the reasons behind the trends observed in product distribution.

5.4 Derivative Thermogravimetry (DTG) Data

The DTG graphs and tables with the summary of the results are presented and discussed in this section. The data in this section should be coupled with the GC-MS of oil and gas analysis to provide a more comprehensive picture of the behaviour of catalysts.

5.4.1 Cellulose

Figure 5-4 presents the graphs for effect of catalysts on derivative weight loss versus time for cellulose pyrolysis (individual graphs in Appendix B). Furthermore, Table 5-2, summarises the peaks, start of pyrolysis temperature and percentage loss for cellulose.

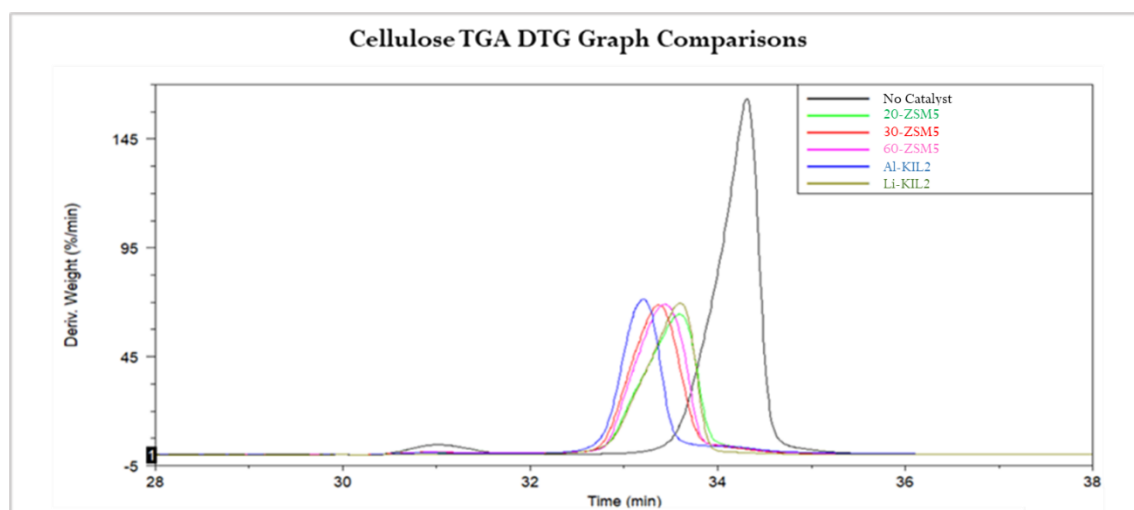


Figure 5-4: Cellulose DTG comparison curve

First of all, the non-catalytic run curve shows a peak at 84°C. Due to the temperature at which the peak occurs, this could be an error or water evaporation. If this peak was omitted, all the catalysts reduced the temperature at which the decomposition started; meaning that the catalysts had facilitated an alternative route with lower activation energy. Comparing the Si/Al ratio in the ZSM-5 catalysts, the higher the ratio, the lower the temperature at which the decomposition started. Also, the least acidic ZSM5, i.e., 30-ZSM5, demonstrated the lower temperatures at both the 2nd and 3rd peak while having high derivative weigh rates. This reverse relationship with acidity could be further solidify by comparing Li-KIL2 (lowest acidity) with Al-KIL2 and the rest of the catalysts which had the lowest decomposition initiation temperature.

Table 5-2: Cellulose DTG data

Cellulose	Pyrolysis Started at (°C)		1 st Peak	2 nd Peak	3 rd Peak
Base	310	Curve Peaks Temperature °C	84.2		406.1
		Derivative Weight (%/min)	4.5		163.3
Al-KIL2	280	Curve Peaks Temperature °C		163	369
		Derivative Weight (%/min)		1	71
Li-KIL2	270	Curve Peaks Temperature °C			407
		Derivative Weight (%/min)			70
20-ZSM5	285	Curve Peaks Temperature °C		169	407.8
		Derivative Weight (%/min)		1	64.6
30-ZSM5	280	Curve Peaks Temperature °C		155	386
		Derivative Weight (%/min)		1	68.7
60-ZSM5	275	Curve Peaks Temperature °C		169	394
		Derivative Weight (%/min)		1	69

5.4.2 Lignin

Figure 5-5 presents the graphs for effect of catalysts on derivative weight loss versus time for lignin pyrolysis (individual graphs in Appendix 2). Furthermore, Table 5-3, summarises the peaks, start of pyrolysis temperature and percentage loss for lignin.

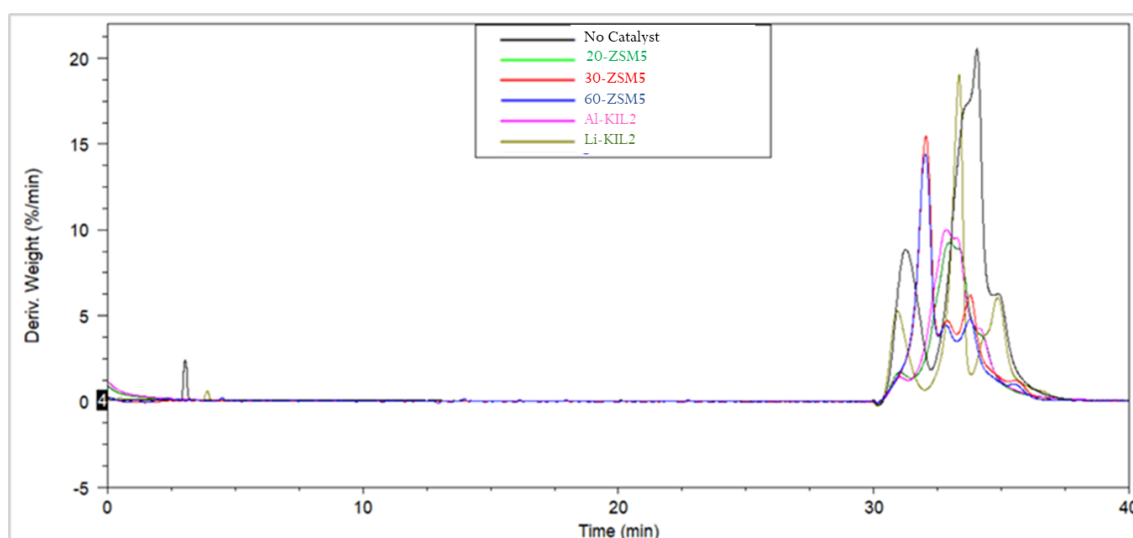


Figure 5-5: DTG graph for lignin

The decomposition curves were more complex and had more peaks compared to cellulose. This was expected due to the more complex nature of lignin. Comparing the ZSM5 catalysts, similar to cellulose, the acidity of the catalysts seems to have a reverse relation to the decomposition temperature. For instance, the most acidic ZSM5 (20-ZSM5) reached the first peak at over 30°C higher temperature compared to other ZSM5 catalysts. Furthermore, the other less acidic catalysts had an extra peak at 503°C. This relation to acidity could also be observed in the KIL2 catalysts. The less acidic Li-KIL2 was the only catalyst with 5 peaks and the one with the highest

decomposition rate. It also had the extra peak at 503°C similar to the less acidic ZSM5 catalysts. Al-KIL2 on the other hand, which was the most acidic catalyst with the highest surface area, seemed to worsen the decomposition of lignin compared to the non-catalytic run.

Table 5-3: Lignin DTG data

Lignin		Pyrolysis Started at (°C)	1 st Peak	2 nd Peak	3 rd Peak	4 th Peak	5 th Peak	6 th Peak
Base	45	Curve Peaks	115		333.3	384.5	468.3	
		Temperature °C						
		Derivative Weight (%/min)	8.9		17.1	20.3	6.3	
Al-KIL2	100	Curve Peaks		159.3	334.6	377.1	468.8	
		Temperature °C						
		Derivative Weight (%/min)		1.4	10	9.5	4.2	
Li-KIL2	45	Curve Peaks	80		316.3	409.5	461.9	503
		Temperature °C						
		Derivative Weight (%/min)	5.3		19	3.8	6	0.5
20-ZSM5	100	Curve Peaks			339	377.3	465.5	
		Temperature °C						
		Derivative Weight (%/min)			9.3	8.9	3.8	
30-ZSM5	150	Curve Peaks			303	386.1	471.6	503.1
		Temperature °C						
		Derivative Weight (%/min)			15.4	4.7	6.1	1.2
60-ZSM5	150	Curve Peaks			306	383.9	478.4	503
		Temperature °C						
		Derivative Weight (%/min)			14.4	4.4	3.8	0.9

5.4.3 Phenylalanine

Figure 5-6 presents the graphs for effect of catalysts on derivative weight loss versus time for phenylalanine pyrolysis (individual graphs in Appendix B). Furthermore, Table 5-4 summarises the peaks, start of pyrolysis temperature and percentage weight loss rate for phenylalanine.

The first behaviour that could be observed is the temperature at which the decomposition is initiated. Al-KIL2 was clearly the catalysts which thermally destabilises phenylalanine the most. Furthermore, regardless of the catalyst utilised, all of the catalysts reduced the decomposition initiation temperature by at least 100 °C. This was a sign that the catalysts have in fact provided an alternative route for the reactions which required lower activation energy.

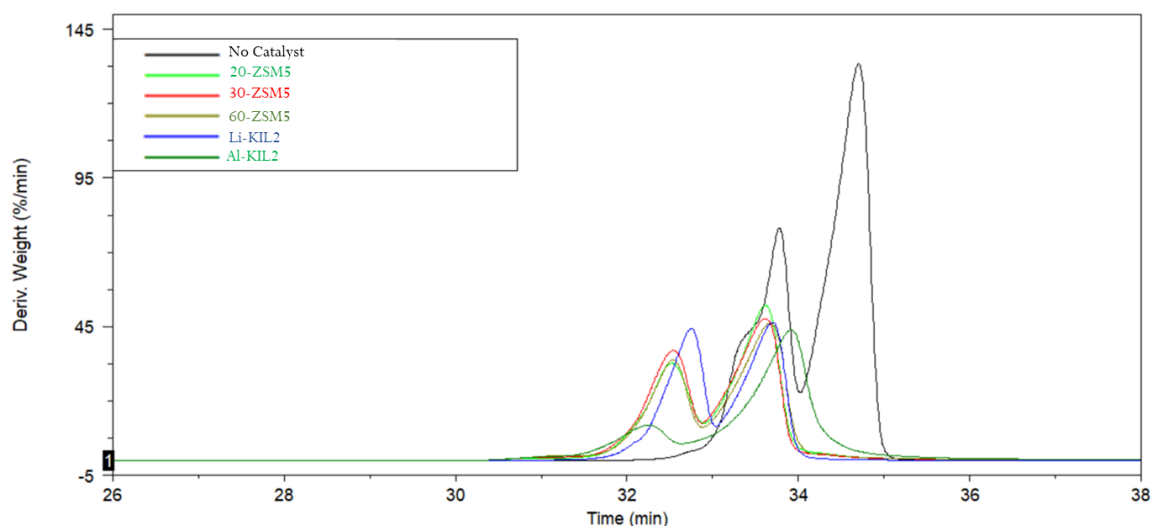


Figure 5-6: Phenylalanine DTG comparison curve

Comparing the Si/Al ratio in the ZSM5 catalysts, there was a clear trend. However, the acidity seemed to play a role. The more acidic 20-ZSM5 favoured the second peak, while the least acidic 30-ZSM5 favoured the first peak. The more acidic catalysts (i.e., 20-ZSM5 and Al-KIL2) reduce the temperature at which the first peak occurred while increasing the temperature at which the second peak occurred compared to other catalysts. The first peak was likely to represent decomposition of light incondensable compounds such as CO₂ and NH₃ while second peak representing heavier aromatics such as toluene and benzeneethanamine [5.8].

Table 5-4: Phenylalanine DTG data

Phenylalanine	Pyrolysis Started at (°C)		1st Peak	2nd Peak	3rd Peak
Base	210	Curve Peaks Temperature °C	312.8	357.7	447.0
		Derivative Weight (%/min)	39.8	77.7	133.3
Al-KIL2	100	Curve Peaks Temperature °C	266.8		428.0
		Derivative Weight (%/min)	11.8		43.9
Li-KIL2	110	Curve Peaks Temperature °C	311.7		404.9
		Derivative Weight (%/min)	44.3		46.2
20-ZSM5	105	Curve Peaks Temperature °C	303.7		410.6
		Derivative Weight (%/min)	32.7		52.3
30-ZSM5	100	Curve Peaks Temperature °C	305.4		410.6
		Derivative Weight (%/min)	37.0		47.6
60-ZSM5	107	Curve Peaks Temperature °C	304.9		415.2
		Derivative Weight (%/min)	33.8		46.1

5.5 Gas Analysis

The pyrolysis gas out of the TGA were analysed in order to observe the gas composition.

5.5.1 Cellulose Gas

As illustrated in Figure 5-7, all of the catalysts reduced the amount of CO₂ and increased the CO produced in cellulose pyrolysis which was a desirable transition due to the possibility of using the produced gas as syngas. The quantity of other components of the gas were insignificant compared to CO and CO₂.

The acidity of the catalysts and the surface area did not seem to have an effect on the gas component distribution trend. For instance, the second acidic catalyst which also had the largest surface area (Al-KIL2) had the reverse gas production trend compared to the most acidic catalyst (20-ZSM5). In case of ZSM5 however, the larger the Langmuir surface area, the more CO was produced. This could be explained by the fact that more area was available immediately on the surface of catalyst for deoxygenation. Since acidity of the catalysts was considered to promote deoxygenation [5.9], the reason behind lower quantities of CO in the more acidic catalysts could be that more oxygens had been removed and further reacted on the surface to form H₂O. This path could be seen in Figure 5-7 where the two most acidic catalysts contained the most amount of water.

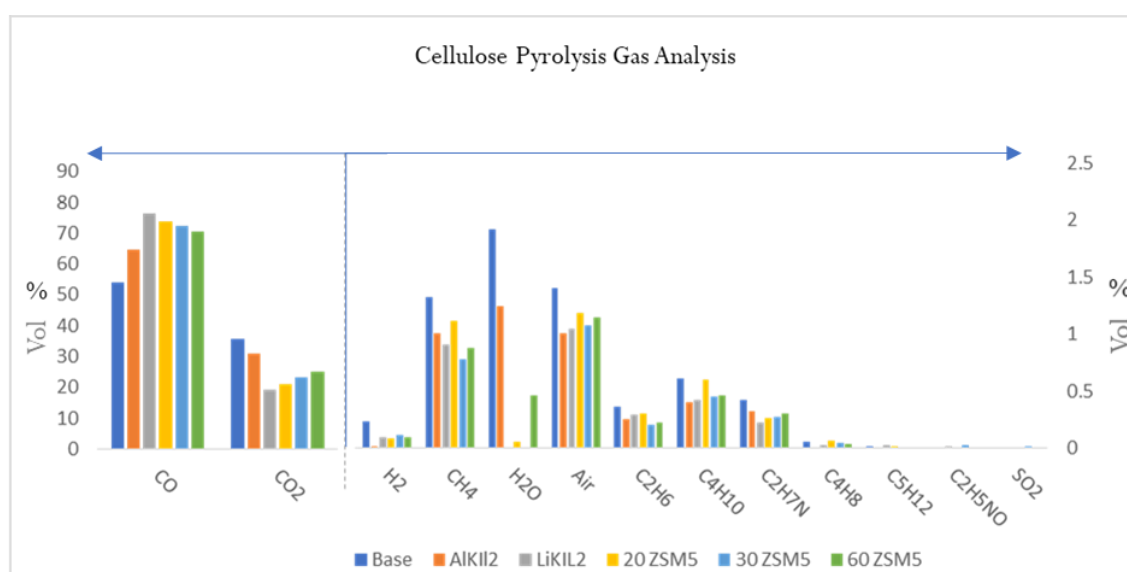


Figure 5-7: Gas analyses of cellulose catalytic pyrolysis

5.5.2 Lignin Gas

In case of lignin (Figure 5.8), the data indicated that the catalysts do not seem to have a significant effect on the gas products distribution. This observation was based on lack of significant difference between the composition of the gas in catalytic and non-catalytic runs. The main products, however, were CO and CO₂ similar to other model compounds. Furthermore, no apparent trend was visible in the obtained figure.

The large surface area of the Al-KIL2 did not come into play since the CO content was not much higher than other samples. In case of ZSM5 catalysts, there was no significant differentiator between the three different one used with respect to CO and CO₂ generation. However, acidity of the ZSM5 seemed to have a reverse correlation with production of HCN. This could have been due to more efficient deamination capability of more acidic catalyst which could have facilitated production of HCN through interaction with radicals.

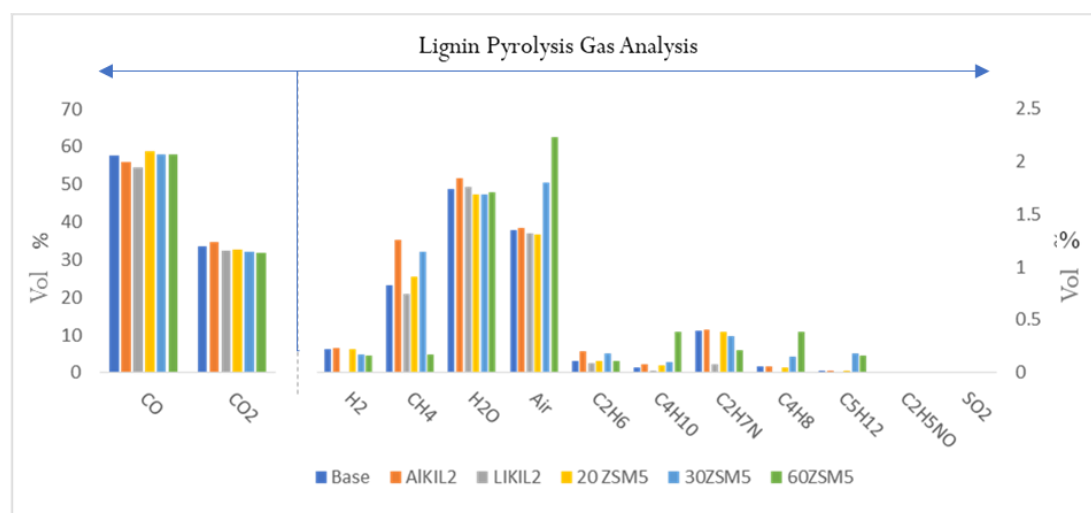


Figure 5-8: Gas analyses of lignin catalytic pyrolysis

5.5.3 Phenylalanine Gas

Analysing the phenylalanine gas (Figure 5-9), as expected, CO and CO₂ were the main products. The large amount of CO₂ was due to the conversion of phenylalanine by decarboxylation at low temperatures. Through use of catalysts, the amount of CO was increased while CO₂ was reduced with the exception of Li-KIL2. Through deamination of phenylalanine, cinnamic acid was produced. One path through which the CO and CO₂ could have been generated was through decomposition of this intermediate (cinnamic acid). R. L. Forman et al. reported that the ratio of CO to CO₂ would be 2 to 1 through this path [5.10] which was smaller than the results in the current experiment. Therefore, other paths should have had complimented this method. Another reason behind the large quantities of CO could have been due to interaction of H₂O and carbon radicals and alkanes in addition to carbon.

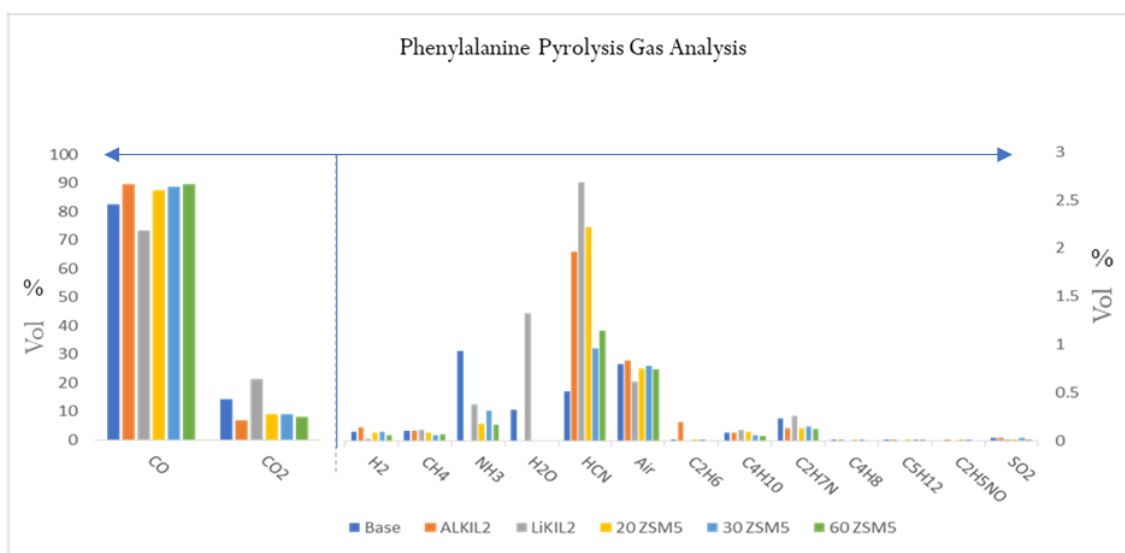


Figure 5-9: Gas analyses of phenylalanine catalytic pyrolysis

5.6 Oil Analyses

Results of oil analyses for each model compound are discussed in this section. The oil samples are obtained from fixed bed runs. The results obtained by GC-MS are sorted by functional groups. The chemical functionalities distribution could be used to understand the activity of the catalyst and linked to their acidity. It should be noted that the GC-MS graphs received, contained some impurities such as phthalates leached out from the GC capillary column, which were removed from the raw data set prior to categorising the oil sample components into functional groups for a clearer comparison between the catalysts. For each model compounds, the raw GC-MS graphs for each catalysts oil product were staggered on top of each other with vertical red lines across them which indicated the same time on all the graphs for simplifying the comparison of them.

5.6.1 Cellulose Oil

The main objective of testing these catalysts was to figure out which catalyst performed best for depolymerizing the model compound and produced desired products such as aromatics. As illustrated in Figure 5-10, the ZSM5 catalysts performed as expected from literature in converting the cellulose in case of aromatic generation. In case of ZSM5 catalysts, the quantity of aromatics increased by increasing the acidity following the order: 20-ZSM5 > 60-ZSM5 > 30-ZSM5. However, with aromatic generation in mind as the main reason for catalyst utilisation, it was observed that only Al-KIL2, 60-ZSM5 and 20-ZSM5 are beneficial since all the other catalytic runs produced less aromatics than the non-catalytic run. Large surface area of Al-KIL2 made it by far the most efficient catalyst for production of aromatics. On the opposing trend, 30-ZSM5 and Li-KIL2 catalysts were active for producing the carbohydrates. This could again be connected to the acidity

of the catalysts in conjunction to the lack of ability of these catalysts in aromatisation. Considering the molecular structure of cellulose and the literature on pyrolysis path of cellulose, the initial stage is dehydration leading to formation of anhydro sugars such as anhydro-oligosaccharide [5.9] (categorised as carbohydrates in this paper). Over acid catalysts or availability of more area for reaction, these carbohydrates could undergo further dehydration, decarboxylation, and reforming (oligomerisation) to produce furans (categorised as ketone in this paper), aldehydes, aromatics or and low molecular weight (till C6) olefins [5.7] [5.11].

The large amount of carbohydrates in Li-KIL2, 30-ZSM5 and 60-ZSM5 illustrated the fact that they performed well in the initial stages of process to produce the dehydrated carbohydrates, while lacked the ability to perform the rest of the steps due to lower acidity. This could further be solidified by considering the quantity of alkenes produced. A competing path to production of aromatics is olefins (alkenes) production [5.12] [5.9]. As it can be seen in Figure 5-10, 20-ZSM5 and Al-KIL2 produced the most quantity of alkene. This can demonstrate that this alternative route was partially presented and 20-ZSM5 preferred this path more compared to Al-KIL2 due to its higher acidity.

Additionally, Ester had the opposite trends in ZSM5 cases. The carbohydrate and ester trends could be connected. In other words, the lack of hydrogen released by the breakage of the carbohydrates in case of 60-ZSM5 could be the reason behind the trend observed in ester generation.

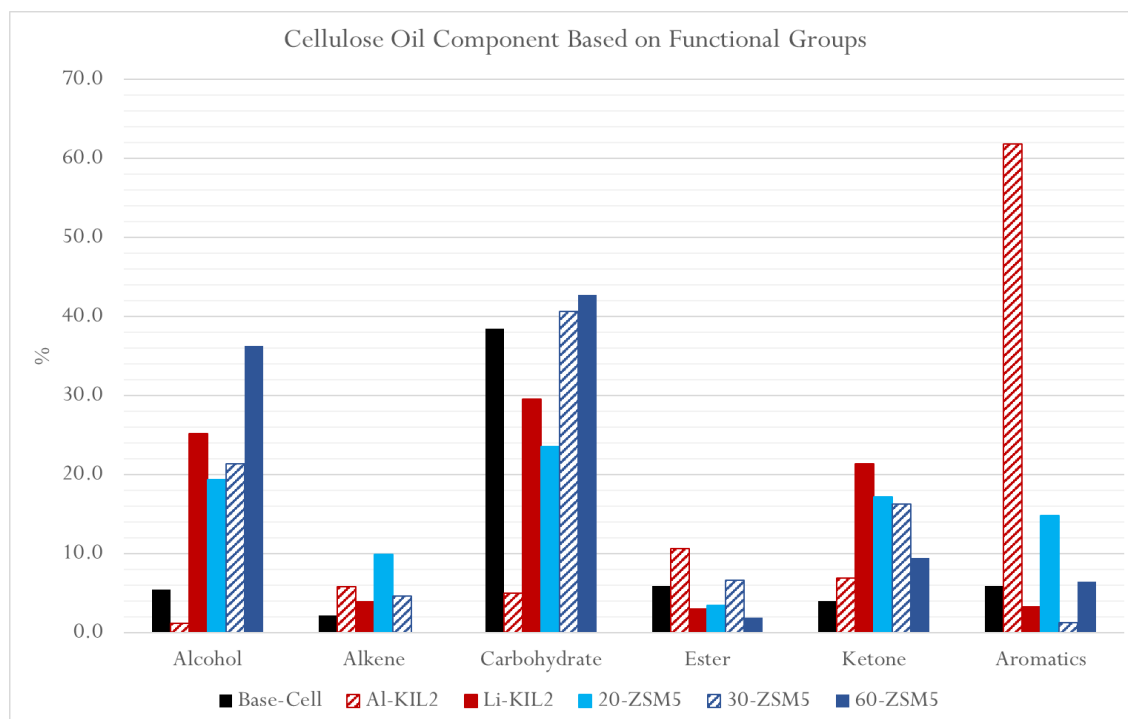


Figure 5-10: Comparison of oil products of Cellulose catalytic runs

Al-KIL2 was the most efficient catalyst in production of aromatic by a large margin. One of the reasons behind this could be the surface area available for cracking the cellulose since the BET surface area of Al-KIL2 was almost triple that of 20-ZSM5. Additionally, the theory mentioned previously that if KIL2 behaves similar to SBA15 upon introduction of aluminium, the addition of aluminium corresponds to an increase in acidity and therefore the high conversion of cellulose to aromatics. The fact that there were almost no alcohol and the least amount of carbohydrates, considering the high aromatics percentage, could lead to two findings. First, the high capability of Al-KIL2 to dehydrate the cellulose and second, the possibility of higher aromatic content if more time or hydrogen was supplied to the system.

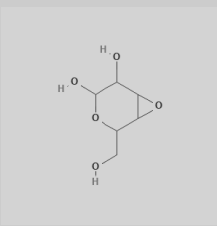
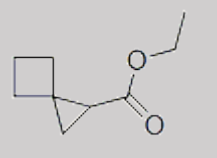
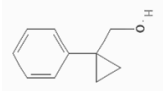
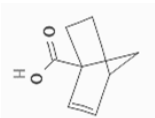
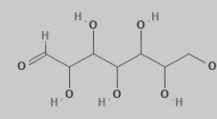
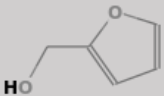
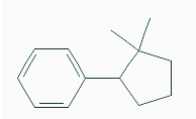
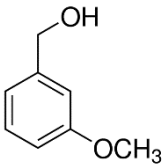
As expected, conversion under Li-KIL2 was not optimal. The low BET surface area and alkalinity was the reason behind this expectation. Comparing with Al-KIL2, the Li clearly hindered the dehydration and aromatization processes.

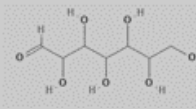
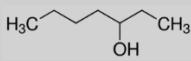
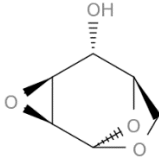
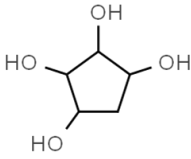
Figure 5-11 compares the peaks observed in the GC-MS results of each catalytic run while Table 5-5 lists the 2 largest products of each run. It was expected that the addition of acid catalysts would lead to production of hydrocarbon and H₂O which then consequently would lead to production of aromatics [5.13]. For example, the two of the most acidic catalysts, namely 20-ZSM5 and Al-KIL2, had aromatics as their main products while the other catalytic runs which were less acidic or not acidic at all had carbohydrates as their main products.

Another sign that demonstrates the effect of catalyst acidity on its behaviour was the identical top products for pyrolysis with Li-KIL2 and 30-ZSM5, the two least acidic catalyst. These simple products, which could also be observed for un-catalytic and 60-ZSM5 catalyst pyrolysis, were considered to be the products of the first step of conversion of cellulose through cleavage of glycosidic bond and lack the capability to further convert the cellulose.

Another interesting aspect that can be seen through Figure 5-11, was the presence of extra peaks between retention times of 45 to 55 min with the use of more acidic catalysts, Al-KIL2 and 20-ZSM5, which represented aromatics such as benzene, 2-propenyl for 20-ZSM5 and cyclopropane methanol, 1-phenyl-for Al-KIL2. It should be noted that the retention times were not identical for the 20-ZSM5 and Al-KIL2.

Table 5-5: Two main components of liquid products of cellulose

	Name	Structure	Group	Area %
Un-Catalytic	3,4-Altrosan		carbohydrate	34.9
	Spiro hexane-1-carboxylic acid, ethyl ester-		ester	2.5
AI-KIL2	Cyclopropane methanol, 1-phenyl-		aromatic	18.0
	Bicyclo [2.2.1] hept-2-ene-1-carboxylic acid, 6-		carboxylic acid	8.7
Li-KIL2	d-Glycero-d-galacto-heptose		carbohydrate	16.8
	2-Furanmethanol		alcohol	8.4
20-ZSM5	Benzene, (2,2-dimethylcyclopentyl)-		aromatic	10.7
	3-Methoxybenzyl alcohol		aromatic	9.1

30-ZSM5	d-Glycero-d-galacto-heptose		carbohydrate	33.3
	3-Heptanol		alcohol	7.3
60-ZSM5	2,3-Anhydro-d-mannosan		carbohydrate	32.0
	1,2,3,4-Cyclopentanetetrol		alcohol	23.9

Cellulose - GC-MS of Oil Comparison

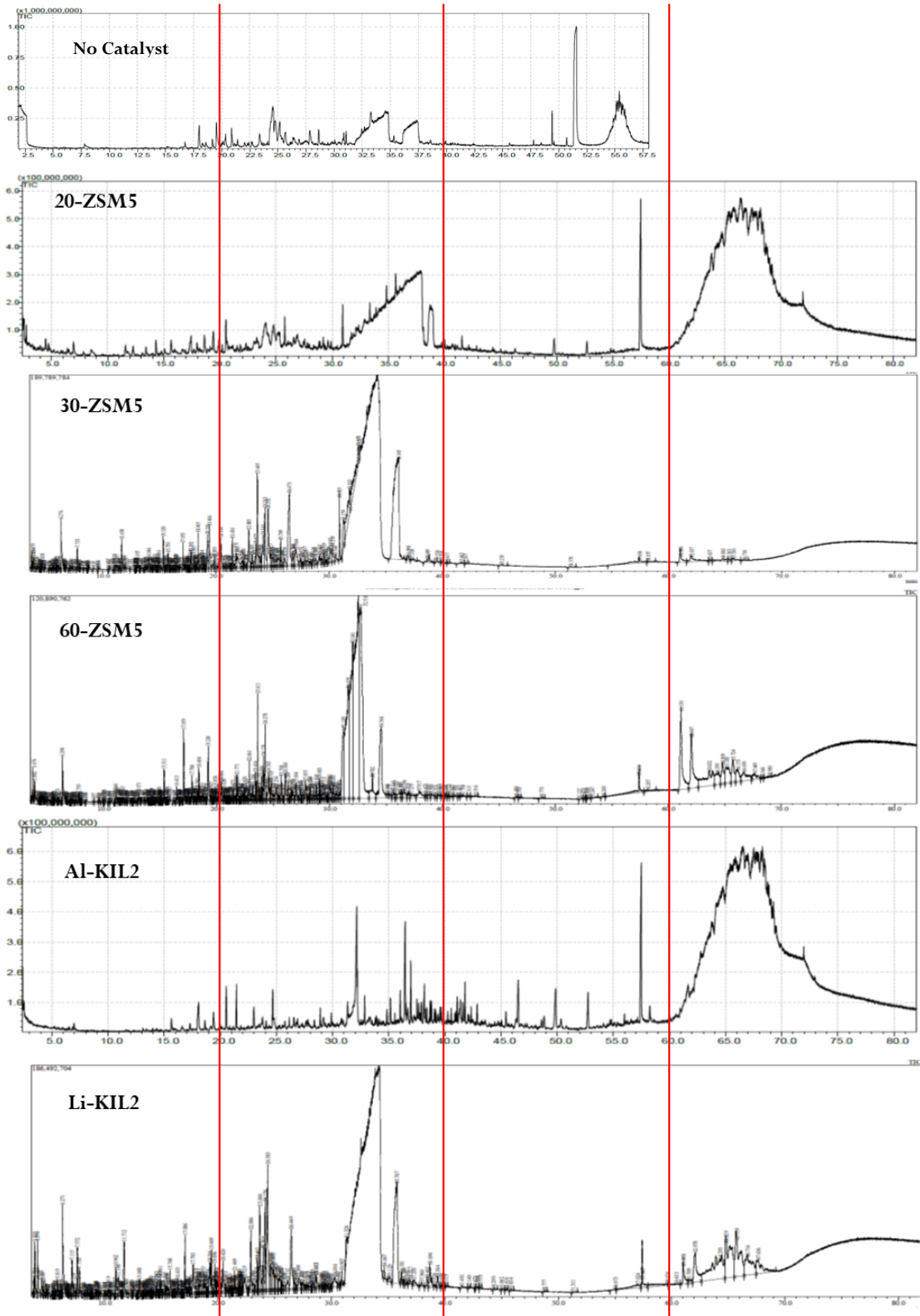


Figure 5-11: Cellulose GC-MS curve comparison

5.6.2 Lignin Oil

As Expected, due to the molecular structure of lignin, aromatics were a larger constituent of the products compared to cellulose and all of the catalysts improved the aromatisation compared to the uncatalyzed run. Due to the dominance of aromatics in the oil products and significantly lower quantities of other functional groups compared to aromatics, only 3 main groups (phenols, mono aromatics, and poly aromatics) are compared in Figure 5-12. Table 5-6 shows the 2 largest components of each run, while Figure 5-13 presents a comparison between the GC-MS curves obtained for each catalyst.

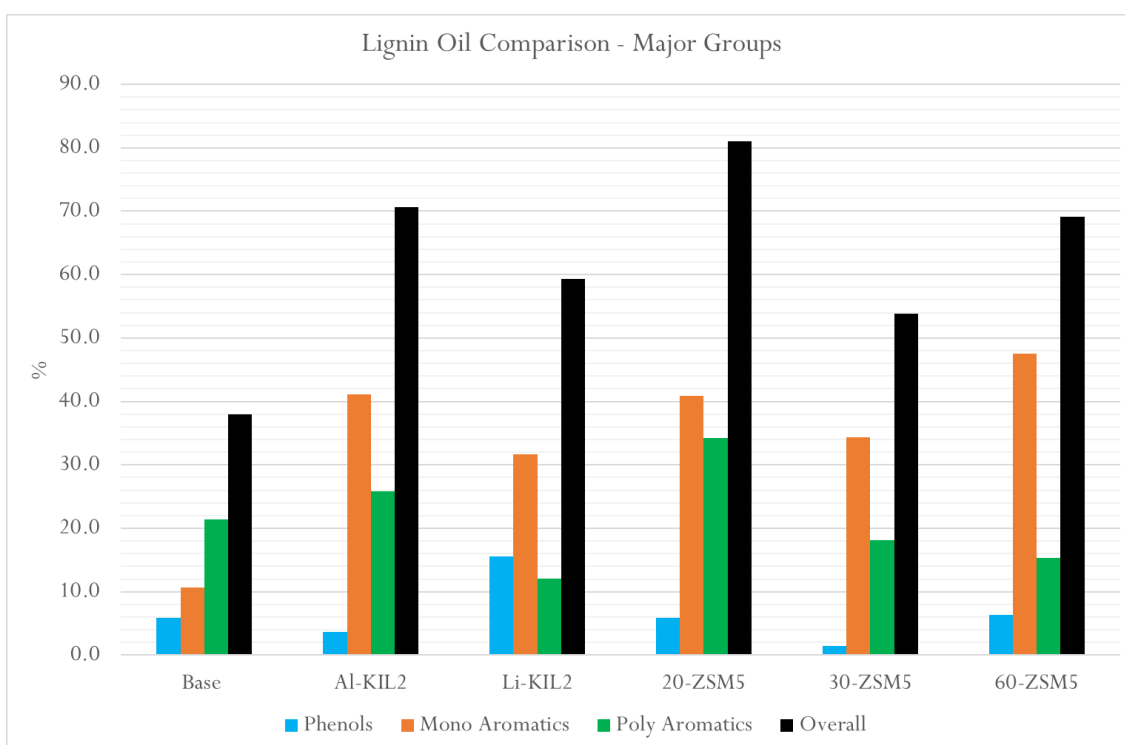


Figure 5-12: Lignin GC-MS functional groups

During the non-catalytic pyrolysis of lignin, the first step is depolymerisation of the feed [5.14]. This depolymerisation will produce alkoxy phenols or dimers of lignin feed. The next step during the pyrolysis of lignin can be varied by acidic catalysts. One path would be conversion of these large alkoxy phenols and dimers to smaller ones through cracking, dealkylation and dehydration. These smaller components can either be converted to alkyl phenols through dealkoxylation, isomerisation and extra oligomerisation or small olefins (C2 to C6) through cracking and dehydration [5.9]. The products from either path can further react together to form other mono or poly aromatics through oligomerisation.

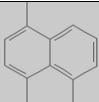
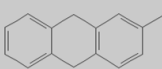
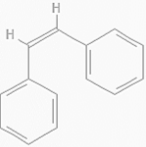
Observing the trends for the overall conversion to aromatics, there was a clear direct correlation between acidity and aromatics production. However, no clear trend was observed in ZSM-5

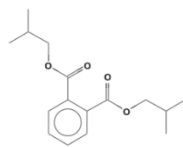
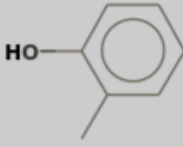
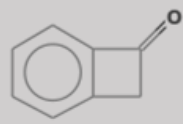
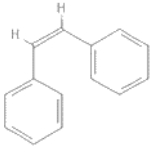
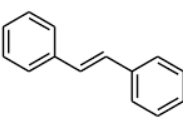
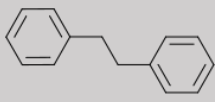
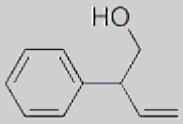
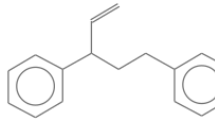
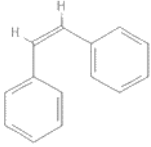
catalysts with the Si/Al ratio in mind in the overall aromatisation even if, as the Si/Al ratio increased, the quantity of poly aromatics decreased.

Li-KIL2 seemed to favour production of phenols by far more than other catalysts. As previously discussed, the first step in pyrolysis of lignin is depolymerisation and conversion to large alkoxy phenols. One reason behind the better performance of Li-KIL2 in production of phenol and overall better performance for lignin conversion to aromatics compared to cellulose could be having the largest median pore width which could assist the first step of pyrolysing the large molecules of lignin. However, once the first step was carried out and smaller components were produced, Li-KIL2 lower acidity restricted further conversion to other products (mono aromatic and poly aromatics) compared to other catalysts.

When comparing the products of the acidic KIL2 catalyst, Al-KIL2, and the least acidic catalyst Li-KIL2, a key observation could be made. “2-methylphenol” is an alkyl phenol while cis-Stilbene is a more complex polyaromatics which was likely to have been produced by dehydration and further oligomerisation of two 2-methylphenol like intermediates. This showed that the acid sites of the catalysts can be determinant when production of certain more complex compounds are targeted. Interestingly, the acidity of ZSM5 catalysts had direct proportionality in production of Stilbene. In more details, all the ZSM5 catalysts had stilbene in their top three products. The amount of Stilbene in the products was largest in 20-ZSM5 and was reduced in 60-ZSM5 and reaches a minimum in 30-ZSM5. This trend was consistent with the acidity relationship of these three catalysts. Furthermore, comparing the overall GC-MS curves, the more acidic 20-ZSM5 and Al-KIL2 demonstrated more prominent peaks at 32 minutes. These peaks also corresponded to stilbene. This also demonstrated that acidity played an important role in pyrolysis of lignin,

Table 5-6: Lignin main components in liquid product

	Name	Structure	Area %
Base	Naphthalene, 1,4,5-trimethyl-		3.3
	Anthracene, 9,10-dihydro-2-methyl-		3.2
Al-KIL2	cis-Stilbene		9.5

	1,2-Benzenedicarboxylic acid, bis (2-methylpro- ester		5.81
Li-KIL2	Phenol, 2-methyl-		8.3
	Benzocyclobuten-1(2H)-one		7.3
20-ZSM5	cis-Stilbene		10.9
	(E)-Stilbene		6.1
30-ZSM5	Bibenzyl		7.7
	Benzene ethanol, beta. -ethynyl-		7.1
60-ZSM5	Benzene, 1,1'-(1-ethenyl-1,3-propanediyl) bis-		10.4
	cis-Stilbene		6.7

Lignin - GC-MS of Oil Comparison

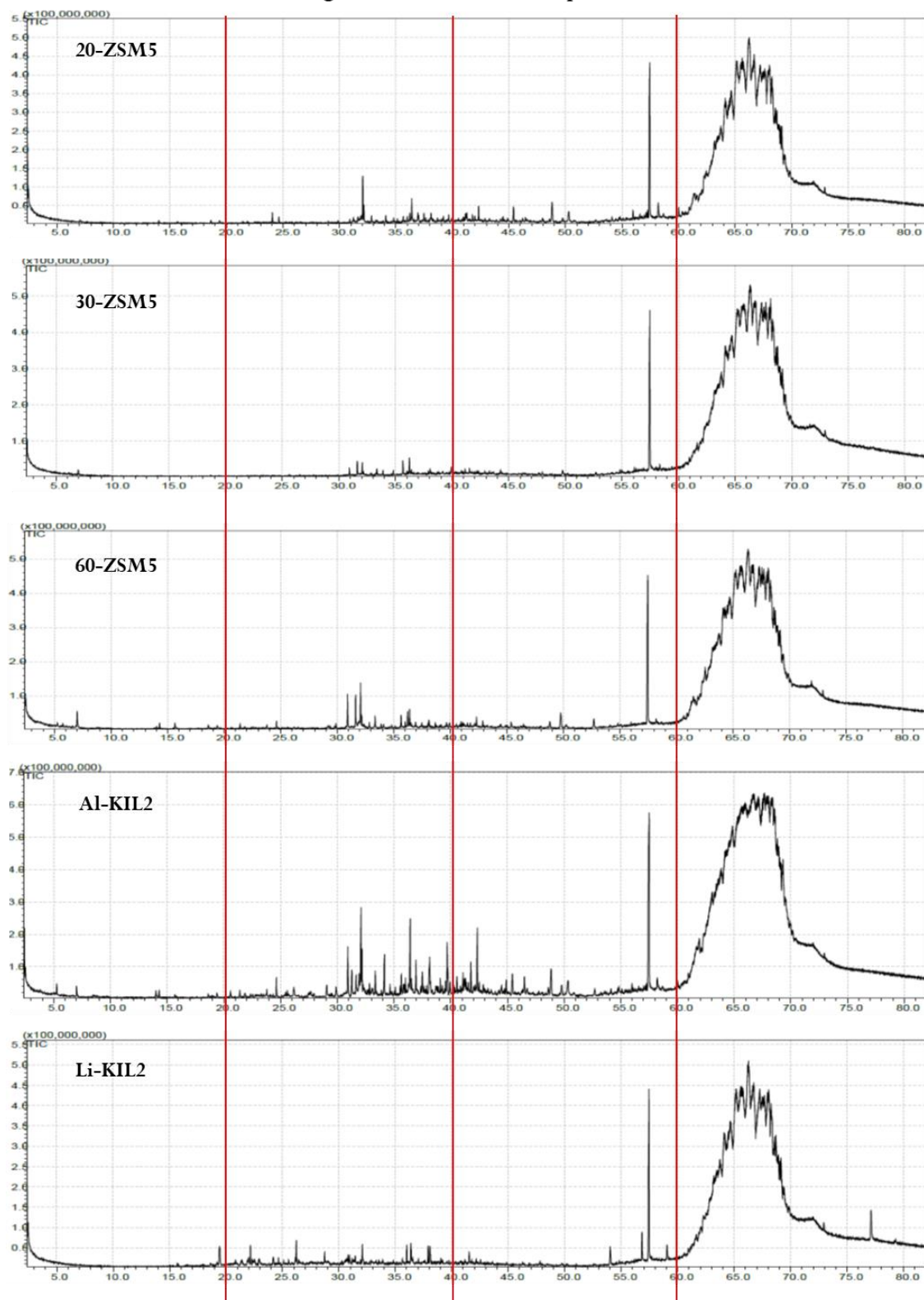


Figure 5-13: Lignin GC-MS comparison curves

5.6.3 Phenylalanine Oil

During the pyrolysis of phenylalanine, the following mechanism can typically be expected: decarboxylation, homolyses, cyclization, deamination. An initial benzylic bond break can be followed by formation of intermediates such as phenyl and unstable molecules. The paths taken can be competitive [5.15]

During the homolyses, CO₂ is released producing unstable compounds which can be followed by removal of H₂. These two steps can lead to generation of aromatic nitriles. The deamination path followed by homolyses can lead to production of benzene derivatives such as styrene (C₈H₈). If hydrogen radicals are available, other aromatic compounds can be formed through addition, reformation, and cyclisation. The additional of carboxyl to phenylalanine can result in production of aromatic aldehydes. On the other hand, removal of carboxyl group will produce a compound with amine radical which can produce indoles through reformation [5.15].

From the phenylalanine monomer and previous works, cyclic and aromatic compounds were expected to be dominant from phenylalanine pyrolysis [5.15] [5.16]. Figure 5-14 illustrates the product component distribution results for the GC-MS of oil. The dominance of aromatics in oil products fell in line with the expectation.

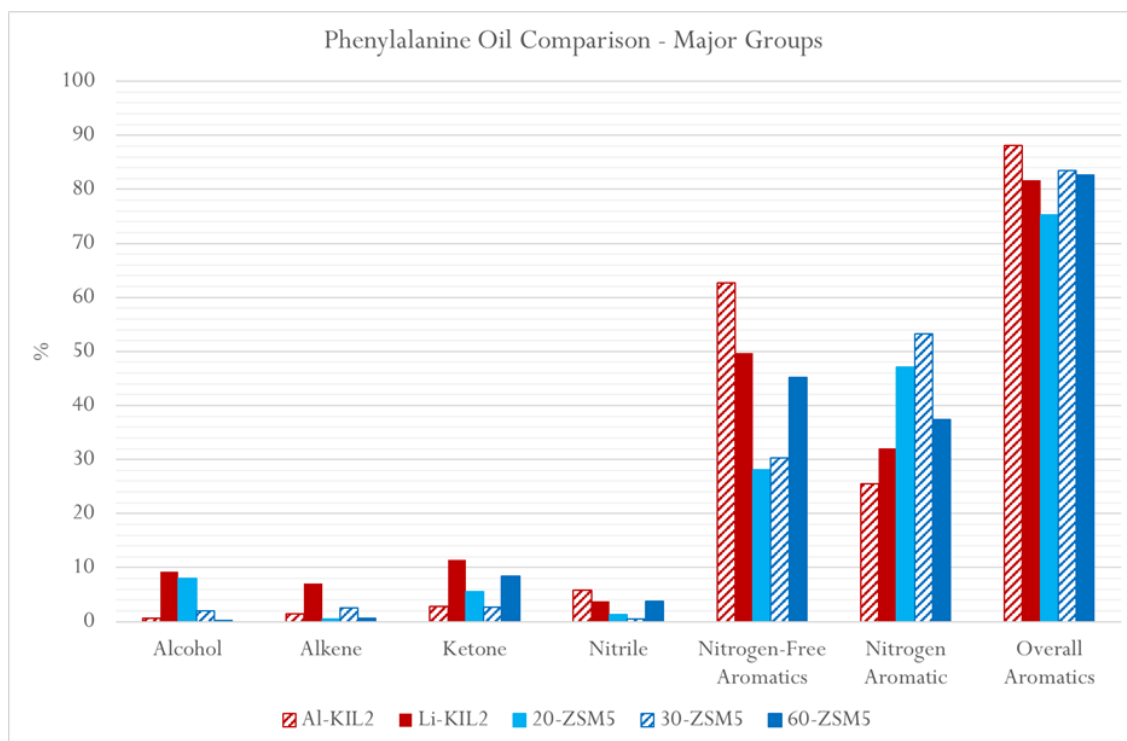
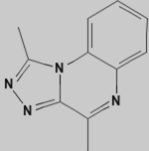
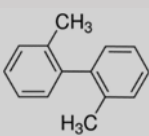
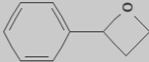
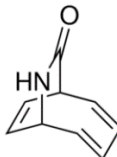


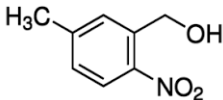
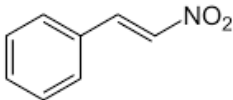
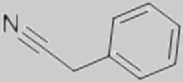
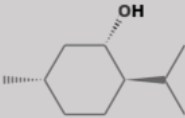
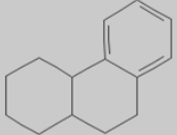
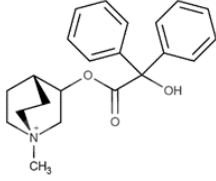
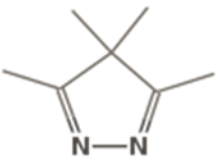
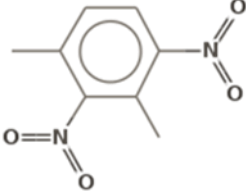
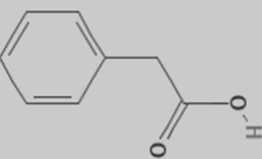
Figure 5-14: Phenylalanine functional group comparison

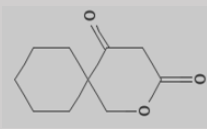
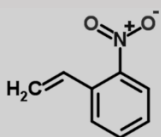
Comparing the ZSM5 catalysts, there did not seem to be a significant difference between overall percentage of aromatics of 60-ZSM5 and 30-ZSM5 (only less than 2% difference). However, regarding the acidity of the three catalysts, there was a reverse correlation with regards to the overall aromatic production. Furthermore, regarding the nitrogen-free aromatics, there seemed to be a direct correlation with increase in Si/Al ratio with the 60-ZSM5 being the most effective in removing nitrogen from the aromatics. However, since phenylalanine feed had aromatics in itself, quantity of the aromatics produced was not deemed a clear determinant in observing the behaviour of the catalysts.

GC-MS analyses showed many components (peaks) in the oil product, indicating that the reactions had not been selective towards one major component. For instance, there were over 80 different components in the oil product of phenylalanine pyrolysis with AL-KIL2. Therefore, to observe which conversion path had been dominant during the application of each catalysts, top 3 products were shortlisted for each run (Table 5-7). Additionally, the curves for the GC-MS analysis (Figure 5-15) were compared.

Table 5-7: Most abundant products in phenylalanine oil

Catalyst	Name	Structure	Area %
Al-KIL2	[1,2,4] Triazolo[4,3-a] quinoxaline, 1,4-dimethyl		17.6
	2,2'-Dimethylbiphenyl		9.0
	2-Phenyl-oxetane		5.7
Li-KIL2	7-Azabicyclo [4.2.2] deca-2,4,9-trien-8-one		9.7

	5-Methyl-2-nitrobenzyl alcohol		4.9
	2-Nitrostyrene		4.4
20-ZSM5	benzene acetonitrile, alpha. - [3-phenyl-2-prope		16.6
	Cyclohexanol, 5-methyl-2-(1-methylethyl)-, be		5.8
	1,2,3,4,4a,9,10,10a-Octahydrophenanthrene		4.0
30-ZSM5	Clidinium		6.6
	Pyrazole, 3,4,4,5-tetramethyl-		5.9
	2,4-Dinitro-1,3-dimethyl-benzene		4.3
60-ZSM5	Benzene acetic acid		17.8

2-Oxaspiro [5.5] undecane-3,5-dione, 1-(3,4-di		7.2
2-Nitrostyrene		5.0

Comparing the most abundant compounds for ZSM5 catalysts, acidity of the catalyst seemed to be important in deoxygenating phenylalanine. This was based on comparing the amount of oxygen in the top three products of 20-ZSM5 with those of the other two ZSM5 catalysts. Furthermore, acidity favoured producing fewer number of components with higher intensity. For instance, only three components made up over 25% of aromatics in the more acidic 20-ZSM5, while this amount for the same quantity of components was 17% for 30-ZSM5.

Two phenomena were dominant in the runs with AL-KIL2; the first one was the minimisation of small compounds such as alkenes while maximisation of complex aromatics occurs. The next one was the fact that 3 components (Table 5-7) made up more than 40% of the products which showed a better selectivity of Al-KIL2 for certain products. However, Al-KIL2 catalyst, due to the large surface area available for contact with model compounds, proved its capability to break down the phenylalanine monomer and form more complex components. One explanation for production of components such as “[1,2,4] Triazolo[4,3-a] quinoxaline, 1,4-dimethyl” could be selectivity of Al-KIL2 for decarboxylation followed cyclisation and oxidation (removal of H).

In the run with Li-KIL2, the component with highest quantity was 7-Azabicyclo [4.2.2] deca-2,4,9-trien-8-one (C₉H₉NO) This could be due to selectivity of Li-KIL2 for a path in which hydroxyl group was removed through a carbocation intermediate followed by a benzene ring cleavage. Another finding through observing the most abundant compounds was the existence of oxygen in the structure of all of them. This could translate to the low selectivity of Li-KIL2 for removal of hydroxyl group and reduction.

Comparing the two KIL2 catalysts indicated that not only Al-KIL2 promoted production of aromatics over other components such as alcohol, but it also performed better for deoxygenating the oil product. This was observed through comparing the top products in the oil sample observed

from catalytic pyrolysis with each catalyst and the larger quantities of oxygen containing compounds such as alcohol and ketone in Li-KIL oil sample.

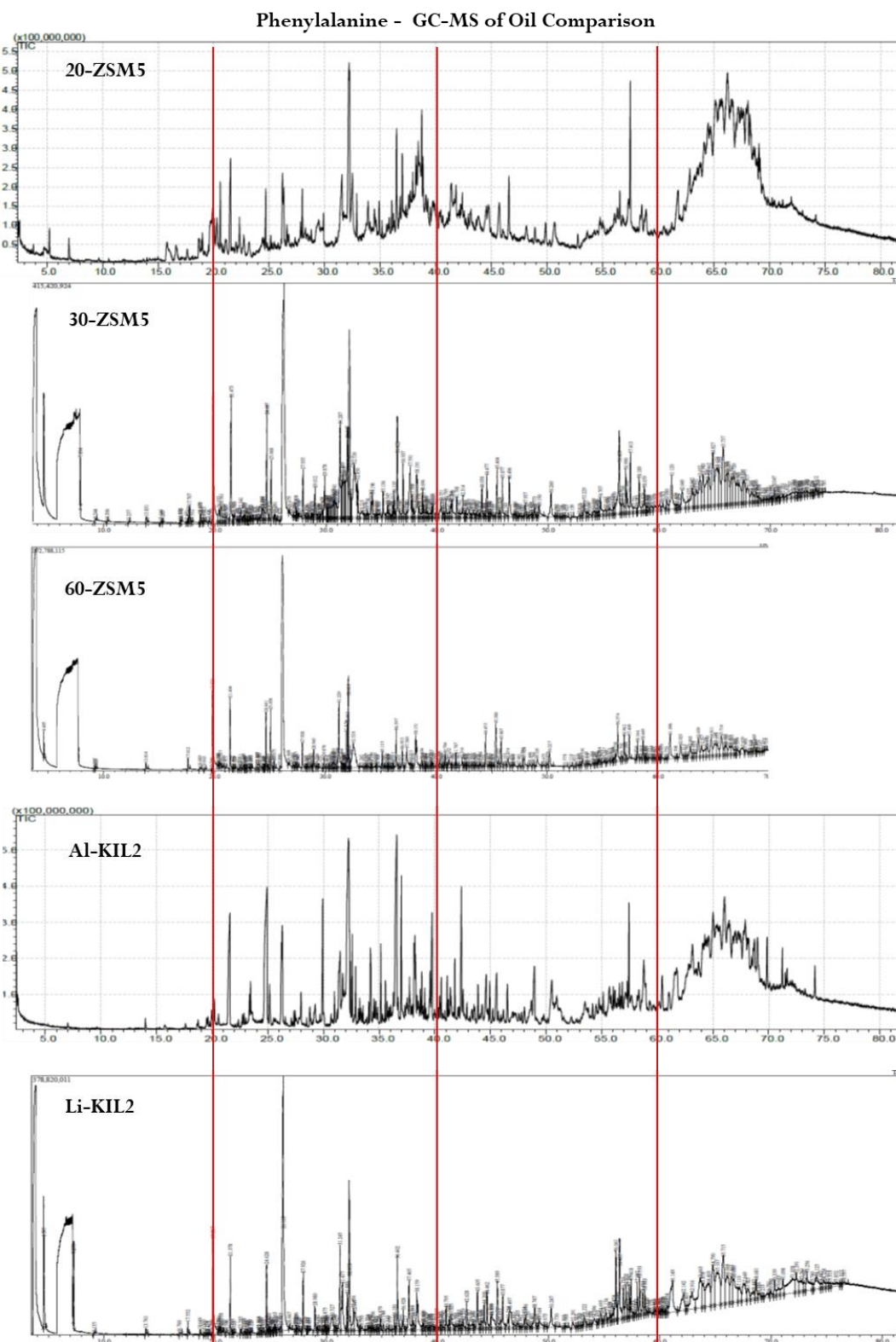


Figure 5-15: Phenylalanine GC-MS comparison curves

5.7 Discussion & Section Conclusion

The runs were carried out to establish which catalysts perform better in conversion of the model compounds to aromatics and deoxygenate the oil. All the catalysts showed that they can modify the properties of the products of model compound's pyrolysis one way or another. However, the ultimate goal of this research was to observe the efficiency of the selected catalysts on wool pyrolysis. Therefore, based on the nature of the catalysts, it was decided to take one KIL2 catalyst and one ZSM5 catalyst forward for wool pyrolysis to observe the behaviour of each catalysts group.

5.7.1 KIL2

The performance of these catalysts for each model compound are summarised in the following sections.

5.7.1.1 Cellulose

Mass balance result indicated that the Al-KIL2 favoured char production while Li-KIL2 promoted volatile (oil and gas) production. However, utilisation of both of them reduced the temperature at which pyrolysis started by at least 30°C through introducing an alternative path to pyrolysis compared to non-catalytic run. In the gas products, both catalysts promoted CO while reducing CO₂ compared to the non-catalytic sample. While Li-KIL2 favoured CO production, Al-KIL2 favoured CO₂, CH₄ and water production.

Al-KIL2 was by far the superior option for aromatisation of the oil product. In more details, the aromatic content of the Al-KIL2 oil sample was over 12 times of that of Li-KIL2. Furthermore, considering the oxygen containing groups such as alcohols and ketones, Al-KIL2 was again the better performing catalyst minimising them. For instance, the alcohol content of Al-KIL2 was less than 2% while Li-KIL2 exceeded 24%.

Overall, Li-KIL2 seemed a better catalyst if reduction in CO₂ in the gas was the aim. However, with aromatisation, deoxygenation, and stabilisation of the oil product in mind, Al-KIL2 was by far the better option. Furthermore, the difference in CO% in gas was not as significant as aromatics percentage in oil.

5.7.1.2 Lignin

Similar to cellulose, mass balance results indicated that Al-KIL2 favoured char production while Li-KIL2 favoured volatiles (oil and gas) production. The results for the DTG indicated that Li-KIL2 results were more similar to the non-catalytic run and showed one more peak compared to Al-

KIL2. This higher decomposition of Li-KIL2 sample compared to Al-KIL2 was in line with mass balance results. Catalysts did not show a significant effect on the composition of the gas product.

Similar to cellulose, Al-KIL2 performed better in aromatising lignin products compared to Li-KIL2. This was the case for both mono and poly aromatics, However, Li-KIL2 performed better in phenol production. Due to the nature of the feed, it was concluded that this could be a result of the large pore median width of Li-KIL2 compared to other catalyst. This conclusion assumed that more space will be available on the pore surface for the large lignin molecule to attach at the first step of pyrolysis (depolymerisation). Furthermore, comparing the top products of these two catalysts, Al-KIL2 performs better in deoxygenation of oil product.

5.7.1.3 *Phenylalanine*

Despite insignificant difference, similar to cellulose and lignin, Al-KIL2 favoured char production while Li-KIL2 favoured volatiles. Both catalysts reduced the pyrolysis initiation temperature by at least 100°C while Al-KIL2 reduced by another 10°C. Contrary to cellulose, Al-KIL2 favoured CO production over CO₂ while Li-KIL2 followed the reverse of this.

Overall, the difference between the catalysts for production of aromatics was not as significant as the case for cellulose. None the less, Al-KIL2 samples contain more aromatics than Li-KIL2. Furthermore, Al-KIL2 produced far less oxygen containing components such as ketones and alcohols.

5.7.2 **ZSM5**

The performance of these catalysts for each model compound will be summarised in the following sections.

5.7.2.1 *Cellulose*

Mass balance results indicated that there was a direct correlation between Si/Al ratio and volatile (oil and gas) production. In other words, the TGA result indicated that by increasing the Si/Al ratio from 20 to 60, the char production is reduced by more than 40%. The same correlation could be observed in reducing the pyrolysis initiation temperature. Regarding gas products, there was not a significant difference between the catalysts in production of CO and CO₂. However, slight increase in CO/CO₂ was observed as Si/Al increased.

In the oil products, 20-ZSM5 was the best performing catalyst for generating aromatics while the other catalysts produced carbohydrates predominantly. This demonstrated the lack of capability of

less acidic catalysts to aromatise the carbohydrates which are produced at the first step of cellulose pyrolysis. Furthermore, over 40% of the 30-ZSM5 and over 55% of 60-ZSM5 oil products were made by 2 components: one carbohydrate and one alcohol. This showed lack of capability of these catalyst in deoxygenating the oil product.

5.7.2.2 *Lignin*

Acidity of the catalysts had direct proportionality with char production. Therefore, based on TGA data, 20-ZSM5 had the highest char production while 30-ZSM5 had the least percentage of char. The pyrolysis initiation temperature was increased by 50°C in less acidic catalysts (i.e., 30 and 60-ZSM5) compared to 20-ZSM5.

Oil GC-MS results indicated that the higher the acidity, the more aromatics are produced. Also, regarding the deoxygenation capability, acidity seemed to be beneficial. For instance, the top two products, which made up over 14% of the oil for all the catalysts, contained no oxygen in case of 20 and 60-ZSM5 catalysts while this non-existence of oxygen containing compounds in the top products did not stand for 30-ZSM5.

5.7.2.3 *Phenylalanine*

All of the catalysts reduced the temperature at which the pyrolysis starts compared to the non-catalytic case. However, the difference between the catalysts was insignificant and less than 8°C. Also, there was not a clear pattern to distinguish the catalysts performance in gas analysis.

Similar to gas analysis results, the difference between catalysts was minimal in overall conversion to aromatics. For instance, the largest difference was observed between 20-ZSM5 and 30-ZSM5, which was less than 8%. Based on observing the largest constituent of the oil, the more acidic catalysts were more effective in deoxygenating the phenylalanine.

5.7.2.4 *Conclusion*

20-ZSM5 was clearly the best performer among the ZSM5 catalyst for aromatisation of lignin and cellulose oil product. However, the difference in effectivity with regards to aromatisation of the products was not as clear for phenylalanine conversion. However, considering the overall performance of the catalysts for pyrolysis of all the model compounds, 20-ZSM5 was selected to be taken forward.

Among KIL2 catalysts, as expected, Al-KIL2 performed better in production of aromatics in pyrolysis of all the model compounds. Furthermore, the high acidity and surface area of Al-KIL2

made it a potentially efficient catalyst to be used for pyrolysis of wool. Therefore, 20-ZSM5 and Al-KIL2 were taken forward to be used for pyrolysis of wool.

5.8 References

- [5.1] L. Shirazi, E. Jamshidi and M. R. Ghasemi, "The effect of Si/Al ratio of ZSM-5 zeolite on its morphology, acidity and crystal size," *Cryst. Res. Technol.*, vol. 43, no. 12, pp. 1300-1306, 2008.
- [5.2] O.A. Anunziata, A.R. Beltramone, M.L. Martinez, "Synthesis and characterization of SBA-3, SBA-15, and SBA-1 Nanostructured catalytic materials," *Journal of Colloid and Interface Science*, pp. 184-190, June 2007.
- [5.3] S.Lin, L. Shi, "Direct Synthesis without addition of acid of Al-SBA-15 with controllable porosity and high hydrothermal stability," *Microporous and Mesoporous Materials*, pp. 526-534, January 2011.
- [5.4] S. E. Volts, "The Catalytic Properties of Supported Sodium and Lithium Catalysts," *Houdry Process Corporation*, 1956.
- [5.5] M.R. Hajaligol, J.B. Howard, J.P. Longwell, and W.A. Peters, "Product Compositions and Kinetics for Rapid Pyrolysis of Cellulose," *Ind. Eng. Chem. Process Des. Dev.*, 1982.
- [5.6] M. Witczak, M. Walkowiak, W. Cichy, M. Komorowicz, "The application of elemental analysis for the determination of the elemental composition of lignocellulosic materials," *Forestry and Wood Technology*, 2015.
- [5.7] P. R. Patwardhan, "Understanding the product distribution from biomass fast pyrolysis," *Iowa State University*, 2010.
- [5.8] L. Jie, L. Yuwen, S. Jingyan, W. Zhiyong, H. Ling, Y. Xi, W. Cunxin, "The investigation of thermal decomposition pathways of phenylalanine and tyrosine by TG-FTIR," *Thermochimica Acta*, 2008.
- [5.9] R. Liu, M. Sarker, M. M. Rahman, C. Li, M. Chai, R. Cotillon, N.R. Scott, "Multi-scale complexities of solid acid catalysts in the catalytic fast pyrolysis of biomass for bio-oil production –A review," *Progress in Energy and Combustion Science*, 2020.

- [5.10] J. Pattersonx, A. F. Haidar, E.P. Papadopoulos, W.T. Smith, "Pyrolysis of Phenylalanine, 3,6-Dibenzyl-2,5-piperazinedione, and Phenethylamine," *J. Org. Chem*, 1972.
- [5.11] H.C. Liu, H. Wang, A. M. Karim, J. Sun, and Y. Wang, "Catalytic fast pyrolysis of lignocellulosic biomass," *Chemical Society Reviews*, 2014.
- [5.12] H X. Li, H. Zhang, J. Li, L. Su, J. Zua, "Improving the aromatic production in catalytic fast pyrolysis of cellulose bt co-feeding low-density polyethylene," *Applied Catalysis A: General*, pp. 114-121, 2013.
- [5.13] X. Han, Y. Guo, X. Liu, Q. Xia, Y. Wang, "Catalytic conversion of lignocellulosic biomass into hydrocarbons: A mini review," *Catalysis Today*, 2019.
- [5.14] L. Hongqiang, Q. Yongshui, J. Xu, "Microwave-Assisted Conversion of Lignin," in *Production of Biofuels and Chemicals with Microwave*, Springer Netherlands, 2014.
- [5.15] S. Wang, B. Liua, Q. Sua, "Pyrolysis–gas chromatography/mass spectrometry as a useful technique to evaluate the pyrolysis pathways of phenylalanine," *Journal of Analytical and Applied Pyrolysis*, pp. 393-403, 2003.
- [5.16] S.S. Choi, J.E. Ko, "Analysis of cyclic pyrolysis products formed from amino acid monomer," *Journal of Chromatography A*, pp. 8443-8455, Sep 2011.
- [5.17] T.R. Carlson, Y.T. Cheng, J. Jae, G. W. Huber, "Production of green aromatics and olefins by catalytic fast pyrolysis of wood sawdust," *Energy Enviromental Science*, pp. 145-161, 2011.
- [5.18] J. Pattersonx, B.F. Haidar, E.P. Papadopoulos, W. T. Smith, "Pyrolysis of Phenylalanine, 3,6-Dibenzyl-2,5-piperazinedione, and Phenethylamine," *J.Org.Chem*, 1987.
- [5.19] N. V. Sidgwick, "The Chemical Elements and Their Compounds," *Pergamon Press*, 1950.
- [5.20] P.D. Muley, C. Henkel, K.K. Abdollahi, "A critical comparison of pyrolysis of cellulose, lignin, and pine sawdust using an induction heating reactor", *Energy Conversion and Management*, pp 273-280, 2016

CHAPTER 6 - SMALL SCALE WOOL PYROLYSIS & GASIFICATION

In this chapter, the results for pyrolysis of wool, both non-catalytic (Section 6.1) and catalytic (Section 6.2) are presented and discussed. Initially, the effect of temperature, carrier gas type, feed size and condensation agent on the products are presented. Afterwards, the effect of catalyst and the possible modification they cause compared to the non-catalytic run are observed.

6.1 Non-catalytic Wool Pyrolysis & Gasification

In this section, initially, the effect of temperature on the products was analysed through pyrolysis with nitrogen as carrier gas with large pieces of wool (see section 3.2.1) at 350, 500 and 800°C, while also observing the effect of the coolant (condensation system) on the oil product. Afterwards, the effect of carrier gas, carbon dioxide and nitrogen, was analysed at 800°C with large pieces of wool. This would be a comparison between pyrolysis (nitrogen as carrier gas) and gasification (carbon dioxide as carrier gas). Next, at 800°C and with nitrogen as the carrier gas, the effect of feed size was evaluated. Finally, the effect of increasing the temperature while reducing the difference in temperature difference with use of carbon dioxide as the carrier gas was evaluated. The products were evaluated separately.

6.1.1 Product Distribution

Three phases of products, namely solids (biochar), liquid (bio-oil) and gaseous (biogas) were expected from the pyrolysis process. Biochar is produced as the result of the release volatiles (in form of biogas and bio-oil) during pyrolysis. Generally, the higher the temperature of the pyrolysis was, the more volatile were expected to be released and therefore a lower yield of char was expected at higher temperatures. The differentiation between the liquid and gas product could be partially correlated to the efficiency of the condensation method and conditions. In other words, higher available surface area for condensation or condensation medium temperature could have shifted the percentage of oil and gas while the char percentage and volatile would not be affected by this. Therefore, during the analysis of the results, more emphasise was put on the effect of variables such as carrier gas and temperature on the amount of char and all the volatiles produced rather than oil and gas individually.

As illustrated in Figure 6-1, as expected, the quantity of volatiles increased as temperature was increased from 350°C to 800°C. Additionally, the increase in volatiles is much more significant in the first temperature increase instance (from 350°C to 500°C) compared to the second increase

(from 500°C to 800°C) despite the smaller size of increase in the former one. This was expected since the main decomposition in untreated wool occurs between 200 to 600°C [6.1]. In more details, water starts to be lost from the wool at temperatures up to 150°C [6.2]. Zhigang Xia et.al observed that 3 other dominant peaks were observed on the DTG curves of wool during decomposition; namely at 238,316 and 434°C [6.3].

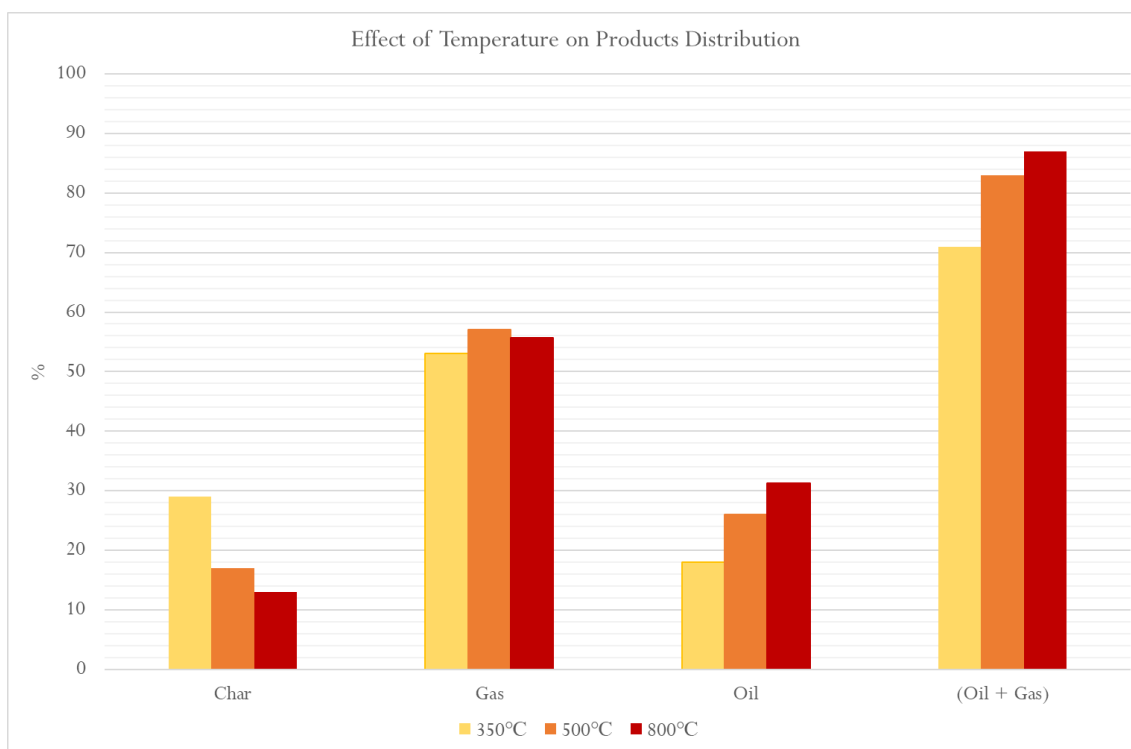


Figure 6-1: Effect of temperature on product distribution with nitrogen injection

The peak at 238°C could correspond to the overall wool crystal decomposition which could have facilitated the further processes occurring afterwards. The breakage of intermolecular chemical bonds such as hydrogen bonds, S-S bonds (the disulphide cross link in the wool (Figure 2.6)) and salt bonds could have corresponded to the second peak at 316°C. Since the breakage of C-C and C-H bonds requires 35% more energy to break compared to S-S, the final peak at 434°C could have corresponded to decomposition of the main macromolecule of wool [6.3]. Since most of the decomposition takes place at temperatures lower than 600°C, the increase in volatiles by increasing the temperature further was expected to be less.

Considering that the error and variance in the product distribution was ± 1.9 , the amount of gas produced was taken as being identical for the samples obtained at 500 and 800°C. Coupled with the increasing trend in oil production with increase in temperature, this indicates that after a certain temperature (around 450°C), a further increase in temperature does not change the amount of gas produced significantly. Differently, higher bio-oil yields are generated by increasing the

temperature further, possibly due to secondary reactions and rearrangement/condensation of volatiles radicals. To check if the Tweed Waste followed the decomposition trend expected for the wool sample from literature, it was pyrolysed in the TGA. The data from literature closely matched the DTG of the tweed waste (Figure 6.2) regarding the major weight loss being at temperatures lower than 600 °C.

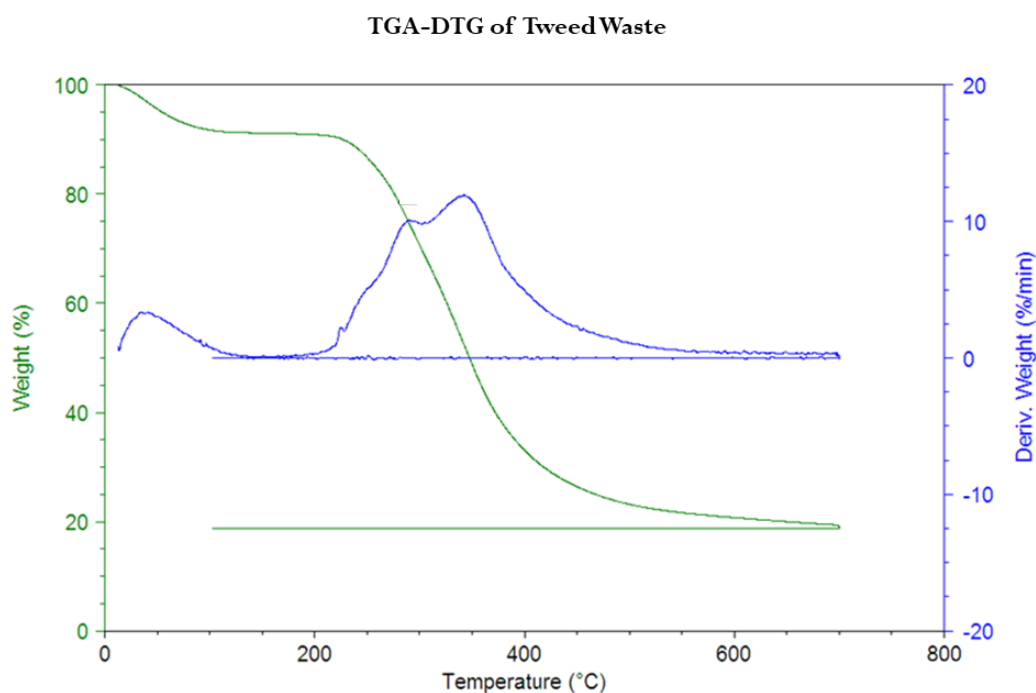


Figure 6-2: TGA-DTG data for the tweed waste

Feed size did not seem to have a clear effect on the product distribution. To observe the effect of switching the carrier gas from N₂ to CO₂ and to observe the effect of another stepwise increase of temperature, pyrolysis was carried out at 700, 800 and 900°C with CO₂ (Figure 6-3). This way, the tests at 800°C was used to compare the effect of type of gas utilised while the 900°C test could be used to observe if any changes occurred at this higher temperature. It should be noted that only char and volatiles percentage are reported at this temperature rather than gas and oil separately. Using CO₂, gas froze in the liquid nitrogen trap due to the freezing point of CO₂ being higher than liquid nitrogen and this phenomenon made the mass balance calculation for these runs inaccurate.

The change of gas (at 800°C) to CO₂ did not change the quantity of char or volatiles significantly. More accurately, the amount of char decreased by less than 2% in CO₂ case and volatiles increased by less than 2%. This decrease in char production was expected and could have been due to the mechanism proposed by C. Guizani et.al. Based on this mechanism, during the pyrolysis in CO₂ environment, after production of the char during the initial pyrolysis, the char goes through

gasification to decompose more [6.4]. The increase of temperature from 800 to 900°C still seems to be effective in decomposing the wool further but as expected, the increase is half of the that shown from 700 to 900°C. This followed the same trend observed with nitrogen as carrier gas.

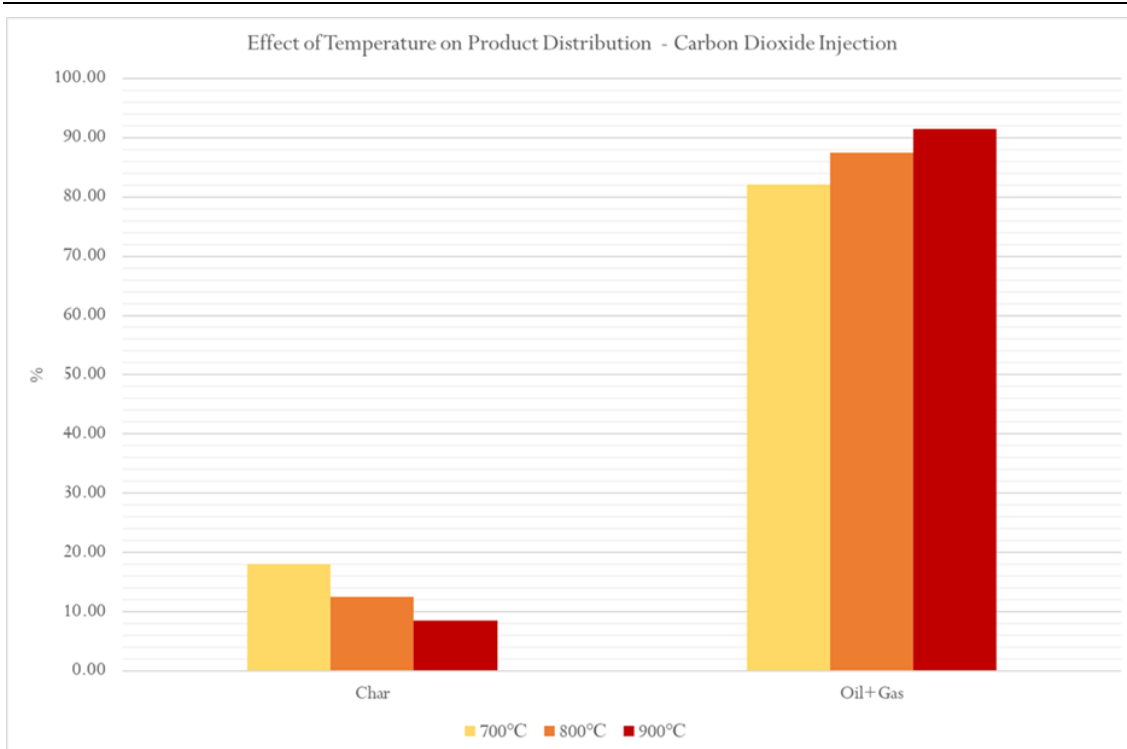


Figure 6-3: Effect of temperature change on product distribution with carbon dioxide injection

6.1.2 Char Analysis

The char obtained from pyrolysis of wool could be categorised as brittle and flaky (Figure 6-4). The visual examination of the solid residues also suggests a “graphitic structure”. Elemental analysis, FTIR analysis and BET tests were carried out on the char samples.



Figure 6-4: Wool before pyrolysis (top), After pyrolysis in the ceramic boat (bottom)

6.1.2.1 BET

In the BET (Brunauer–Emmett–Teller) analysis, the available surface area of a solid material is determined based on the assumption that the absorption occurs on multiple layers rather than on a monolayer. Therefore, this analysis plays an important role in assessing the suitability of the biochar for adsorption applications. For instance, for biochar to be used as activated carbon it should have a BET area of at least 400 m²/g and ideally around 900 m²/g. With the use of the current arrangement, i.e., pyrolysis with no catalyst or activated carbon activation, the maximum surface area achieved was 208 m²/g.

Despite the fact that the BET of the char obtained did not reach the threshold for the char to be classified as activated carbon, it still exceeded the BET of several other biomass generated char such as coconut shells, palm oil and orange peel [6.5]. These biomasses have been reported to be efficient as fertilisers due to their good water retention properties [6.6] [6.5] despite the fact that they have lower BET surface area than the wool BET. This observation made the wool char promising as a useful by-product.

The effect of carrier gas, feed size and increase in temperature on the BET of the char were observed. Char from pyrolysis at 800°C with large pieces of wool was selected to observe the effect of variation in injected gas on BET of the char. BET values of 113 m²/g with an error margin of ±24 and 192 m²/g with error margin of ±16 were obtained for CO₂ and N₂ char samples, respectively. By changing the gas, the BET surface area could increase by 40% despite the fact that product distribution was not affected by the change in gas. The lower available surface area in the char obtained from the pyrolysis with CO₂ as the carrier gas could be that some of the CO₂ was absorbed on the pores of the char and therefore reduced the BET. However, this trend was opposed to the findings reported by C. Guizani [6.4]. Another explanation could have been that nitrogen, an inert gas, only had the effect of removing the volatiles from the reaction zone while carbon dioxide facilitated further reactions (for example with the water moisture of the wool) on the surface of the char [6.7]. This could have then resulted in partial filling of the pores of the char which in turn could have caused the reduction in the surface area of the char [6.5].

Another comparison was carried out between the char samples collected with different feed sizes at 800 °C in presence of CO₂. As expected, the shredded wool sample produced a char with higher surface area. The large piece wool samples produced a char with BET of 40 m²/g, while the shredded wool sample char had a BET of 113 m²/g. This increase was most likely explainable by that small, shredded pieces of wool provided more space for the evolved gases to be evaporated while avoiding condensation.

Temperature increase had a direct correlation with increase in the char surface area. For instance, the char at 700 °C had a BET of 59 m²/g while 900 °C char sample had a BET of 190 m²/g (both samples obtained from pyrolysis with CO₂). This increase was in line with the literature [6.8].

6.1.2.2 *Elemental Analysis*

By evaluating the percentage of C, H, N and O in the residues, the EA can help determined if the chars can be classified formally as biochar and also gives an indication on their likelihood to be used as soil amendment. For instance, if the carbon content of the solid product is less than 50%, it cannot be categorised as biochar. However, this is not the case for the char obtained from the processed wool waste, whose C content is higher than 70 wt% when the temperature of the process is higher than 700°C. The raw wool itself has a carbon content of 50%. Due to the high protein content of the raw processed wool waste (15.9%), the existence of nitrogen in the product was expected. This high nitrogen content could be an asset if the biochar is going to be used as a mean of soil amendment. The oxygen and hydrogen content of the raw wool was 26.6 and 7.3 % respectively.

Figure 6-5 compares the effect of temperature on the on elemental content of char. The increase of temperature has direct correlation with increase of carbon content of the char, while having a reverse effect of nitrogen and hydrogen content of the char. This trend fell within the expectation from literature [6.9]. The oxygen content could not be used as a definite value similar to carbon and nitrogen since it was calculated by difference and raw wool (and consequently char) were likely to contain sulphur as well as oxygen.

Figure 6.6 demonstrates the effect of change in carrier gas on char elemental analysis. Nitrogen seemed to perform better in stabilisation of char through more deoxygenation of char. Similar to the results of the BET, the higher oxygen content of the char obtained under CO₂ injection could be the filling of some the char pores with products.

Figure 6-7 demonstrates the comparison of char elemental analysis between the shredded and whole pieces of wool. Given that the pyrolysis tests could have had some errors during product collection and the elemental analysis itself could have been subject to slight errors, the difference between these two cases seemed to be negligible. Therefore, it was concluded that the wool sample size did not contribute to any difference in wool char carbon richness.

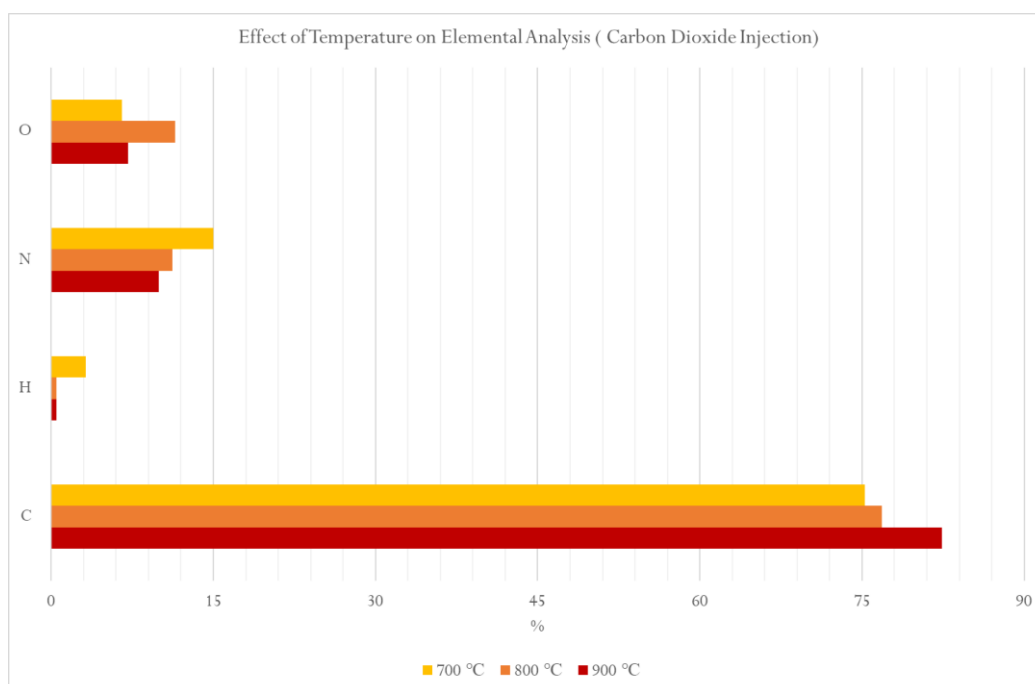


Figure 6-5: Effect of temperature on elemental analysis of char with carbon dioxide injection

The importance of H/C ratio is in the determination of the stability of the solid product. In other words, the higher the value of H/C is, the better the chemical functionalities in the solid are. As a result, the product is less stable. The threshold H/C ratio in considering the biochar as stable is 0.7 [6.10] [6.14]. Also, the value of H/C can be used as an index of aromaticity. The estimated aromaticity given by the relationship between H/C ratio and production temperature can be linked to the potential adsorption capacity of the biochar. All the char samples had lower than 0.7 H/C values with the highest value being 0.15 which belonged to the pyrolysis at 350°C. The char samples obtained at 800 and 900°C had very low H/C ratio (0.01). This suggested that the chars produced at 800 and 900 °C could have a very good activity for the removal of pollutants such as naphthalene and phenanthrene, since good adsorbents are characterised by low H/C ratios.

Similar to the H/C ratio, the O/C ratio is used to differentiate the biochar from other possible by-products. The O/C ratios of all the samples fell between the range of 0.04 to 0.32, which were lower than the threshold value of 0.4 [6.10]. It should be noted that O/C values of less than 0.2 could make the char to have a half-life of thousand years [6.15]. These results indicated that the char obtained from wool pyrolysis could be categorised and marketed as biochar.

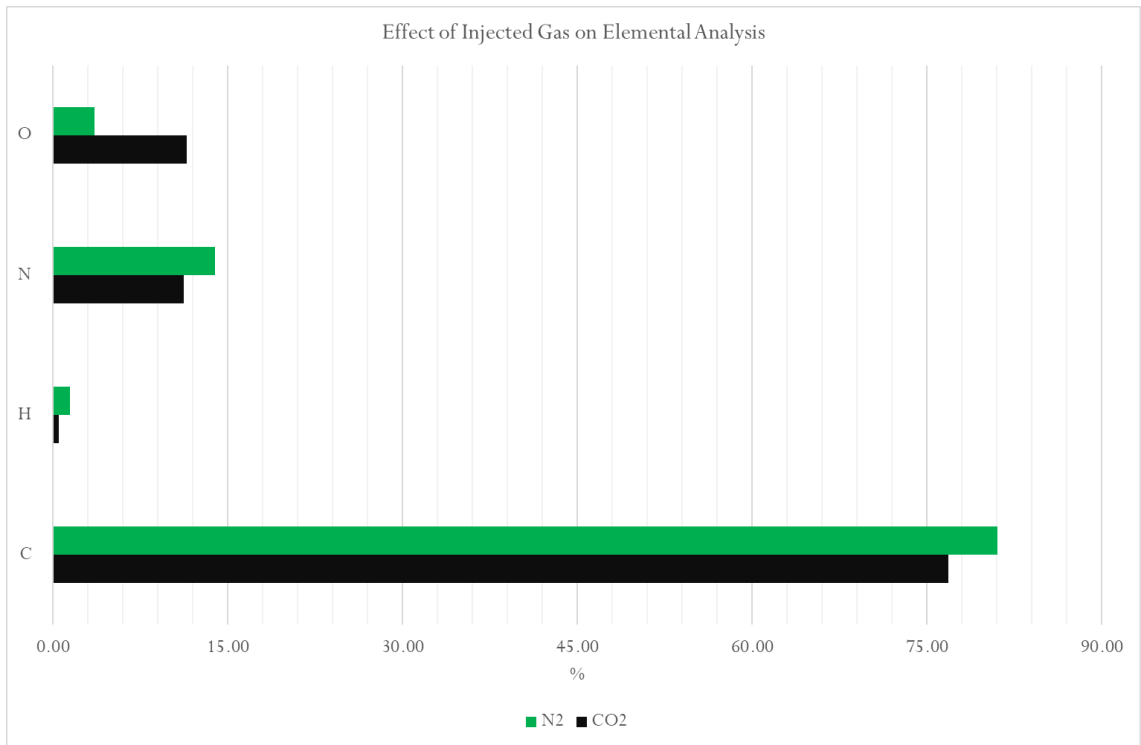


Figure 6-6: Effect of injected gas on elemental analysis of char

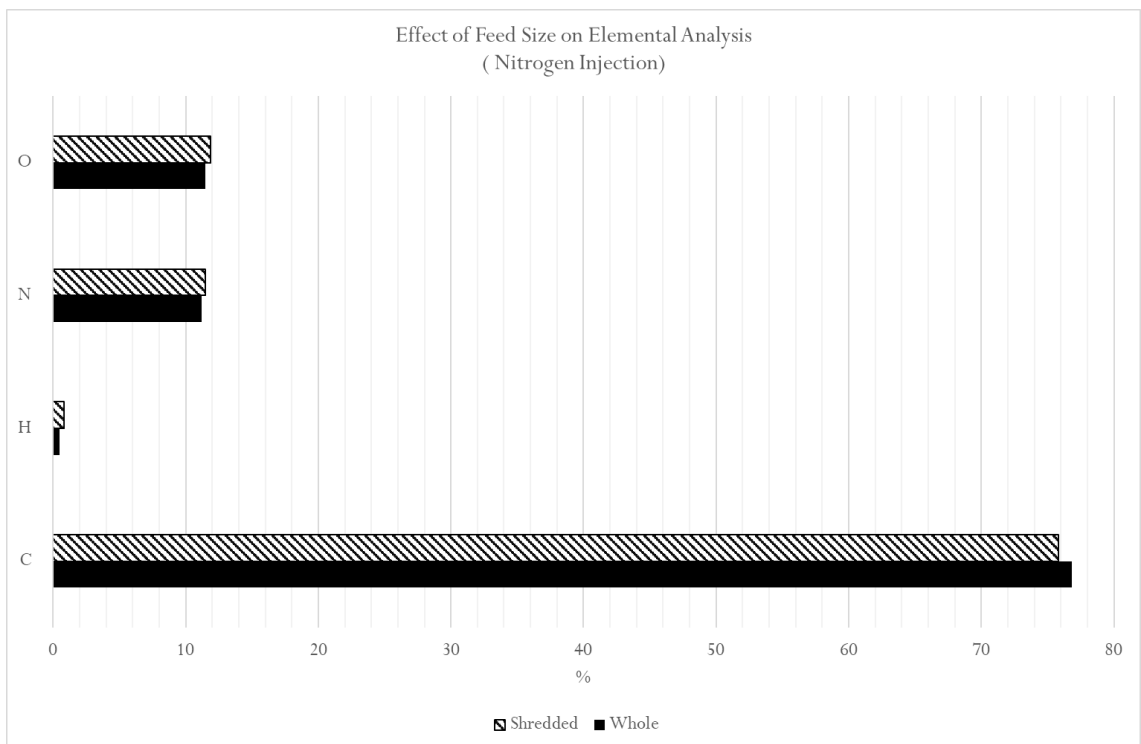


Figure 6-7: Effect of feed size on elemental analysis of char

6.1.2.3 FTIR Analysis

FTIR analysis was carried out to observe the functional groups which were likely to be present in the char. Three main peaks were observed (Figure 6-8) that potentially corresponded to stretching $O=C=O$, stretching $N=N=N$ and stretching $C=O$. Coupling the FTIR results to the elemental analysis, a clearer image could be observed. For instance, the elemental analysis indicated that nitrogen content of the char decreased through increasing the pyrolysis temperature. Similarly, the $N=N=N$ bonds transmittance decreased as the temperature increased. Another general observation was that as the temperature increased, less predominant and strong peaks were observed in the char FTIR analysis. This fell in line with the fact that as temperature increased, less char and consequently less unstable compounds were remained in the char.

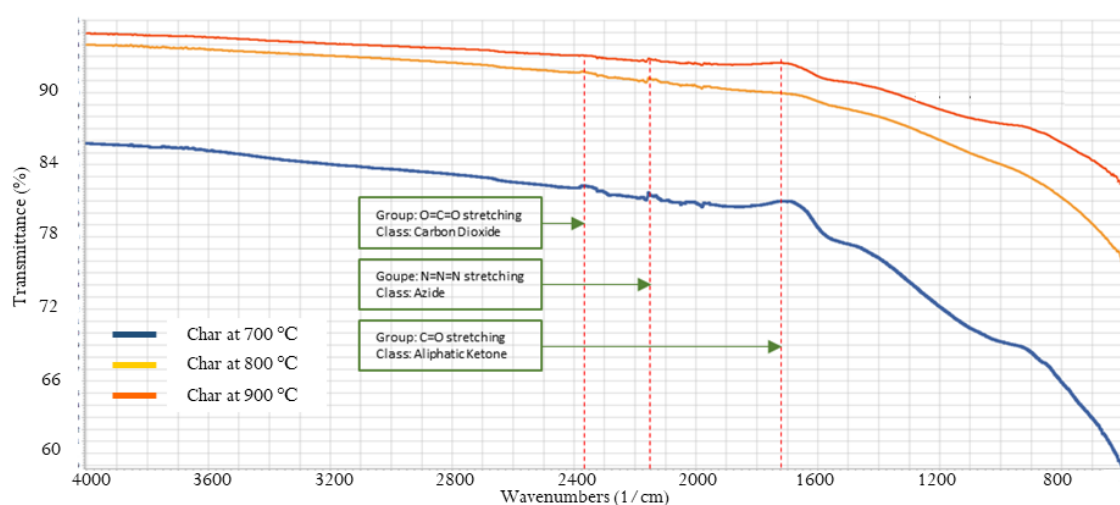


Figure 6-8: FTIR results on comparison of temperature variation effect on char products (700, 800 and 900 °C)

6.1.3 Gas Analysis

The composition of the gases produced in the experiments at 700, 800 and 900 °C with CO_2 are shown in Figure 6-9. CO_2 was the main product at 700 °C, while CO becomes the main gas product when the temperature increased to 800 and 900 °C. More precisely, at 900 °C, CO made up over 65% of the gas while CO_2 content was only 21%. This phenomenon demonstrated that the reverse of the Boudouard reaction ($C + CO_2 \rightleftharpoons 2CO$) is favoured as the temperature is increased. In other words, as expected, the decarboxylation of wool amino acid groups produced CO_2 . This CO_2 is further reacted with the carbon radicals to form CO .

Another reason behind the direct relation between increasing the temperature and CO production could be further decomposition of intermediates such as cinnamic acid at higher temperatures which can promote production of CO over CO_2 . Observing the higher quantity of water and CO at higher

temperature could also introduce another reason behind lower CO₂ content at higher temperatures. In other words, in water gas shift reaction ($\text{CO} + \text{H}_2\text{O} \rightleftharpoons \text{CO}_2 + \text{H}_2$), since the reaction is exothermic, sensitive to temperature and based on Le Chatelier's principle, favours the reactants as the temperature increases. This process seemed to have taken place based on higher quantities of water and CO at higher temperatures.

Besides CO and CO₂, relatively small quantities of C1-C4 hydrocarbons were present at all the temperatures, with their abundance decreased when the temperature increased due to enhanced cracking activity at higher temperatures and gasification with CO₂.

Since the wool waste is mainly a protein-based material containing nitrogen and sulphur content were expected due to the dye structure, pyrolysis was expected to lead to production of N-compounds and sulphur containing compound. Figure 6-10 compares the three-gas analysis at different temperatures. Ammonia (NH₃) was the main compound among the identified N-compounds. Hydrogen cyanide (HCN) and dimethylamine (C₂H₇N) were also identified in quantifiable amounts. HCN and NH₃ had direct proportionality with increasing the temperature. This was in line with the elemental analysis of the char under the same conditions (Figure 6-4). Since less nitrogen was observed in the char at higher temperatures, the released nitrogen was expected to be observed in the volatiles.

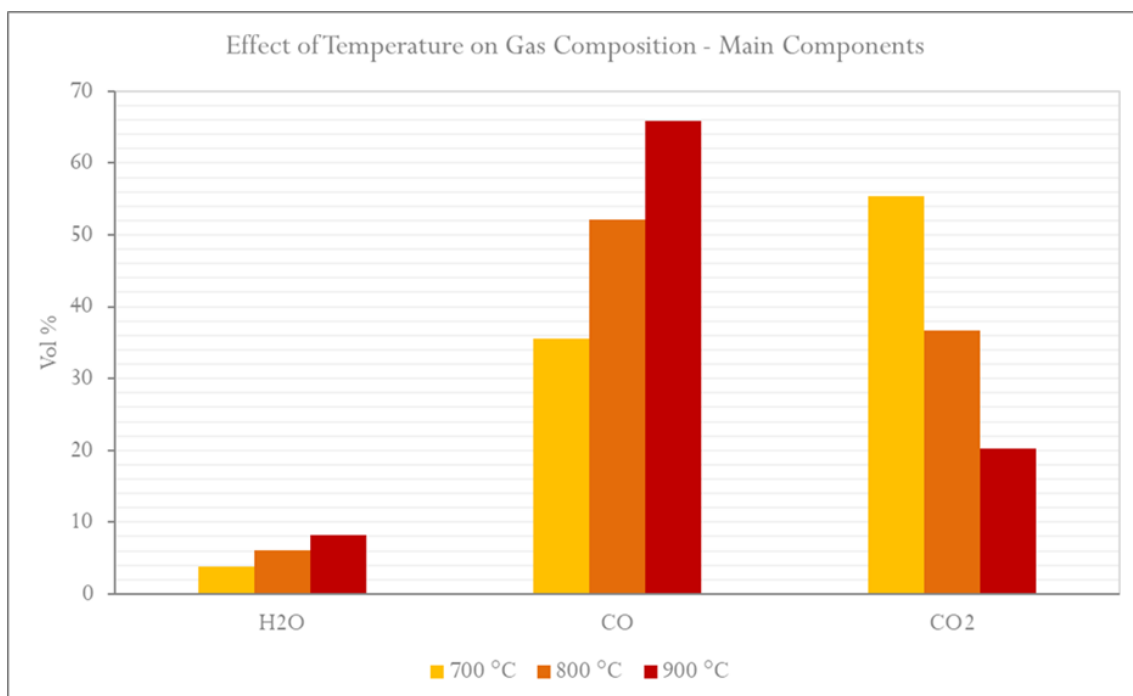


Figure 6-9: Effect of temperature variation on main products of wool gasification (with CO₂)

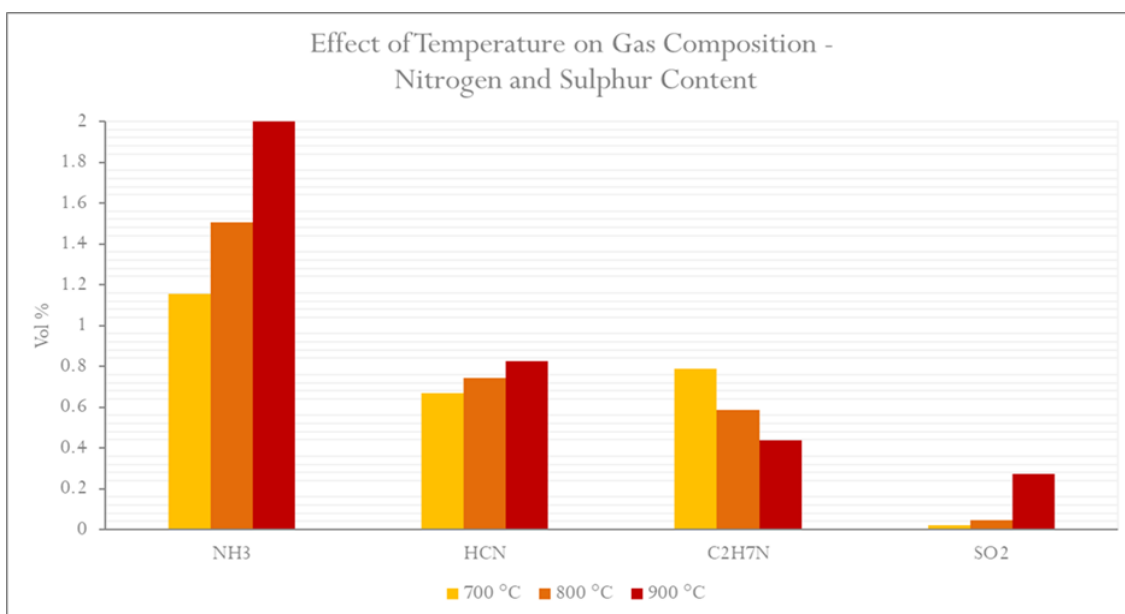


Figure 6-10: Effect of temperature variation on nitrogen and sulphur containing products of wool gasification (with CO₂)

Hydrogen cyanide (HCN) is extremely poisonous and a flammable liquid that boils slightly above room temperature at 25.6 °C. HCN is produced on an industrial scale and is a highly valuable precursor to many chemical compounds ranging from polymers to pharmaceuticals. Dimethylamine is a secondary amine flammable gas with an ammonia-like odour. Dimethylamine is commonly encountered commercially as a solution in water at concentrations up to around 40%. Acetamide, another product observed in the gas analysis in small quantities, is the simplest amide derived from acetic acid. It finds some use as a plasticizer and as an industrial solvent (Solubility in water: 2000g/L; BP: 221.2°C). All these compounds are flammable and could be combusted together to other syngas flammables. However, their combustion will be leading to Nitrogen oxides and therefore should be avoided. Therefore, since all the above substances are soluble in water, water (or other solvents) scrubbing of the produced gas prior to releasing it to the atmosphere could be a solution in view of recovering valuable chemicals.

6.1.4 Oil Analysis

GC-MS method was used to identify the chemical component of the oils. As mentioned previously, two different oils were collected at each temperature, one salted ice water and one liquid nitrogen. Furthermore, two types of gas and two different type of feed (shredded and large pieces of wool) were pyrolysed. In this section, the effect of changing these variables were discussed.

Generally, the most abundant products found in the oil samples were phenolics and indoles. This was expected due to the structure of the reactive and acid dyes used in dyeing process of the wool. All of the dyes which were applied to the wool contained benzene rings which was either attached

to a carbon or nitrogen (Chapter 3). Furthermore, both acid blue 25 and acid green 25 contain several oxygens which are attached to carbon through double bonds which can facilitate generation of phenols.

Another group of compounds which were observed in the products were simple ketones such as 4-hydroxy-4-methyl- 2-Pentanone. These compounds could have been as a result of the breakage of the wool hydrogen bonds and isopeptide cross-links. In general, due to the nature of the wool feed used (existence of amino acids such as histidine and proline in the wool), high quantities of nitrogen containing compounds were expected in the oil. These were observed in forms of pyrazines, amines, amides, nitriles and aziridines. However, opposed to the phenols where large quantities of one or few compounds was produced, smaller quantities of several nitrogen containing compounds in smaller quantities were produced.

Overall, as the temperature increased, the number of components produced increased. For instance, in the sample obtained at 350°C, only 25 unique compounds were found while this number increased to over 130 at 800°C with all the other variables staying constant. However, in all the samples, regardless of the temperature, the top 20 compounds with regards to their abundance in the GC-MS results made up over 55% of the products. Therefore, to facilitate the comparison of the samples, only these components with the largest quantity were compared.

6.1.4.1 Effect of Condensation System and Injected Gas

Figure 6-11 illustrates the two appearance of the two samples obtained from pyrolysis at 800°C in presence of nitrogen with the difference being the condensation stage. The samples condensed in liquid nitrogen bath had a darker appearance and higher viscosity, resembling that of heavy oil. This could have indicated that heavier (higher molecular weight) compounds were condensed in liquid nitrogen. Alternatively, it could have indicated that simply put, liquid nitrogen was more efficient at condensing the volatiles and therefore contained higher concentration of compounds.



Figure 6-11: Comparison between the appearance of the oil products obtained from pyrolysis at 800 Celcius

Figure 6-12 presents the GC-MS curves for pyrolysis at 800°C with different gases and condensation mediums. Comparing the effect of change in condensation medium in the case of nitrogen injection, the peaks seem to be occurring at the same retention times for both cases, meaning that same compounds were formed in both cases. However, the heights of the peaks are different between the samples. For instance, at retention time of 20, p-cresol (4-methyl phenol), one of the main components observed in most of samples, is detected in both samples. However, the height of the peak in the liquid nitrogen is twice of that in the ice case while. Despite this difference, since the boiling point of cresol is at 202°C, it seemed that the main reason behind this difference is the residence time that the pyrolysis gases had for condensation. In other words, if only one of the condensation methods were used but gases spent more time in the bath through extending the contact area, more heat transfer would have occurred.

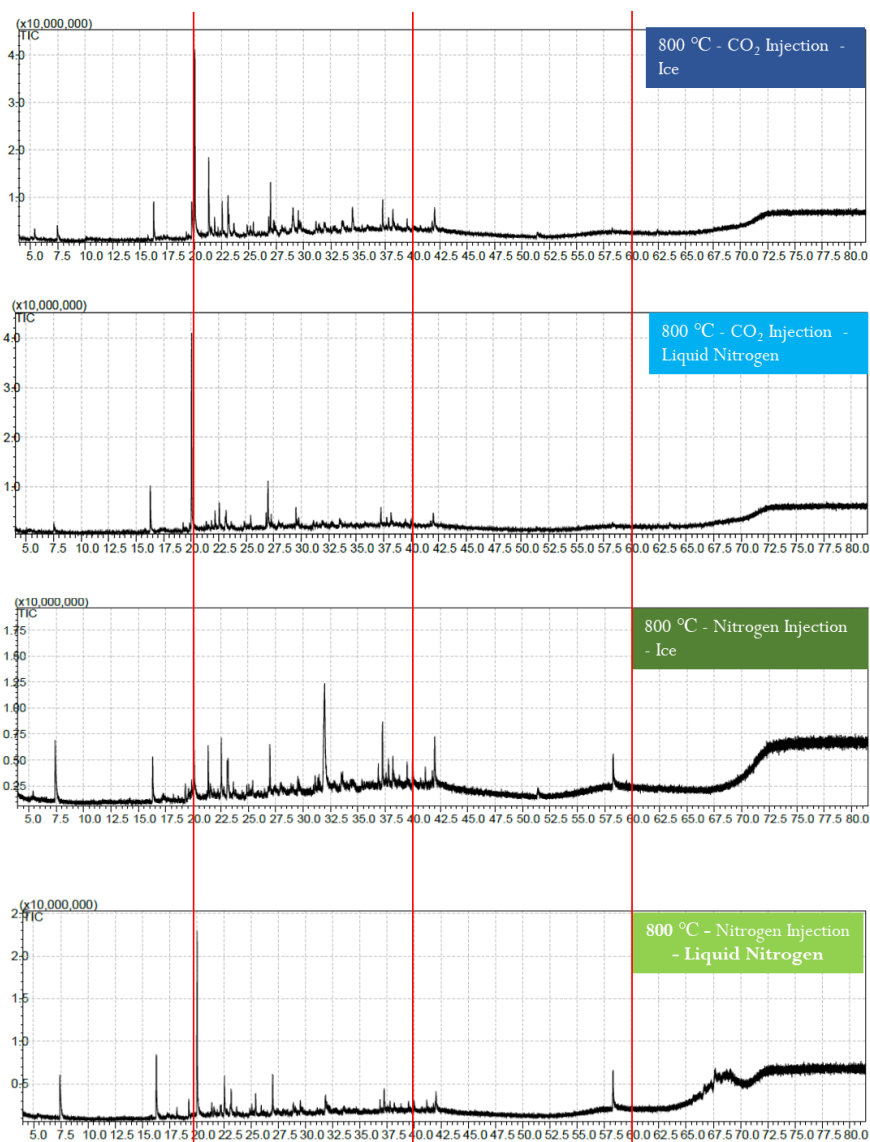


Figure 6-12: Effect of injected gas and condensation system on pyrolysis oil

Another comparison which could have been made from Figure 6-12 was the effect of carrier gas on oil samples composition. Both of the samples had a substituted phenol, namely cresol, as their main component, the main difference was the type of cresol and the percentage of the overall area. To elaborate, m-cresol constituted to 18% of the oil in the CO₂ sample, while p-cresol made up 13% of the N₂ sample.

Another difference was the number of unique compounds which were produced. For instance, 166 unique compounds were found in the GC-MS result of the nitrogen case, while over 240 were found for the carbon dioxide case.

Since it was expected that use of CO₂ would promote generation of mono phenols while reducing the methoxy containing compounds [6.11, 6.12], this larger variation in compounds for the CO₂ case was justifiable. Comparing the overall percentage of the phenols, indoles and methoxy containing groups, the above statement stood through. As presented in Figure 6-13, the quantity of phenols increased by 2% by changing the gas to carbon dioxide while methoxy containing compounds decreased by 1%.

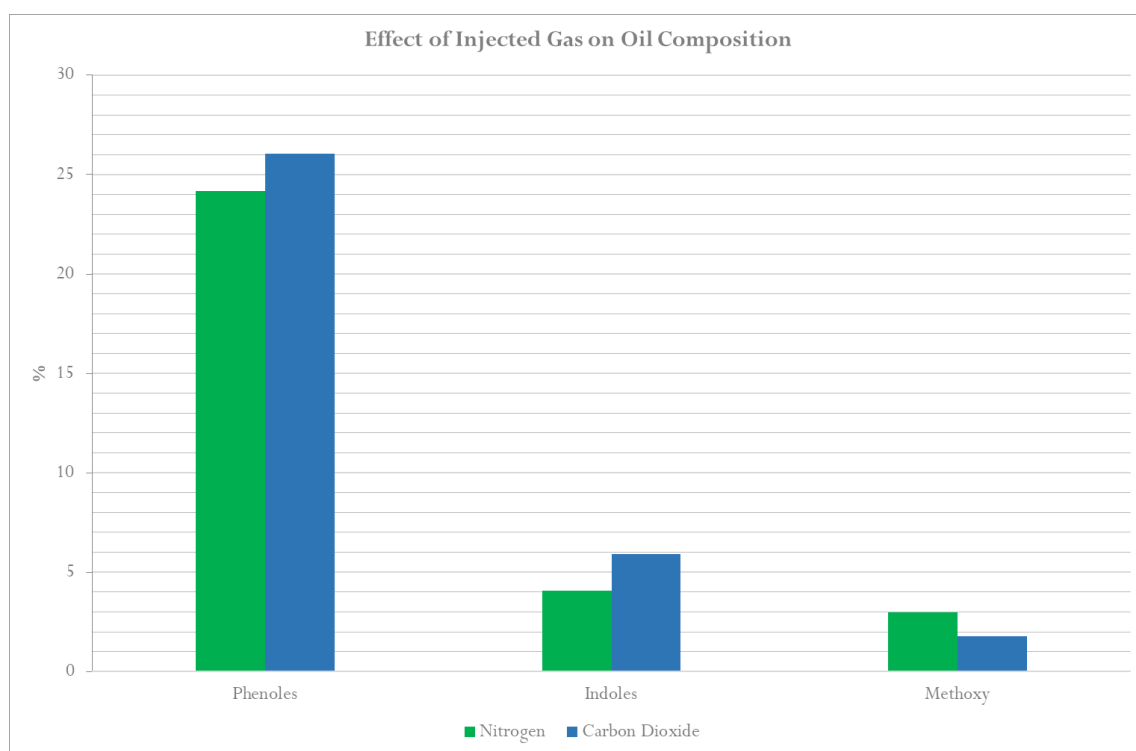


Figure 6-13: Effect of injected gas on the oil composition

6.1.4.2 Effect of feed Size

Figure 6-14 compares the GC-MS data obtained for the pyrolysis oil samples for two different feed size while all the other variables are the same. As it can be seen, almost all the peaks are identical and only the intensity of the peaks in the shredded case is higher for some of the peaks. For instance, both samples have peaks which corresponded to cresol (component with the largest difference in the two samples) and other phenols while only the intensity being slightly different. Due to similarity of the components observed in the samples and slight difference in the quantities, it was concluded that the sample size did not affect the products significantly but can affect the products abundance.

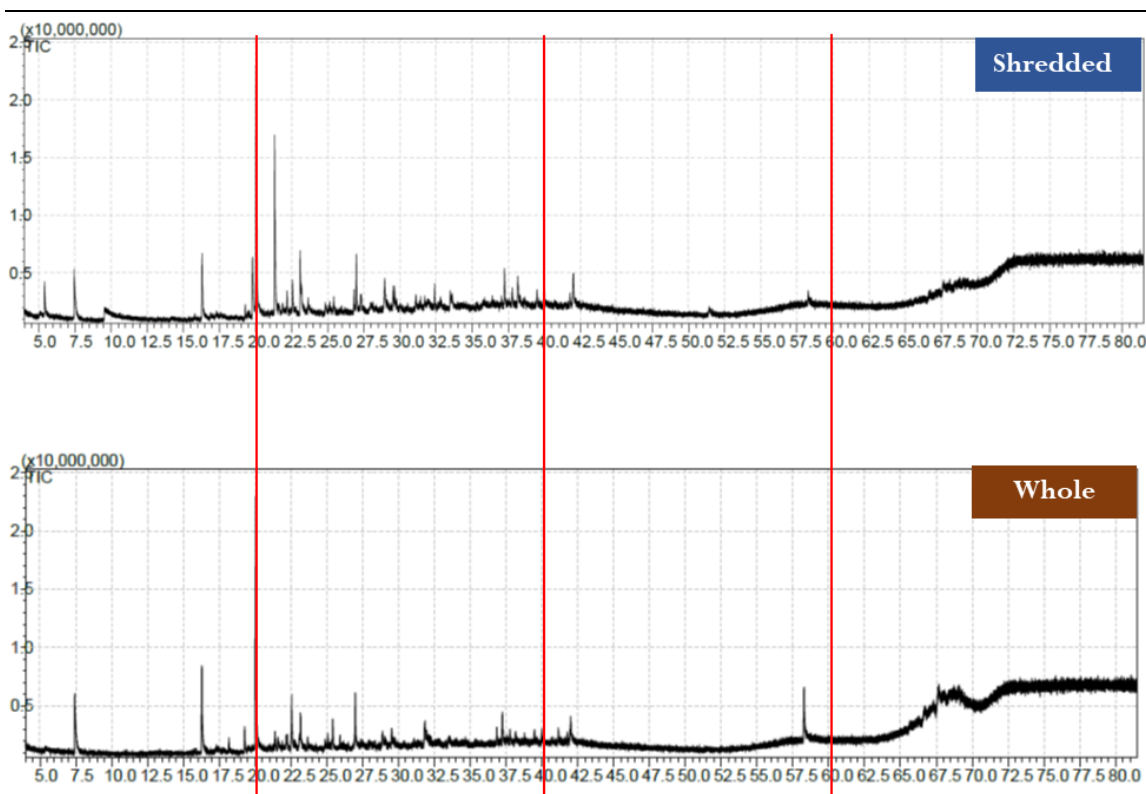


Figure 6-14: Effect of feed size on oil product

6.1.4.3 Effect of Temperature

Figure 6-15 presents the GC-MS curves for the oil samples obtained from pyrolysis at 700, 800 and 900 and can be used to observe the effect of temperature change on the oil compounds. All of the samples seemed to have similar peaks from the curves and the intensity of the heights were varied. Since the curves presented in Figure 6-15 were only representing the results for salted ice trap and not the liquid nitrogen trap, it was decided to compare the results more comprehensively through combining the results of both condensation traps.

Doing so, the first phenomenon observed was the significant increase in the number of unique compounds produced when the temperature was increased from 700°C (141 compounds) to 800°C (over 240 compounds). This behaviour was not observed by the temperature increase from 800°C to 900°C. This observation could have been due to the promotion of gasification at 900. Since the main products of gasification are volatiles, the increase in temperature could have affected the gas product rather than the oil. Furthermore, as illustrated in Figure 6-16, the increase in the quantity of phenols produced by increasing the temperature was much more predominant passing from 700 to 800°C (10% increase), compared to the increase from 800 to 900°C (2%).

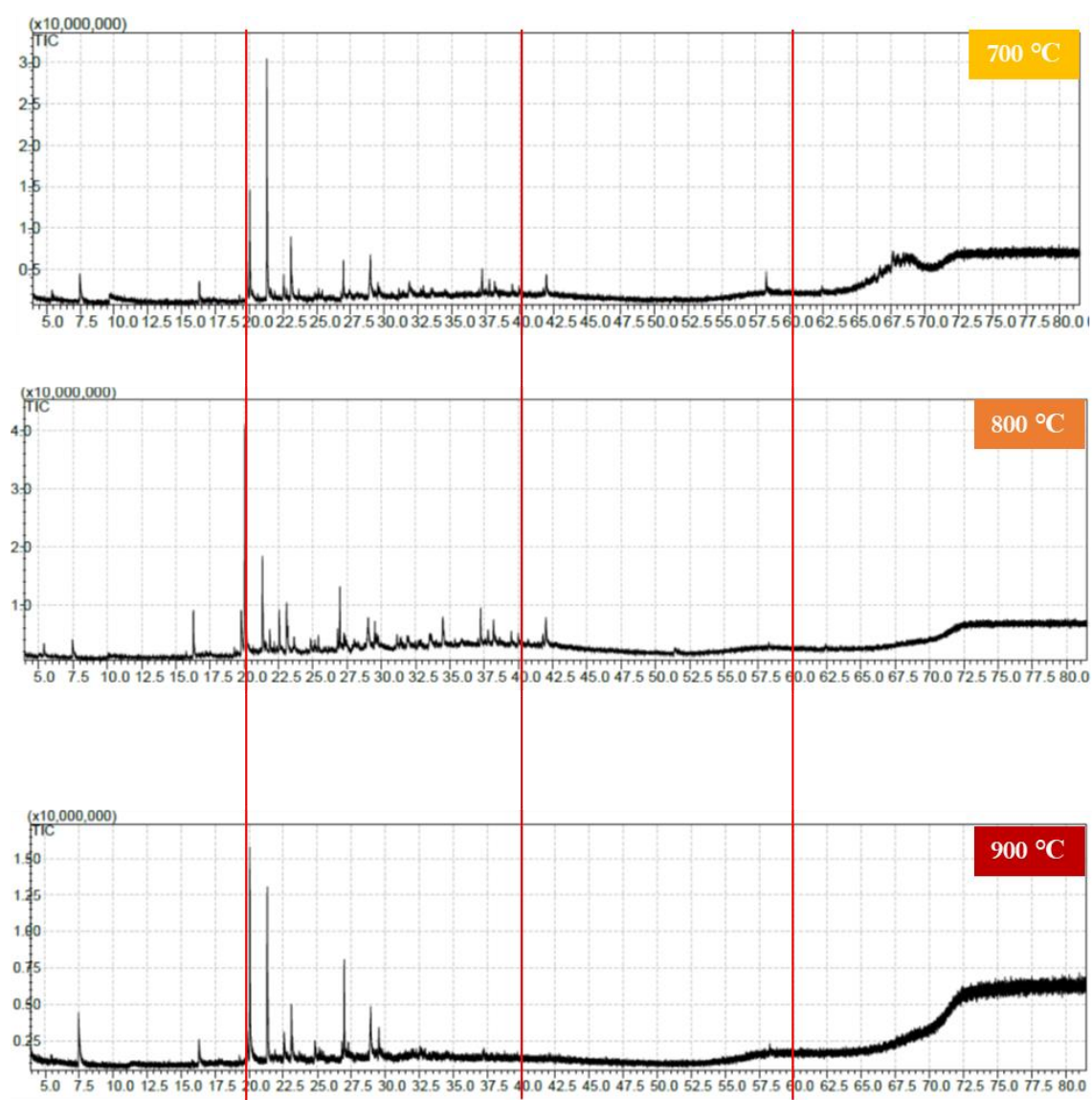


Figure 6-15: Effect of temperature (carbon dioxide injection) on oil product

On the contrary, the increase in indole production is much more significant in the second temperature increase. To evaluate what could be the reasons behind these behaviours, it was decided to compare the actual compounds produced in each run rather than comparing the curves

and groups of chemicals. It was decided to narrow than the comparison to the top products to make the comparison clearer. This decision and method were feasible since the top 20 components made up at least over 55% of the products, while the top 10 products made up at least over 45% of the products.

Table 6-1 presents the 10 most abundant products obtained in the oil from the pyrolysis at 700, 800 and 900 °C. One observation was that despite the larger number of products produced by increasing the temperature (such as intermediates), the number of products available in large quantities decreased. One potential explanation behind this behaviour could be that as temperature increases, the efficiency in breaking bonds such as the ionic ones is increased. This resulted in large number of intermediates as the temperature increases. Consequently, these intermediates interact to form more favourable products such as phenols.

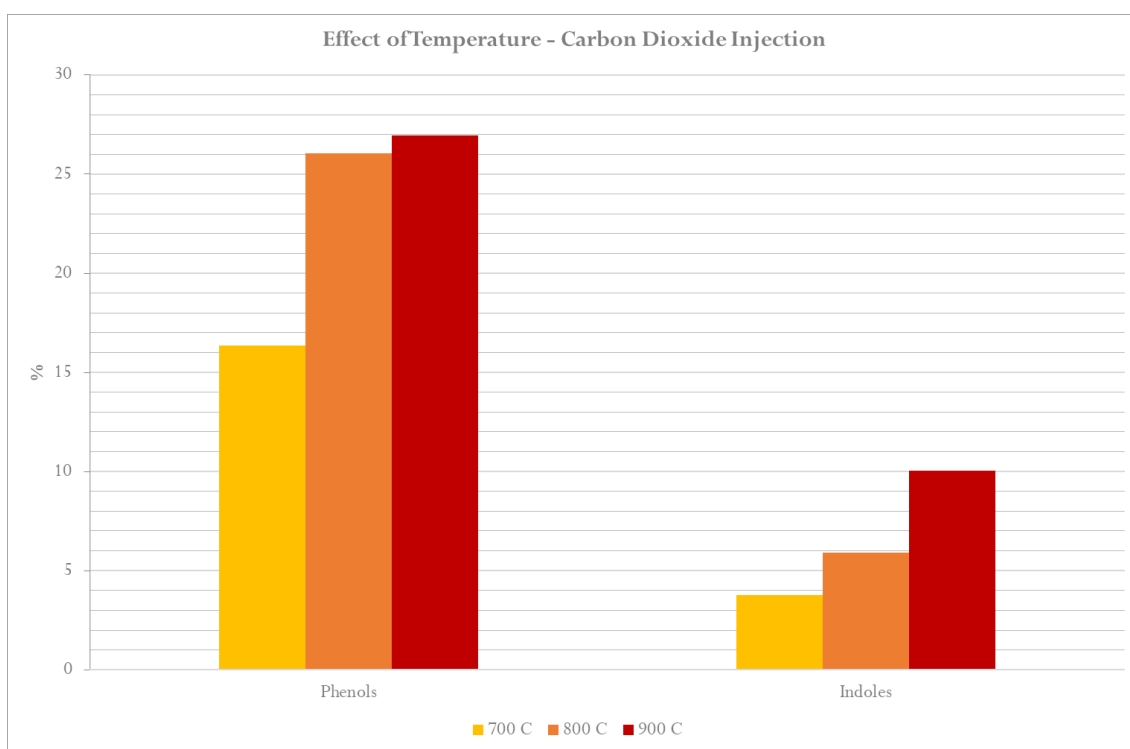


Figure 6-16: Effect of Temperature on phenols and indoles in oil

The product with largest area in the GC-MS analysis, regardless of the temperature, belonged to the phenolic groups. Furthermore, all of them were different arrangements of cresols; namely o-cresol (2-methyl phenol), m-cresol (3-methyl phenol) and p-cresol (4-methyl phenol). The increases in the quantity of the compounds with methyl groups attached to the phenol could potentially be correlated to the dyes used and the gas analysis. To elaborate, one of the main dyes utilised in the wool samples was acid green 25. This dye contains a benzene ring attached to a methyl group and SO_3Na . In the gas analysis, as the temperature increased, the quantity of SO_2 in the gas

were increased. This could mean that as the temperature were increased, more SO₂ were decomposed, resulting in more cresol being produced from the green dye.

Another product which was produced in significant quantities was 2,4-Imidazolidinedione, 5,5-dimethyl- (second most abundant product at 700 and 900°C). Similarly, indole is the second most abundant component in the 800°C sample. The structure of these components indicates that they potentially decomposed from the Indigoid chromophore of the wool samples through deoxygenation.

Existence of “4-Piperidinone, 2,2,6,6-tetramethyl” could have been due to the deoxygenation of the “3,6-Dioxo-1,4-cyclohexadiene-1,2,4,5-tetraide” group, which was part of the structure of the acid blue 25 followed by addition of N-H. The fact that nitrogen content of the char decreased as the temperature increased could be justified by the trend of increase in nitrogen containing compound in the oil as the temperature is increased.

Table 6-1: The top 10 products in the bio-oil samples to observe the effect of pyrolysis temperature variation

700°C		800°C		900°C	
Compound	Area %	Compound	Area %	Compound	Area %
Phenol, 2-methyl-	9.1	Phenol,3-methyl-	18.2	p-Cresol	18.4
2,4-Imidazolidinedione, 5,5-dimethyl-	7.2	Indole	4.7	2,4-Imidazolidinedione, 5,5-dimethyl-	10.4
4-Piperidinone, 2,2,6,6-tetramethyl-	4.8	Phenol	4.2	Indole	7.3
Pyrrolo[1,2-a]pyrazine-1,4-dione, hexahydro-3-(2-methylpropyl)-. beta. -D-Glucopyranose, 1,6-anhydro-	3.4	4-Piperidinone, 2,2,6,6-tetramethyl-	3.9	4-Piperidinone, 2,2,6,6-tetramethyl-	5.5
Phenol	3.3	2-Propen-1-amine, N, N-bis(1-methylethyl)-	3.0	Phenol	3.7
5,10-Diethoxy-2,3,7,8-tetrahydro-1H,6H-dipyrrolo[1,2-a:1',2'-d] pyrazine	3.2	4-Aminoresorcinol	2.4	4-Aminoresorcinol	2.4
		5,10-Diethoxy-2,3,7,8-tetrahydro-1H,6H-dipyrrolo[1,2-a:1',2'-d] pyrazine	2.4	4-Piperidinone, 4-Piperidinone, 2,2,6,6-tetramethyl-	2.1

2,4-Imidazolidinedione, 5-(2-methylpropyl)-, (S)-	2.8	Pyrrolo[1,2-a]pyrazine-1,4-dione, hexahydro-	2.3	Phenol, 4-ethyl-	1.6
Indole	2.8	Cyclopropylamine, N-isobutylidene-	2.1	Aziridine, 1,2-diisopropyl-3-methyl-, trans-	1.5
Pyrrolo[1,2-a]pyrazine-1,4-dione, hexahydro-	2.2	Hexahydropyrrolizin-3-one	2.0	2-Pentanone, 4-hydroxy-4-methyl-	1.5
p-Cresol	1.9	Aziridine, 1,2-diisopropyl-3-methyl-,	1.9	Benzofuran, 2,3-dihydro-	1.3
Overall	44.0	Overall	47.0	Overall	55.7

Interestingly, the run at 700°C contained “. beta. -D-Glucopyranose, 1,6-anhydro- “, a carbohydrate, which was not as clear to justify. However, this compound could have been a by-product of cotton (cellulose) pyrolysis. Since the textile waste feed used did not have a uniform colour/structure and included some cotton stitching (labels), the existence of this compound could have in fact been as a result of the cotton impurities pyrolysis.

6.2 Catalytic Wool Pyrolysis

In this section, the effect of catalysts on modifying the pyrolysis products were evaluated. The wool samples were pyrolysed with 20-ZSM5 and Al-KIL2 in addition to a non-catalytic run at 500°C. As discussed in chapter 5, 20-ZSM5, the most acidic ZSM5, performed better than other ZSM5 catalysts in deoxygenating protein model compounds (phenylalanine). Among KIL2 catalysts, Al-KIL2 demonstrated more potential compared to Li-KIL2 in conversion of model compounds which was mainly associated with its high surface area and acidity.

6.2.1 Product distribution

As illustrated in Figure 6-17, catalyst affected the distribution of all the 3 phases. However, if only the char and volatiles were to be compared rather than char with oil and gas, the effect of catalysts were not significant. The biggest differentiation between the catalysts that could be observed was the distribution between oil and gas. Al-KIL2 maximised the oil product while 20-ZSM5 favoured gas production compared to Al-KIL2. However, both of the catalysts increased the amount of oil produced.

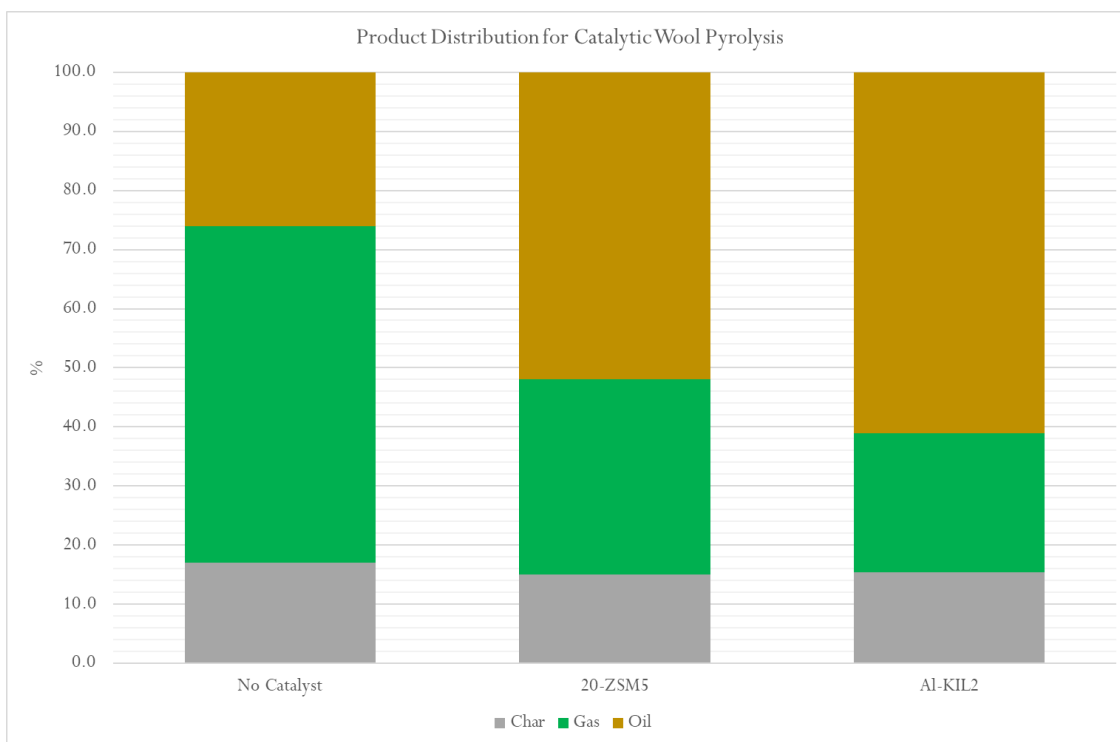


Figure 6-17: Product distribution comparison of catalytic and non-catalytic samples in fixed bed

In the non-catalytic pyrolysis (Figure 6-1), it was observed that the higher the temperature, the higher the quantity of the oil obtained. Use of the catalysts double the quantity of oil produced compared to the non-catalytic run at the same temperature while the change in char content was insignificant. Since the initial decomposition would result in release of lighter and less complex compounds, the reduction in gas in catalytic runs while the oil is increased many folds indicate that catalysts were successful in introducing a path to reduce the activation energy required for the secondary reactions which produce heavier condensable products. High acidity and high surface area of Al-KIL2 facilitated the decomposition and secondary reactions better than more acidic and less porous 20-ZSM5.

6.2.2 Char Analysis

As stated in section 6.1.2.2., several factors such as carbon percentage, H/C ratio and O/C ratio can be used to identify the char type. As illustrated in Figure 6-18, the trends observed in the elemental analysis were not as clear as the ones in the non-catalytic ones. However, with the goal in mind to reduce the quantity of oxygen in char and therefore reduce the O/C ratio, both of the catalysts performed satisfactorily. For instance, the O/C ratios of the run with catalysts were decreased by at least 25% compared to the non-catalytic one. Since this low O/C was potentially the result of dehydration reactions, which in turn decreased the hydrophilicity of the surface of the biochar, long-term stability behaviour could be expected from this char which would make it a good

soil amendment. Furthermore, the high nitrogen content of the catalytic runs (specially Al-KIL2 run) made it a good fertiliser.

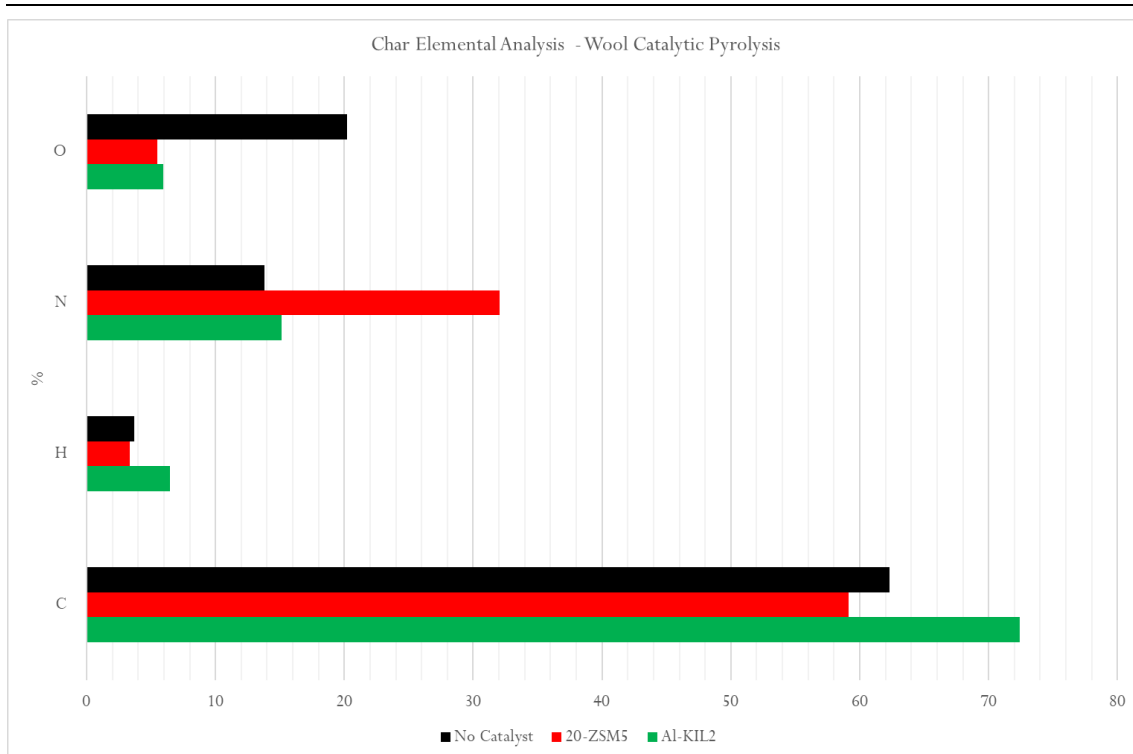


Figure 6-18: Elemental analysis comparison of catalytic and non-catalytic char samples

The high H/C ratio could be due to high aromaticity of char caused by high quantities of volatiles during pyrolysis. This high aromaticity makes the char more stable. The Al-KIL2 increased the char H/C ratio by over 25%.

6.2.3 Oil Analysis

Similar to the non-catalytic runs, there seemed to be a correlation between the overall number of the compounds produced in addition to the quantity of the overall products which are made of the most abundant ones with the variation in pyrolysis conditions. As illustrated in Figure 6-19, the number of unique compounds produced reduced significantly with use of catalysts. This can indicate by introduction of catalysts, the smaller compounds which are initially decomposed at 500°C, were reacted further to form other compounds and therefore the number of smaller intermediates were reduced. Comparing the two catalysts, the larger available surface area of the Al-KIL2 seemed to facilitate this behaviour more efficiently.

Another observation which could solidify or compliment the above theory could be the increase in the share of the ten most abundant compounds in the oil product. This meant that by being able to extract over 70% of the products through 10 different compounds, the separation and identification of the products was simplified. This behaviour also demonstrated that catalysts were selective

towards production of certain products, while the non-catalytic pyrolysis included several competing paths.

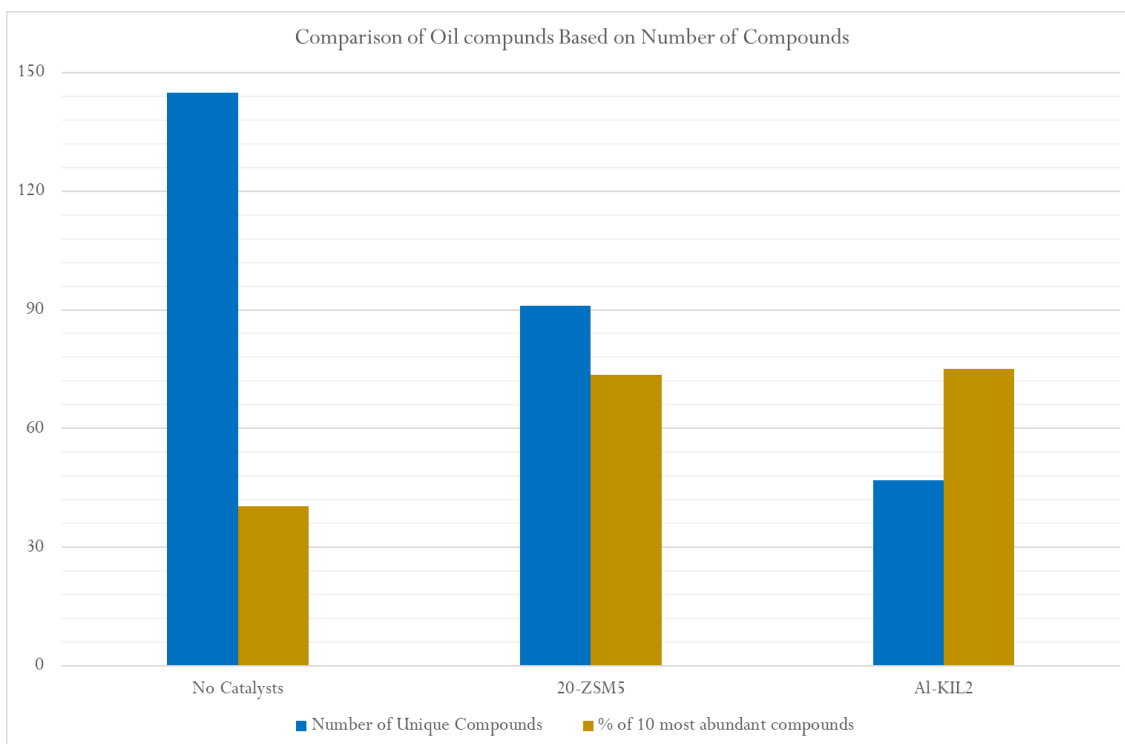


Figure 6-19: Effect of catalysts on the number of compounds produced and the percentage of top 10 main compounds

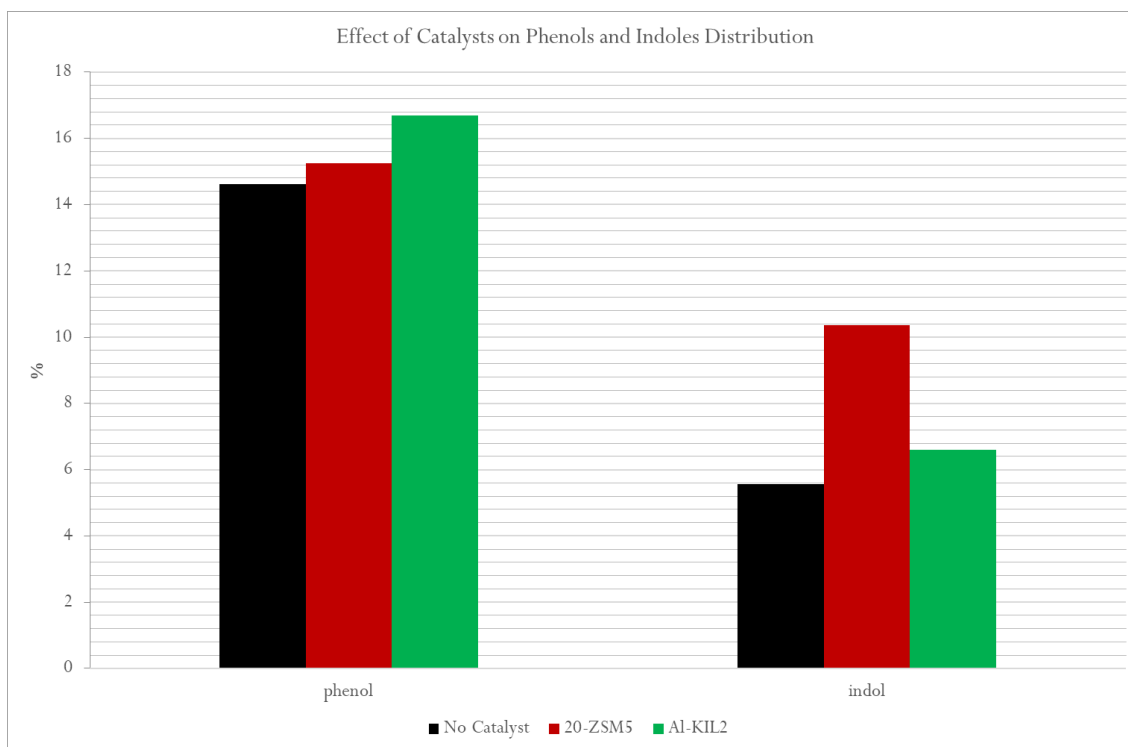


Figure 6-20: Effect of catalysts on phenols and indoles

As illustrated in Figure 6-20, catalysts were effective in increasing the aromatics, specifically indoles and phenols (oxygenated aromatics). Production of the phenols could have been to the cracking of the tyrosine amino acid or addition of hydroxyl to the various benzene intermediates available during the pyrolysis of wool.

The trend observed in the indoles was different to the one regarding the phenols. The increase of indoles could indicate the ability of the catalysts, in particular 20-ZSM, in breaking down the carbon bond in the indigoid chromophore. Another explanation for the higher amount of the indoles in 20-ZSM5 sample compared to Al-KIL2 could be the capability of Al-KIL2 to break the indoles further down into its constituents such as pyrroles or further break down and conversion to other nitrogen containing compounds such as imidazole due to the availability of higher surface area. Upon further investigation, it was observed that this was not the case. As illustrated in Figure 6-21, the increase in pyrroles in the case of 20-ZSM5 was the most significant effect. Coupling the data presented in Figure 6-21 with Table 6-2, could give a better image of the effect of catalysts. A pyrrole that existed in all the three samples was “Pyrrolo[1,2-a] pyrazine-1,4-dione, hexahydro-3-(2-methylpropyl)”. This compound is the most abundant compound in the non-catalytic and 20-ZSM5 sample. The quantity is more than tripled with use of 20-ZSM5, while reduced by around 25% with use of Al-KIL2. This compound could be produced through the removal of hydroxyl group from several proline amino acid of the wool structure.

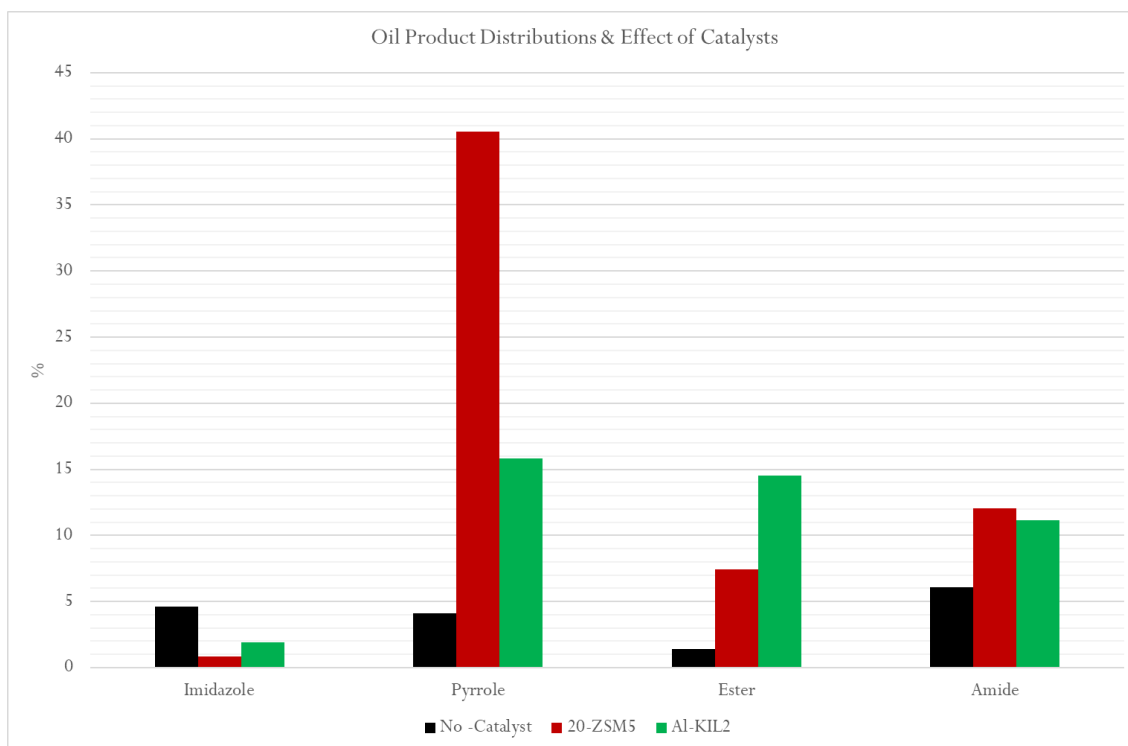


Figure 6-21: Effect of catalysts on oil product distribution

Catalysts behaviour regarding production of amides was not significantly different while esters are predominant in the Al-Kil2 samples. Esters and carboxylic acids could have been generated from cracking of several amino acids and dye molecules such as phenylalanine.

Table 6-2: The ten most abundant products in the oil samples

No Catalyst		20-ZSM5		Al-KIL2	
Compound	Area %	Compound	Area %	Compound	Area %
Pyrrolo[1,2-a] pyrazine-1,4-dione, hexahydro-3-(2-methylpropyl)-	8.1	Pyrrolo[1,2-a] pyrazine-1,4-dione, hexahydro-3-(2-methylpropyl)-	28.9	2,5-Piperazinedione, 3,6-bis(phenylmethyl)-	14.7
p-Cresol	7.5	p-Cresol	8.7	p-Cresol	10.9
Phenol	4.3	3-Methyl-1,4-diazabicyclo [4.3.0] nonan-2,5-dione, N-acetyl-	6.5	Hexanedioic acid, bis(2-ethylhexyl) ester	9.6
5,10-Diethoxy-2,3,7,8-tetrahydro-1H,6H-dipyrrolo[1,2-a:1',2'-d] pyrazine	3.7	5,10-Diethoxy-2,3,7,8-tetrahydro-1H,6H-dipyrrolo[1,2-a:1',2'-d] pyrazine	6.4	13-Docosenamide, (Z)-	7.3
Pyrazine, trimethyl-	3.1	Indole	4.7	Pyrrolo[1,2-a] pyrazine-1,4-dione, hexahydro-3-(2-methylpropyl)-	6.0
3-Methyl-1,4-diazabicyclo [4.3.0] nonan-2,5-dione, N-acetyl-	3.0	13-Docosenamide, (Z)-	3.7	3-Methyl-1,4-diazabicyclo [4.3.0] nonan-2,5-dione, N-acetyl-	5.7
Indole	3.0	Cyclobutylamine	3.7	Indole	5.5
Furaldehyde phenylhydrazone	2.1	2,5-Piperazinedione, 3,6-bis(phenylmethyl)-	3.2	Glutarimide	4.4
Hexanamide	1.9	Cyclopentane carboxylic acid, 3-methylbutyl ester	2.7	Propanoic acid, 2-hydroxy-, ethyl ester	3.9
2,5-Piperazinedione, 3,6-bis(phenylmethyl)-	1.9	Hexanamide	2.5	5,10-Diethoxy-2,3,7,8-tetrahydro-1H,6H-dipyrrolo[1,2-a:1',2'-d] pyrazine	3.6
2-Isopropylidene-2,5,6,7,8,9-hexahydroimidazo[1,2-a] azepin-3-one	1.8	Phenol	2.5	2-Propyn-1-ol, acetate	3.5

Figure 6-22 illustrates the difference between the FTIR of the oil samples. Existence or lack of a peak can demonstrate if a functional group exists or no longer exists. For instance, the peak between 2050 and 2075 cm^{-1} indicates that a cyanate existed in oil sample for the non-catalytic run. However, this is removed when catalysts are used in pyrolysis. Another peak, appearing between 1650 and 1700 cm^{-1} indicates the existence of an oxime, which does not show in the Al-KIL2 sample. This matches with the GC-MS analysis results. Production of imines generally occurs through reaction of primary amines with ketones or aldehydes in presence of acidic catalyst to increase the rate of reaction. The fact that the peak is more significant in the case of 20-ZSM5 compared with non-catalytic run, shows that the acidity of catalysts came into effect. Additionally, the large quantities of ester in the Al-KIL2 catalyst can indicate that this reactions path was not favoured by this catalyst.

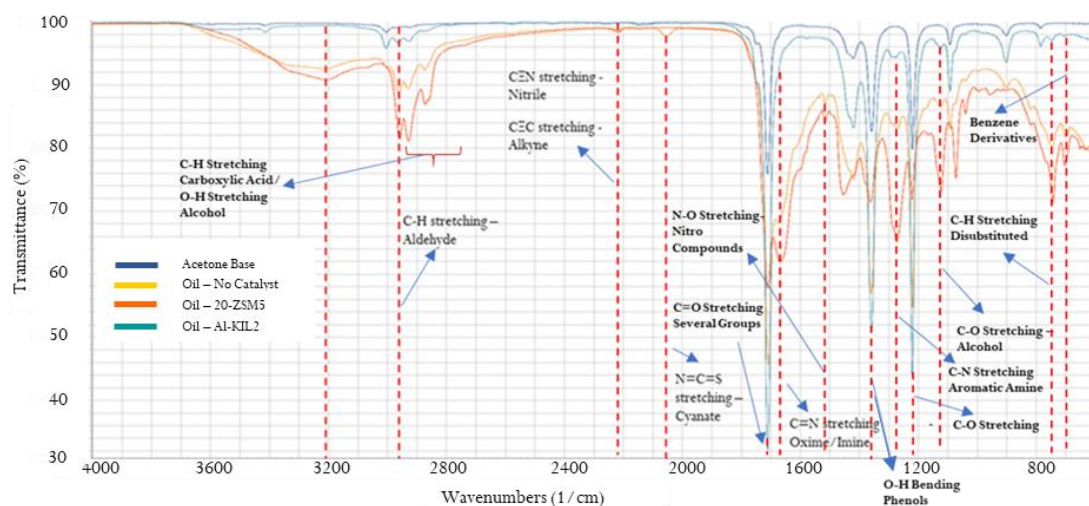


Figure 6-22: FTIR of catalytic and non-catalytic oil products [6.13]

Another observable effect that catalysts had was variation in the quantity of C-H groups at different wavelengths. These groups increased in the oil samples with use 20-ZSM5 compared to the non-catalytic tests while Al-KIL2 seemed to reduce this value. This result could be coupled with the char elemental analysis where the quantity of carbon and hydrogen were higher in the Al-KIL2 char sample compared to the other two samples.

Another major peak occurring between 1350 and 1400 cm^{-1} could belong to O-H group. Given the trend observed at this peak (Al-KIL2 > 20-ZSM5 > non-catalytic), this peak was indicative of presence of phenols in the oil.

Overall, data suggested that use of 20-ZSM5 resulted in increase of nitrogen containing compounds in oil. This was observed in GC-MS results where “Pyrrolo[1,2-a] pyrazine-1,4-dione, hexahydro-3-2-methylpropyl” quantity was more than quintuple of Al-KIL2 and triple of non-catalytic run

while pyrroles and indoles were the dominant groups. Furthermore, FTIR peaks illustrated that imines/oximes and amines were presented in the oil. On the other hand, GC-MS and FTIR data suggested that Al-KIL2 promoted generation of esters and compounds with oxygen contains functional groups.

6.3 Summary and Conclusion

A summary of this chapter and what the next chapter presents are discussed in this section.

6.3.1 Non-Catalytic Pyrolysis

Increase of temperature reduced char by-product in favour of volatile production. This increase in volatile was predominantly due to increase in oil production rather than gas. Feed size did not seem to affect the product distribution while changing the gas to carbon dioxide reduced produced char.

BET analysis of char showed that a maximum BET of 208 m²/g could be achieved at high temperatures. The char had higher BET when nitrogen was utilised instead of carbon dioxide. Char produced from shredded wool had BET value three times larger than the one with large piece of wool and therefore should be preferred for char applications. As expected, increasing pyrolysis from 700 to 900°C increased the BET by more than 300%.

Elemental analysis indicated that wool carbon content of 50% could be increased to more than 70% through pyrolysis at temperatures higher than 700°C. Furthermore, biochar obtained from wool has high nitrogen content (over 12%), low H/C and low O/C, which made the biochar nutrient-rich and stable and consequently usable as fertiliser or as soil amendment. Wool feed size did not seem to affect the char properties, while use of nitrogen generated char with higher carbon content compared to carbon dioxide case.

Gas analysis indicated that increase in temperature favoured production of CO over CO₂. This observation indicated that by increasing the temperature, the gas (after scrubbing away of toxic component) can be integrated as part of a CHP (Combined Heat and Power) system. Furthermore, as nitrogen content of char was reduced through increasing temperature, nitrogen containing compounds such as HCN and NH₃ were increased in gas with increasing the temperature. Therefore, if high temperature is selected to improve the gas potential for use as fuel source, gas clean-up procedure should be mediated.

The main compounds found in the oil were phenolics and indoles with their quantities increasing proportionally with temperature increase. Generally, increasing the temperature increased the number of unique compounds found in the oil. The condensation trap type did not seem to affect

the oil properties significantly and the more important factor was the degree to which heat transfer occurred. This was thought to be a function of surface area and contact period rather than the temperature of the trap.

CO₂ as carrier gas, compared to nitrogen, seemed to favour phenols and indoles generation while methoxy groups were favoured through use of nitrogen. Feed size did not seem to affect the produced oil properties significantly. The effect of temperature increase on indoles and phenols production became less significant as the temperature increased.

Overall, running reactions at higher temperatures are favourable since the BET of the char increased, char became more stable, CO content of gas increased, and valuable phenol and indole by-products increased as the temperature increased. While increasing the temperature was beneficial to improve qualities such as high CO content of gas and a more stable char, there were some downsides such as increased NH₃ in the gas, reduction in the nitrogen content of the char and increase cost of heating. Therefore, an operational temperature of around 800 °C could balance the costs and benefits of increase in temperature increase. Finally, pyrolysis of wool with the aim of converting it to valuable by-products (i.e., stable char, CO in gas syngas and saleable oil by-products such as indole and phenol) was deemed feasible to be taken forward for scale-up.

6.3.2 Catalytic Pyrolysis

Use of catalysts increased volatiles production significantly while decreasing char production slightly. However, the main observed behaviour of the catalysts was in distribution of oil and gas. Both catalysts increased oil yield significantly compared to the non-catalytic runs, while the oil produced through Al-KIL2 was just under 10% more than the 20-ZSM5 sample.

The char oxygen content reduced significantly through use of catalysts and therefore more stable. Use of 20-ZSM5 resulted in char with high nitrogen content which further improved the potential of the char as saleable by-product for fertilisation.

Use of catalysts reduced the number of unique compounds found in the oil while increasing the concentration of most abundant compounds. Also, use of catalysts increased both indoles and phenols. However, opposed to the trend observed during increasing the temperature in non-catalytic tests where the phenols and indoles were the increasing products, pyrroles were the main products in case of 20-ZSM5 while esters were the second most abundant compounds instead of indoles in case of Al-KIL2.

Overall, catalysts improved the pyrolysis products. Both catalysts made the char more stable through reducing the oxygen content while improving the oil quality through reducing the number

of unique compounds in it. This would make the separation procedure more feasible. However, the high nitrogen content of the char obtained from pyrolysis with 20-ZSM5 made it a better choice if market demand for char as fertiliser was high. On the other hand, the oil sample with fewer number of unique compounds would make the oil sample obtained from pyrolysis with Al-KIL2 a better choice if oil had a higher demand.

6.3.3 Next Chapter

In the next chapter, results for wool pyrolysis using scaled-up reactor are presented. Also, the possible utilisation of some of the main products is listed.

6.4 References

- [6.1] W. Falix, M. McDowall, H. Eyring, "The differential thermal analysis of natural and modified wool and mohair," *Textile Research Journal*, 1963.
- [6.2] G. Menefee, E. Yee, "Thermally-induced structural changes in wool," *Textile Research Journal*, 1965.
- [6.3] Z. Xia, C. Yao, J. Zhou, W. Ye and W. Xu, "Comparative study of cotton, ramie and wool fiber bundles' thermal and dynamic mechanical thermal properties," *Textile Research Journal*, 2015.
- [6.4] C. Guizani, F.J. Escudero Sanz, S. Salvador, "Effects of CO₂ on biomass fast pyrolysis: Reaction rate, gas yields and char reactive properties," *Fuel*, 2014.
- [6.5] E. Batista, J. Shultz, T. Matos, M.R. Fornari, T.M. Ferreira, B. Szpoganicz, R. Freitas & A.S. Mangrich, "Effect of surface and porosity of biochar on water holding capacity aiming indirectly at preservation of the Amazon biome," *Scientific Reports*, 2018.
- [6.6] F. Zhao, G. Zou, Y. Shan, Z. Ding, M. Dai & Z. He, "Coconut shell derived biochar to enhance water spinach (*Ipomoea aquatica* Forsk) growth and decrease nitrogen loss under tropical conditions," *Scientific Reports*, 2019.
- [6.7] Q. Yan, H. Toghiani, F. Yu, Z. Cai, J. Zhang, "Effects of Pyrolysis Conditions on Yield of Biochars from Pine Chips," *Forest Products Journal*, 2011.

- [6.8] R. Chatterjee, B. Sajjadi, W. Chen, D. L. Mattern, N. Hammer, V. Raman and A. Dorris, "Effect of Pyrolysis Temperature on PhysicoChemical Properties and Acoustic-Based Amination of Biochar for Efficient CO₂ Adsorption," *Energy Research*, 2020.
- [6.9] C. Guizani, M. Jeguirim, S. Valin, L. Limousy and S. Salvador, "Biomass Chars: The Effects of Pyrolysis Conditions on Their Morphology, Structure, Chemical Properties and Reactivity," *Energies*, 2017.
- [6.10] B. G. S. Schimmelpfennig, "One step forward towards characterization: some important material properties to distinguish biochars," *Chemosphere*, 2012.
- [6.11] A. Pattiya, "Fast pyrolysis," in *Direct Thermochemical Liquefaction for Energy Applications*, Maharakham University, Kamriang, 2018, pp. 3-28.
- [6.12] H. Zhang, R.X. Deng, H. Wang, G. He, S. Shao, J. Zhang, Z. Zhong, "Biomass fast pyrolysis in a fluidized bed reactor under N₂, CO₂, CO, CH₄ and H₂ atmospheres," *Bioresource Technology*, 2011.
- [6.13] Sigma-Aldrich, "IR Spectrum Table & Chart," [Online]. Available: sigmaaldrich.com/technical-documents/articles/biology/ir-spectrum-table.html. [Accessed 2020].
- [6.14] International Biochar Initiative, "Standardized Product Definition and Product Testing Guidelines for Biochar That Is Used in Soil", 2014
- [6.15] K.A. Spokas, "Review of the stability of biochar in soils: predictability of O:C molar ratios", *Food and Agriculture Organisation of United States*, 2010

CHAPTER 7 - SCALE-UP WOOL PYROLYSIS AND GASIFICATION EXPERIMENTS USING A CUSTOMISED AUGER REACTOR

In this chapter, the results for the pyrolysis of wool using the customised auger reactor discussed in chapter 4 are presented. The aim of this chapter is to verify the feasibility of wool waste pyrolysis at a maximised feeding rate. The reactor was designed to hold over 1 kg of feed in the designated hopper and with the second auger speed mentioned in section 4.6, the reactor had the potential to process over 10 kg/h wool waste. There were no dedicated reactors available in literature which was capable to handle this volume of wool waste. Furthermore, this chapter compares the scale-up results with those obtained using the small, fixed bed scale reactor.

To do the above tasks, pyrolysis was carried at 350, 500 and 800 and 900°C with carbon dioxide and at 800°C with nitrogen, to observe the effect of increase in temperature and change of gas in large scale. The main focus was put on the char and bio-oil products due to the more accuracy during the collection of them and attempts were made to analyse the gas characteristics by deduction.

7.1 Process Considerations

The comparison between the two processes (auger Vs. fixed bed reactors) was carried out with the realisation in mind that the nature of the two processes were different. Since the scale up was carried out as a mean to test the viability of the designed reactor to be used practically in an industrial scale, it needed to be designed in a continuous arrangement rather than a batch one. Therefore, the basic nature of the reactors was different.

One main difference was the residence time of the pyrolysis vapours in the heated zone, with the gas retention time in the small-scale and large-scale reactors being respectively 28 and 205 seconds. Another difference was represented by the time the wool spent in the reactor. In the fixed bed experiment, wool was introduced into the heated bed when the reactor reached the desired temperature (heating rate of at least 11 °C/s). Furthermore, the feed was pyrolysed until pyrolysis was completed (overall 15 minutes spent at elevated temperatures) and the reactor was cooled for disassembly. In the auger reactor, same approach was taken, and wool was introduced when the desired temperature was reached in the furnace. Wool theoretically should have taken 35 seconds (heating rate of at least 10 °C/s) to be moved to the end of the reactor and discharged (as char/ash) in the char receiver. However, in reality, the time spent by some wool pieces could be affected by

the formation of wool agglomerates that would be carried over by the auger blades (up to 1 minute in the auger).

Other difference was the efficiency of the condensation train. In the fixed bed experiment, due to the small size of the feed (1g), it was possible to use a very efficient tar-trap sink (such as ice and liquid nitrogen) to maximise condensation with minimal heat transfer area. In contrary, using liquid nitrogen or ice bath was deemed impractical and for commercialisation purposes, costly. Therefore, a system with two Quickfit jacketed coil water condensation system was selected for maximisation of surface area and accessibility of the condensation medium (tap-water). This change could have changed the composition of the bio-oil compared to using the fixed bed.

Another change introduced in the auger reactor was scrubbing of gas prior to release into atmosphere by water to reduce the toxic content of the gas. Therefore, the properties of the scrubbing water were used to determine the toxic content of gas and to establish if water scrubbing was effective.

Determining the product distribution using the auger reactor was not as straightforward as using the small-scale fixed bed and it proved to be significantly erroneous with the current system. The reason behind this was the inability to weigh all the process equipment in an error free manner prior to pyrolysis due to their large size and heavy weight. This was coupled with the fact that char by-product was found to some stick to the auger itself. Furthermore, due to the fact that oil condensed at temperatures as high as 300 °C, some oil was found to condense in connection tubes upstream of the gas outlet despite the use of heating tapes and insulation material.

Therefore, all the above considerations have to be accounted for the set-up's comparison.

7.2 Mass Balance

As stated in the previous section, error free measurement of the equipment/products and consequently obtaining an exact mass balance was not practical. However, to obtain an approximate range for the quantity of char and volatiles produced, tests at 500 and 800 °C were carried out 3 times. Afterwards, attempts were made to collect as much of the char produced as possible (from the solid collection container and auger blades). The mass of char obtained was subtracted from the quantity of tweed wasted fed into the system to obtain the conversion percentage to char and volatiles. The mean value of the minimum and maximum values was taken with the deviation from this value being taken as the error margin. The char quantity was calculated to be 24% \pm 6 and 21% \pm 7 for the tests at 500 and 800°C respectively. Despite the fact that these values deviated from the runs in the fixed bed, the values were not deemed unreasonable and showed that auger reactor

was capable of converting the tweed to the products similar to the fixed bed with minor adjustments if needed.

7.3 Char analysis

Similar to fixed bed, char appearance characteristics were brittle and flaky. However, the sample obtained at 350 °C was except from this observation. At this temperature, the product seemed to be only partially pyrolysed and at the core of char particles, wool structure was still present Figure 7-1. The difference between these two (350°C runs in small and large reactor) could be due to higher residence time of the char in the small scale which provides more time for the wool to be pyrolysed. This phenomenon is not observed at higher temperatures.



Figure 7-1: Char appearance in the auger feeder

7.3.1 Elemental Analysis of Char

Figure 7-2 presents the results for the elemental analysis of the char obtained at different temperatures. Furthermore, at 800°C, the results for both the auger and the fixed bed reactors are presented to facilitate their comparison. Similar to the fixed bed, the increase in temperature increased the carbon content of the char. Similarly, nitrogen and hydrogen decreased with the increase in temperature as per the fixed bed char. There are two anomalies to the trends described above and with regards to the fixed bed results.

The first difference is the trend of oxygen content in relation to temperature increase. In auger feeder, the quantity of oxygen content in the char was reverse correlation with increasing the temperature. This trend was expected since as temperature increased, more oxygen containing volatiles were expected to be decomposed and therefore the char would have become more stable. The same trend was observed for the fixed bed, apart for the run at 700°C, possibly due to an error in the elemental analysis.

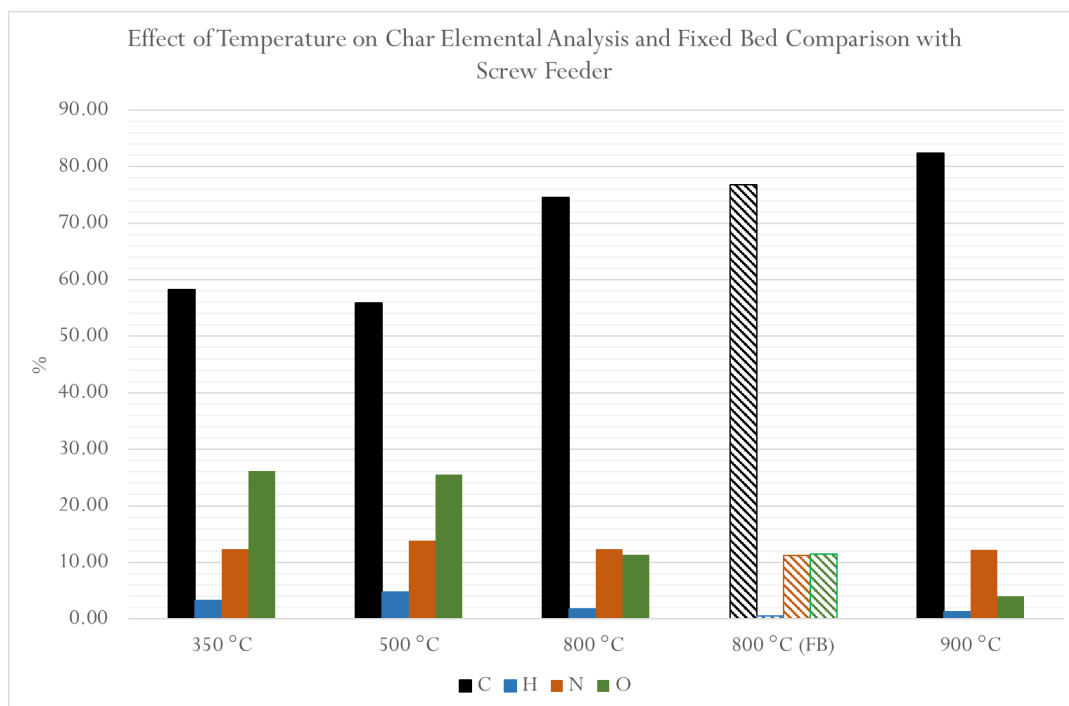


Figure 7-2: Elemental analysis of auger feeder char samples at different temperatures and fixed bed at 800°C

Sample obtained at 350°C did not fall into the trend observed in analysis of the samples observed at other temperatures. Carbon quantity is higher than the sample obtained at 500°C which was opposite to the trend observed. Lack of occurrence of the final step of decomposition corresponding to release of main macro molecules of wool (occurring at 434°C (Chapter 6)), could explain this difference. High carbon concentration of these, which remained in the wool (char) structure at this temperature resulted in this observed difference. Furthermore, the physical appearance of the char demonstrated that the original structure of wool was still intact at the core of the char sample at 350°C; something which was not observed at higher temperatures. Therefore, complete pyrolysis was not successful at 350°C.

Direct comparison of the char obtained from the fixed bed and the auger reactor was carried out on samples obtained at 800°C. Fixed bed sample contained 2% more carbon and 1% less hydrogen. Since the fixed bed sample spent more time in the heated zone, a higher decomposition degree

could have taken place for this sample, resulting in higher carbon content, or this minor difference could have been due to errors in measurements. Overall, the results indicate a very similar behaviour in the two set-ups.

7.3.2 FTIR of Char

Figure 7-3 presents the results for FTIR analysis of the char samples obtained at 500 and 800°C for both fixed bed and auger reactors.

Comparing the results indicates that peaks were almost identical for the samples obtained at 800°C, while the differences were minimal at 500°C. One difference that could be observed was the transmittance percentage. At 800°C, the char from the auger reactor absorbed more light compared to that from the fixed bed, while this was reversed at 500°C. This could indicate that at 500°C, heat transfer efficiencies were close for fixed bed and the auger reactor as a result of primary decomposition. However, as temperature was increased, more secondary reactions occurred in the fixed bed arrangement, due to the higher residence time.

Comparing char samples at 500°C, a peak at around 3000 cm⁻¹ could be seen in the auger reactor sample, which was missing in the fixed bed sample. This could have belonged to an alkene stretch vibration, confirming that complete decomposition did not take place at this temperature using the auger reactor.

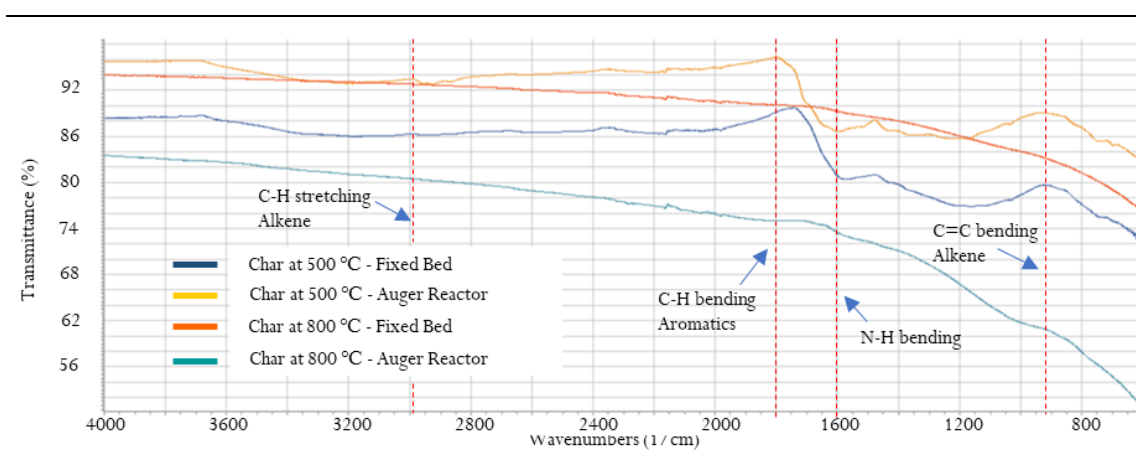


Figure 7-3: Comparison of FTIR results for fixed bed and auger reactor

7.4 Scrubbing Water & Gas

Since char elemental and FTIR analysis indicated the similarity of the products, it was expected that volatiles composition as a whole would be similar to that of fixed bed. The difference, therefore, was expected to be mainly due to the effectivity of the condensation system. Since the gas produced were expected to have toxic nitrogenates and sulphur containing compounds, gas needed to be

cleaned prior to exit to atmosphere. Water was selected as the medium to scrub the gas as indicated in literature [7.1, 2, 3]. GC-MS analysis of scrubbing water was used to identify the trapped species.

Using the auger feeder, the appearance of the smoke produced from wool could be observed. As illustrated in Figure 7-4, condensation colour got lighter as the gas started to move down the condensation train. For instance, at the top of the spiral in the first condenser, condensed gas had dark black colour and it got lighter downstream. This could be due to the condensation of heavier and denser compounds during the initial stages of condensation, while lighter compounds condense further downstream as temperature is further increased through contact with cooling water.

The appearance of the condensable gas from lower temperature and higher ones were also distinctively different. As shown in Figure 7-5, the gas from the run at 350 °C had a light yellowish fog appearance, while the gas from the run at 900 °C had a dark black smoke like appearance. This could have indicated that as temperature is increased, heavier compounds are formed through direct decomposition (till around 500°C) or secondary reactions. This phenomenon could be used for a stepwise process in which products are collected in separate condensation trains or multiple auger feeders, facilitating easier separation of useful by-products.

Figure 7-6 presents the appearance of the scrubbing water. It was observed that small particles of wool were swept with the gas and were either captured on the surface of the water or precipitated to the bottom of the water container, suggesting that a cyclone should be used in an improved system. The water colour changed from transparent to different shades of yellow based on the temperature at which pyrolysis took place. Large accumulation of gas formed on the top of water during the process. This coupled with the fact that pale yellow condensed steam appeared in the tubing out of the water scrubber meant that if condensation train improved through either increasing the contact surface area or reduction in temperature, more bio-oil could have been condensed.



Figure 7-4: Appearance of gas as it enters the condensation train and gas scrubbing



Figure 7-5: Effect of pyrolysis temperature on appearance of the gas (350°C on left, 900 on right°C)

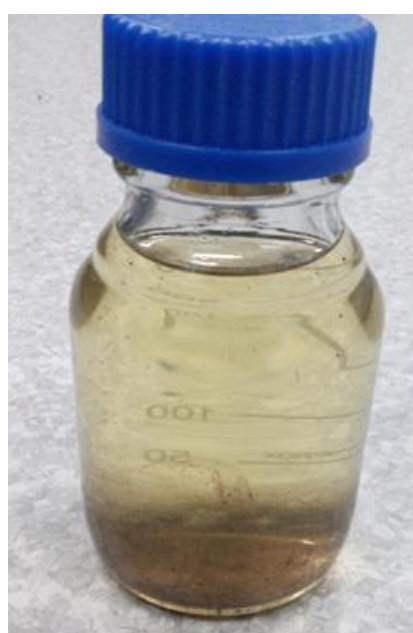


Figure 7-6: Appearance of the scrubbing water during process (left) and after collection (right)

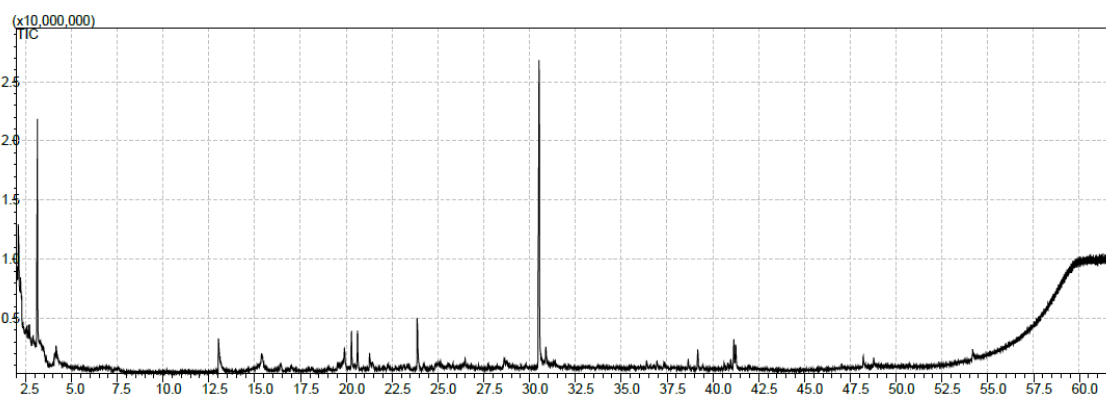


Figure 7-7: GC-MS curve for the scrubbing water at 800°C

Figure 7-7 presents the GC-MS curve of the scrubbing water obtained from the run at 800°C. The first observation was that the number of unique compounds (peaks) in the sample were much larger than oil samples. Namely, over 550 unique compounds were present in the sample. However, the more abundant peak including the predominant one at 30.5 minutes were in lower number compared to the ones in the bio-oil.

The peak at 30.5 minutes belonged to “3,3'-thiobis Propanenitrile” ($C_6H_8N_2S$), which is a poisonous compound. Existence of this chemical, which if heated will produce NO_x , CN and SO_x , alongside other nitrogen containing components such as “Pyrrole[1,2-a] pyrazine-1,4-dione” and “hexahydro-3-(2-methylpropyl)” in the scrubbing water indicated that this arrangement was successful in removing toxic nitrogen and sulphur containing compounds from gas to a degree. Also, 3,3'-thiobis Propanenitrile, constituted over 25% of the chemicals in the scrubbing water while only constituted to less than 1% of some of the oil samples. It should be noted that “3,3'-thiobis Propanenitrile” is colourless, but could have a light-yellow colour. Therefore, the colour of the scrubbing water was the function of existence of this compound.

In addition to unique compounds such as “3,3'-thiobis Propanenitrile”, other compounds that were predominant in the condensed bio-oils were also present in the scrubbing water but in much lower concentration. Some of these were, acetic acid (second prominent compound occurring at after minutes in GC-MS curve), p-cresol, butanedinitrile, propanoic acid and Undecane. This clearly confirm the fact that the condensation set-up should be enhanced to maximise the retention of compounds in bio-oil. These compounds could also be separated from the wastewater and sold separately as useful commodities but would require energy intensive post-processing.

7.5 Bio-oil Analysis

Bio-oil samples colour were similar to that of fixed bed samples. As illustrated in Figure 7-8, the quantity of bio-oil obtained at the first stage of condensation (right bottle) was more than the second

stage. Furthermore, condensation took place in the tubes upstream of the oil collection bottle between the two condensation steps. However, the quantity of oil condensed was minimal in the outlet of the water scrubber compared to the connections upstream of the scrubbing water, which translated to the effectivity of the condensation system to capture volatiles to an acceptable degree.



Figure 7-8: Appearance of oil obtained at different stages of condensation

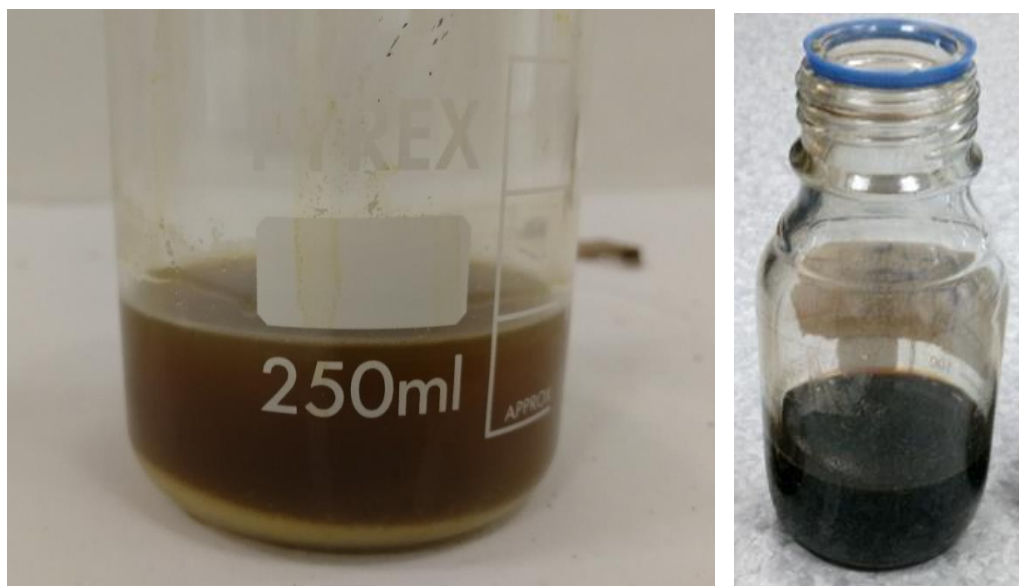


Figure 7-9: Difference in the oil obtained at 350°C (two layers) and 800 °C

As illustrated in Figure 7-9, the appearance of oil changed significantly as temperature increased. More precisely, the increase of temperature from 350°C to 500°C changed the colour and texture

of the oil obtained significantly. Oil at high temperatures (500°C and above) had a dark brown colour without any form of separation. At 350°C, however, oil had a phase separation, an organic rich phase on top and a bottom organic-water-phase. Elemental analysis, GC-MS and FTIR were carried out on oil samples to evaluate these differences.

7.5.1 Elemental Analysis of Oil

Figure 7-10 presents the elemental analysis data for bio-oils obtained at different conditions using the auger reactor in addition to the sample obtained at 500°C in the fixed bed for comparison.

Comparing the top and bottom samples of the oil obtained at 350°C, the differences were not significant. Carbon content of the top dark layer (organic rich) was slightly higher than the cream-coloured bottom layer (organic-water phase) while the trend observed in the oxygen content were reversed. The lower carbon and higher carbon content of the bottom layer coupled with the appearance of it, could have indicated more fatty acids were present in this part of the sample. This was further supported by the fact that at this lower temperature, the decomposition of wool could not be completed, while secondary reactions could not be completed to the same degree as higher temperatures.

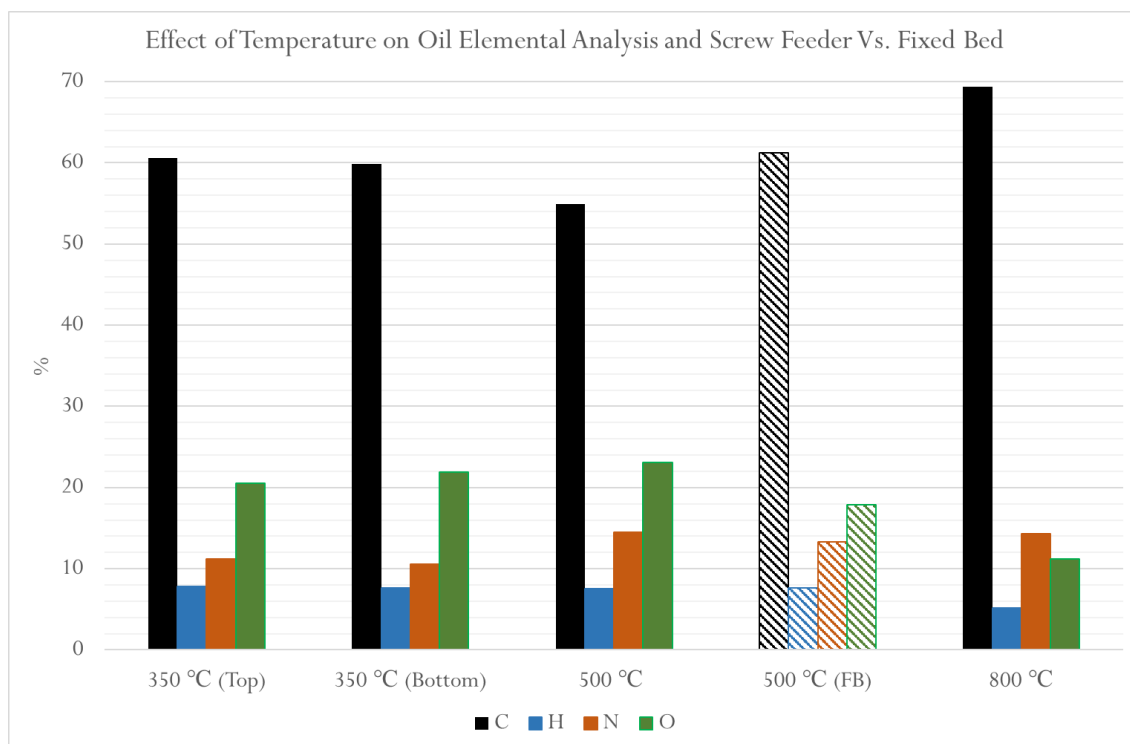


Figure 7-10: Elemental analysis of oil samples obtained from wool pyrolysis (all the tests besides the “FB” were carried out in the Auger reactor)

Observing the effect of temperature, same effect observed in char analysis was observed. This meant that with increase of temperature, oxygen content was reduced, while carbon content was increased

with the exception of the sample produced at 350°C. The higher carbon content at 350°C, compared to the 500°C sample, could be compensated by higher nitrogen content of the 500°C sample. In other words, the macro structure of wool, which contains large quantities of nitrogen were not broken at 350°C. This meant that higher concentrations of nitrogen (and sulphur) were presented in samples obtained at higher temperature, where nitrogen were released. This meant that concentration of carbon decreased at higher temperatures due to the increase in nitrogen concentration.

7.5.2 GC-MS of bio-oils

First comparison was carried out to observe the difference between the two layers of the sample obtained at 350°C (Figure 7-11). Some peaks were identical between the two samples. Examples of these were peaks at 20.2 minutes (p-cresol), 21.2 minutes (4-Piperidinone, 2,2,6,6-tetramethyl) and 26.8 minutes (indole). These products existed on samples obtained at higher temperatures and at samples obtained from fixed bed tests too. Furthermore, their quantities are more prominent in the top layer of oil sample. Therefore, they could not be the reason behind the difference appearance of the bottom layer.

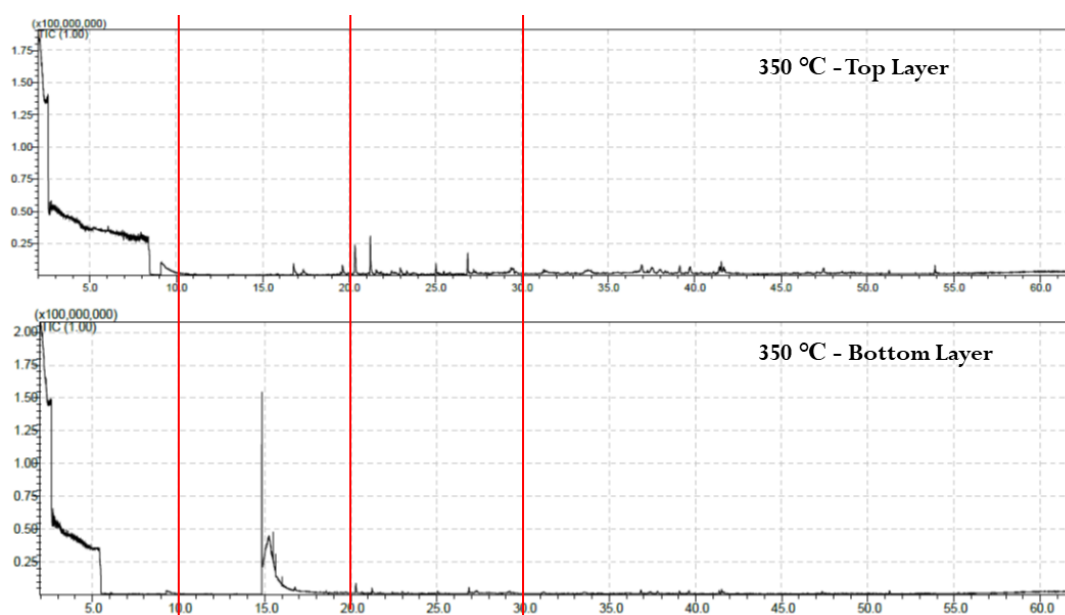


Figure 7-11: Comparison of GC-MS results obtained for top and bottom layers of pyrolysis oil sample at 350°C

Peaks occurring just before 15 minutes till 16 minutes are unique to the bottom layer sample. The peak occurring at 14.8 and 15.3 belonged to “5-(3,7-Dimethylocta-2,6-dienyl)-4-methyl-2,3-dihydrothiophene 1,1-dioxide” and “5-(2-Bromoethyl)-bicyclo [2.2.1] hept-2-ene” respectively. More importantly, “5-(2-Bromoethyl)-bicyclo [2.2.1] hept-2-ene” constituted to over 70% of the sample. Bromine was observed in almost all of the samples in small quantities, typically constituting

to less than 2% of overall area in GC-MS curves. The existence was expected due to structure of some of the red or orange acidic dyes (such as C.I. Acid Red 87 - $C_{20}H_6Br_4Na_2O_5$, EOSIN Y - $C_{20}H_8Br_4O_5$ and Acid Red 92 - $C_{20}H_2Br_4Cl_4Na_2O_5$) used in the processed wool. This dominance of this bromine containing compounds and its polarity could have been the reason behind the separation of the oil sample into two different layers (oily non-polar phase on the top and layer with polar compounds on the bottom).

As illustrated in Figure 7-12, none of these compounds are aromatics and they contain double carbon bonds. As discussed previously, at this temperature, wool was not decomposed completely. Therefore, breakage of intermolecular bonds such as hydrogen bonds were predominant. Shape of these compounds justifies these assumptions. It appears that at higher temperatures, these small linear compounds break down further and form more complex compounds and therefore behave as intermediates. Therefore, despite low temperature pyrolysis (350°C) is not efficient in decomposing the whole wool waste, a staged pyrolysis with an initial low temperature stage could be used to recover these specific bromine compounds.

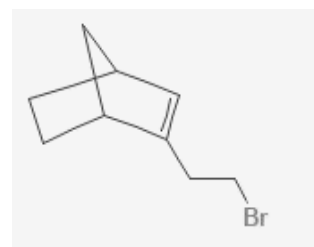
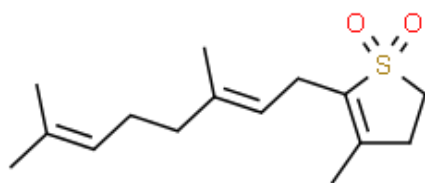


Figure 7-12: Structure of 5-(3,7-Dimethylocta-2,6-dienyl)-4-methyl-2,3-dihydrothiophene 1,1-dioxide (left) and 2-(2-Bromoethyl) bicyclo [2.2.1] hept-2-ene (right)

Figure 7-13 presents the results obtained from analysis of auger feeder and fixed bed oil samples. However, it should be re-instated that pyrolysis residence time and condensation train were different. Despite this, most of peaks occurred at retention times. For instance, peak at 21.3 minutes (4-Piperidinone, 2,2,6,6-tetramethyl-) was significant in both samples. One other behaviour observable from the curves was the number of unique compounds. Over 250 compounds were present in fixed bed oil sample and this number was reduced to 100 using the scale-up set-up. This behaviour of reduction in number of compounds was observed in fixed bed oil result by reducing temperature (Chapter 6). This could have been another sign that the decrease in wool residence time in the auger reactor process reduced the degree of pyrolysis and secondary reactions.

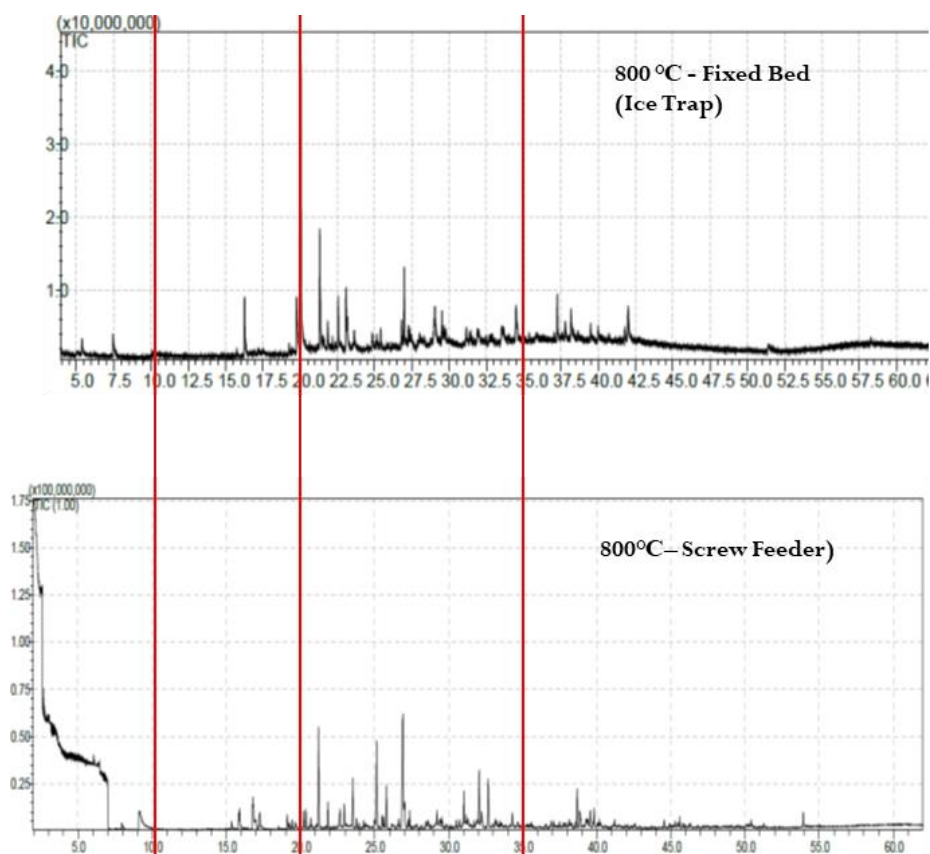


Figure 7-13: Comparison of GC-MS results of fixed bed and auger feeder at 800 °C

To clarify the difference between fixed bed and auger reactor, products were categorised into main functional groups (Figure 7-14). The only compounds in which minimum amount of change occurred during scale-up were indoles. The most significant change was the shift from phenols dominance in products to quinoline and nitriles. With regards to the structure of these compounds, it could be concluded that pyrolysis in fixed bed allowed more steps of reaction due to the longer residence time and therefore better heat transfer. For instance, black reactive dye and indigoid chromophore were expected to be used during dyeing process. For phenols to be produced, the structure of these dyes needed to be broken down through several processes such as desulfurization, deamination, deoxygenation, and reformation. However, through fewer steps were required for nitriles to form.

To observe the effect of increasing the temperature on oil sample in auger reactor and compare it with fixed bed, top ten most abundant compounds in each sample at 800°C and 900°C for both arrangements were compared (Table 7-1). The first observation was the shift from phenol to ketones as the most abundant functionality using the auger reactor. For instance, at 900°C, most abundant product was “benzocyclobuten-1(2H)-one” in the sample, which could have been generated from deoxygenation of indigoid followed by detachment of benzene ring. On the other

hand, in fixed bed, most abundant compound was p-cresol, which could have been formed by further reforming of benzocyclobuten-1(2H)-one through carbonyl reduction followed by addition of hydroxyl group. However, existence of p-cresol in the auger derived bio-oil but with much less concentration showed the effect of increased residence time in fixed bed. Products from the auger reactor at 800 and 900°C were compared to observe the effect of temperature. The complexity of products seemed to reduce as temperature increased, while the concentration of top product increased. For instance, the top 10 most abundant compounds constituted over 65% of bio-oil at 900°C, while this number reduced to less than 48% at 800°C.

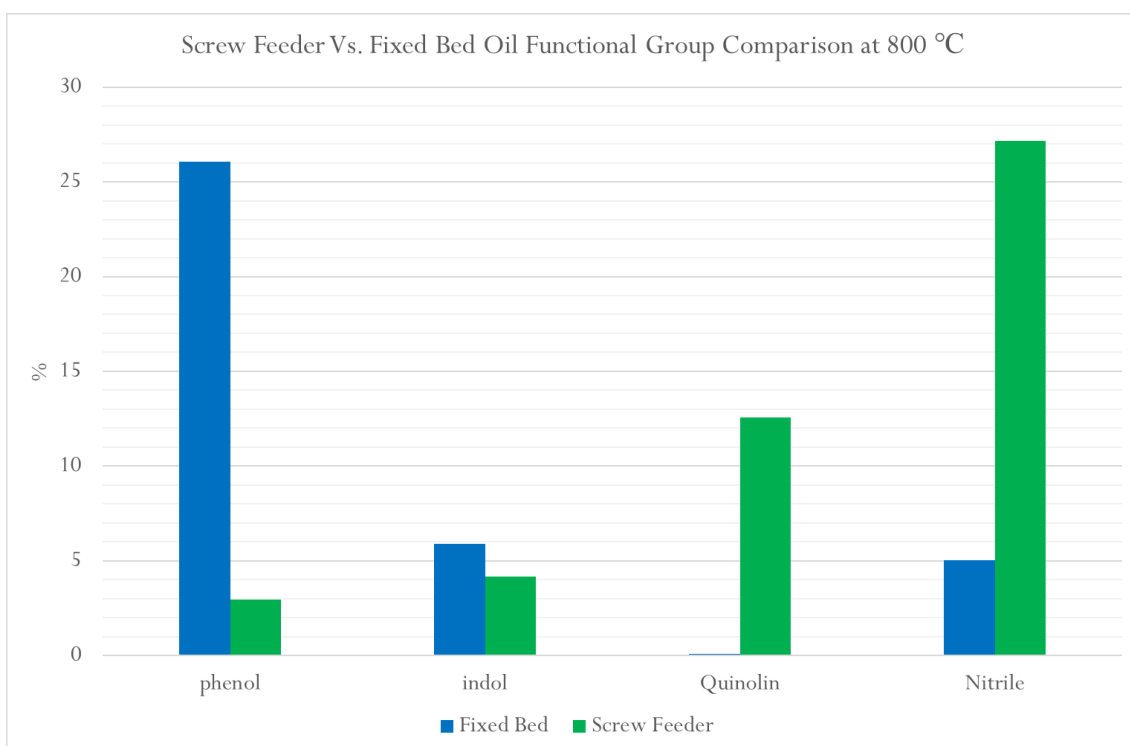


Figure 7-14: Comparison of auger feeder and fixed bed oil samples via main functional groups

Table 7-1: Effect of increasing temperature on oil composition in auger feeder compared with fixed bed

800°C (FB)		800°C (Auger)		900°C (FB)		900°C (Auger)	
Compound	Area %	Compound	Area %	Compound	Area %	Compound	Area %
Phenol,3-methyl-	18.2	Benzocyclobuten-1(2H)-one	10.9	p-Cresol	18.4	4-Isobutyl-2-pyrrolidinone	32.48
Indole	4.7	1-Naphthalenecarbonitrile	6.9	2,4-Imidazolidinedione, 5,5-dimethyl-	10.4	Cycloprop[a]indene, 1,1a,6,6a-tetrahydro-	6.45
Phenol	4.2	4-Piperidinone, 2,2,6,6-tetramethyl-	6.1	Indole	7.3	Bis-(2,2,6,6-tetramethylpiperidin-4-yl)-amine	4.58
4-Piperidinone, 2,2,6,6-tetramethyl-	3.9	Phenylpropynal	5.5	4-Piperidinone, 2,2,6,6-tetramethyl-	5.5	1-Naphthalenecarbonitrile	3.68
2-Propen-1-amine, N, N-bis(1-methylethyl)-	3.0	1H-Pyrrole-2-carbonitrile	3.2	Phenol	3.7	1,2,4,5-Tetrazin-3-amine, 6-methyl-	3.40
4-Aminoresorcinol	2.4	Azulene	3.0	4-Aminoresorcinol	2.4	Isoquinoline	2.64
5,10-Diethoxy-2,3,7,8-tetrahydro-1H,6H-dipyrrolo[1,2-a:1',2'-d] pyrazine	2.4	Isoquinoline	2.8	4-Piperidinone, 4-Piperidinone, 2,2,6,6-tetramethyl-	2.1	Hexahydro-1,3,5-trinitroso-1,3,5-triazine	2.63
Pyrrolo[1,2-a] pyrazine-1,4-dione, hexahydro-	2.3	Biphenylene	2.4	Phenol, 4-ethyl-	1.6	p-Cresol	2.28
Cyclopropylamine, N-isobutylidene-	2.1	Phenanthridine	2.3	Aziridine, 1,2-diisopropyl-3-methyl-, trans-	1.5	2-Ethynyl pyridine	2.21
Hexahydropyrrolizin-3-one	2.0	Anthracene	2.2	2-Pentanone, 4-hydroxy-4-methyl-	1.5	Pyrene	2.15

Aziridine, 1,2-diisopropyl-3-
methyl-,

1.9 Benzo[h]quinoline

2.0 | Benzofuran, 2,3-
dihydro-

1.3 Phenanthrene

2.04

7.5.3 FTIR of Oil

Figure 7-15 compares the FTIR analysis result of the auger reactor bio-oil. The wide peaks observed between 3200 to 3600 cm^{-1} which were much more significant at 350°C, represent NH and OH intermolecular bonds [7.4]. Due to the broadness of the peak however, the probability of OH intermolecular bonds were higher. These could have represented long unbroken chains, which were broken down as temperature increased.

One peak that did not occur at 350°C and got more significant as temperature increased was at 2200 cm^{-1} . This could have belonged to nitriles or alkynes. Coupled with elemental analysis of oil, this peak most likely belonged to alkynes since temperature increased, carbon content of char increased, while hydrogen decreased.

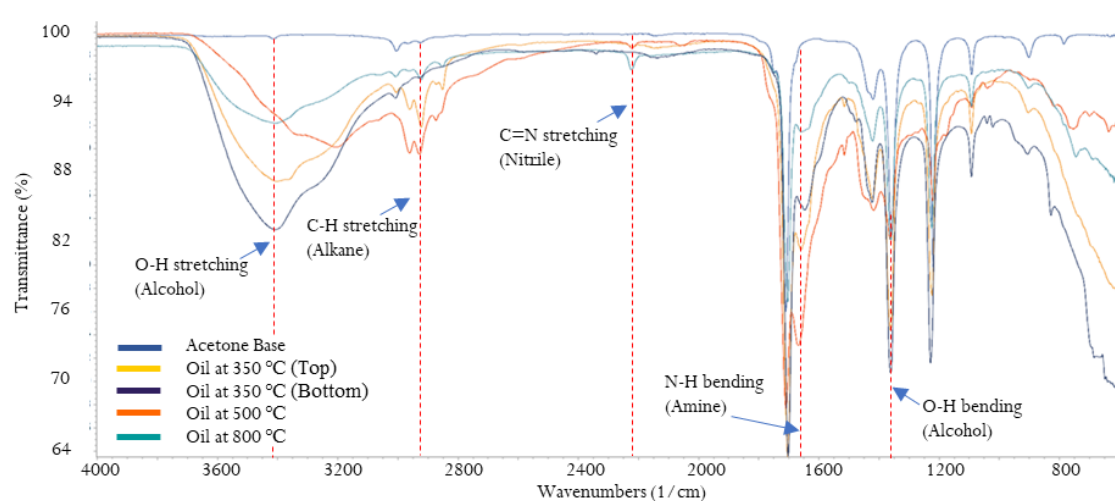


Figure 7-15: FTIR result comparison for oil products of screw feeder pyrolysis

7.6 Potential Application for Products and Separation Methods

In this section, the applications of some of the by-products and potential methods to separate them from the other by-products are discussed. To do so, products which were obtained with significant quantities which were deemed to have possible commercial utilisation are listed in

Table 7-2: Wool pyrolysis products with potential commercial applications

Product	Application	Density (kg/m ³)	Boiling Point (°C)
P-Cresol	> Precursor for organic synthesis	1034	202.5

	<ul style="list-style-type: none"> › Raw feedstock for antioxidant production › Raw material for dye and pesticide manufacturing [7.5] 		
Other Phenols	<ul style="list-style-type: none"> › Plastic manufacturing › Production of Bakelite › As drugs (e.g., Antiseptic) › Food additive and packaging [7.14] 	-	-
4-Piperidinone, 2,2,6,6-tetramethyl-	It can be used as starting feedstock for Hindered Amine Stabilisers production [7.6]	882	205
Azulene	Azulene based optoelectronics materials could be used as fuel cells and transistors [7.7]. Also, it has been used as skincare and cosmetic product	1000	242
2-(2-butoxyethoxy) ethanol	<ul style="list-style-type: none"> › Hydraulic and heating transfer fluid › Cosmetics and perfume manufacturing › Plant protection and wastewater treatment processes › Cleaning and washing products [7.8] 	954	209
4-Isobutyl-2-pyrrolidinone	Use in pharmaceutical manufacturing (intermediate for pregabalin production) [7.9]	-	269
Benzocyclobuten-1(2H)-one	Alkene derivative has several applications such fabrication agent, dielectric material, and adhesive bonding material [7.10]	1214	70

Depending on the components of the bio-oil, either distillation (through difference in boiling point) or liquid/liquid extraction (through difference in density) can be used to separate the more valuable by-products from the rest. For instance, separation of “Benzocyclobuten-1(2H)-one” could be carried out with either of the methods due to the large difference in both density and boiling compared with other compounds. However, compounds such as 4-Piperidinone, 2,2,6,6-tetramethyl- and 2-(2-butoxyethoxy) ethanol cannot be separated though distillation and liquid/liquid

extraction would be the method to do so. On the other hand, Cresol and Azulene would require application of distillation rather than liquid/liquid extraction due to the close proximity of their boiling point. Therefore, due to the large number of compounds presented in the bio-oil, a multiple stage separation method consisting of both of these methods would be required to obtain high quality and pure products.

The char product can have several applications. For instance, Lehmann indicated that char produced at high temperatures would have high potential to adsorb metal ions from aqueous media due to its high surface area, pH, and capacity for cation exchange [7.15]. Also, the char products obtained had a high nitrogen content which made them a good candidate for fertilisation. Furthermore, the high pH char can be applied to acidic soils and increase their fertility through neutralisation [7.16].

7.7 Chapter Summary

Char analysis revealed that similar to fixed bed, increasing temperature increased carbon content while nitrogen content decreased. Overall, there was not a significant difference between char samples obtained from fixed bed and auger reactor.

Analysing scrubbing water showed that this system has good potential to remove toxic NO_x and SO_x from gas and potentially recover 3,3'-thiobis Propanenitrile. It also showed that through improving the condensation train by either increasing the surface area available for heat transfer or decreasing the trap temperature, more oil could have been condensed.

Oil analysis showed the most observable difference between the two configurations. Oil sample from fixed bed contained predominantly phenols and indoles, while ketones, nitriles and quinolines were main products in auger reactor. It was concluded that longer feed residence time in the fixed bed allowed more conversion of intermediates.

Overall, scale-up procedure (from fixed bed to auger) proved to be promising and feasible. This conclusion was based on the fact that wool was converted to by-products and wool flew through the auger system with acceptable flowrate after removing some of the issues such as gas back flow and stagnation of wool in the reactor tube (Chapter 4).

7.8 References

- [7.1] EPA, "Monitoring by Control Technique - Wet Scrubber For Gaseous Control," EPA, 2019. [Online]. Available: epa.gov/air-emissions-monitoring-knowledge-base/monitoring-control-technique-wet-scrubber-gaseous-control.
- [7.2] EPA, "Wet Scrubbers for Particulate Matter," in *EPA Air Pollution Control Cost Manual*, EPA, 2002.
- [7.3] CR Clean Air, "The Chemical Aspect of NO_x Scrubbing," 2020. [Online]. Available: crleanair.com/library-2/technical-articles/the-chemical-aspect-of-nox-scrubbing/.
- [7.4] SigmaAldrich, "IR Spectrum Table & Chart," 2020. [Online]. Available: <https://www.sigmaaldrich.com/technical-documents/articles/biology/ir-spectrum-table.html>.
- [7.5] Chemical Book, "P-Cresol," [Online]. Available: https://www.chemicalbook.com/ChemicalProductProperty_EN_CB5453502.htm.
- [7.6] J. Kirchhoff, F. Kraushaar, "Triacetoneamine derivatives: Industrial applications and recent developments," *Polymers and Polymer Composites*, 2000.
- [7.7] H. Xin, G. Xike, "Application of Azulene in Constructing Organic Optoelectronic Materials: New Tricks for an Old Dog," *ChemPlusChem*, 2017.
- [7.8] European Chemical Agency, "Substance Info Card," ECHA, 2020. [Online]. Available: <https://echa.europa.eu/da/substance-information/-/substanceinfo/100.003.601#:~:text=This%20substance%20is%20used%20for%20the%20manufacture%20of%3A%20textile%2C%20leather,release%20and%20formulation%20in%20materials..>
- [7.9] Holzel-Biotech, "4-Isobutyl-2-pyrrolidinone (pregabalin lactam impurity)," [Online]. Available: <https://www.hoelzel-biotech.com/en/molecule-trc-i786502-10mg-4-isobutyl-2-pyrrolidinone-13c3-pregabalin-lactam-impurity.html>. [Accessed 2020].
- [7.10] Sigma Aldrich, "Benzocyclobutene," 2020. [Online]. Available: <https://www.sigmaaldrich.com/catalog/product/aldrich/164410?lang=en®ion=U>

S&gclid=Cj0KCCQjwp4j6BRCRARIsAGq4yMGBqi1XvVfU1vZUjcm2RY9nn1ftSMJiQR
GlnRM5L3mEFxd5cvh6rVsaAmKDEALw_wcB.

- [7.11] Sigma Aldrich, “5,6-DIBROMO-BICYCLO(2.2.1)HEPT-2-ENE,” [Online]. Available: <https://www.sigmaaldrich.com/catalog/product/aldrich/s326410?lang=en®ion=US>. [Accessed 2019].
- [7.12] Sigma Aldrich, “Chloroethane solution,” 2020. [Online]. Available: <https://www.sigmaaldrich.com/catalog/product/aldrich/338303?lang=en®ion=US>.
- [7.13] Sigma Aldrich, “p-Cresol for Synthesis,” [Online]. Available: <https://www.sigmaaldrich.com/catalog/product/mm/805223?lang=en®ion=US>.
- [7.14] S. Martillanes, J. Rocha-Pimienta, M. Cabrera-Bañegil, D. Martín-Vertedor and J. Delgado-Adámez, “Application of Phenolic Compounds for Food Preservation: Food Additive and Active Packaging”, *InTechOpen*, 2016
- [7.15] N.A. Qambrani, M.M.Rahman, S. Won, S. Shim, C. Ra, “Biochar properties and eco-friendly applications for climate change mitigation, waste management, and wastewater treatment: A review”, *Renewable and Sustainable Energy Review*, 2017
- [7.16] M.K. Hossain, V. Strezov, K.Y.Chan, A.Ziolkowski,P.F. Nelson“Influence of pyrolysis temperature on production and nutrient properties of wastewater sludge biocha”, *Journal of Environmental Management*, 2009

CHAPTER 8 - CONCLUSION

Due to decrease in garment production costs and evolvement of fast fashion, textile waste generation has increased significantly. A large proportion of these wastes are currently being sent to landfills which can cause several environmental issues such as soil contamination and release of greenhouse gases. Parallely, use of non-renewable energies sources such as fossil fuels have been one of the major causes of environmental issues. This research focused on proposing a method to reduce the negative environmental effects of textile waste through conversion of them to fuels and useful commodities. Following this path, proposal of an integrated solution for addressing the environmental issues arose from both use of fossil fuels, petroleum-based products and textile waste generation was set as the objective of the research.

To achieve the mentioned objectives, three major tasks should have been carried out. The first task was to figure out a process which was capable of converting wool waste to useful commodities and to arrange a set up to test the potentials of such a method in laboratory scale. The second and main task was to propose a method to carry out wool waste management in a scaled-up process (compared to the laboratory scale). This would be done to observe the potential of commercialising the proposed wool waste management method.

To carry out the first and seconds tasks, a review of the available technologies to process wool waste was performed. A wide range of categories of methods such as biochemical, thermochemical, recycling and reusing were considered. After consideration and evaluation of the methods, pyrolysis and gasification, thermochemical methods, were selected as the suitable technologies. Pyrolysis and gasification of wool produce by-products in forms of oil, gas, and char.

Due to the properties of protein biomass such as wool, i.e., high nitrogen and oxygen content, it was envisaged that the products would need be modified to become more valuable. For instance, the high oxygen would have resulted in unstable oil product while the high nitrogen content could have ended up in the gaseous product and eventually caused acidic rains. Therefore, the third task was to attempt and find methods or conditions which improved/modified the qualities of the by-products through paths such as deoxygenation. To do so, it was decided to modify the operating conditions and evaluate the effect of heterogeneous catalysts on wool waste pyrolysis.

After consideration of the available pyrolysing technologies such as rotary kiln, fluidised bed, and rotating cone, it was decided to carry pyrolysis in a laboratory sized fixed bed due to the proven records and simplicity of it. This was done to check the feasibility of pyrolysis of wool at different operating conditions (temperature and with or without catalysts). Due to the complexity of the wool structure, model compounds were used to observe the effect of catalysts on the reaction path taken during pyrolysis. The catalysts used in model compounds pyrolysis were 20-ZSM5, 30-ZSM5, 60-ZSM5, Al-KIL2 and Li-KIL2. The results of the model compounds indicated that 20-ZSM5 and Al-KIL2 were the more promising catalysts for improving the quality of the wool pyrolysis products due to their high acidity and surface area.

Wool was pyrolysed in the fixed bed at different conditions (feed size, type of gas, temperature, and condensation medium) with and without catalysts. The results of the non-catalytic tests indicated that temperature was the most influential variable. Furthermore, increase of temperature increased the quantity of phenols and indoles (main products in the oil samples) in the oil, increased the BET of the char and increased the CO content of the gas. These all indicated that running the pyrolyser at higher temperatures was beneficial. However, undesirable compounds such as NH_3 increased in the gas while char nitrogen content reduced (high nitrogen content increases the favourability of char as soil amendment). Therefore, it could be concluded that a balance between these properties could be obtained at the pyrolysis at 800 °C.

In the catalytic runs, it was observed that both catalysts increased the char stability through reducing the oxygen content. Furthermore, the number of compounds found in the oil was reduced through use of both catalysts which made the oil easier to process and extract useful by-products from it. This effect of reduction in number of unique compounds was more predominant in case of the Al-KIL2. Therefore, this behaviour, followed by the fact that Al-KIL2 increased the oil fraction by over than 100% compared to non-catalytic one, made use of this catalyst as a recommendation where demand for oil product is preferable. Alternatively, due to the high nitrogen content, pyrolysis with 20-ZSM5 can be more beneficial if char product is in higher demand.

To scale the pyrolysis up, an auger reactor which used a hopper as the mean to introduce the feed was designed, built, and modified. Overall, this system reached uninterrupted flowrate of 2 kg/h. The char obtained from the auger reactor demonstrated similar properties to the fixed bed while the oil samples properties were significantly different. While phenols and indoles were obtained in the fixed bed, the products shifted towards nitriles, ketones and quinoline. The higher solid

residence time of the fixed could have been the reason behind this observed difference. The gas was scrubbed using water prior to release to the atmosphere. The high content of 3,3'-thiobis Propanenitrile in the scrubbing water demonstrated that the system had the potential to remove the toxic content from the gas.

Overall, the auger reactor proved to be capable of processing wool waste on its own and without it being mixed with other material, as the design intended. Product collection was successfully carried out and gas was scrubbed to show potential for integration of a dedicated gas scrubbing facility to the system. Furthermore, useful marketable by-products were collected as char and bio-oil while gas by-product showed promise to be used as fuel.

8.1 Recommendations and Future Work

The auger reactor system can be further modified to improve its efficiency and increase its capacity. For instance, a CHP unit can be incorporated to make the reactor partially self-sufficient. Also, the cooling medium of the condensers can be recirculated and used as a heating medium if the system is installed in a textile processing facility/mill. Furthermore, increasing the capacity of the current system would be a less cost intensive step compared to the current system due to the availability of the current design data.

As another modification of the auger arrangement, gas collection point can be added in series at difference points on the reactor tube for better control over product quality and thermal control of the system. This gas can pass through a series of condensation trains which use cooling mediums with different temperatures. This would result in initial separation of useful components. Alternatively, these gas collection points can be joined together and flow into a bed loaded with catalysts to alter the properties of the products. Furthermore, future study on optimising the methods to extract oil components such as phenols with marketable qualities would be valuable. Also, a dedicated study on an optimised method to purify the gas which is obtained from the wool pyrolysis and/or study on an optimised method for removal of the toxic material from the scrubbing water would be beneficial.

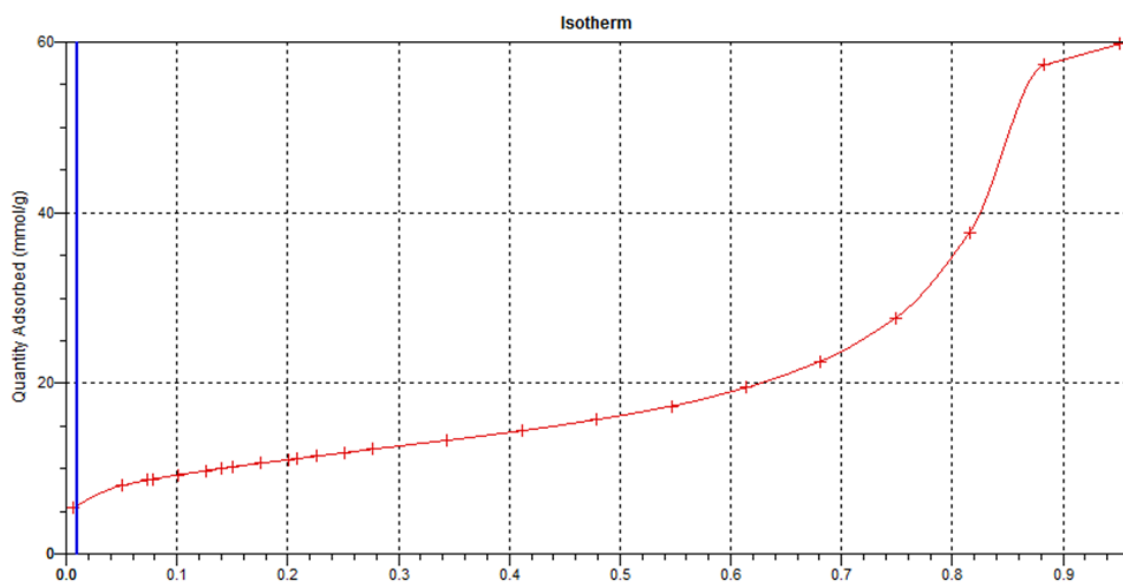
Due to the closeness of the blades of the auger to the tube wall, high carrier gas flowrates were required to facilitate the flow of evolved gas in the system. To reduce this high required gas rate and consequently make the process less cost intensive, small holes can be made on the middle of auger blades which would reduce the resistance to gas flow in the system.

The wool which was pyrolysed in this study had a complex structure due to the fact that the tweed pieces each included several dyes in their structure. This made the assignment of the reaction path taken during pyrolysis (both catalytic and non-catalytic) challenging. Therefore, to understand the reaction mechanisms involved during the pyrolysis of wool, dyes could be bleached out of the wool in the future studies and then the same experiments can be carried out on the wool. Furthermore, since the fixed bed pyrolysis produced oil products with higher phenolics, the residence time of the feed in the auger reactor can be increased in the future work to observe if the products quality would shift towards the fixed bed or not. To do this while aiming for the same high flowrates, the reactor would need to be re-designed.

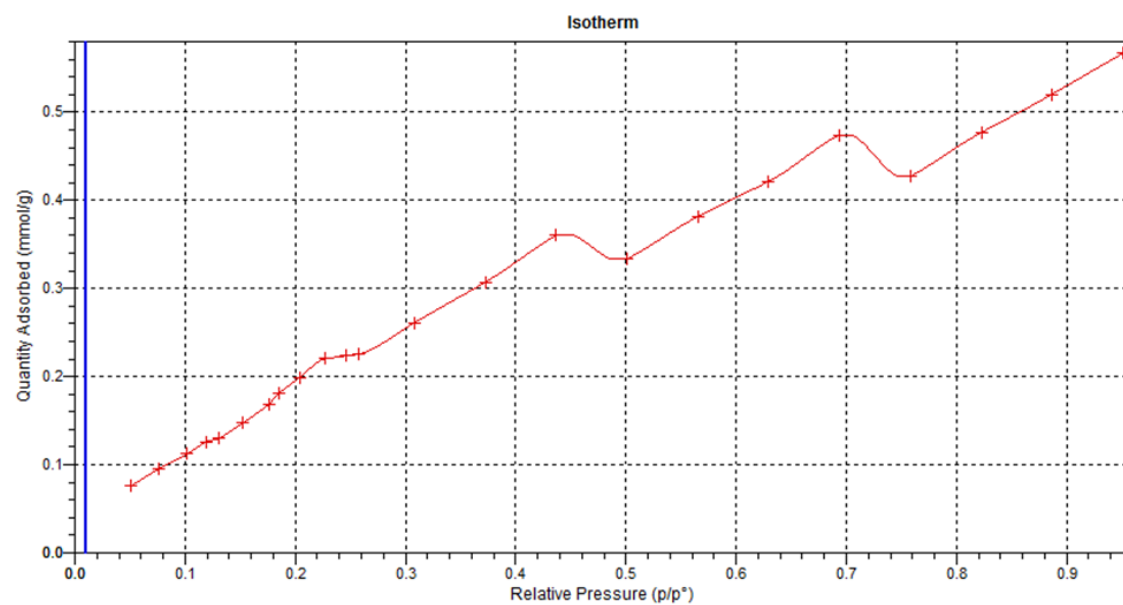
APPENDICES

9.1 Appendix A: Catalyst's Isotherms

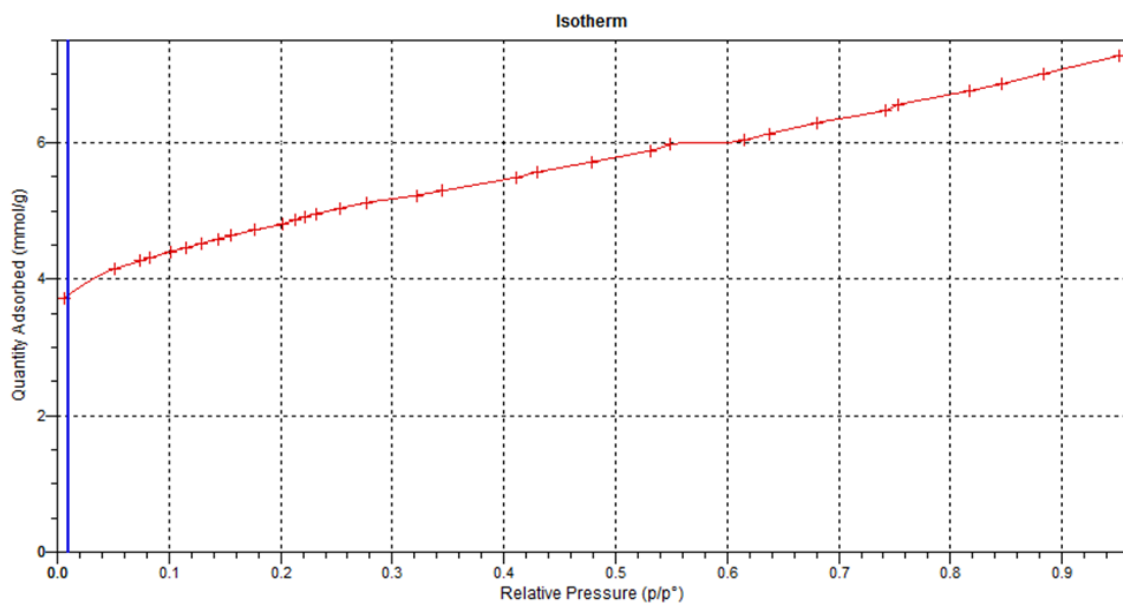
9.1.1 Al-KIL2



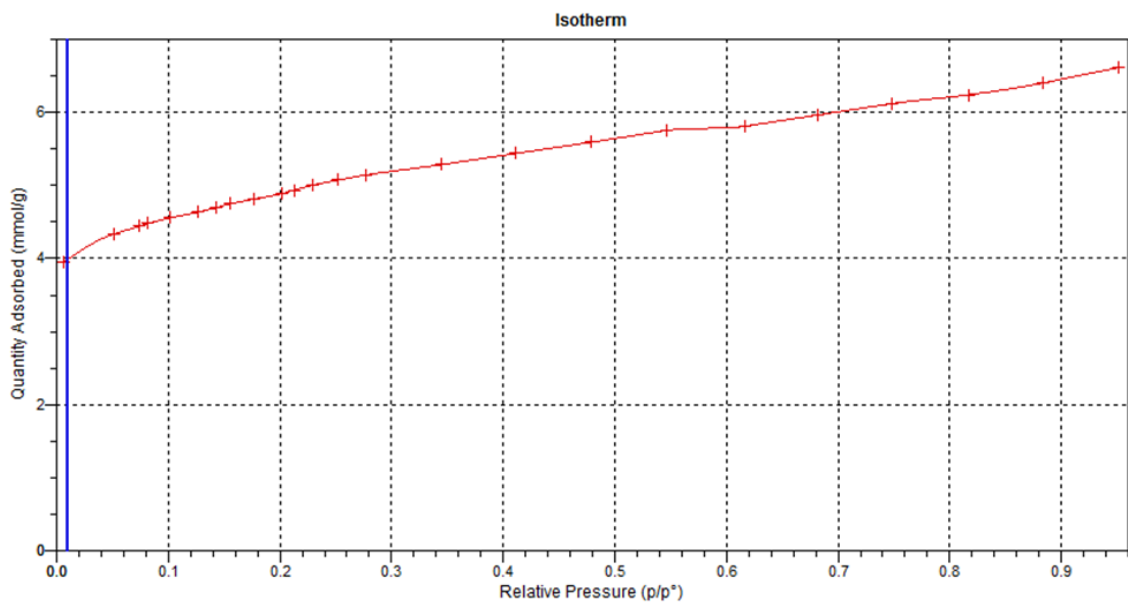
9.1.2 Li-KIL2



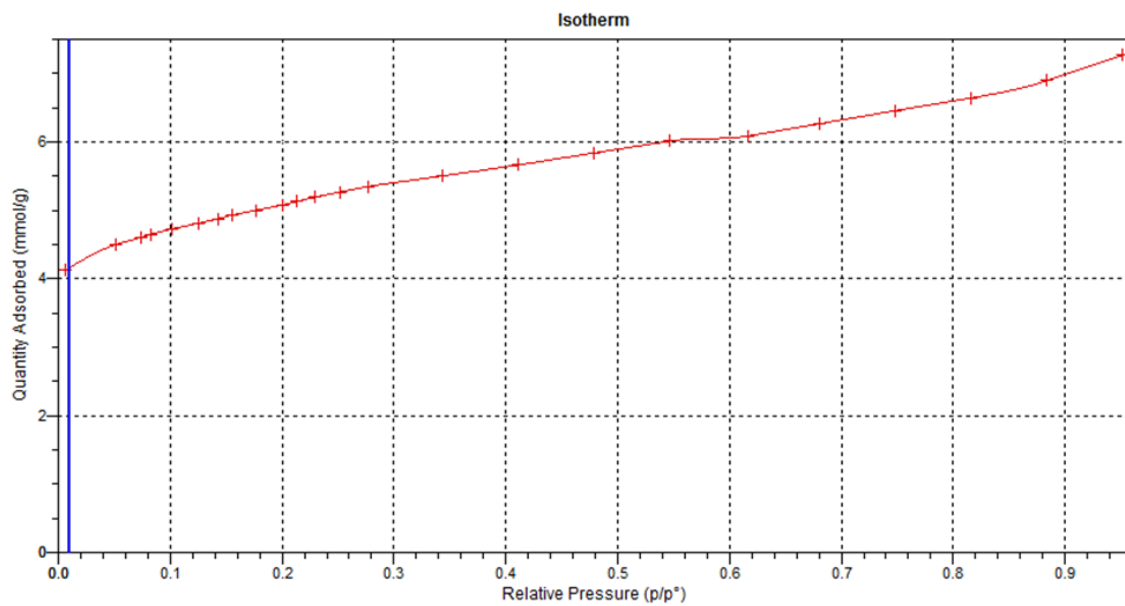
9.1.3 20-ZSM5



9.1.4 30-ZSM5



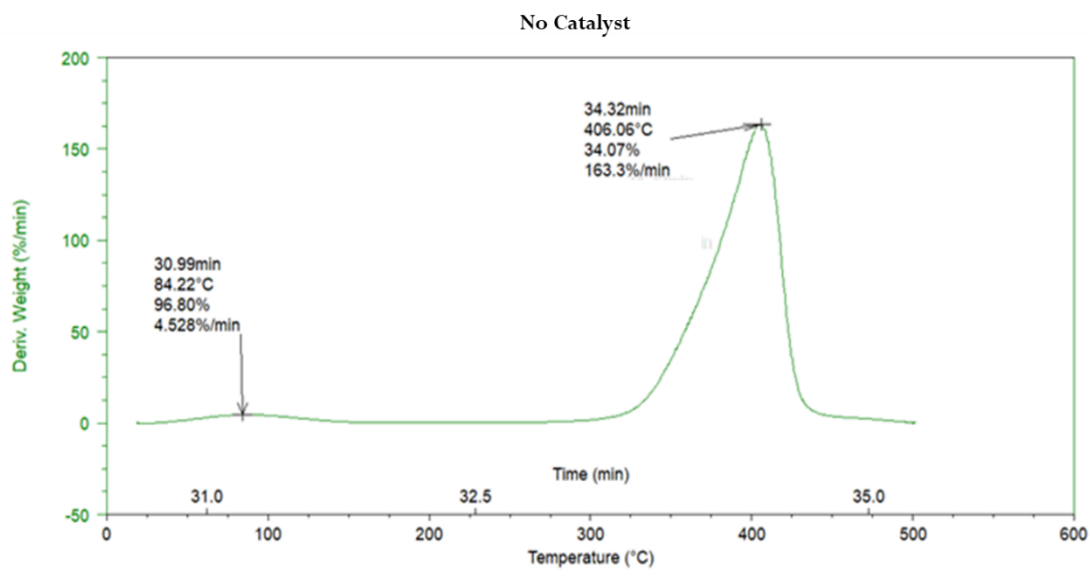
9.1.5 60-ZSM5



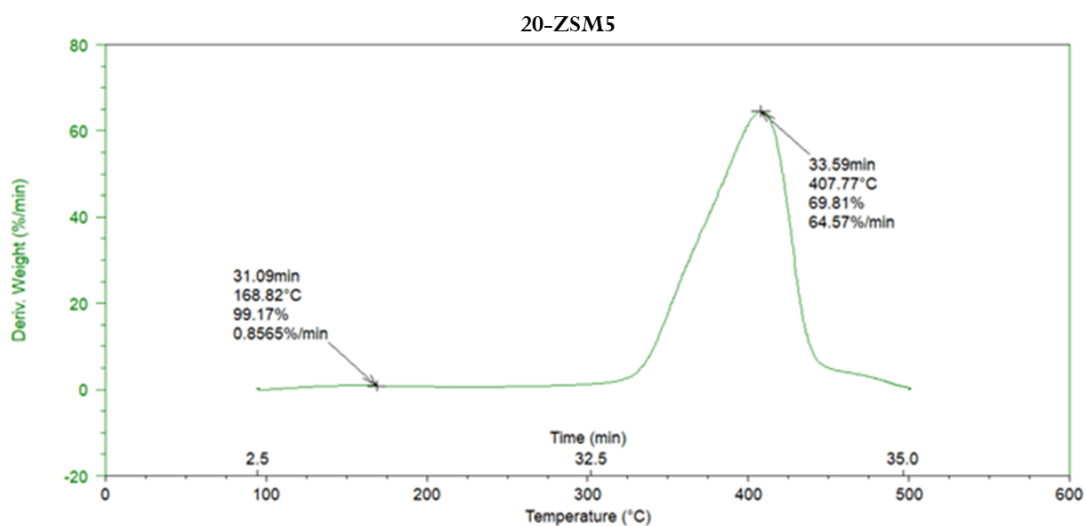
9.2 Appendix B: DTG Vs. Temperature

9.2.1 Cellulose

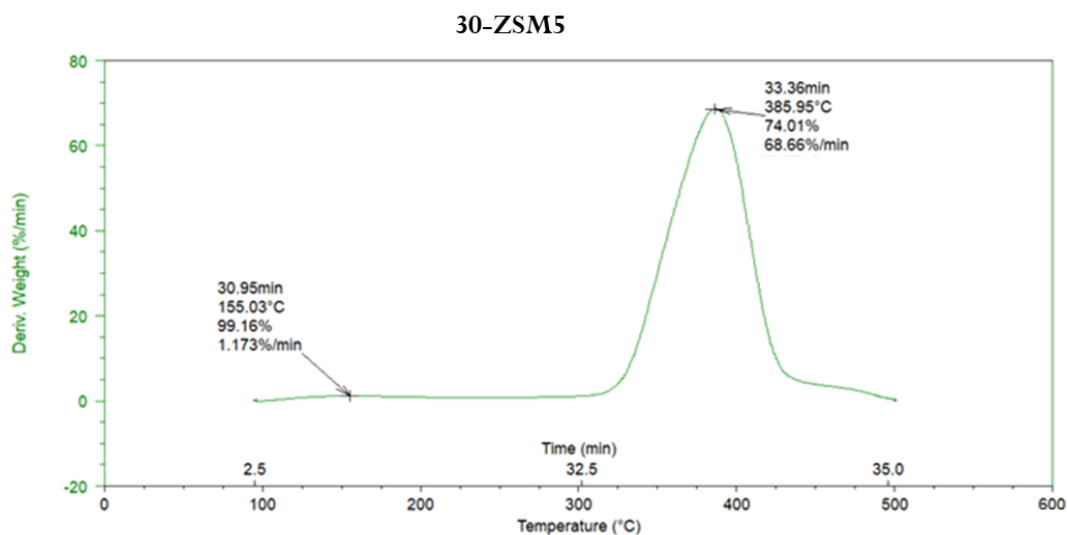
9.2.1.1 No Catalyst



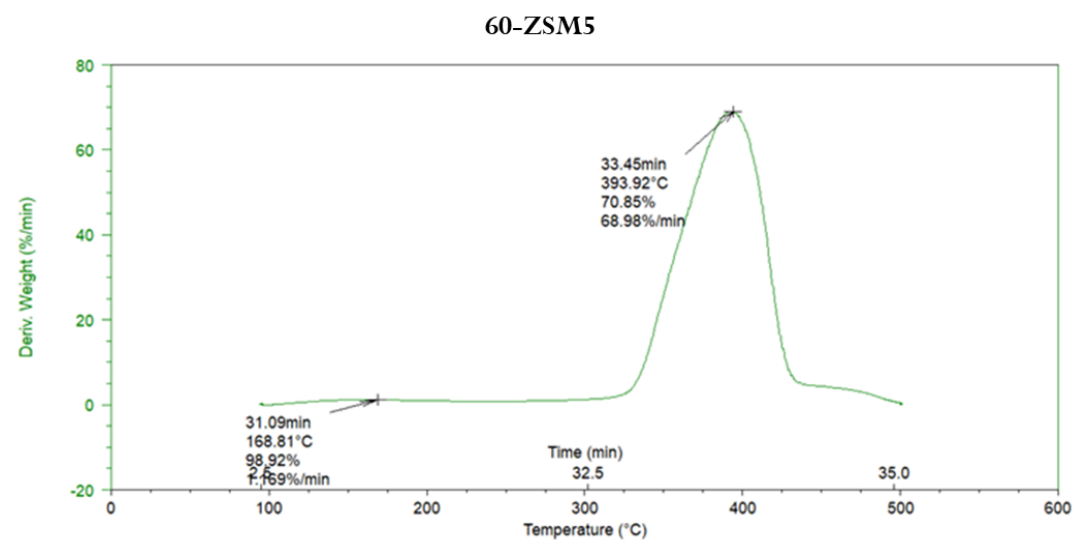
9.2.1.2 20-ZSM5



9.2.1.3 30-ZSM5

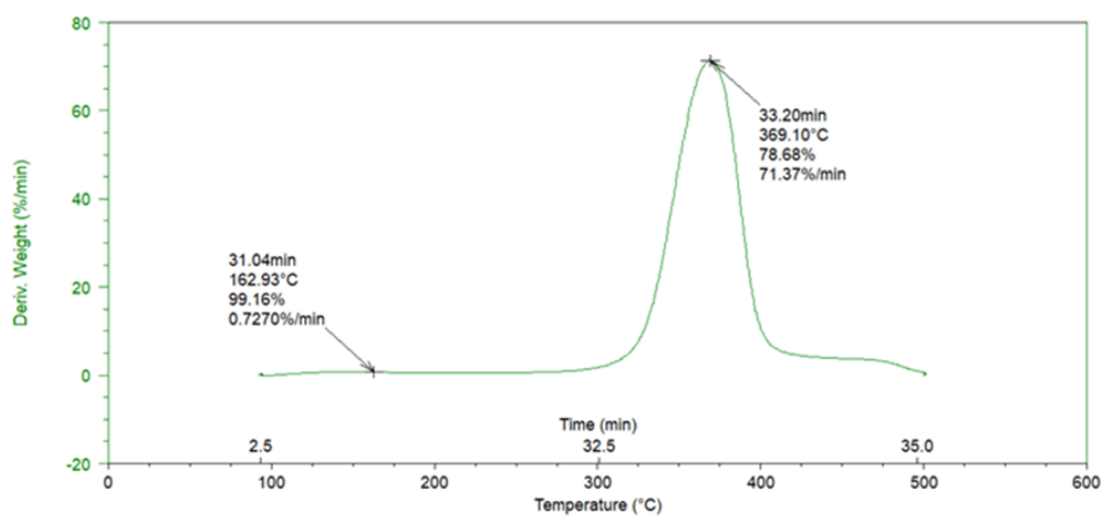


9.2.1.4 60-ZSM5



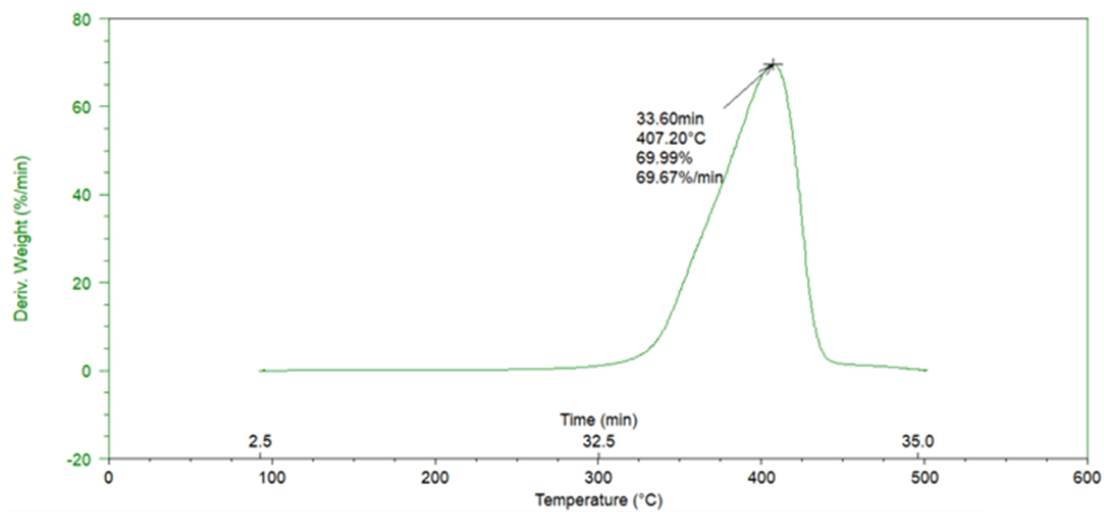
9.2.1.5 AL-KIL2

AL-KIL2



9.2.1.6 Li-KIL2

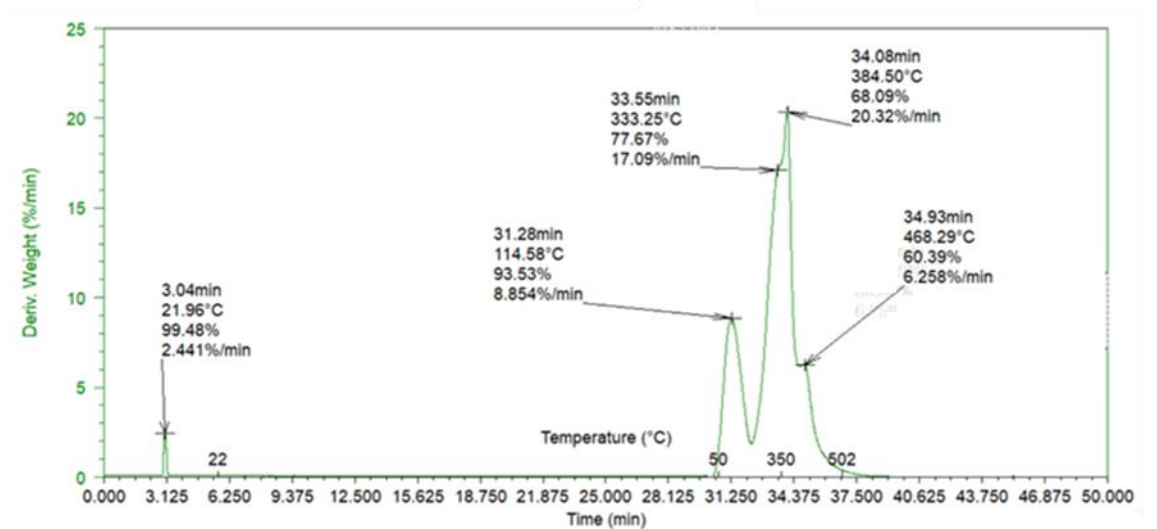
Li-KIL2



9.2.2 Lignin

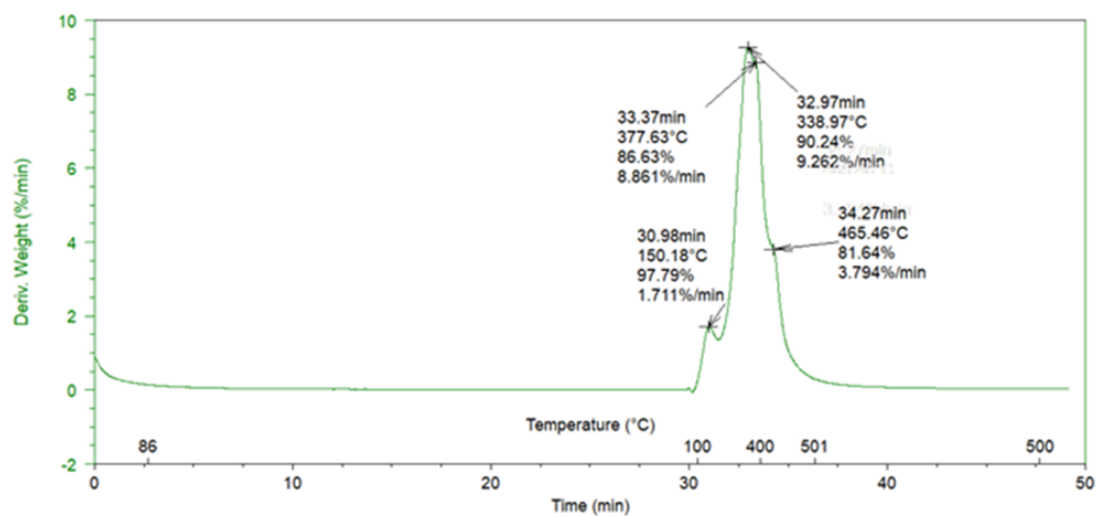
9.2.2.1 No Catalyst

No Catalyst

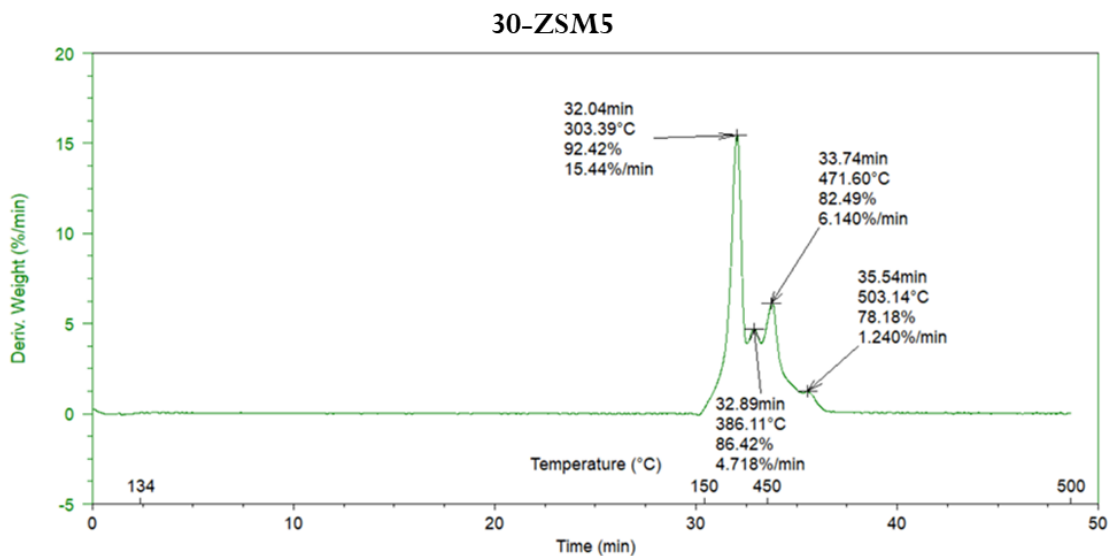


9.2.2.2 20-ZSM5

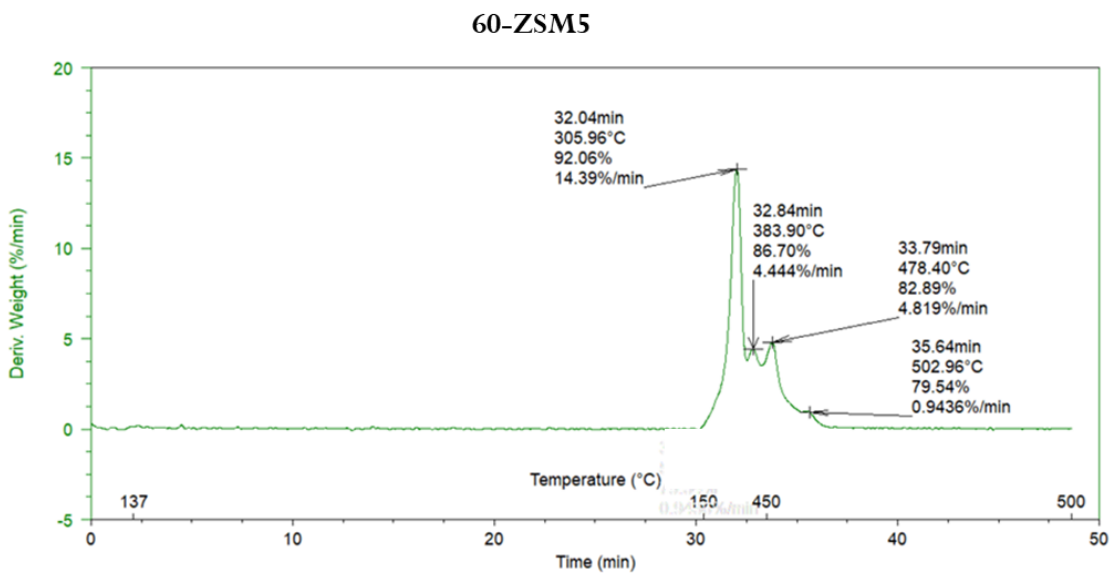
20-ZSM5



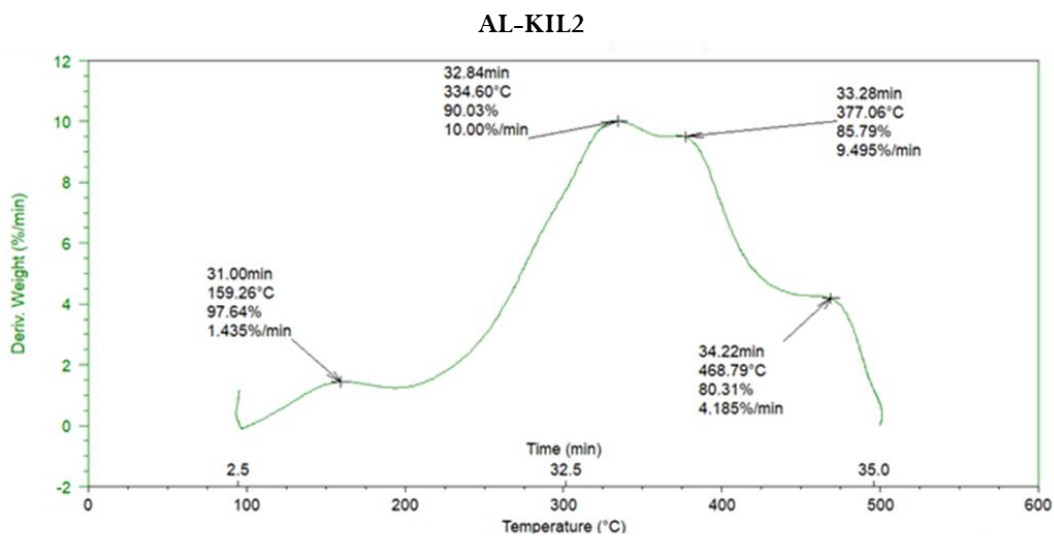
9.2.2.3 30-ZSM5



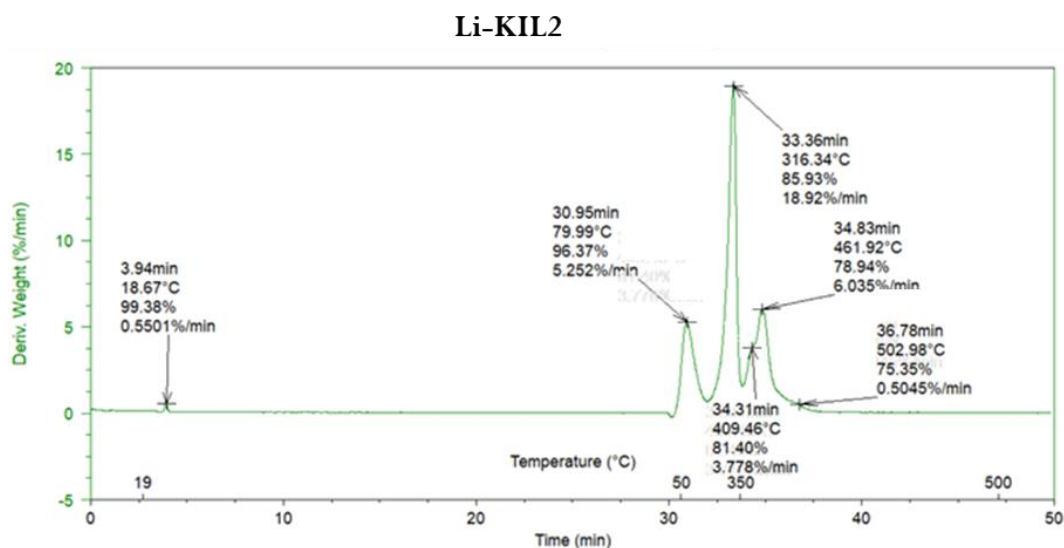
9.2.2.4 60-ZSM5



9.2.2.5 AL-KIL2

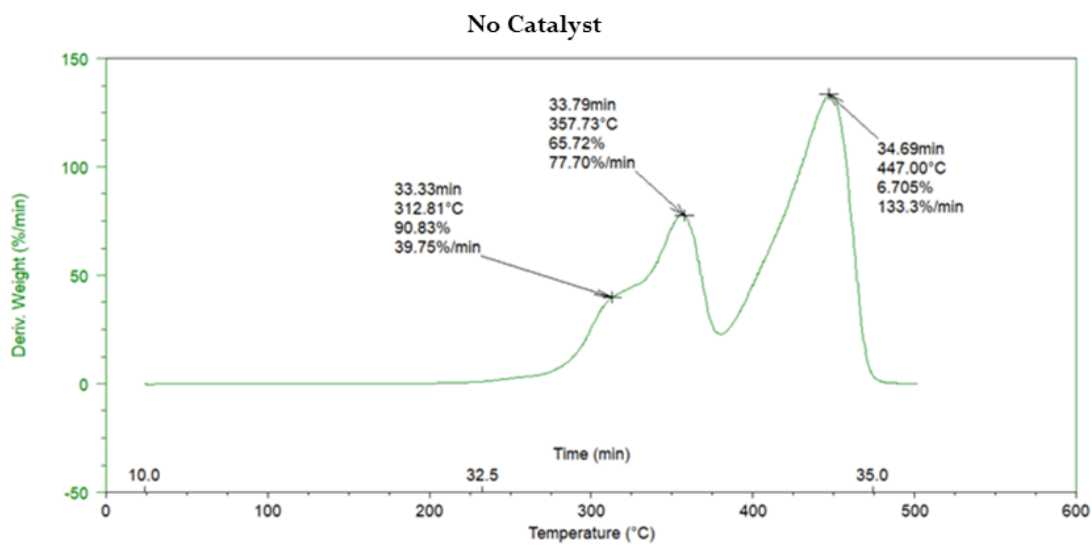


9.2.2.6 Li-KIL2

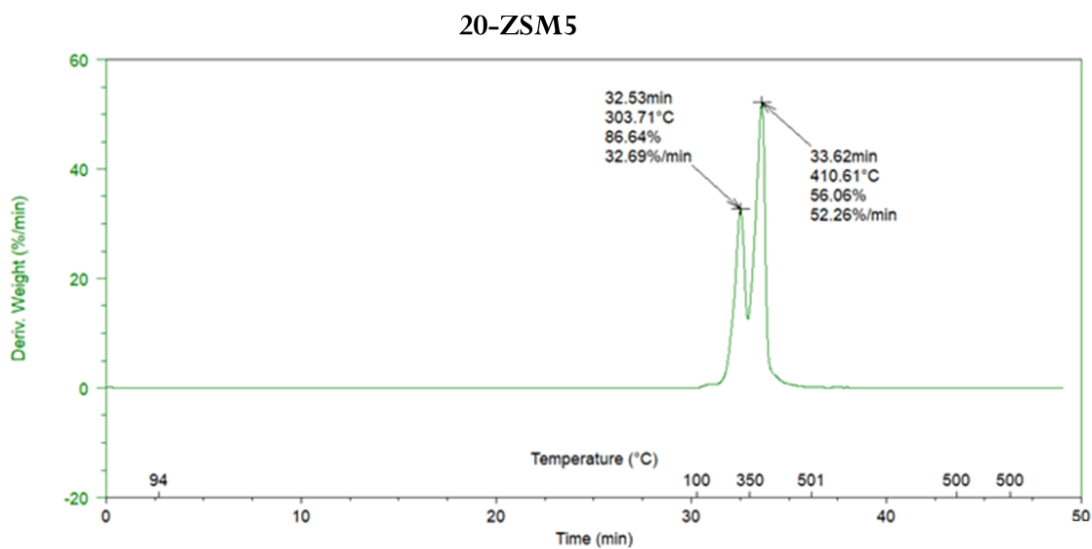


9.2.3 Phenylalanine

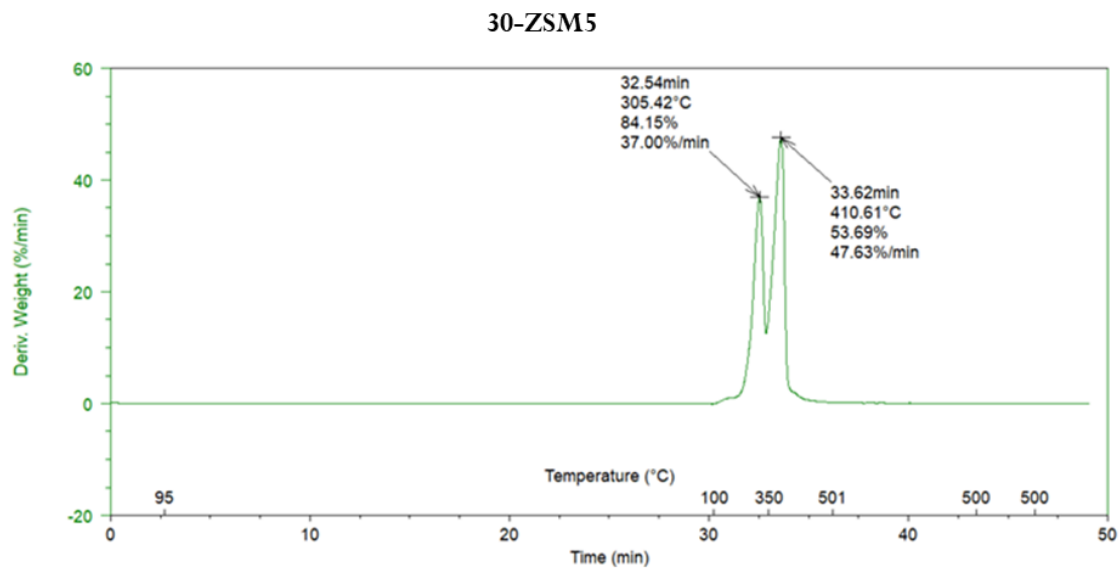
9.2.3.1 No Catalyst



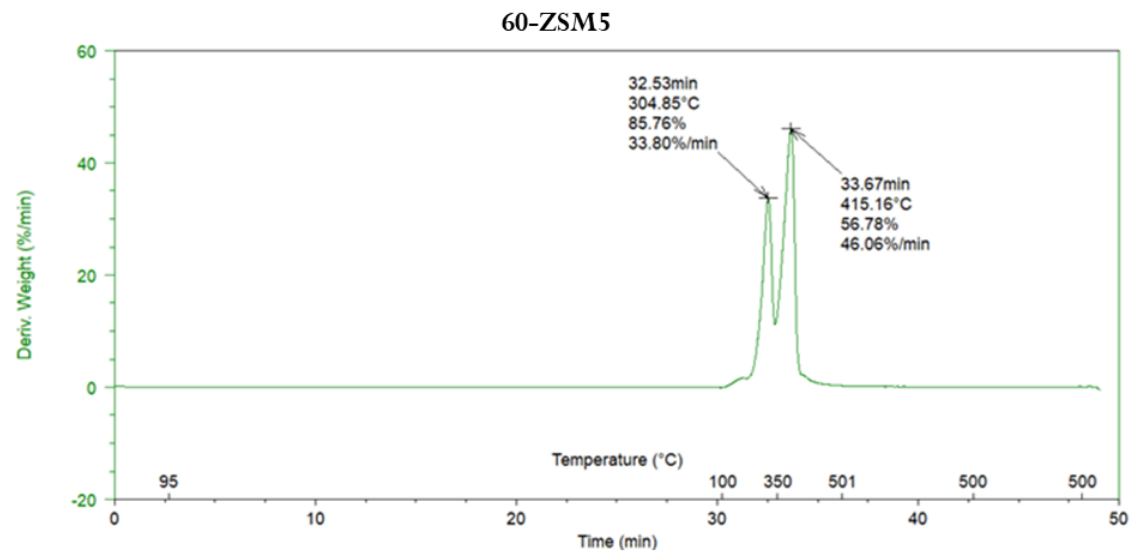
9.2.3.2 20-ZSM5



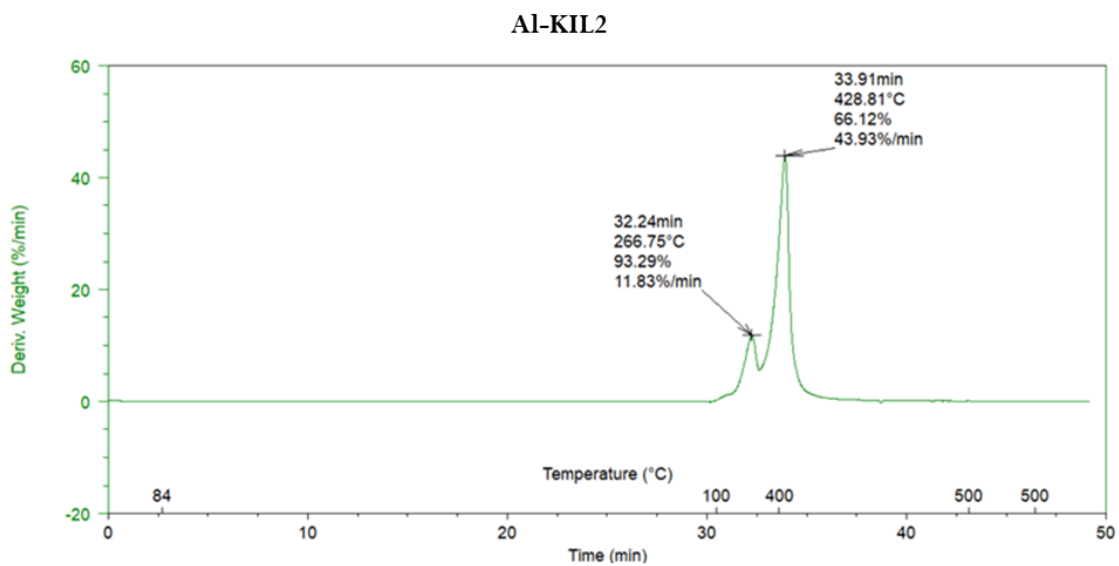
9.2.3.3 30-ZSM5



9.2.3.4 60-ZSM5



9.2.3.5 Al-KIL2



9.2.3.6 Li-KIL2

